Narrabri Mine Modification 5

Environmental Assessment

APPENDIX A

Subsidence Assessment

Resource Strategies

WHITEHAVEN COAL

Ditton Geotechnical Services Pty Ltd
82 Roslyn Avenue Charlestown NSW 2290
PO Box 5100 Kahibah NSW 2290

DgS

Ditton Geotechnical Services

Narrabri Coal Operations Pty Ltd

Mine Subsidence Assessment on the Proposed 75W Modification to the Stage 2 Mining Layout at the Narrabri Mine, Narrabri

DGS Report No. NAR-004/1

Date: 17 August, 2015

DgS

17 August, 2015

Mr Steve Farrar
Environmental Officer - Narrabri Mine
Whitehaven Coal Ltd
10 Kurrajong Creek Road
Baan Baa NSW 2390

DGS Report No. NAR-004/1

Dear Steve,

Subject: Mine Subsidence Assessment on the Proposed 75W Modification to the Stage 2 Mining Layout at the Narrabri Mine, Narrabri.

This report has been prepared in accordance with the brief for the above project.

Please contact the undersigned if you have any questions regarding this matter.

For and on behalf of
Ditton Geotechnical Services Pty Ltd

Steven Ditton
Principal Engineer

Executive Summary

This report presents a mine subsidence assessment for the proposed 75W Modification to the Stage 2 mining layout at Narrabri Mine (NM). The Project Approval for the Stage 2 Area within mining lease (ML1609) was issued in 2010 by the Director General of the NSW Department of Planning for longwall (LW) panels 1 to 26 (PA 08_0144). The longwalls were 305.4 metres (m) wide (void) with 24.6 m to 37.6 m wide chain pillars (solid).

The proposed modification to the 2009 Environmental Assessment (EA) mining layout would include six (6) Approved longwalls (LW 101 to 106) that would be 306.5 m wide and fourteen (14) proposed longwalls (LW 107 to 120) that would be 408.9 m wide[1]. The modified layout would be extended approximately 60 m to the west of the approved layout but remains within ML1609.

Based on an effective cover depth range of 180 m to 360 m, the modified longwalls 107 to 120 will have *supercritical* width/height (W/H) ratios ranging from 1.1 to 2.3. The Approved longwalls 101 to 106 will have similar W/H ratios that range from 1.2 to 1.9 for cover depths from 165 m to 255 m.

Chain pillar widths for LW101 to LW106 have been changed from a range of 24.6 m to 29.6 m in the 2009 EA to a range of 29.8 m to 39.5 m in the 101 to 106 Extraction Plan (EP). Chain pillar widths for LW107 to LW120 have been changed from a range of 24.6 m to 37.6 m in the 2009 EA to a range of 28 m to 36 m. There will also be two rows of chain pillars instead of one formed between each of the wider panels.

The original EA proposed mining height of 4.2 m in the Hoskissons Seam has been increased to 4.3 m for LW 103 to 120. Main headings and longwall gate roads remain unchanged at 3.5 m high with a nominal width of 5.4 m.

The predicted subsidence effects and likely impacts for the proposed modification to the approved Narrabri Mine layout have been compared to the previously assessed predictions provided in the 2009 EA submission. From this comparison, the Modification would not change the approved level of subsidence impact for the existing/approved underground mine layout. Predicted mine subsidence impacts to the following features within the Project Area have been re-assessed:

- Semi-cleared, gently undulating terrain (that is owned by the Narrabri Coal Operations Pty Ltd).

- Five ephemeral watercourses and creeks (Pine Creek, Pine Creek Tributary 1 and 2, Kurrajong Creek and Kurrajong Creek Tributary 1).

- Poor quality sub-surface groundwater aquifers at depths ranging from 5 m to 50 m.

---

[1]   Void widths are quoted in this report, rather than block widths.

- Six (6) Aboriginal cultural heritage sites of 'High' archaeological significance, comprising two scattered artefact sites (No. 38 and 39), two grinding groove sites (No. 10b and 122), one open camp site (No. 43) and one scarred tree (No. 123).

- One Hundred & twenty-nine (129) Aboriginal cultural heritage sites of 'Low' archaeological significance, comprising scattered and individual artefacts.

- Two disused orchard groves, 11 residential/farm buildings (to be vacated prior to subsidence effects occurring) and 13 above ground tanks.

- Forty unsealed access roads and several kilometres of property fencing.

- Forty-one earth embankment dams for stock and orchard watering.

- Single-phase suspended power lines and 15 timber power poles (disused domestic).

- Soil conservation banks (contour banks).

Assessment

Subsidence effect and impact predictions (**Sections 7** to **9**) for the features above the proposed longwalls have been based on **ACARP, 2003** (see **Section 4** and **Appendix A**) and subsidence effect data from the NM to date (LW 101 to 104). At the time of report preparation, NM had extracted (and reported on) three of six 306.5 m wide longwalls in the Hoskissons Seam.

The subsidence prediction model used in the 2009 EA estimated a maximum subsidence of 2.44 m or 0.58 mining height (T) above the 305.4 m wide longwalls. Although the predicted values for LW 101 to 104 have been within 15% of the measured results, the model has now been adjusted to reflect the actual 95% Confidential Levels (CLs) for subsequent panels as follows:

- Single Panel S_{max}/T increased from 0.58 to 0.60 for LW101 and 0.63 from LW102 to 120.

- Final maximum panel S_{max}/T has been increased to 0.61T for LW101 and 0.64T for LW 102 to 120.

- Supercritical width appears to occur at 1.2H instead of 1.4H, based on measured tilts and strains to-date.

Based on the available subsidence data it is assessed that no spanning behaviour associated with the Garrawilla Volcanics, Basalt Sill or Digby Conglomerate units has occurred to date. Subsidence predictions have therefore only considered 'Low' Subsidence Reduction Potential (SRP) for the worst-case scenario (Cases 1 and 3 in the 2009 EA Report).

Statistical inference techniques have been applied to estimate confidence levels for the predicted values and allow a probabilistic assessment of the potential range of impacts to the environmental and man-made surface features. Credible worst case (CWC) predictions have

been based on Upper 95% Confidence Levels in this study. Revised subsidence profiles and contours have subsequently been derived for LW 101 to 120.

The key outcomes of the results of the study are presented below for the modified layout:

(i)   Final maximum panel subsidence is likely to range between 2.69 m and 2.75 m (64% of the mining height).

(ii)   Final maximum chain pillar subsidence is estimated to range between 0.11 m and 0.76 m above twin chain pillar widths ranging from 28 m to 36 m. The vertical stress acting on the pillars are estimated to range from 9.4 to 28.3 MPa with pillar Factor of Safety (FoS) values of 3.20 to 1.09 estimated for a 3.5 m pillar height.

(iii)   Yielding of the chain pillars is not expected for the proposed mining layout (i.e. the predicted FoS values are > 1). However, strain-hardening of the pillars due to core confinement and goaf materials within the panels themselves will limit and result in eventual cessation of subsidence if overloading conditions were to occur.

(v)   Maximum panel tilts are estimated to range from 17 to 46 millimetre per metre (mm/m) for 'smooth' profile subsidence, with occasional tilts from 25 mm/m to 68 mm/m due to discontinuous strata behaviour (i.e. localised strata block rotations).

(vi)   The maximum compressive strains are expected to range from 3 mm/m to 13 mm/m for 'smooth' profile subsidence, with strains ranging from 8 mm/m to 32 mm/m due to discontinuous strata behaviour (i.e. cracking).

(vii)   The maximum tensile strains are expected to range from 2 mm/m to 10 mm/m for 'smooth' profile subsidence, with strains ranging from 6 mm/m to 25 mm/m due to discontinuous strata behaviour (i.e. cracking).

Based on the predicted CWC maximum panel subsidence, tilt and strain values for the longwall panel layouts, the potential for the following subsidence related impacts and their likely effect on natural and man-made features have been assessed:

Surface cracking and shearing (Section 9.2): Surface cracking within tensile strain zones and ranging in width from 20 millimetres (mm) to 250 mm at cover depths ranging from 360 m to 160 m respectively. Surface shearing and uplift within compressive strain zones and ranging in widths from 30 mm to 330 mm at cover depths ranging from 360 m to 160 m respectively.

Height of continuous sub-surface fracturing above the panels (Section 9.3): Direct hydraulic connection to the surface due to sub-surface fracturing above the panels is unlikely to occur where cover depths are > 160 m. Sub-surface aquifers within 144 m to 281 m above the proposed panels however, may be impacted by direct hydraulic connection to the workings, with significant long-term increases in vertical permeability. The predicted A-Zone ranges from 78% to 88% of the cover depth; 0.61 to 0.69 times the effective panel width and 34 to 65 times the mining height. It is also predicted that the height of A-Zone fracturing may extend to within 21 m to 79 m of the surface.

Height of discontinuous sub-surface fracturing above the panels (Section 9.3):
Discontinuous fracturing would be expected to occur above these limits and increase rock mass storage capacity and horizontal permeability by 10 to 100 times without direct hydraulic connection to the workings. Rock mass permeability is unlikely to increase significantly outside the limits of extraction.

In-direct or discontinuous sub-surface fracturing could interact with surface cracks where cover depths are < 255 m. Creek flows could be re-routed to below-surface pathways and re-surfacing down-stream of the mining extraction limits in these areas due to this interaction. This behaviour usually only occurs where shallow surface rock is present and unlikely to occur where deep soil profiles exist.

Surface gradient changes (Section 9.4): Surface gradients are likely to increase or decrease by up to 3.5% (+/- 2°) along creeks, with occasional increases of up to approximately 5% (or 3°) (note that consistent with experience to date, higher values are likely to be due to discontinuous strata behaviour and unlikely to be representative of gradient changes along a creek).

Ponding (Section 9.5): Potential ponding depths of 0.1 to 2.6 m may develop above several of the longwalls and creeks in the flatter areas of the site, based on post-mining contour predictions.

Slope Instability (Section 9.4): General and localised slope instability along low-level hills is considered 'very unlikely' due to the predicted cracking and tilting above LW 101 - 120.

Valley Closure (Section 9.6): Based on measured results along Pine Creek Tributary No. 1, the development of valley closure and associated uplift in valley floors and along creek beds is unlikely to exceed 200 mm.

Far-field horizontal displacements and strains (Section 9.7): Far-field displacements (FFDs) are horizontal movements outside the angle of draw and generally only have the potential to damage long, linear features such as pipelines, roads, bridges and dam walls. The Werris Creek Mungindi Railway and Kamilaroi Highway with their associated infrastructure are the only public utilities that exist to the east of the proposed modification area and are outside the 5 times cover depth range.

Archaeology (Section 9.8): One-hundred and twenty nine scattered and isolated artefact sites of 'Low' archaeological significance plus six sites of 'High' archaeological significance, comprising two scattered artefact sites (No. 38 and 39), two semi-detached grinding groove sites (No. 10b and 122), one open camp site (No. 43) and one scarred tree (No. 123) exist within the mine subsidence area for LW 101 to 120.

It is assessed that the potential for cracking is 'Likely' at the 'High' archaeologically significant Scattered Artefact site No. 38 to 39 after extraction of LW104. It unlikely that the cracking will result in direct damage to the artefacts themselves, however, individual artefacts could be lost into cracks that occur.

Cracking of the Grinding Groove Sites (No. 10b) due to LW105 is 'unlikely' because they are on sandstone 'floaters' in soil and not attached to bedrock. It is noted that similar 'floating' grinding grooves in a significant tensile strain zone above LW102 (Site No. 122) were not impacted by cracking.

It is 'unlikely' that the scarred tree (with 'High' archaeological significance) will be damaged by surface cracking and tilting.

Roads (Section 9.9): The various unsealed roads and tracks around the site are likely to be subject to cracking and shearing during mine subsidence development. Maximum tensile crack widths across or along roads are estimated to range between 20 mm and 250 mm. Surface 'steps' or humps due to compressive shear failures are estimated to range between 30 mm and 320 mm. Some sections of road may require re-grading or drainage remediation works after subsidence development. Mine subsidence warning signs and possibly closure of the roads should be considered where public safety risks are identified.

Farm Dams (Section 9.10): Stock watering dams are 'likely' to be damaged by mine induced cracking and/or shearing, resulting in dam wall breach or storage losses through the floor of the dam storage areas. Repairs to the dams and temporary supplies of water may be required by the stakeholders. Windmills and fences around the dams could also be damaged and require repairs after mining. Several dams have already been subsided by LW101 to 104 but have not required remedial works to be implemented.

Houses, Sheds and Above-Ground Tanks (Section 9.10): Vacant residential dwellings and farm machinery sheds are also likely to be significantly impacted during mining (i.e. 'Moderate' to 'Severe' impact rating in accordance with Australian Standard [AS] 2870:2011).

Fences, Livestock and Orchards (Section 9.11): Impacts to the fences and orchards may include the loss of function due to structural failure of wire strands and fence posts and/or the disruption of the orchard's water and drainage system.

Power lines (Section 9.13): The fifteen power line and poles to the various residences and orchards within the ML 1609 will be subsided by above LW 101 to 105 by between 0.0 m and 2.72 m. The differential subsidence between subsided and non-subsided poles with chain pillars in between them may have conductor clearances decreased by up to 1.96 m or increased by up to 0.16 m.

The poles would be affected by transient and final tilts towards the centre of the goaf of up to 41 mm/m. The ground strains at the poles are likely to range from +/- 12 mm/m. The predicted tilts and strains have the potential to damage the poles and ceramic conductor isolators. Flexible/roller-type conductor sheathing on the poles to control the conductor tension during/after mining impacts have already been implemented.

Comparison of Predicted Subsidence Effects and Impacts (2009 EA v. 2015 Modification) (Sections 6 and 9): The results presented in this study generally indicate changes in subsidence effect predictions between the EA and proposed mining layout

Modification by approximately +/- 20% (i.e. some increases and some decreases). The predicted increases in subsidence effect are unlikely to result in significantly higher impacts or environmental consequences, based on observed impacts to-date.

It is noted that the height of continuous fracturing predicted using the 2014 Geology Pi-Term Model are 26 to 83 m higher than the EA Report indicated. The overall impact should therefore be re-assessed by the groundwater modelling consultant.

The above items will require further discussion with the stakeholders to enable acceptable Extraction Plans (EP) to be developed. A suggested program for monitoring subsidence, tilt and strain at the relevant locations has been provided for the purpose of implementing and reviewing the EP. The use of remote Aerial Laser Scanning (ALS) is considered an appropriate subsidence monitoring technique in lieu of some of the traditional ground based subsidence survey lines.

Based on the observation that a finite range of subsidence effect values can occur at a given location above an extracted longwall panel of known mining geometry and geology, it is possible to provide a range of predictions that are likely to occur within a nominal confidence limit (i.e. usually 95%). This approach will allow specialist consultants and stakeholders to apply risk management principles in a practical way. On-going monitoring and review of subsidence effects and associated impacts will be conducted during mining in order to implement the proposed impact management strategies for the Project Area.

Each of the key features of the Project Area that have been assessed have been provided with impact management strategies as follows:

- **Surface cracking (Section 9.2.3)**
  Surface crack repair works may need to be implemented around the affected areas of the site, and in particular, if public roads, watercourses and steep slopes are impacted.

  Crack repairs in the flatter areas may involve ripping, backfilling and top dressing works or the pouring of cement-based grout or crushed rock into wider, deeper cracks. Crack repairs should not be attempted until the majority of active mine subsidence has occurred.

- **Watercourses (Sections 9.2 and 9.4)**
  Extraction Plans will need to include Trigger Action Response Plans and remediation strategies if cracking does occur along creeks and streams. Surface piezometers will be necessary to monitor ground water level adjustment and recovery for several years after each panel undermines a creek.

- **Sub-surface Fracturing (Section 9.3):**
  Consideration of further deep borehole extensometers and Vibrating Wire Piezometers the Project Area would allow a more comprehensive review of groundwater interaction with the extracted longwall panels.

  Inspections and monitoring of underground workings stability, groundwater makes and goaf air entry should continue to be recorded and included with subsidence monitoring data.

- **Residences (Sections 9.12):** It is recommended that the machinery sheds are vacated and all equipment/property of value removed before mining impacts. It is considered likely that subsidence movements will affect undermined properties for periods of at least 2 years after mining. Some of the structures may not be repairable after mining is completed.

- **Archaeology (Section 9.8):** It is assessed that none of the 'Highly' significant sites are likely to be impacted by cracking and erosion damage by mine subsidence. It is 'unlikely' that the scarred tree (with 'High' archaeological significance) will be damaged by surface cracking and tilting.

  There have been no impacts to the sites as a result of subsidence effects above LW101 to LW104, however, the Registered Aboriginal Parties (RAPs) have raised the temporary salvage artefacts as a management measure. This is yet to be approved in a revision to the sites Aboriginal Cultural Heritage Management Plan (ACHMP).

- **Power lines (Sections 9.13)**
  Power lines should continue to be managed in accordance with the Mine's Public Safety Management Plan in consultation with Essential Energy and the Mine Subsidence Board. Flexible/roller-type conductor sheathing on the poles to control the conductor tension during/after mining impacts have already been implemented in accordance with the Essential Energy Management Plan (EEMP).

- **Roads (Sections 9.9)**
  Public Roads should continue to be managed by the Mine's Public Safety Management Plan to provide signage and traffic control measures to affect repairs and maintain safety for road users during active subsidence periods. Some sections of road may also require re-grading or drainage remediation works after subsidence development.

- **Fences (Section 9.11):** The impact of subsidence on fencing and the grazing of livestock would primarily require either the installation of temporary fencing or re-location of the livestock during repair of surface cracking and damaged fences. The location and suggested methods of repair to surface cracking is discussed further in **Section 9.2**.

Overall, it is concluded that the Modification would result in some increases in subsidence effect predictions, however, these would not change the level of impact or environmental consequences. The assessed range of potential subsidence and far-field displacement impacts after the mining of the proposed longwall panels would be manageable for the majority of the site features, based on the analysis outcomes and discussions with the stakeholders to-date.

Impact management plans and strategies (**Section 9**) can then be developed that allow appropriate Trigger Action Response Plans and mine planning adjustments or mitigation measures necessary to deliver satisfactory outcomes to the feature and the stakeholders.

Surface and sub-surface monitoring recommendations are detailed in **Section 10**.

Table of Contents

Appendix A - Empirical Subsidence Prediction Model Details

GLOSSARY

Angle of Draw The angle (normally no greater than 26.5^o from the sides or ends of an extracted longwall block) from the vertical of the line drawn between the limits of extraction at seam level to the 20 mm subsidence contour at the surface. The 20 mm subsidence contour is an industry defined limit and represents the practical measurable limit of subsidence.

Chain Pillar The pillar of coal left between adjacent longwall panels. This forms a barrier that allows the goaf to be sealed off and facilitates tailgate roof stability.

Compressive Strain A decrease in the distance between two points on the surface. This can cause shear cracking or steps at the surface if > 2mm/m. Compressive strains are usually associated with concave curvatures near the middle of the panels.

Confidence Limits A term used to define the level of confidence in a predicted subsidence impact parameter and based on a database of previously measured values above geometrically similar mining layouts.

Cover Depth The depth from the surface to the mine workings.

Critical Longwall Panels Longwall panels that are almost as deep (H) as they are wide (W) (i.e. 0.6 <W/H < 1.4) and is the point where natural arching stops and failure of the overburden starts to occur. The presence of massive strata units however, can still provide spanning capability through flatter voussoir arching behaviour. Maximum subsidence will be a function of panel width, mining height and geology.

Curvature The rate of change of tilt between three points (A, B and C), measured at set distances apart (usually 10 m). The curvature is plotted at the middle point or point B and is usually concave in the middle of the panel and convex near the panel edges.

i.e. curvature = (tilt between points A and B - tilt between points B and C)/(average distance between points A to B and B to C) and usually expressed in 1/km.

Radius of curvature is the reciprocal of the curvature and is usually measured in km (i.e. radius = 1/curvature). The curvature is a measure of surface 'bending' and is generally associated with cracking.

CWC Values	The Credible Worst-Case (CWC) prediction for the predicted impact Parameter and normally based on the Upper 95% or U99% Confidence Limit line determined from measured data and the line of 'best fit' used to calculate the mean value. The CWC values are typically 1.5 to 2 times the mean values.
Development Height	The height at which the first workings (i.e. the main headings and gateroads) are driven; usually equal to or less than the extraction height on the longwall face.
Dynamic Subsidence Effects	**see Transient Subsidence Effects.**
Extraction Height	The height at which the seam is mined or extracted across a longwall face by the longwall shearer.
Extraction Plan	Refers to the approval process for managing mine subsidence impacts, in accordance with the Department of Planning and Development Consent document. The mine must prepare an Extraction Plan (EP) to the satisfaction of the Director-General, before the commencement of operations that will potentially lead to subsidence of the land surface.
Factor of Safety	The ratio between the strength of a structure divided by the load applied to the structure. Commonly used to design underground coal mine pillars.
Far-Field Displacement	Horizontal displacement outside of the angle of draw, associated with movement are due to horizontal stress relief above an extracted panel of coal. The strains due to these movements are usually < 0.5 mm/m and do not cause damage directly. Such displacements have been associated with differential movement between bridge abutments and dam walls in the Southern Coalfield, but generally have not caused significant damage.
First Workings	The tunnels or roadways driven by a continuous mining machine to provide access to the longwall panels in a mine (i.e. main headings and gate roads). The roof of the roadways is generally supported by high strength steel rock bolts encapsulated in chemical resin. Subsidence above first workings pillars and roadways is generally <20 mm.
Gate Roads	The tunnels or roadways driven down both sides of the longwall block (usually in pairs), to provide airways and access for men, materials, and the coal conveyor to the longwall face. The conveyor side of the block is called the 'maingate' and dust laden air and coal seam gases are exhausted on the opposite side (called the 'tailgate').

Goaf	The extracted area that the immediate roof or overburden collapses into, following the extraction of the coal. The overburden above the 'goaf' sags, resulting in a subsidence 'trough' at the surface.
Greenfields Site	Refers to a mining area where no local data of ground response to underground mining exists. Subsidence predictions must therefore be based on experience gained from mining in other areas with similar geological conditions and appropriate engineering models.
Horizontal Displacement	Horizontal displacement of a point after subsidence has occurred above an underground mining area within the angle of draw. It can be predicted by multiplying the tilt by a factor derived for the near surface lithology at a site (e.g. a factor of 10 is normally applied for the NSW Coalfields).
Inbye	An underground coal mining term used to describe the relative position of some feature or location in the mine that is closer to the coal face than the reference location.
Inflexion Point	The point above a subsided area where tensile strain changes to compressive strain along the deflected surface. It is also the point where maximum tilt occurs above an extracted longwall panel.
Longitudinal Subsidence Profile	Subsidence measured (or predicted) along a longwall panel or centre line.
Longwall	The method of extracting a wide block of coal using a coal shearer and armoured face conveyor. Hydraulic shields provide roof support across the face and protect the shearer and mine workers. The longwall equipment is installed along the full width of the block in an 8 to 10 m wide installation road at the start of the block before retreating 2 to 3 km back to the end of the block. The shields are progressively advanced across the full width of the face, as shearing continues in a sequence of backwards and forwards motions across the face. Depending on the geological and longwall equipment conditions, the longwall retreats at an average rate of about 80 m/week.
Maingate	Refers to the tunnels or roadways down the side of a longwall block which provides access for mine operations personnel, power, materials and clean air to the longwall face. It is usually located on the side of the longwall panel adjacent to unmined panels or solid coal.
Mean Values	The average value of a given impact parameter value (i.e. of subsidence, tilt and strain) predicted using a line of 'best fit' through a

set of measured data points against key independent variables (e.g. panel width, cover depth, extraction height). The mean values are typically two-thirds to half of the credible worst-case values.

Mining Height   Refers to the height or thickness of coal extracted along a longwall face.

Outbye   An underground coal mining term used to describe the relative position of some feature or location in the mine that is closer to the mine entry point than the reference location.

Outlier   A data point well outside the rest of the observations, representing an anomaly (e.g. a measurement related to a structural discontinuity or fault in the overburden that causes a compressive strain concentration at the surface, in an otherwise tensile strain field).

Panel Width   The width of an extracted area between chain pillars.

Shearing   The shortening effect of compressive strains due to mine subsidence on surface terrain, which results in localised shearing movements of soils and rock.

Strain   The change in horizontal distance between two points at the surface after mining, divided by the pre-mining distance between the points.

i.e. Strain = ((post-mining distance between A and B) - (pre-mining distance between A and B))/(pre-mining distance between A and B) and is usually expressed in mm/m.

Strain can be estimated by multiplying the curvature by a factor derived for the near surface lithology at a site (e.g. a factor of 10 is normally applied for the Newcastle Coalfield).

Study Area   The area which may have features in it that could be impacted by the proposed mine. It is usually defined by a 26.5^o to 35° angle of draw to 20 mm of vertical subsidence and up to 3 to 5 times the cover depth to limits of possible far-field horizontal displacement.

Subsidence   The difference between the pre-mining surface level and the post-mining surface level at a point, after it settles above an underground mining area.

Subsidence   Reducing the impact of subsidence on a feature by modifying the

Control	mining layout and set back distances from the feature (normally applied to sensitive natural features that can't be protected by mitigation or amelioration works).
Subsidence Impact	The effect that subsidence has on natural or man-made surface and sub-surface features above a mining area.
Subsidence Mitigation/ Amelioration	Modifying or reducing the impact of subsidence on a feature, so that the impact is within safe, serviceable, and repairable limits (normally applied to moderately sensitive man-made features that can tolerate a certain amount of subsidence).
Subsidence Reduction Potential	Refers to the potential reduction in subsidence due to massive strata in the overburden being able to either 'bridge' across an extracted panel or have a greater bulking volume when it collapses into the panel void (if close enough to seam level). The term was defined in an **ACARP, 2003** study into this phenomenon and is common in NSW Coalfields.
Super-Critical Longwall Panels	Longwall panels that are not as deep (H) as they are wide (W) (ie W/H > 1.4) and will cause complete failure of the overburden and maximum subsidence that is proportional to the mining height (i.e. 0.58 to 0.6 T).
Tailgate	Refers to the tunnels or roadways down the side of a longwall block which provides a ventilation pathway for bad or dusty air away from the longwall face. It is usually located on the side of the longwall panel adjacent to extracted panels or goaf.
Tilt	The rate of change of subsidence between two points (A and B), measured at set distances apart (usually 10 m). Tilt is plotted at the mid-point between the points and is a measure of the amount of differential subsidence. i.e. Tilt = (subsidence at point A - subsidence at point B)/(distance between the points) and is usually expressed in mm/m.
Tensile Strain	An increase in the distance between two points on the surface. This is likely to cause cracking at the surface if >2 mm/m. Tensile strains are usually associated with convex curvatures near the sides (or ends) of the panels.
Transverse Subsidence Profile	Subsidence measured (or predicted) across a longwall panel or cross line.
Transient Subsidence	Refers to the subsidence tilt and strains associated with the subsidence 'wave' at the surface that travels behind the retreating longwall face.

Effects	The transient tilts and strains are generally less than final subsidence profile values due to the retreat velocity of the longwall face.
Valley Closure	The inward (or outward) movement of valley ridge crests due to subsidence trough deformations or changes to horizontal stress fields associated with longwall mining. Measured movements have ranged between 10 mm and 400 mm in the NSW Coalfields and are usually visually imperceptible.
Valley Uplift	The phenomenon of upward movements along the valley floors due to **Valley Closure** and buckling of sedimentary rock units. Measured movements have ranged between 10 mm and 400 mm in the NSW Coalfields and may cause surface cracking in exposed bedrock on the floor of the valley (or gorge).

DgS

1.0 Introduction

This report presents a mine subsidence assessment for the proposed 75W Modification to the Stage 2 mining layout at Narrabri Mine (NM).

The Project Approval for the Stage 2 Area within the mining lease (ML1609) was given in 2009 by the Director General of the NSW Department of Planning for longwall (LW) panels 1 to 26 (PA 08_0144). The longwalls were 305.4 metres (m) wide (void) with 24.6 m to 37.6 m wide chain pillars (solid).

The Modification includes the following changes to the approved mining layout:

- An increase in longwall panel void width for LW107 to LW120 from

  305.4 m to 408.9 m.

- A reduction in the number of longwall panels from 26 to 20.

- The extension of the underground longwall areas relative to the existing/approved project by approximately 60 m to the west but remain within ML 1609.

- Chain pillar widths for LW101 to LW106 have been changed from a range of 24.6 m to 29.6 m to a range of 29.8 m to 39.5 m.

- Chain pillar widths for LW107 to LW120 have been changed from a range of 24.6 m to 37.6 m to a range of 28 m to 36 m. There will also be two rows of chain pillars instead of one formed between each panel.

- Continuation of hydraulic fracturing of the Digby Conglomerate to prevent or minimise the impact of wind blast in the underground workings.

The purpose of the report is to (i) provide subsidence effect and sub-surface fracture height predictions for LW 101 to 120 to allow specialist environmental consultants to assess the likely impacts of the proposed modifications, and (ii) form part of a 75W Modification under the Environmental Planning and Assessment Act 1979 (EP&A Act).

The mine is currently extracting LW104 under the existing Extraction Plan (EP) Approval for LW 101 to 105 and is in the process of extending the EP to include LW106, the last of the proposed 306.5 m void width panels.

This report also provides:

(i)   a review of predicted v. measured subsidence effects and their impacts for LW101 to 104 to-date; and

(ii) a comparison between the subsidence effects and impact predictions for the Modified mining layout and the 2009 Environmental Assessment (EA) layout predictions.

The predictions have been prepared using the same methodology that was used to assess the proposed EP extension for LW 101 to 106 (refer **DgS, 2015**).

2.0   Mining Geometry

2.1   Proposed Mining Geometry

The Modified mining layout presented in this report is summarised below:

- LW101 to LW106 have void widths of 306.5 m, generally with 2-heading gate roads (Maingate 106 has 3-headings) and a single row of chain pillars with widths of 29.8 m for LW101 and 102 Maingates; 35 m for LW103 and 104 Maingates and 39.5 m for LW105 Maingate. All chain pillars are 94 m long.

- LW107 to LW120 have void widths of 408.9 m with 3-heading gate roads and two rows of chain pillars with widths ranging from 28 m to 36 m. All chain pillars are 94 m long (solid).

- The seven-heading mains pillars for LW101 to LW106 to the north are 27 m to 36 m wide and 30 m to 96 m long. The mains in this section would also provide access to the southern panels, LW117 to LW120.

- The seven-heading mains pillars for LW107 to 111 to the north are 27 m to 36 m wide and 30 m to 96 m long. The mains in this section would also provide access to the southern panels, LW112 to LW116.

- The main headings and gate roads remain unchanged at a height of 3.5 m and nominal width of 5.4 m.

- The panel width to cover depth ratio (W/H) for the proposed mining layout would range from 1.13 to 2.25, indicating both critical and supercritical subsidence behaviour (assumed to occur when W/H >0.6 and >1.2 respectively). The chain pillars would have w/h ratios of 8.5 to 11.3 and expected to strain-harden (if overloaded) after mining is completed.

The EA approved and modified mine plans with cover depth contours are shown in **Figure 1a**. The modified mine plan in the northern and southern areas is shown in **Figures 1b** and **1c** respectively.

2.2   Previous Environment Impact Assessment Mining Geometry

The longwall panels that were originally assessed for Stage 2 were 305.4 m wide with chain pillar widths ranging from 24.6 m to 37.6 m wide. The proposed longwall mining height and roadway development height was 4.2 m and 3.5 m respectively. Roadway widths were nominally 5.5 m wide. This has been reduced slightly to 5.4 m in the Modified mining layout.

The current extraction plan longwalls LW101 to 106 are < 1% wider than the proposed panels assessed in the 2009 EA Report. The proposed chain pillars are approximately 20% wider than the EA mining layout for these panels.

The proposed longwalls LW107 to 120 will be 408.9 m wide and are 33% wider than the EA mining layout. The proposed double row of chain pillars are 85% to 91% wider than the approved single row of chain pillars for the EA mining layout.

3.0 Surface Features

3.1 LW 101 to 120

The land above the proposed LW101 - 120 comprises private land holdings used primarily for livestock grazing with some cereal crop farming. It is understood that NM now owns most of the private land holdings above the proposed longwalls. The land to the west of the proposed longwalls is overlain by native woodlands and the Jacks Creek and Pilliga East State Forests.

Topographic relief above the proposed longwalls ranges from 270 m AHD to 350 m AHD. The surface terrain is generally flat with slopes 2° - 5°. Slopes increase to 10° - 15° in several of the ephemeral creeks and tributaries (or gullies) of Pine Creek and Kurrajong Creek, which drain the mine site towards the north-east. There are a few ridges with steep slopes between 15° and 25° above longwalls LW110 to 117.

Sandy alluvial deposits (up to 15 m deep) exist along the creek channels with no rock exposures evident. Silty sand and sandy clay surface soils present on the mine site are mildly to highly erosive / dispersive if exposed to concentrated runoff.

Vegetation across the Project Area include several stands of cypress pine and box gum forest with shrubs and grasses across the agricultural land use areas and riparian zones along creeks.

The existing surface features within the zone of expected subsidence due to LW101 to 120 include the following:

- Semi-cleared, gently undulating terrain (that is owned by the mine).

- Five ephemeral watercourses and creeks (Pine Creek, Pine Creek Tributary 1 and 2, Kurrajong Creek and Kurrajong Creek Tributary 1).

- Poor quality groundwater aquifers at depths ranging from 5 m to 50 m.

- Six (6) Aboriginal cultural heritage sites of 'High' archaeological significance, comprising two scattered artefact sites (No. 38 and 39), two grinding groove sites (No. 10b and 122), one open camp site (No.43) and one scarred tree (No. 123).

- One Hundred & twenty-nine (129) Aboriginal cultural heritage sites of 'Low' archaeological significance, comprising scattered and individual artefacts.

- Two disused orchard groves, 11 residential/farm buildings and 13 above ground water tanks.

- Forty unsealed access roads and several kilometres of property fencing.

- Forty-one earth embankment dams for stock and orchard watering.

- Single-phase suspended power lines and 15 timber power poles (disused domestic).

- Soil conservation banks (contour banks).

Mine site infrastructure includes temporary gas drainage pipe lines to drainage wells above the panels and gate roads. The pipes are inspected for subsidence damage and decommissioned as required as mining progresses.

Pit top infrastructure and the Kamilaroi Highway and Werris Creek Mungindi Railway are > 1.9 kilometres (km) to the east of LW101 to 120 and outside the limits of far-field displacement and strain.

The study area with the above feature locations are shown in **Figures 1a-d** and **2a-c**.

3.2 Subsidence Monitoring Lines

The following subsidence monitoring lines have been installed above LW 101 to 104:

- Lines 101 and 102 are full centrelines above LW101 and 102.

- Line A cross line above LW101 to 105.

- Line 103 North and South are partial centre lines above the start and finishing ends of LW103.

- Line 104 North is a partial centreline above LW104.

- Line B is a longitudinal line along Pine Creek Tributary 1 with transverse lines C, E to G at 300 m spacing.

- Line D is a longitudinal line along Pine Creek.

- Power pole survey markers at base and tops of poles above LW101 to 105.

The survey line locations are shown in **Figure 3**.

The subsidence lines consist of pheno markers installed at 10 m spacing and anchored into the soil profile to a depth of 1 m. The pegs are surveyed using total station with static point control before and after mining effects. The surveys indicate systematic errors between surveys ranging from -20 millimetres (mm) to 45 mm, mainly due to seasonal soil moisture movement effects.

4.0 Subsidence Prediction Methodology

Single panel subsidence may be estimated using the empirical subsidence curves presented in **ACARP, 2003**. The prediction curves were initially developed from measured subsidence and mining geometry from the Newcastle Coalfield longwall mines with a wide range of geological conditions. Data from other NSW Coalfields has been added by DgS over the past 8 years. Single panel subsidence is mostly due to strata sag above an extracted longwall panel with compression of goaf edges also contributing.

The collapsed ground above the extracted panel of coal collapses into the void to form the 'goaf' which provides some support to the sagging strata and mitigates the magnitude of subsidence to a proportion of the mining height. The subsidence above a single longwall panel depends on the Subsidence Reduction Potential (SRP) of strata units within the overburden (see **Figures 4a** to **4c**), the width of the panel, the cover depth and mining height; see **Figures 5a** and **5b**.

When several panels are extracted adjacent to each other, further subsidence occurs due to the compression of the row of chain pillars left between the extracted panels. The prediction of the chain pillar subsidence is based on another empirical model developed using measured subsidence data for a given pillar and panel geometry. The subsidence is estimated based on the total pillar stress and mining height; see **Figures 6a** and **6b**. *Note: the pillar stress estimates for single pillar rows assumes double abutment loading conditions. The stress acting on the double pillar rows assume single abutment loading is applied to each pillar.*

Multiple-panel effects are determined by the **ACARP, 2003** model by adding a proportion of the predicted chain pillar subsidence to the predicted single panel subsidence. Estimates of first and final subsidence above a given set of longwalls use this general approach. The definition of First and Final S_{max} is as follows.

First $S_{max} =$ the maximum subsidence above a longwall panel after it is first extracted, including the effects of previously extracted longwall panels adjacent to the subject panel.

Final $S_{max} =$ the final maximum subsidence over an extracted longwall panel after at least three more panels have been extracted, or when mining is completed.

The subsidence above chain pillars has been defined in this study as follows.

First $S_p =$ subsidence over chain pillars after longwall panels have been extracted on both sides of the pillar for the first time.

Final $S_p =$ the total subsidence over a chain pillar, after at least another three more panels have been extracted, or when mining is completed.

First and Final S_{max} for the NM longwalls have been predicted by adding 50% and 100% of the predicted subsidence over the chain pillars between the previous and current panels, less the goaf edge subsidence above the Maingate (as it is already included in the chain pillar subsidence prediction).

A conceptual model of multiple longwall panel subsidence mechanics is given in **Figure 7**.

First and Final Subsidence profiles above the modified mining area are then estimated after each panel is extracted, based on the maximum panel subsidence, chain pillar subsidence, goaf edge subsidence and the angle of draw distance to 20 mm of subsidence. The profiles are used to calibrate the Surface Deformation Prediction System (SDPS[®]), 2007, which uses a 3-D Influence Function to generate subsidence contours. **Surfer 12**[®] software has then been used to generate enhanced subsidence, tilt, horizontal displacement, and strain contours above the panels from the **SDPS**[®] output files and measured subsidence profile data at the mine.

Further details of the subsidence predictions models used in this study are summarised in **Appendix A**.

DgS

5.0 Sub-Surface Conditions

5.1 Overburden

Typically, the overburden comprises thin to medium bedded siltstone and sandstone laminite with minor claystone between several massive 15 to 49 m thick units of conglomerate and basalt sills and lava flows. The depth of cover ranges from 160 to 250 m with depth of weathering typically varying from about 15 m to 35 m from the surface, although it can be as deep as 80 m below surface where there is also thick alluvial cover along some creek flats.

Previous reviews of available borehole data (see **Figure 4a** for borehole locations) suggested there may be potential subsidence reducing units in the overburden (e.g. Digby Conglomerate, intrusive basalt sill in the Napperby Formation and basalt lava flows of the Garrawilla Volcanics.

A summary of the thickness of the massive units and their location in the overburden sequence (in descending order) is presented in **Table 1**.

Table 1 - Summary of Massive Strata Units above LW 101 to 120

Lithological Unit	Massive Unit Thickness, t (m)	Unit Distance Above Proposed LW, y (m)	Laboratory UCS Strength Range [Mean] (MPa)
Garrawilla Volcanics*	1 - 62	42 - 258	65 - 252 [140]
Intrusive Basalt Sill	7 - 27	38 - 82	91 - 189 [140]
Digby Conglomerate	13 - 25	0.2 - 39	21- 42 [28]

* - The first 15 to 80 m below the surface may be affected by weathering. Unit may have a maximum thickness of only 20 m (**MGS, 2006**)
MPa = megapascal

Based on a review of subsidence data above LW 101 to 104 in **Section 6**, it is concluded that none of the massive units have reduced subsidence to-date. Subsequent predictions of maximum subsidence above all of the remaining longwalls have therefore assumed the overburden will have 'Low' SRP.

5.2 Immediate Mine Workings Conditions

The Hoskissons Seam ranges in thickness from 4.6 to 10 m in the Project Area, sub-cropping to the east at 130 m AHD. Based on bore core testing results, the proposed mining section of the seam comprises low to moderate strength coal (UCS of 20 to 40 MPa) with minor carbonaceous siltstone / mudstone bands. The proposed mine roof coal consists of similar strength coal with a higher proportion of low strength carbonaceous siltstone / mudstone (35% to 40% of roof section thickness).

The immediate roof of the proposed development roads consists of 0.4 to 5 m of coal, with overlying interbedded siltstone and sandstone laminite with minor mudstone (UCS ranges from 33 MPa to 36 MPa) and/or conglomerate of the Digby Formation (UCS ranges from 21 MPa to 42 MPa).

The floor of the development roadways comprises medium strength carbonaceous siltstone/ mudstone and sandstone (UCS ranges from 30 to 45MPa) with low slaking potential.

It is assessed that the immediate roof and floor strata conditions are within the range of the empirical database cases and may be used to estimate the chain pillar subsidence reliably at NM.

The prediction model outcomes have also been validated against measured subsidence data for LW 101 to 104 (Note: not all of LW104 was completed at time of writing); see **Section 6**.

6.0   Review of Subsidence Predictions v. Measured Data

The measured subsidence effects above LW 101 to 104 are compared to predicted mean and U95%CL values presented in **Tables 2A** and **2B**.

The review of measured First Maximum Subsidence above LW 101 to 102 full centrelines indicates that the 95th percentile S_{max} along centreline for LW101 was 0.6T or 2.52 m, and 0.63T or 2.65 m for LW102 (for a mining height of 4.2 m) - see **Figures 8a** and **8b**.

The partial centreline profiles for the start and finishing ends of LW103 and start end of LW104 are shown in **Figures 8c** and **8d** respectively. The U95%CL values of 0.63T are considered to be reasonable estimates for these two panels, as first goafing subsidence is usually higher than the rest of the panel once the goafing process has been established. The increase in panel subsidence after the first panels has been extracted is also due to tailgate chain pillar compression; see **Figure 8e**.

The subsidence prediction model (DgS modified **ACARP, 2003**) used in the 2009 EA estimated a maximum subsidence of 2.44 m or 0.58T would occur. The observed maximum subsidence has exceeded the predicted values for LW 101 to 104 but are within 15% of the measured results. The model has now been adjusted to match to reflect the actual 95%CLs for subsequent panels as follows:

- Single Panel S_{max}/T increased from 0.58 to 0.60 for LW101 and 0.63 from LW102 to 120 (see **Figures 5a,b**).

- Final maximum panel S_{max}/T has been increased to 0.61T for LW101 and 0.64T for LW102 to 120.

The chain pillar subsidence model appears to be conservative, with measured values to-date plotting below the mean curve (see **Figure 6a,b**).

The empirical models used to estimate maximum tilt, curvature and strain are presented with measured NM data in **Figures 9a** to **9d** respectively. Points of note include:

- The maximum tilt database is satisfactorily captured by the empirical model; see **Figure 9a**.

- Convex and concave curvature models now also capture 95% of the database (see **Figures 9b-9c**) with U95%CL Curvature = 2.5 x Mean Curvature.

- The Maximum Horizontal Strain = 10 x Maximum Curvature. Discontinuous movements such as cracking and compression humping may increase the maximum values by 2 to 4 times. The U95%CL Strain value has been assessed to be approximately 25 x mean curvature or 10 x U95%CL Curvature; see **Figure 9d**.

- Supercritical width appears to occur at 1.2H instead of 1.4H, based on measured tilts, curvatures and strains to-date; see **Figures 9a** to **9c**.

The DgS Modified **ACARP, 2003** models have been calibrated / validated against the measured data, with adjustments made to the maximum panel subsidence as described above.

The predicted values for the Modified mining layout for LW 101 to 120 are presented in **Section 7**.

Table 2A - Summary of Measured v. Predicted EA Subsidence above LW 101 to 104

LW#	Survey Line	Panel Width W (m)	Cover Depth H (m)	W/H	Chain Pillar Width w$_{cp}$ (m)	Mining Height T (m)	Total Pillar Stress (MPa)	First Maximum Subsidence First S$_{max}$ (m)		Final Chain Pillar Subsidence S$_p$ (m)		Final Maximum Subsidence Final S$_{max}$ (m)	
								Pred.	Meas.	Pred.	Meas.	Pred.	Meas.
101	CL101N	306.4	165	1.86	29.8	4.2	15.3	2.44	2.57	0.42	-	2.44	2.62
	CL101S	306.4	175	1.75	29.8	4.2	16.5	2.44	2.49	0.49	-	2.44	2.55
	XLA	306.4	165	1.86	29.8	4.2	15.0	2.44	2.45	0.44	0.118	2.44	2.52
102	CL102N	306.4	180	1.70	28.8	4.2	18.1	2.44	2.60	0.52	-	2.44	2.64
	CL102S	306.4	185	1.66	28.8	4.2	18.9	2.44	2.64	0.54	-	2.44	2.66
	XLA	306.4	175	1.75	28.8	4.2	17.6	2.44	2.52	0.50	0.183	2.44	2.58
103	CL103N	306.4	195	1.57	34.8	*4.3*	18.1	2.44	2.67	0.44	-	2.44	-
	CL103S	306.4	200	1.53	34.8	*4.3*	18.9	2.44	2.49	0.55	-	2.44	-
	XLA	306.4	195	1.57	34.8	*4.3*	17.6	2.44	2.59	0.53	-	2.44	-
104	CL104N	306.4	180	1.70	39.8	*4.3*	16.0	2.44	2.75	0.57	-	2.44	-

italics - predictions based on mining height of 4.2 m, which was increased to 4.3 m after EA report.

Table 2B - Summary of Measured and Predicted EA Subsidence Effects above LW 101 to 104

LW#	Survey Line	Final Goaf Edge Subsidence S$_{goe}$ (m)		Angle of Draw to 20mm Subsidence Contour (o)		Maximum Tilt T$_{max}$ (mm/m)		Maximum Compressive Strain -E$_{max}$ (mm/m) [meas/pred]		Maximum Tensile Strain +E$_{max}$ (mm/m) [meas/pred]	
		Pred.	Meas.	Pred.	Meas.	Pred.	Meas.	Pred.	Meas.	Pred.	Meas.
101	CL101N	0.22	0.31	21.2	32.7	47	46.3	14.4 [1.1]	15.9	11.4 [1.0]	11.4
	CL101S	0.23	0.12	21.4	13.9	41	31.1	12.0 [1.3]	**15.6**	9.5 [0.6]	5.9
	XLA	0.22	0.09 - 0.10	21.2	9.2 - 11.1	47	50.4 - 54.3	14.4 [1.0]	10.9 - 14.3	11.4 [1.3]	13.5-**14.7**
102	CL102N	0.24	0.205	21.7	15.5	40	43.7	11.4 [4.1]	**46.7**	9.0 [2.3]	**20.5**
	CL102S	0.24	0.16	21.7	20.6	38	29.8	10.8 [0.6]	6.4	8.5 [0.9]	7.4
	XLA	0.24	0.17	21.7	14.0	41	**48.5** - **56.3**	12.0 [2.2]	12.3 - **26.7**	9.5[1.6]	10.9-**15.2**
103	CL103N	0.24	0.25	21.9	23.4	43	39	12.8 [2.2]	**27.9**	10.1[1.5]	**14.7**
	CL103S	0.24	0.16	21.9	14.0	34	29.3 - 30.3	9.2 [0.9]	8.5	7.3[1.3]	**9.3**
	XLA	0.24	0.25	21.9	23.2	35	29.3 - 36.6	9.7 [1.0]	5.9 - 9.6	7.6[1.5]	**11.0-11.6**
104	CL104N	0.24	0.18	21.8	17.3	40	41.7	11.4 [3.1]	**35.6**	9.0 [4.7]	**42.6**

Bold - measured value exceeds smooth profile prediction by > 15% (indicating discontinuous behaviour).

7.0   Subsidence Effect Predictions for LW 101 to 120

7.1   General

Total and differential subsidence predictions have been assessed across the study area after:

(i)   each longwall block has been extracted, and

(ii) after mining of all of the proposed longwall panels is complete.

The assessment requires consideration of the following:

- The subsidence reduction potential (SRP) of the overburden and the influence of proposed mining geometry on single panel subsidence development (i.e. whether the panels are likely to *sub-critical, critical* or *supercritical*).

- The behaviour of the chain pillars and immediate roof and floor system under double - abutment loading conditions when longwalls have been extracted along both sides of the pillars.

- The combined effects of single panel and chain pillar subsidence to estimate final subsidence profiles and subsidence contours for subsequent impact assessment.

As mentioned previously, it is considered that the development of subsidence impacts will be not be affected by the spanning potential of the Garrawilla Volcanics, Basalt Sill or Digby Conglomerate units and the subsidence above the chain pillars between the panels. Subsidence predictions have therefore only considered Low SRP for the worst-case scenario and measured subsidence profiles for LW 101 to 104.

The outcomes of the subsidence assessment are presented in the following sections.

7.2   Maximum Single Panel Subsidence

The maximum subsidence above a single longwall panel will depend upon its width (W), cover depth (H), seam thickness (T), and the SRP of the overburden.

Based on reference to the **ACARP, 2003** model, the relevant depth categories for LW 101 - 120 are the 200 m and 300 m +/- 50 m categories. The depth categories were developed in the **ACARP, 2003** study to cater for the influence of scale on the overburden spanning behaviour above panels of a given geometry. Upper and lower subsidence predictions for all the panels are shown in **Figures 5a** and **5b**.

The maximum subsidence, S_{max} for a single 306.5 m wide longwall panel at 160 to 250 m depth with 'Low' SRP overburden is summarised in **Table 3A** and based on face extraction heights of 4.2 m or 4.3 m. The 408.9 m wide panel predictions for LW107 to 120 are presented in **Table 3B**.
The values were determined along ten representative cross lines (XL1 - 10); see **Figures 1b** and **1c** for their locations above the proposed mining layout.

Table 3A - Predicted Maximum Single Panel Subsidence for LW 101 to 106

LW	XL	Cover Depth, H (m)	W/H	Mining Height T (m)	SRP	Single S_{max}* (m)	
						Mean	U95%CL
101	3	165	1.86	4.2	Low	2.44	2.52
	4	165	1.86	4.2	Low	2.44	2.52
	5	177	1.73	4.2	Low	2.48	2.52
102	3	180	1.70	4.2	Low	2.48	2.52
	4	175	1.75	4.2	Low	2.48	2.52
	5	188	1.63	4.2	Low	2.48	2.52
103	2	190	1.61	4.3	Low	2.52	2.58
	3	195	1.57	4.3	Low	2.52	2.58
	4	195	1.57	4.3	Low	2.49	2.58
	5	200	1.53	4.3	Low	2.54	2.58
104	1	180	1.70	4.3	Low	2.46	2.58
	2	200	1.53	4.3	Low	2.41	2.58
	3	210	1.46	4.3	Low	2.41	2.58
	4	215	1.43	4.3	Low	2.49	2.58
	5	215	1.43	4.3	Low	2.35	2.58
105	1	200	1.53	4.3	Low	2.32	2.58
	2	215	1.43	4.3	Low	2.32	2.58
	3	225	1.36	4.3	Low	2.38	2.56
	4	235	1.30	4.3	Low	2.30	2.53
	5	235	1.30	4.3	Low	2.28	2.53
106	1	220	1.39	4.3	Low	2.28	2.58
	2	240	1.28	4.3	Low	2.44	2.52
	3	245	1.25	4.3	Low	2.44	2.51
	4	255	1.20	4.3	Low	2.48	2.49
	5	250	1.23	4.3	Low	2.48	2.50

SRP - Subsidence Reduction Potential: L = Low, M = Moderate, H = High.
* - Maximum subsidence limited to 60% of mining height for the mean and U95%CL (refer to **ACARP, 2003**).

Table 3B - Predicted Maximum Single Panel Subsidence for LW 107 to 120

LW	XL	Cover Depth, H (m)	W/H	Mining Height T (m)	SRP	Single Panel S_{max}* (m)	
						Mean	U95%CL
107	2	240	1.70	4.3	Low	2.54	2.58
	3	270	1.51	4.3	Low	2.53	2.58
	4	280	1.46	4.3	Low	2.54	2.58
	5	285	1.43	4.3	Low	2.54	2.58
108	1	275	1.49	4.3	Low	2.54	2.58
	2	265	1.54	4.3	Low	2.53	2.58
	3	275	1.49	4.3	Low	2.54	2.58
	4	290	1.41	4.3	Low	2.54	2.58
	5	305	1.34	4.3	Low	2.48	2.58

DgS

Table 3B (Cont…) - Predicted Maximum Single Panel Subsidence for LW 107 to 120

LW	XL	Cover Depth, H (m)	W/H	Mining Height T (m)	SRP	Single Panel S_{max}* (m)	
						Mean	**U95%CL**
109	1	295	1.39	4.3	Low	2.52	2.58
	2	290	1.41	4.3	Low	2.54	2.58
	3	300	1.36	4.3	Low	2.50	2.58
	4	305	1.34	4.3	Low	2.48	2.58
	5	325	1.26	4.3	Low	2.40	2.58
110	1	320	1.28	4.3	Low	2.42	2.58
	2	310	1.32	4.3	Low	2.46	2.58
	3	330	1.24	4.3	Low	2.38	2.58
	4	320	1.28	4.3	Low	2.42	2.58
	5	335	1.22	4.3	Low	2.36	2.57
111	1	330	1.24	4.3	Low	2.38	2.58
	2	325	1.26	4.3	Low	2.40	2.58
	3	350	1.17	4.3	Low	2.31	2.52
	4	360	1.14	4.3	Low	2.28	2.49
	5	350	1.17	4.3	Low	2.31	2.52
112	6	355	1.15	4.3	Low	2.29	2.51
	7	340	1.20	4.3	Low	2.34	2.56
	8	355	1.15	4.3	Low	2.29	2.51
	9	360	1.14	4.3	Low	2.28	2.49
	10	355	1.15	4.3	Low	2.29	2.51
113	6	350	1.17	4.3	Low	2.31	2.52
	7	320	1.28	4.3	Low	2.42	2.58
	8	330	1.24	4.3	Low	2.38	2.58
	9	340	1.20	4.3	Low	2.34	2.56
	10	345	1.19	4.3	Low	2.33	2.54
114	6	330	1.24	4.3	Low	2.38	2.58
	7	310	1.32	4.3	Low	2.46	2.58
	8	300	1.36	4.3	Low	2.50	2.58
	9	320	1.28	4.3	Low	2.42	2.58
	10	325	1.26	4.3	Low	2.40	2.58
115	6	305	1.34	4.3	Low	2.48	2.58
	7	305	1.34	4.3	Low	2.48	2.58
	8	275	1.49	4.3	Low	2.54	2.58
	9	285	1.43	4.3	Low	2.54	2.58
	10	300	1.36	4.3	Low	2.50	2.58
116	6	270	1.51	4.3	Low	2.53	2.58
	7	270	1.51	4.3	Low	2.53	2.58
	8	245	1.67	4.3	Low	2.54	2.58
	9	255	1.60	4.3	Low	2.54	2.58
	10	280	1.46	4.3	Low	2.54	2.58
117	6	230	1.78	4.3	Low	2.54	2.58
	7	240	1.70	4.3	Low	2.54	2.58
	8	225	1.82	4.3	Low	2.54	2.58
	9	225	1.82	4.3	Low	2.54	2.58
	10	245	1.67	4.3	Low	2.54	2.58
118	6	200	2.04	4.3	Low	2.54	2.58
	7	205	1.99	4.3	Low	2.54	2.58
	8	205	1.99	4.3	Low	2.54	2.58
	9	210	1.95	4.3	Low	2.54	2.58

Table 3B (Cont…) - Predicted Maximum Single Panel Subsidence for LW 107 to 120

LW	XL	Cover Depth, H (m)	W/H	Mining Height T (m)	SRP	Single Panel S$_{max}$* (m)	
						Mean	**U95%CL**
118	10	225	1.82	4.3	Low	2.54	2.58
119	8	190	2.15	4.3	Low	2.54	2.58
	9	200	2.04	4.3	Low	2.54	2.58
	10	210	1.95	4.3	Low	2.54	2.58
120	8	180	2.27	4.3	Low	2.54	2.58
	9	190	2.15	4.3	Low	2.54	2.58
	10	205	1.99	4.3	Low	2.54	2.58

SRP - Subsidence Reduction Potential: L = Low, M = Moderate, H = High.
* - Maximum subsidence limited to 60% of mining height for the mean and U95%CL (refer to **ACARP, 2003**).

The results of the single panel spanning assessment indicate that the maximum panel subsidence for the no spanning volcanic units) will range between 2.44 and 2.58 m (58% to 60% mining height, T).

The single panel subsidence values predicted above will be used with the chain pillar and goaf edge subsidence to estimate the multi-panel subsidence in the following sections.

7.3   Maximum Predicted Subsidence above Chain Pillars

The predicted subsidence values above the chain pillars have been estimated based on an empirical model of the roof-pillar-floor system.

The empirical model has been developed from measured subsidence data over chain pillars (S$_p$) divided by the face extraction height (T) v. the total pillar stress after longwall panel extraction on both sides, see **Figure 6a** and **6b**.

The database indicates that when pillar stresses are < 20 MPa, chain pillar subsidence is generally between 5% - 10% T. Between 20 and 40 MPa, the chain pillars start to 'soften' or yield with subsidence increasing to around 15% - 25%T. Above 40 MPa the subsidence does not increase over 30%T, which indicates that strain hardening behaviour is occurring and suggests that some of the pillar load will be re-distributed to the adjacent goaf (which also strain hardens) after yielding of the pillar starts to occur.

It is apparent from the measured data that the subsidence above the pillars is a function of the strength and stiffness of the coal and surrounding rock mass (i.e. higher subsidence was measured above a pillar with a weak shale roof compared to a pillar with a strong sandstone floor, all other strata and coal properties were similar).

The database includes longwall mining heights of 2 m to 4.8 m with pillar development heights of 2.0 m to 3.5 m. Pillar widths range from 18 m to 40 m (and one case of 80 m) with corresponding w/h ratios of 7.4 to 25.8.

The proposed chain pillar geometries are within the database limits.

7.3.1 Empirical Model Stress

The estimate of the total stress acting on the chain pillars on each side of the panel under double or single abutment loading conditions is based on the formulae presented in **ACARP, 1998a**; see **Figure 7**. The total stress acting on the chain pillars after mining is completed was estimated as follows:

σ = pillar load/area = $(T+A_1+A_2)/wl$

where:

T   = full tributary area load of column of rock above each pillar;

     = $(l+ r)(w + r).\rho.g.H$;

$A_{1,2}$ = total abutment load from each side of pillar in MN/m, and

     = $(l+r)\rho g(0.5W'H - W'^2/8\tan\phi)$ (for sub-critical panel widths) or

     = $(l+r)(\rho gH^2\tan\phi)/2$ (for super-critical panel widths);

w   = pillar width (solid);

l   = pillar length;

r   = roadway width;

H   = depth of cover;

ϕ = abutment angle (normally taken to be 21º); and

W'   = effective panel width (rib to rib distance minus the roadway width).

A panel is deemed sub-critical when $W'/2 < H\tan\phi$.

7.3.2 Empirical Model Pillar Strength and FoS

As presented in **ACARP, 1998b** the Factor of Safety (FoS) of the chain pillars were based on the strength formula for 'squat' pillars with w/h ratios > 5 as follows:

S   = $27.63\Theta^{0.51}(0.29((w/5h)^{2.5} - 1) + 1)/(w^{0.22}h^{0.11})$

where:

h   = pillar development height;

Θ = a dimensionless 'aspect ratio' factor or w/h ratio in this case.

The FoS was then calculated by dividing the pillar strength, S, with the pillar stress, σ.

7.3.3 Results

The predicted mean and Upper 95%CL subsidence values above the proposed chain pillars (under double or single abutment loading conditions and a mining height of 4.2 and 4.3 m) are summarised for representative cross lines XL1 to 10 in **Table 4**.

Table 4 - Predicted Maximum Chain Pillar Subsidence for Modified LW 101 to 120 based on the DgS Modified ACARP, 2003 Empirical Model

LW	XL	Cover Depth, H (m)	Mining Height T (m)	Chain Pillar Width w (m)	Pillar w/h	Chain Pillar Stress (MPa)	Pillar FoS under DA or SA Loading Conditions	Chain Pillar Subsidence			
								S_p First (m)		S_p Final (m)	
								mean	U95%	mean	U95%
101	3	165	4.2	30	8.5	*15.3*	*1.67*	0.18	0.26	0.21	0.30
	4	165	4.2	30	8.5	*15.0*	*1.70*	0.17	0.25	0.20	0.29
	5	177	4.2	30	8.5	*16.9*	*1.51*	0.21	0.37	0.25	0.42
102	3	180	4.2	30	8.5	*11.6*	*2.20*	0.12	0.20	0.14	0.23
	4	175	4.2	30	8.5	*11.3*	*2.26*	0.11	0.20	0.14	0.22
	5	188	4.2	30	8.5	*12.3*	*2.08*	0.13	0.21	0.15	0.24
103	3	195	4.3	35	10.0	*11.8*	*2.67*	0.12	0.20	0.14	0.23
	4	195	4.3	35	10.0	*12.1*	*2.60*	0.12	0.21	0.15	0.23
	5	200	4.3	35	10.0	*12.4*	*2.54*	0.13	0.21	0.15	0.24
104	2	180	4.3	35	10.0	*10.7*	*2.92*	0.11	0.19	0.13	0.21
	3	205	4.3	35	10.0	*13.0*	*2.42*	0.14	0.22	0.17	0.25
	4	215	4.3	35	10.0	*13.9*	*2.26*	0.15	0.24	0.18	0.27
	5	215	4.3	35	10.0	*13.9*	*2.26*	0.15	0.24	0.18	0.27
105	2	200	4.3	40	11.3	*11.7*	*3.20*	0.12	0.20	0.14	0.23
	3	225	4.3	40	11.3	*13.9*	*2.70*	0.15	0.24	0.18	0.27
	4	235	4.3	40	11.3	*14.8*	*2.53*	0.17	0.25	0.20	0.28
	5	235	4.3	40	11.3	*14.6*	*2.56*	0.16	0.25	0.20	0.28
106	2	220	4.3	28	8.0	**16.5**	**1.44**	0.20	0.37	0.24	0.41
	3	245	4.3	28	8.0	**19.8**	**1.20**	0.27	0.44	0.32	0.49
	4	255	4.3	28	8.0	**21.0**	**1.13**	0.30	0.47	0.36	0.53
	5	250	4.3	28	8.0	**20.9**	**1.14**	0.30	0.46	0.36	0.52
107	2	240	4.3	30	8.6	**18.3**	**1.41**	0.24	0.40	0.28	0.45
	3	270	4.3	30	8.6	**21.0**	**1.23**	0.30	0.47	0.36	0.53
	4	280	4.3	30	8.6	**22.5**	**1.14**	0.34	0.50	0.40	0.57
	5	285	4.3	30	8.6	**23.6**	**1.09**	0.37	0.53	0.44	0.61
108	1	275	4.3	32	9.1	**21.4**	**1.30**	0.31	0.48	0.37	0.54
	2	265	4.3	32	9.1	**20.4**	**1.36**	0.28	0.45	0.34	0.51
	3	275	4.3	32	9.1	**21.6**	**1.29**	0.31	0.48	0.38	0.55
	4	290	4.3	32	9.1	**23.0**	**1.21**	0.35	0.52	0.42	0.59
	5	305	4.3	32	9.1	**25.2**	**1.11**	0.41	0.58	0.49	0.66
109	1	295	4.3	34	9.7	**23.2**	**1.30**	0.35	0.52	0.43	0.59
	2	290	4.3	34	9.7	**22.3**	**1.35**	0.33	0.50	0.40	0.57
	3	300	4.3	34	9.7	**24.0**	**1.25**	0.38	0.55	0.45	0.62
	4	305	4.3	34	9.7	**23.9**	**1.26**	0.37	0.54	0.45	0.62
	5	325	4.3	34	9.7	**26.2**	**1.15**	0.44	0.60	0.52	0.69
110	1	320	4.3	36	10.3	**24.6**	**1.33**	0.39	0.56	0.47	0.64
	2	310	4.3	36	10.3	**23.6**	**1.38**	0.37	0.54	0.44	0.61

Table 4 (Cont…) - Predicted Maximum Chain Pillar Subsidence for Modified LW 101 to 120 based on the DgS Modified ACARP, 2003 Empirical Model

LW	XL	Cover Depth, H (m)	Mining Height T (m)	Chain Pillar Width w (m)	Pillar w/h	Chain Pillar Stress* (MPa)	Pillar FoS under DA or SA Loading Conditions	Chain Pillar Subsidence			
								Sp First (m)		Sp Final (m)	
								mean	U95%	mean	U95%
110	3	330	4.3	36	10.3	**26.3**	**1.24**	0.44	0.61	0.53	0.70
	4	320	4.3	36	10.3	**26.1**	**1.25**	0.43	0.60	0.52	0.69
	5	335	4.3	36	10.3	**26.7**	**1.22**	0.45	0.62	0.54	0.71
112	6	355	4.3	36	10.3	**28.3**	**1.15**	0.49	0.66	0.59	0.76
	7	340	4.3	36	10.3	**25.7**	**1.27**	0.42	0.59	0.51	0.67
	8	355	4.3	36	10.3	**27.3**	**1.19**	0.47	0.63	0.56	0.73
	9	360	4.3	36	10.3	**28.2**	**1.16**	0.49	0.66	0.59	0.76
	10	355	4.3	36	10.3	**28.1**	**1.16**	0.49	0.65	0.58	0.75
113	6	350	4.3	34	9.7	**28.0**	**1.08**	0.48	0.65	0.58	0.75
	7	320	4.3	34	9.7	**24.6**	**1.23**	0.39	0.56	0.47	0.64
	8	330	4.3	34	9.7	**24.9**	**1.21**	0.40	0.57	0.48	0.65
	9	340	4.3	34	9.7	**26.7**	**1.13**	0.45	0.62	0.54	0.71
	10	345	4.3	34	9.7	**27.3**	**1.10**	0.47	0.63	0.56	0.73
114	6	330	4.3	32	9.1	**26.2**	**1.06**	0.44	0.60	0.52	0.69
	7	310	4.3	32	9.1	**24.6**	**1.13**	0.39	0.56	0.47	0.64
	8	300	4.3	32	9.1	**22.4**	**1.24**	0.33	0.50	0.40	0.57
	9	320	4.3	32	9.1	**24.4**	**1.14**	0.39	0.56	0.47	0.63
	10	325	4.3	32	9.1	**25.5**	**1.09**	0.42	0.59	0.50	0.67
115	6	305	4.3	32	9.1	**22.6**	**1.23**	0.34	0.51	0.41	0.57
	7	305	4.3	32	9.1	**22.6**	**1.23**	0.34	0.51	0.41	0.57
	8	275	4.3	32	9.1	**19.2**	**1.45**	0.26	0.43	0.31	0.48
	9	285	4.3	32	9.1	**20.4**	**1.37**	0.28	0.45	0.34	0.51
	10	300	4.3	32	9.1	**22.6**	**1.23**	0.34	0.51	0.41	0.58
116	6	270	4.3	32	9.1	**18.3**	**1.52**	0.24	0.40	0.28	0.45
	7	270	4.3	32	9.1	**18.7**	**1.49**	0.24	0.41	0.29	0.46
	8	245	4.3	32	9.1	**16.3**	**1.70**	0.20	0.28	0.23	0.32
	9	255	4.3	32	9.1	**17.0**	**1.63**	0.21	0.29	0.25	0.34
	10	280	4.3	32	9.1	**19.6**	**1.42**	0.27	0.43	0.32	0.49
117	6	230	4.3	32	9.1	**14.5**	**1.92**	0.16	0.25	0.19	0.28
	7	240	4.3	32	9.1	**15.3**	**1.82**	0.18	0.26	0.21	0.30
	8	225	4.3	32	9.1	**14.3**	**1.95**	0.16	0.24	0.19	0.27
	9	225	4.3	32	9.1	**14.5**	**1.93**	0.16	0.25	0.19	0.28
	10	245	4.3	32	9.1	**16.3**	**1.70**	0.20	0.28	0.23	0.32
118	6	200	4.3	32	9.1	**9.3**	**2.98**	0.09	0.18	0.11	0.19
	7	205	4.3	32	9.1	**9.7**	**2.88**	0.10	0.18	0.11	0.20
	8	205	4.3	32	9.1	**12.5**	**2.22**	0.13	0.22	0.16	0.24
	9	210	4.3	32	9.1	**13.2**	**2.12**	0.14	0.22	0.17	0.25
	10	225	4.3	32	9.1	**14.5**	**1.93**	0.16	0.25	0.19	0.28
119	8	190	4.3	32	9.1	**11.3**	**2.46**	0.11	0.20	0.14	0.22
	9	200	4.3	32	9.1	**12.2**	**2.28**	0.13	0.21	0.15	0.24
	10	210	4.3	32	9.1	**13.3**	**2.09**	0.14	0.23	0.17	0.26

italics - DA = Double abutment loading conditions.

bold - SA = Single abutment loading conditions.

* - The chain pillars referred to in the above table are on the Maingate side or leading goaf edge for a given LW. Predictions for the end panels 111 and 120 are therefore not applicable to the assessment.

h = Pillar height = 3.5 m.

The predicted First Subsidence over the chain pillars (S_p) between the extracted panels 101 to 120 is estimated to range from 0.08 m to 0.66 m for the range of pillar sizes and geometries proposed. The Final Subsidence over the chain pillars (after mining is completed) is estimated to range from 0.10 m to 0.76 m (an increase of approximately 20% above the First Subsidence).

The vertical stress acting on the pillars are estimated to range from 9.4 to 28.3 MPa with pillar FoS values of 3.20 to 1.09 estimated for a 3.5 m pillar height. The FoS is used in the empirical model to estimate the error band or U95%CL setting as follows:

- for cases with FoS ≥ 1.6, U95%CL error = 0.024T

- for cases with FoS < 1.6, U95%CL error = 0.048T

7.3.4 Bearing Capacity of Roof and Floor Strata

The bearing capacity of the roof/floor strata and chain pillar strength was firstly checked before appropriate rock mass Young's Modulii values were assigned for subsidence prediction under the assessed loading conditions.

Reference to **Pells *et al*, 1998** indicates that the bearing capacity of sedimentary rock under shallow footing type loading conditions is 3 to 5 times its UCS strength. Based on the estimated range of UCS values of 31 MPa and 33 MPa in the immediate floor and roof strata respectively, the general bearing capacity of the strata is estimated to range between 93 and 165 MPa.

The estimated pillar stresses of 9.4 MPa to 28.3 MPa gives a FoS range (based on the maximum pillar stress) of 3.2 to 5.8, which indicates that the roof and floor strata are likely to behave elastically over the majority of the site.

7.4 Goaf Edge Subsidence Prediction

Based on the modified **ACARP, 2003** model (see **Figure 7**) the U95%CL goaf edge subsidence predictions of 0.09 to 0.36 m for LW101 to 120 have been derived from the prediction curves shown in **Figure 10a** and the maximum final panel subsidence range (see **Section 7.6**).

The measured results presented in **Table 2B** for LW101 to 104 are also shown in **Figure 10a** for model validation purposes.

7.5 Angle of Draw Prediction

Reference to the **ACARP, 2003**, longwall panel angle of draw predictions have been derived from the U95%CL goaf edge subsidence predictions.

The U95%CL AoD to the 20 mm subsidence contour are estimated to range from 22.7^o to 33.2^o for the LW101 to 120, based on the empirical model presented in **Figure 10b**.

The measured results presented in **Table 2B** for LW101 to 104 are also shown in **Figure 10b** for model validation purposes.

7.6   Multiple Panel Subsidence Prediction

Based on the predicted maximum single panel, chain pillar and goaf edge subsidence values derived from the **ACARP, 2003** model, the mean and worst-case first and final maximum multi-panel subsidence predictions (and associated impact parameters) are summarised in **Table 5** for representative cross lines (XLs 1 to 10) the proposed LW 101 to 120.

As mentioned earlier, the review of measured subsidence, tilt and strain above LW 101 to 104 has resulted in the previous assumption that supercritical subsidence effectively occurred at 1.4H to be reduced to 1.2H.

The mean and U95%CL values for tilt and strain now also represent continuous and discontinuous strata behaviour respectively. This supersedes the previous requirement to multiple the U95% values by 2 times or the mean values by 4 times to estimate the later scenario.

If the model has been calibrated correctly, the measured tilts and strains should not be exceeded by more than 1.2 and 1.5 times the U95%CL values respectively. The exceedance frequency should also be < 5% of the predictions made (i.e. occasionally).

In regards to the subsidence predictions, the measured subsidence should not exceed the U95%CL values by more than 15%.

Table 5 - Predicted First and Final Maximum Subsidence Effects for LW 101 to 120 (Mean - Upper 95% Confidence Limits)

LW Panel #	Cross Line #	Cover Depth H (m)	Panel Width W (m)	Mining Height T (m)	W/H Ratio	Maingate Chain Pillar Width w_{cp} (m)	First S_{max} (m) mean	First S_{max} (m) U95	Final S_{max} (m) mean	Final S_{max} (m) U95	First Pillar S_p (m) mean	First Pillar S_p (m) U95	Final Pillar S_p (m) mean	Final Pillar S_p (m) U95	Max Tilt T_{max} (mm/m) mean	Max Tilt T_{max} (mm/m) U95	E_{max} tensile mean	E_{max} tensile U95	E_{max} compressive mean	E_{max} compressive U95
101	3	165	306.5	*4.2*	1.86	*29.8*	2.44	2.52	2.52	2.56	0.18	0.26	0.21	0.30	46	68	10	25	13	32
	4	165	306.5	*4.2*	1.86	*29.8*	2.44	2.52	2.52	2.56	0.17	0.25	0.20	0.29	46	68	10	25	13	32
	5	177	306.5	*4.2*	1.73	*29.8*	2.48	2.52	2.52	2.56	0.21	0.37	0.25	0.42	41	62	9	22	11	28
102	3	180	306.5	4.2	1.70	*29.8*	2.49	2.56	2.69	2.69	0.12	0.20	0.14	0.23	41	61	9	21	11	27
	4	175	306.5	4.2	1.75	*29.8*	2.49	2.55	2.69	2.69	0.11	0.20	0.14	0.22	43	64	9	22	11	29
	5	188	306.5	4.2	1.63	*29.8*	2.50	2.57	2.69	2.69	0.13	0.21	0.15	0.24	39	58	8	20	10	25
103	3	195	306.5	4.3	1.57	*35*	2.54	2.61	2.75	2.75	0.12	0.20	0.14	0.23	37	56	7	18	9	24
	4	195	306.5	4.3	1.57	*35*	2.54	2.61	2.75	2.75	0.12	0.21	0.15	0.23	38	56	7	18	9	24
	5	200	306.5	4.3	1.53	*35*	2.51	2.59	2.75	2.75	0.13	0.21	0.15	0.24	36	54	7	17	9	22
104	2	180	306.5	4.3	1.70	*35*	2.54	2.59	2.75	2.75	0.11	0.19	0.13	0.21	42	63	9	22	11	27
	3	205	306.5	4.3	1.50	*35*	2.48	2.57	2.71	2.75	0.14	0.22	0.17	0.25	34	51	7	17	8	21
	4	215	306.5	4.3	1.43	*35*	2.44	2.54	2.67	2.75	0.15	0.24	0.18	0.27	31	47	6	15	8	19
	5	215	306.5	4.3	1.43	*35*	2.44	2.55	2.67	2.75	0.15	0.24	0.18	0.27	31	47	6	15	8	19
105	2	200	306.5	4.3	1.53	*39.5*	2.50	2.57	2.74	2.75	0.12	0.20	0.14	0.23	35	53	7	17	9	22
	3	225	306.5	4.3	1.36	*39.5*	2.38	2.49	2.61	2.72	0.15	0.24	0.18	0.27	28	43	5	13	7	17
	4	235	306.5	4.3	1.31	*39.5*	2.35	2.47	2.59	2.70	0.17	0.25	0.20	0.28	26	40	5	12	6	15
	5	235	306.5	4.3	1.31	*39.5*	2.35	2.47	2.59	2.70	0.16	0.25	0.20	0.28	26	39	5	12	6	15
106	2	220	306.5	4.3	1.39	**28**	2.41	2.57	2.68	2.75	0.20	0.37	0.24	0.41	31	46	6	14	7	18
	3	245	306.5	4.3	1.25	**28**	2.33	2.55	2.60	2.75	0.27	0.44	0.32	0.49	26	39	5	11	6	15
	4	255	306.5	4.3	1.20	**28**	2.31	2.57	2.58	2.75	0.30	0.47	0.36	0.53	25	37	4	11	5	14
	5	250	306.5	4.3	1.23	**28**	2.32	2.57	2.59	2.75	0.30	0.46	0.36	0.52	26	38	4	11	6	14
107	2	240	408.9	4.3	1.70	**30**	2.58	2.71	2.75	2.75	0.24	0.40	0.28	0.45	29	44	5	13	6	16
	3	270	408.9	4.3	1.51	**30**	2.58	2.71	2.75	2.75	0.30	0.47	0.36	0.53	25	37	4	10	5	13
	4	280	408.9	4.3	1.46	**30**	2.58	2.71	2.75	2.75	0.34	0.50	0.40	0.57	23	35	4	9	5	12
	5	285	408.9	4.3	1.43	**30**	2.58	2.71	2.75	2.75	0.37	0.53	0.44	0.61	23	34	4	9	5	11
108	1	275	408.9	4.3	1.49	**32**	2.54	2.71	2.75	2.75	0.31	0.48	0.37	0.54	24	36	4	10	5	12
	2	265	408.9	4.3	1.54	**32**	2.58	2.71	2.75	2.75	0.28	0.45	0.34	0.51	25	38	4	10	5	13

Table 5 (Cont…) - Predicted First and Final Maximum Subsidence Effects for LW 101 to 120 (Mean - Upper 95% Confidence Limits)

LW Panel #	Cross Line #	Cover Depth H (m)	Panel Width W (m)	Mining Height T (m)	W/H Ratio	Maingate Chain Pillar Width w_{cp} (m)	First S_{max} (m)		Final S_{max} (m)		First Pillar S_p (m)		Final Pillar S_p (m)		Max Tilt* T_{max} (mm/m)		Maximum Strain* E_{max} (mm/m)			
																	tensile		compressive	
							mean	U95	mean	U95	mean	U95	mean	U95	mean	U95	mean	U95	mean	U95
108	3	275	408.9	4.3	1.49	**32**	2.58	2.71	2.75	2.75	0.31	0.48	0.38	0.55	24	36	4	10	5	12
	4	290	408.9	4.3	1.41	**32**	2.58	2.71	2.75	2.75	0.35	0.52	0.42	0.59	22	33	3	9	4	11
	5	305	408.9	4.3	1.34	**32**	2.58	2.71	2.75	2.75	0.41	0.58	0.49	0.66	21	31	3	8	4	10
109	1	295	408.9	4.3	1.39	**34**	2.58	2.71	2.75	2.75	0.35	0.52	0.43	0.59	22	33	3	8	4	11
	2	290	408.9	4.3	1.41	**34**	2.58	2.71	2.75	2.75	0.33	0.50	0.40	0.57	22	33	3	9	4	11
	3	300	408.9	4.3	1.36	**34**	2.58	2.71	2.75	2.75	0.38	0.55	0.45	0.62	21	32	3	8	4	10
	4	305	408.9	4.3	1.34	**34**	2.58	2.71	2.75	2.75	0.37	0.54	0.45	0.62	21	31	3	8	4	10
	5	325	408.9	4.3	1.26	**34**	2.55	2.71	2.75	2.75	0.44	0.60	0.52	0.69	19	28	3	7	4	9
110	1	320	408.9	4.3	1.28	**36**	2.55	2.71	2.75	2.75	0.39	0.56	0.47	0.64	19	29	3	7	4	9
	2	310	408.9	4.3	1.32	**36**	2.58	2.71	2.75	2.75	0.37	0.54	0.44	0.61	20	30	3	8	4	10
	3	330	408.9	4.3	1.24	**36**	2.52	2.71	2.75	2.75	0.44	0.61	0.53	0.70	18	28	3	7	3	9
	4	320	408.9	4.3	1.28	**36**	2.56	2.71	2.75	2.75	0.43	0.60	0.52	0.69	19	29	3	7	4	9
	5	335	408.9	4.3	1.22	**36**	2.53	2.71	2.75	2.75	0.45	0.62	0.54	0.71	18	27	3	7	3	8
111	1	330	408.9	4.3	1.24	**36**	2.53	2.69	2.75	2.75	n.a	n.a	n.a	n.a	18	27	3	7	3	8
	2	325	408.9	4.3	1.26	**36**	2.53	2.71	2.75	2.75	n.a	n.a	n.a	n.a	19	28	3	7	4	9
	3	350	408.9	4.3	1.17	**36**	2.47	2.66	2.70	2.75	n.a	n.a	n.a	n.a	17	26	2	6	3	8
	4	360	408.9	4.3	1.14	**36**	2.43	2.64	2.66	2.75	n.a	n.a	n.a	n.a	17	25	2	6	3	8
	5	350	408.9	4.3	1.17	**36**	2.48	2.67	2.71	2.75	n.a	n.a	n.a	n.a	17	26	2	6	3	8
112	6	355	408.9	4.3	1.15	**36**	2.29	2.71	2.57	2.75	0.49	0.66	0.59	0.76	18	26	3	6	3	8
	7	340	408.9	4.3	1.20	**36**	2.34	2.71	2.62	2.75	0.42	0.59	0.51	0.67	18	26	3	6	3	8
	8	355	408.9	4.3	1.15	**36**	2.29	2.71	2.57	2.75	0.47	0.63	0.56	0.73	18	26	3	6	3	8
	9	360	408.9	4.3	1.14	**36**	2.28	2.71	2.55	2.75	0.49	0.66	0.59	0.76	18	26	3	6	3	8
	10	355	408.9	4.3	1.15	**36**	2.29	2.71	2.57	2.75	0.49	0.65	0.58	0.75	18	26	3	6	3	8
113	6	350	408.9	4.3	1.17	**34**	2.50	2.71	2.75	2.75	0.48	0.65	0.58	0.75	18	26	3	6	3	8
	7	320	408.9	4.3	1.28	**34**	2.58	2.71	2.75	2.75	0.39	0.56	0.47	0.64	19	29	3	7	4	9
	8	330	408.9	4.3	1.24	**34**	2.56	2.71	2.75	2.75	0.40	0.57	0.48	0.65	18	28	3	7	3	9

Table 5 (Cont…) - Predicted First and Final Maximum Subsidence Effects for LW 101 to 120 (Mean - Upper 95% Confidence Limits)

LW Panel #	Cross Line #	Cover Depth H (m)	Panel Width W (m)	Mining Height T (m)	W/H Ratio	Maingate Chain Pillar Width w_{cp} (m)	First S_{max} (m)		Final S_{max} (m)		First Pillar S_p (m)		Final Pillar S_p (m)		Max Tilt* T_{max} (mm/m)		Maximum Strain* E_{max} (mm/m)			
																	tensile		compressive	
							mean	U95	mean	U95	mean	U95	mean	U95	mean	U95	mean	U95	mean	U95
113	9	340	408.9	4.3	1.20	**34**	2.53	2.71	2.75	2.75	0.45	0.62	0.54	0.71	18	26	3	6	3	8
	10	345	408.9	4.3	1.19	**34**	2.51	2.71	2.75	2.75	0.47	0.63	0.56	0.73	18	26	3	6	3	8
114	6	330	408.9	4.3	1.24	**32**	2.57	2.71	2.75	2.75	0.44	0.60	0.52	0.69	18	28	3	7	3	9
	7	310	408.9	4.3	1.32	**32**	2.58	2.71	2.75	2.75	0.39	0.56	0.47	0.64	20	30	3	8	4	10
	8	300	408.9	4.3	1.36	**32**	2.58	2.71	2.75	2.75	0.33	0.50	0.40	0.57	21	32	3	8	4	10
	9	320	408.9	4.3	1.28	**32**	2.58	2.71	2.75	2.75	0.39	0.56	0.47	0.63	19	29	3	7	4	9
	10	325	408.9	4.3	1.26	**32**	2.58	2.71	2.75	2.75	0.42	0.59	0.50	0.67	19	28	3	7	4	9
115	6	305	408.9	4.3	1.34	**32**	2.58	2.71	2.75	2.75	0.34	0.51	0.41	0.57	21	31	3	8	4	10
	7	305	408.9	4.3	1.34	**32**	2.58	2.71	2.75	2.75	0.34	0.51	0.41	0.57	21	31	3	8	4	10
	8	275	408.9	4.3	1.49	**32**	2.58	2.71	2.75	2.75	0.26	0.43	0.31	0.48	24	36	4	10	5	12
	9	285	408.9	4.3	1.43	**32**	2.58	2.71	2.75	2.75	0.28	0.45	0.34	0.51	23	34	4	9	5	11
	10	300	408.9	4.3	1.36	**32**	2.58	2.71	2.75	2.75	0.34	0.51	0.41	0.58	21	32	3	8	4	10
116	6	270	408.9	4.3	1.51	**32**	2.58	2.71	2.75	2.75	0.24	0.40	0.28	0.45	25	37	4	10	5	13
	7	270	408.9	4.3	1.51	**32**	2.58	2.71	2.75	2.75	0.24	0.41	0.29	0.46	25	37	4	10	5	13
	8	245	408.9	4.3	1.67	**32**	2.58	2.71	2.75	2.75	0.20	0.28	0.23	0.32	28	43	5	12	6	16
	9	255	408.9	4.3	1.60	**32**	2.58	2.71	2.75	2.75	0.21	0.29	0.25	0.34	27	40	4	11	6	14
	10	280	408.9	4.3	1.46	**32**	2.58	2.71	2.75	2.75	0.27	0.43	0.32	0.49	23	35	4	9	5	12
117	6	230	408.9	4.3	1.78	**32**	2.58	2.70	2.75	2.75	0.16	0.25	0.19	0.28	31	46	5	14	7	18
	7	240	408.9	4.3	1.70	**32**	2.58	2.71	2.75	2.75	0.18	0.26	0.21	0.30	29	44	5	13	6	16
	8	225	408.9	4.3	1.82	**32**	2.58	2.69	2.75	2.75	0.16	0.24	0.19	0.27	32	48	6	14	7	18
	9	225	408.9	4.3	1.82	**32**	2.58	2.69	2.75	2.75	0.16	0.25	0.19	0.28	32	48	6	14	7	18
	10	245	408.9	4.3	1.67	**32**	2.58	2.71	2.75	2.75	0.20	0.28	0.23	0.32	28	43	5	12	6	16
118	6	200	408.9	4.3	2.04	**32**	2.58	2.61	2.75	2.75	0.09	0.18	0.11	0.19	36	54	7	18	9	22
	7	205	408.9	4.3	1.99	**32**	2.58	2.62	2.75	2.75	0.10	0.18	0.11	0.20	35	53	7	17	9	21
	8	205	408.9	4.3	1.99	**32**	2.58	2.66	2.75	2.75	0.13	0.22	0.16	0.24	36	54	7	17	9	22
	9	210	408.9	4.3	1.95	**32**	2.58	2.67	2.75	2.75	0.14	0.22	0.17	0.25	35	52	7	16	8	21
	10	225	408.9	4.3	1.82	**32**	2.58	2.69	2.75	2.75	0.16	0.25	0.19	0.28	32	48	6	14	7	18

Table 5 (Cont…) - Predicted First and Final Maximum Subsidence Effects for LW 101 to 120 (Mean - Upper 95% Confidence Limits)

LW Panel #	Cross Line #	Cover Depth H (m)	Panel Width W (m)	Mining Height T (m)	W/H Ratio	Maingate Chain Pillar Width w_{cp} (m)	First S_{max} (m)		Final S_{max} (m)		First Pillar S_p (m)		Final Pillar S_p (m)		Max Tilt* T_{max} (mm/m)		Maximum Strain* E_{max} (mm/m)			
																	tensile		compressive	
							mean	U95	mean	U95	mean	U95	mean	U95	mean	U95	mean	U95	mean	U95
119	8	190	408.9	4.3	2.15	**32**	2.56	2.62	2.75	2.75	0.11	0.20	0.14	0.22	39	59	8	20	10	25
	9	200	408.9	4.3	2.04	**32**	2.57	2.64	2.75	2.75	0.13	0.21	0.15	0.24	37	55	7	18	9	23
	10	210	408.9	4.3	1.95	**32**	2.58	2.67	2.75	2.75	0.14	0.23	0.17	0.26	35	52	7	16	8	21
120	8	180	408.9	4.3	2.27	**32**	2.56	2.57	2.75	2.75	n.a	n.a	n.a	n.a	41	62	9	21	11	27
	9	190	408.9	4.3	2.15	**32**	2.56	2.59	2.75	2.75	n.a	n.a	n.a	n.a	38	58	8	19	10	25
	10	205	408.9	4.3	1.99	**32**	2.57	2.61	2.75	2.75	n.a	n.a	n.a	n.a	35	52	7	17	9	21

* - Predicted tilt and strains include 'smooth' profile (mean values) and 95% of the discontinuous profile (U95%CL values). Subsidence, tilt and strain measurements may exceed the predicted U95%CL values by up to 1.15, 1.2 and 1.5 times respectively 5% of the time (i.e. occasionally); *italics* - one row of Maingate chain pillars; **bold** - two rows of Maingate chain pillars of width shown.

The predicted mean and credible worst-case (U95%CL[2]) subsidence effect results for LW 101 to 120 are summarised below:

- **First maximum panel subsidence** ranges from 2.28 m to 2.75 m (53% to 64%T).

- **Final maximum panel subsidence** ranges from 2.47 m to 2.75 m (57% to 64%T).

- **Final maximum chain pillar subsidence** ranges from 0.11 m to 0.76 m (3% to 18%T)

- **Final maximum panel tilt** ranges from 17 to 46 millimetres per metre (mm/m) for 'smooth' profile behaviour and from 25 to 68 mm/m due to discontinuous movements.

- **Final maximum panel concave curvatures** range from 0.3 to 3.2 km^{-1} (radii of curvature 3.2 km to 0.45 km).

- **Final maximum panel convex curvatures** range from 0.4 to 2.5 km^{-1} (radii of curvature 4 km to 0.4 km).

- **Final maximum panel compressive strains** range from 3 to 13 mm/m for 'smooth' profile behaviour and from 8 to 32 mm/m due to discontinuous movements.

- **Final maximum panel tensile strains** range from 2 to 10 mm/m for 'smooth' profile behaviour and from 6 to 25 mm/m due to discontinuous movements.

7.7   Modified Mining Layout v. 2009 EA Subsidence Effect Predictions

A comparison between the Modified mining layout and the 2009 EA subsidence effect predictions for the 'smooth' profile case are summarised in **Table 6**.

Overall, the Modified mining layout would not change the level of impact assessed in the EA or current extraction plan. However, based on a review of measured subsidence data for LW 101 to 104 and minor model input assumption and output definition changes (i.e. discontinuous strata behaviour effects are now included in the U95%CL values provided), the revised subsidence effect predictions are now marginally lower than the EA layout predictions (i.e. <20%).

The impact of the increased subsidence predictions will be discussed in **Section 9**.

---

[2]   Note: The predicted U95%CL values may be exceeded occasionally (<5% of the time) due to local discontinuous strata movements associated with geological structure or topographic interaction.

Table 6 - Comparison of Proposed LW 101 - 120 Mining Geometries and Predicted Subsidence Effects with Values Presented in the 2009 EA Report

Parameter	EA Report (refer DgS, 2009)	Modified Mining Layout (this study)	
	LW 1 - 26	LW 101 - 106	LW 107-120
Panel Width, W (m)	305	306.8	408.9
Cover Depth, H (m)	165 - 360	165 - 255	180 - 360
Mining Height (T)	4.2	4.2 - 4.3	4.3
Chain Pillar Width (w)	24.6 - 37.6	29.8 - 39.5	29.8 - 39.5
W/H	1.85 - 0.95	1.86 - 1.20	1.70 - 1.14
Final Maximum Subsidence (m)	2.44	2.56 - 2.75	2.75
Maximum Tilt (mm/m)*	30 (45) - 45 (68)	25 (37) - 45 (68)	17 (25) - 41 (62)
Maximum Tensile Strain (mm/m)*	4 (8) - 11 (22)	6 (11) - 13 (25)	3 (6) - 11 (21)
Maximum Compressive Strain (mm/m)*	8 (16) - 14 (28)	7 (14) - 16 (32)	4 (8) - 14 (27)
Final Chain Pillar Subsidence (m)	0.51 - 1.32	0.21 - 0.53	0.19 - 0.76
Final Goaf edge Subsidence (m)	0.22 - 0.59	0.13 - 0.32	0.09 - 0.36
Final Angle of Draw (o)	26.5 - 31	25.3 - 32.2	22.7 - 33.2

* - Predicted tilts and strains for 'smooth' subsidence profiles. Cracking or discontinuous displacements may cause the 'smooth' profile tilt and strain values to increase by 1.5 to 2 times respectively (bracketed values).

The results indicate the following changes to subsidence effect predictions due to the Modified mining layout compared to the values provided in the 2009 EA:

- Maximum subsidence is expected to increase by approximately 13%.

- Maximum tilt and strain have changed by +/- 15% due to model and mining geometry changes based on measured results.

- Maximum goaf edge and angle of draw predictions have changed by +/- 20% due to model and mining geometry changes based on measured results.

It should be noted that the tilt and strain prediction models are based on power rule relationships between the ratio of measured subsidence/panel width[n] (as identified in **ACARP, 2003**). Net increases in panel width v. subsidence ratios can therefore result in a *decrease* in tilt and strain over wider, *critical* longwalls (i.e. W/H < 1.2).

7.8 Subsidence Profile Predictions

For completeness, the predicted subsidence profiles for LW 101 to 111 panels for XL4 are presented on **Figures 11a** to **11c**.

The predicted subsidence profiles for LW 112 to 120 panels for XL9 are presented in **Figures 12a** to **12c**.

The subsidence effect profile predictions have been derived after (i) each panel is extracted and (ii) on the completion of mining. The profiles are based on U95%CL panel subsidence and 'mean' chain pillar subsidence values, to be consistent with previous assessments of worst-case scenarios in the EA.

8.0 Prediction of Subsidence Impact Parameter Contours

8.1 Calibration of SDPS 3D-Influence Function Model

Credible worst-case subsidence contours for the extended mining layout have been derived using the **SDPS®** program from the predicted subsidence profiles along XLs 1 to 10. The **SDPS®** model was calibrated to the predicted subsidence profiles to within 10%.

The outcome of the SDPS model calibration exercise is summarised in **Table 7**

Table 7 - SDPS® Model Calibration Summary

Input Parameters	Value
Panel No. (refer to **Figures 1b** and **1c**)	101-120
Panel Void Width, W (m)	306.5 - 408.9
Cover Depth, H (m)	165 - 360
Mining Height, T (m)	4.2 to 4.3
W/H range	1.20 - 1.86
SRP for Mining Area	Low
Maximum Final Panel Subsidence Range, S_{max}(m)	2.69 - 2.75
S_{max}/T Range for Panels	0.63 - 0.64
Chain Pillar Widths (m)	29.8 - 39.5
Gate road Heading and Cut-through Widths (m)	5.4
Chain Pillar Subsidence (m)	0.21 - 0.54
Modified **ACARP, 2003** Inflection Point Location (d) from Rib-side/Cover Depth (H): d/H	0.30 - 0.31
Modified **ACARP, 2003** Inflection Point Location from Rib-side, d (m)	65 – 90
Calibration Results for Best Fit Solution to the Modified ACARP, 2003 Model Predictions[^]	**Optimum Value**
Influence Angle (tan(beta))	1.5 - 2.0*
Influence Angle (degrees)	56.3 - 63.4*
Angle of Draw (degrees)	33.7 - 26.6*
Supercritical Subsidence Factor for Panels and Pillars (S_{max}/T)	63.0 - 83.7*
Mean Distance to Inflexion Point from Rib-Sides (m)	50 - 107*

[^] - See SDPS manual extract in Appendix A of **DgS, 2012** for explanation of methodology and terms used.
* - These values provide best fit to Modified **ACARP, 2003** profiles only and are due to the effect of calibrating SDPS to multiple panels with compressing chain pillars (i.e. they should not be used other than for SDPS input values).

Representative SDPS v. ACARP model outcomes are presented in **Figures 13a** to **13c** for subsidence, tilt and strain profiles along XL 4. Similarly, **Figures 13a** to **13c** show SDPS v. ACARP model outcomes for XL 9.

The predicted **SDPS®** subsidence and tilt profiles were generally located within +/- 10% of the predicted modified **ACARP, 2003** model. This outcome is considered a reasonable fit considering that the **ACARP, 2003** profiles represent measured tilt profiles that are invariably affected by 'skewed' or kinked subsidence profiles.

The results of the analysis indicate that the majority of the predicted tensile and compressive **SDPS**® strains fell within +/- 50% of the modified **ACARP, 2003** model predictions. This result is also considered reasonable in the context that the **ACARP, 2003** model represents measured profile data that includes strain concentration effects such as cracking and shearing.

As mentioned earlier, this 'discontinuous' type of overburden behaviour can increase 'smooth' profile strains by 2 to 4 times locally. The predicted worst-case subsidence effects provided in this study should encapsulate approximately 95% of the measured values if the model is calibrated to a representative range of data for a given mining geometry in similar geological conditions.

8.2   Predicted Subsidence Effect Contours

Based on the calibrated SDPS® model, predictions of final subsidence contours for the northern LW 101 to 111 are shown in **Figure 15a**. Associated final subsidence effect contours (principal tilt and horizontal strain) have been subsequently derived using the calculus module provided in **Surfer12**® and the predicted final subsidence contours. The outcomes are shown in **Figures 15b** and **15c**.

Predictions of final subsidence effect contours for the southern LW 112 to 120 are shown in **Figures 16a** to **16c**.

The pre and post-mining surface levels above the northern and southern longwalls have also been generated from the final subsidence contours and are shown in **Figures 17a** and **17b** respectively.

Predicted impacts to the natural and built surface features due to the subsidence effect contours mentioned above are assessed in **Section 9**.

9.0 Subsidence Impacts

9.1 General

Due to the uncertainties associated with mine subsidence prediction for a given mining geometry and geology, a credible range of impact outcomes (based on probabilistic design methodologies) have been provided to assist with the development of effective subsidence management plans for the existing site features.

Discussions of likelihood of impact occurrence in the following sections generally refer to the qualitative measures of likelihood described in **Table 8**, and are based on probabilistic terms used in **AGS, 2010** and **Vick, 2002**.

Table 8 - Qualitative Measures of Likelihood

Likelihood of Occurrence	Event implication	Indicative relative probability of a single event
Almost Certain	The event is expected to occur.	90-99%
Very Likely	The event is expected to occur, although not completely certain.	75-90%
Likely[+]	The event will probably occur under normal conditions.	50-75%
Possible	The event may occur under normal conditions.	10-50%
Unlikely*	The event is conceivable, but only if adverse conditions are present.	5-10%
Very Unlikely	The event probably will not occur, even if adverse conditions are present.	1-5%
Not Credible	The event is inconceivable or practically impossible, regardless of the conditions.	<1%

Notes:
+ - Equivalent to the mean or line-of-best fit regression lines for a given impact parameter presented in **ACARP, 2003**.
* - Equivalent to the worst-case or U95%CL subsidence impact parameter in **ACARP, 2003**.

It should be also be understood that the terms 'mean' and 'CWC' used in this report generally infer that the predictions will be exceeded by 50% and 5% of panels mined with similar geometry and geology etc. Using lower probability of exceedance values (i.e. <5% probability of exceedance) may result in false-positives or potentially uneconomic mining layouts.

9.2   Surface Cracking

9.2.1   Predicted Effects and Impacts

The development of surface cracking above a longwall panel is caused by the bending of the overburden strata as it sags down into the newly created void in the coal seam. The sagging strata is supported by previously collapsed roof material (goaf), which then slowly compresses until maximum subsidence is reached.

The tensile fractures generally occur between the panel ribs and the point of inflexion, which is where convex curvatures and tensile strains will develop. The point of inflexion is assessed to be located 65 to 90 m from the panel ribs for the range of mining geometries proposed. Tensile fractures can also develop above chain pillars that are located between extracted panels. The compressive shear fractures or shoving zones will generally develop in the area above the longwall panel and inside the inflexion points.

Surface crack widths (in mm) have been estimated by multiplying the predicted tensile strains by 10 (and assuming a 10 m distance between survey pegs). The above crack width estimation method assumes all of the strain will concentrate at a single crack between the survey pegs. This can occur where near surface bedrock exists, but is more likely to develop as two or three smaller width cracks in deep alluvial soil profiles. Therefore, the crack widths are expected to be wider on ridges than along sandy-bottomed creek beds (generally).

Based on the predicted range of maximum transverse tensile strains (i.e. 2 to 25 mm/m) for cover depths of 160 m to 360 m, maximum surface cracking widths of between 20 mm to 250 mm may occur above the panels and within the limits of extraction.

It should be understood that the above crack widths are U95%CL values, which means that may be exceeded 5% of the time (by definition) due to adverse topographic or geological conditions. For example, it has been noted that in steep terrain around Newcastle, that the crack widths are increased (once they occur) in direct proportion to the measured tilts due to rigid body rotation of the subsided slope. Whilst this effect is unlikely to occur above LW 101 - 120 generally, the crack widths may exceed the predicted range near steep creek banks along the creeks and tributaries.

Based on reference to **ACARP, 2003**, the cracks will probably have developed by the time the longwall face has retreated past a given location for a distance equal to 1 to 2 times the cover depth. Cracks will usually develop within several days after a mine has retreated beneath a given location, with some of the cracks closing in the compression zone in the middle of the fully developed subsidence trough, together with new cracks developing in the tensile zones along and inside the panel sides several weeks later.

The cracks in the tensile strain zones will probably be tapered and extend to depths ranging from 5 to 10 m. Cracks within compressive strain zones are generally low-angle shear cracks caused by failure and shoving of near surface strata. Some tensile type cracks can also be present due to buckling and uplift of near surface rock, if it exists (see **Section 9.6**).

DgS

The cracks usually develop in groups of two or three over a tensile zone of 20 m in width. Once the cracks develop, the strain is usually relieved in the adjacent ground, however, the topography and near surface geology also can influence the extent of cracking.

Undermining ridges can also result in surface cracks migrating up-slope and outside the limits of extraction for significant distances due to rigid block rotations. This phenomenon will depend upon the slope angle, vertical jointing and the subsidence at the toe of the slope.

9.2.2   Review of Observed Surface Cracking

Reference to **NM, 2015** indicates that surface cracks observed above LW 101 to 104 have typically ranged from 50 mm to 100 mm wide, with some cracking up to 200 mm.

The measured cracks have therefore been within the predicted crack width ranges of between 40 mm and 220 mm in the current EP Report for LW 101 to 105. The revised cracking width range of 20 mm to 250 mm for LW 101 to 120 is therefore likely to be conservative.

9.2.3   Impact Management Strategies

The practical options available for controlling surface fracturing are (in order of increasing impact to mining):

* Regularly inspect the surface during subsidence development above a given panel and map crack locations and their widths in Autocad.

* Repair large surface cracks if they occur, but usually after subsidence development for a given longwall. *Note: Temporary fencing may be necessary before effective repairs can be completed.*

* Decrease mining height and/or panel width to limit subsidence and hence tensile strains; *Note: This option will require local subsidence and sub-surface monitoring data to make effective and reliable changes to the mining layout.*

* Leave a barrier pillar beneath a sensitive area or limit mining to first workings.

Surface crack repair works (such as ripping or ploughing and re-seeding or pouring gravel or grout into large, deep cracks) may need to be implemented around the affected areas of the lease, and in particular, any public (or private) access roads or ephemeral watercourses that do not infill naturally with sediment due to natural geomorphic processes.

9.3 Sub-Surface Cracking

9.3.1 Sub-Surface Fracturing Zones

As noted in **Li *et al*, 2006**, "the transmission of water through the overburden strata may [occur] via a number of mechanisms such as (i) inter-granular porosity, (ii) mining induced voids, fractures and strata dilation/bed separations and (iii) structural discontinuities / geological defects [faults and dykes]".

The void created by extracting coal invariably results in the collapse of the immediate roof strata which is subject to bending and shearing stresses as the overburden tries to span the void. The extent of fracturing and shearing up through the strata is dependent on mining geometry and overburden geology.

International and Australian research on longwall mining interaction with groundwater systems indicates that the overburden may be divided into essentially four or five zones of surface and subsurface fracturing; see **Figures 18a** and **18b**. The zones are based on the **Forster, 1995** and **ACARP, 2007** models and are defined (in descending order) as follows:

- Surface Zone (D-Zone) - Unconstrained

- Elastic Zone (C-Zone) - Constrained

- Discontinuous Fracture Zone (B-Zone) - Constrained

- Continuous Fracture Zone (A-Zone) - Unconstrained

- Caved Zone (included in the A-Zone) - Unconstrained

Further details of the sub-surface fracture mechanics, including the strain and permeability increases in the A, B and C-Zones is presented in **Appendix A**.

9.3.2 Sub-Surface Fracture Height and Constrained Zone Thickness Prediction Models

The prediction of connective subsurface fracture network heights above longwall panels over the past 40 years have been based on several simple empirical models that have allowed successful mining beneath permanent water bodies such as Lake Macquarie in the Newcastle Coalfield, water supply dams in the Southern Coalfield and relatively shallow depths of cover (< 150 m) below creeks and rivers without causing surface to seam or aquifer to seam connection.

Several instances of unanticipated cracking and drainage of near-surface alluvial and confined aquifers have occurred over the years in NSW (and internationally) however, and have led to further research into improving our understanding of the sub-surface crack development process and the height of fracture zone estimates above longwall and pillar extraction panels.

The research to-date has identified the following key parameters should be considered when making robust sub-surface fracture height predictions:

- Panel width (W)

- Mining height (T)

- Cover depth (H)

- Panel criticality (i.e. sub-critical or supercritical)

- Presence of massive sandstone or conglomerate strata that may control continuous fracture height development.

- Constrained Zone lithology and thickness required to control inter-connective cracking between surface and seam or aquifer and seam.

- Presence of geological structure (faults/dykes/joint swarms) that have an increased level of fracturing and therefore higher secondary conductivity.

Several of the current models in use in NSW consider only one or two of above parameters such as W or T because they were developed in a coalfield with a particular geometry and consistent geology, and generally provided satisfactory results. However, it is apparent that as mines are developed in other coalfields or mining geometries and/or geology changes within a coalfield, these models can significantly under-predict or over-predict the sub-surface fracture heights (if the key controlling factor or factors present at the new locations are no longer included in the simplified models).

All of the above factors have now been considered by DgS for the NM site using recently developed Pi-Term empirical models (**Ditton & Merrick, 2014**). The models have been validated to measured NSW case studies with a broad range of mining geometries and geological conditions. Details of the *Geometry* and *Geology* Pi-Term Model's development are presented further below and in **Attachment A**.

The Pi-term models are based on a conceptual model of the subsurface fracturing that develops above a longwall panel with varying mining geometry and geology; see **Figure 18c**. A database of measured (interpreted) heights of A and B-Zone fracturing have been linked to several dimensionless ratios of the key parameters mentioned above. Non-linear regression techniques have been applied to derive curves of best fit with a R^2 of 0.80 for the A-Zone and 0.86 for the B-Zone (using the Geology Pi-Term Model). The R^2 value for the Geometry Pi-Term model decreases to 0.61 (when no geological parameter included).

The conceptual model demonstrates that longwall panel geometries and overburden geology determine the height of 'continuous' and 'discontinuous' fracturing. Continuous fractures above the mine workings tend to form up into the overburden at an angle of 12° to 19° from the rib sides, based on physical and numerical modelling observations and subsidence data; see **Figure 18d**. The extent of vertical fractures above the mine workings (i.e. the A-Zone) will also be dependent on the effective strata thickness that either (i) spans the goaf or (ii) sags down onto it with limited fracturing through the 'beam'.

A review of measured heights of A-Zone fracturing and borehole data above longwall panels in NSW and Queensland Coalfields in **Ditton and Merrick, 2014** demonstrates the overburden develops an effective strata unit thicknesses (t') that limits the A-Zone at a given height above a longwall; see **Figure 18e**. The results indicate that the effective thickness of the strata units is influenced by the geology of the coalfield and the mining geometry. Ignoring this parameter may result in data base bias when applying the model in different coalfields. The t' may also be calibrated to local mine site data.

Continuous sub-surface fracture height predictions (A) for LW 101 to 106 have been made based on the following empirical prediction models from several NSW Coalfields:

- Geometry Pi-Term Model ($A = 2.215W'^{0.357} H'^{0.271}T^{0.372}$) (**Ditton and Merrick, 2014**)

- Geology Pi-Term Model ($A = 1.52W'^{0.4}H'^{0.535}T^{0.464} t'^{-0.4}$) (**Ditton and Merrick, 2014**)

- Panel Width-based model (A=1.0W - 1.5W) (**SCT, 2008**)

- Mining Height-based model (A= 21 - 33T) (**Forster, 1995**)

Details of the development of each model and their limitations are provided in **Appendix A.**

9.3.3   Geometry Pi-Term Model

The model was developed in 2013-14 in response to several Planning Assessment Commission concerns in regards to large apparent differences between established prediction methods that use only one parameter in a particular coalfield (eg the mining height v. panel void width models).

The Geometry Pi-Term model considers the influence of the panel width, cover depth and mining height on the height of continuous fracturing above a longwall panel. A dimensionally consistent product and power rule has been derived using non-linear regression analysis of measured cases. The model considers the key mining geometries and indirectly includes the influence of a wide range of geological conditions.

A-Zone Prediction Model:

The Pi-terms have been derived (by experiment) using Buckingham's Pi-term theorem and refer to the dimensionless ratios of key independent variables with a repeating variable of influence (the panel width) as follows:

$$\underline{\text{Mean } A/W' = 2.215 \ (H/W')^{0.271}(T/W')^{0.372}} \qquad\qquad R^2 = 0.61 \ (\text{rmse}=21\%)$$

$$\underline{\text{U95\%CL} \ \ A/W' = \text{Mean } A/W' + a}$$

where

a = 0.16 for *sub-critical*, 0.16 - 0.085(W/H-0.7) for *critical* and 0.1 for *supercritical* panels

H = cover depth = maximum potential goaf load height

W' = effective panel width = minimum of W and 1.4H.

T = mining height.

Re-arranging the above equation in terms of A gives:

$$\underline{A = 2.215W^{0.357}H^{,0.271}T^{0.372}} \qquad\qquad +/- \ aW'$$

B-Zone Prediction Model:

The heights of the B-Zone may also be estimated using a similar approach to the A-Zone methodology:

$$\underline{\text{Mean } B/W' = 1.621 \ (H'/W')^{0.55}(T/W')^{0.175}} \qquad R^2 = 0.86 \ \& \ \text{rsme} = 0.12W' \ (13\%)$$

$$\underline{\text{U95\%} \ B/W' = \text{Mean } B/W' + b}$$

where b = 0.16 for sub-critical panels, 0.16-0.085(W/H-0.7) for critical panels and 0.10 for supercritical panels.

Re-arranging the above equation in terms of B gives:

$$\underline{B = 1.621 \ W^{,0.275}H^{0.55}T^{0.175}} \quad +/- \ bW'$$

9.3.4   Geology Pi-Term Model

Further to the Geometry Model, the Pi-Term Geology model also considers the influence of the panel width, cover depth and mining height with the inclusion of the effective strata unit thickness. The effective strata unit thickness refers to the thickness of the beam that limits the height of continuous fracturing above a longwall panel. Using a product and power rule and non-linear regression analysis of measured cases, the range of effective beam thicknesses for a given mining geometry was derived for the NSW and Queensland Coalfields; see **Figure 18d**.

A-Zone Prediction Model:

The Pi-terms have been derived (by experiment) using Buckingham's Pi-term theorem and refer to the dimensionless ratios of key independent variables with a repeating variable of influence (the panel width) as follows:

$$\underline{\text{Mean A/W'} = 1.52\ (H/W')^{0.535}(T/W')^{0.464}(t'/W')^{-0.4}} \qquad R^2 = 0.8\ (\text{rmse}=15\%)$$
$$\underline{\text{U95\%CL A/W' = Mean A/W' + a}}$$

where

a = 0.15 for *sub-critical*, 0.15 - 0.0714(W/H-0.7) for *critical* and 0.1 for *supercritical* panels

H = cover depth = maximum potential goaf load height.

W' = effective panel width = minimum of W and 1.4H.

T =   mining height.

t' = effective strata unit thickness in the overburden above the A-Zone and ranges between 16 m and 54 m across the Newcastle Coalfield with a median value of 20 m.

Re-arranging the above equation in terms of A gives:

$$\underline{A = 1.52 W^{0.4} H'^{0.535} T^{0.464} t'^{-0.4}} \qquad\qquad \text{+/- aW'}$$

B-Zone Prediction Model:

It is considered that the Pi-Term Geology model is superior to the Pi-Term Geometry model as the t' factor may be back-analyzed to local height of A-Zone fracture height measurements once mining commences.

The two models are likely to provide conservative predictions if massive strata are present in the overburden with the capability to span the goaf and 'truncate' the A-Zone heights.

The heights of the B-Zone may also be estimated using a similar approach to the A-Zone methodology:

$$\underline{\text{Mean B/W' } = 1.873 \ (H'/W')^{0.635}(T/W')^{0.257}(t'/W')^{-0.097}} \quad R^2 = 0.86 \ \& \ rmse = 0.13W'(15\%)$$

$$\underline{\text{U95\% B/W' } = \text{Mean B/W' } + b}$$

where b = 0.15 for sub-critical panels; 0.15-0.0714(W/H-0.7) for critical panels and 0.10 for supercritical panels.

Re-arranging the above equation in terms of B gives:

$$\underline{B = 1.873 \ W'^{0.205} H^{0.635}T^{0.257}t'^{-0.097}} \quad \quad \text{+/- bW'}$$

9.3.5   Panel Width-Based Models

The width-based model published in **SCT, 2008** was originally defined as a 'height of fracturing' models that did not distinguish between discontinuous and continuous zones of fracturing. The models were based on numerical Flac2-D outcomes and a FISH program that tracked tensile and compressive fracturing and bedding shear above a longwall goaf. The model is therefore likely to provide conservative estimates of the A-Zone and possibly includes the B-Zone fractures/dilated strata as well in some cases.

It is considered that whilst the program is a reasonable attempt at predicting fracture heights numerically, the model is still a 'continuous strata model' program that is trying to model part-discontinuous and part-continuous strata behaviour. Whilst the program appears to be able to identify caving zones and zones of large displacement (i.e. the A-Zone), the predicted heights of fracturing have only been related to one parameter, the panel width, W, as follows:

$$A = 1.0W \text{ to } 1.5W$$

The width-based models do not consider the effect of cover depth or mining height and also assume the A-Zone will continue to increase above *supercritical* panel geometries. This usually means that surface to seam connectivity will always be predicted for critical and supercritical panel widths, which is at odds with industry experience.

A review of published industry experience of critical and supercritical panels presented in **Appendix A** indicate that only 2 or 3 cases out of 14 (15% - 20%) or 1 in 5 supercritical longwalls have resulted in surface to seam connectivity; see **Figure 18d**.

This outcome suggests that factors such as cover depth, mining height and geological conditions should also be considered other than just the panel width alone when estimating heights of fracturing above longwall panels. The model may therefore indicate conservative A-Zone heights in some cases, and will depend on differences in mining height, cover depth and mining geology for a given panel width.

9.3.6   T-Based Model

The height of the A-Zone fracturing has been successfully predicted from relationships established with extensometer and piezometeric monitoring data above supercritical panels in the Newcastle Coalfield. A supercritical panel relationship between A and T was developed by **Forster, 1995** in the Lake Macquarie Region as follows:

A=21T to 33T above *supercritical* panel geometries

Massive conglomerate or sandstone strata units located at horizons just above the extracted coal seams where the continuous fracturing extended to. The model has been validated against Wyee LW 17 to 23 in **Li *et al*, 2006** and provides a simple method by which to compare other model results. Caution is advised when making A-Zone predictions in other coalfields with less massive lithology present however.

9.3.7   Continuous Sub-Surface Fracture Height Predictions (A-Zone)

The predicted values for continuous (A-Zone) sub-surface fracture heights above NM LW 101 to 106 are summarised in **Table 9A**, with LW 107 to 120 in **Table 9B**. Predicted A-Zone horizons of 21T to 33T from **Forster, 1995** for 'critical' to 'supercritical' panel width geometries are also provided for comparison with the proposed panels.

An effective strata unit thickness t' = 20 m has been back-analysed for the Pi-Term Geology Model from measured height of fracturing data (**Figure 19a**) and the maximum strain / curvature regression analysis (**Figure 9c**) for the completed NM LW 101 to 104. *Note: the effective bending beam thickness at the surface is approximately twice the horizontal strain/curvature ratio.*

The *continuous* sub-surface fracture heights (A-Horizon) have been plotted against cover depth in **Figure 19b** for LW 101 to 111 and **Figure 19c** for LW 112 to 120.

Table 9A - Summary of Predicted Sub-Surface Fracturing Heights (A-Zone) above the Proposed LW 101 to 106

Longwall Panels	Cover Depth, H (m)	Mining Height, T (m)	Effective Panel Width W' (m)	Predicted Continuous (A Horizon) Fracture Heights (m)					Depth to A-Zone (m)
				Pi-Term Geology Model		Forster, 1995	Pi-Term Geometry Model		Geology Model
				mean	U95%CL	33T	U95%CL	U95%CL	U95%CL
101	165	4.2	231.0	121	144	139	105	128	21
	160	4.2	224.0	117	140	139	103	126	20
	175	4.2	245.0	128	152	139	109	134	23
102	175	4.2	245.0	128	152	139	109	134	23
	180	4.2	252.0	131	156	139	111	136	24
	185	4.2	259.0	135	160	139	113	139	25
103	190	4.3	266.0	139	166	142	116	143	24
	195	4.3	273.0	143	170	142	118	145	25
	195	4.3	273.0	143	170	142	118	145	25
	200	4.3	280.0	146	174	142	120	148	26
104	180	4.3	252.0	133	158	142	112	137	22
	200	4.3	280.0	146	174	142	120	148	26
	210	4.3	294.0	153	183	142	123	153	27
	215	4.3	301.0	157	187	142	125	155	28
	215	4.3	301.0	157	187	142	125	155	28
105	200	4.3	280.0	146	174	142	120	148	26
	215	4.3	301.0	157	187	142	125	155	28
	225	4.3	306.4	162	193	142	128	159	32
	235	4.3	306.4	165	198	142	129	162	37
	235	4.3	306.4	165	198	142	129	162	37
106	220	4.3	306.4	160	190	142	127	158	30
	240	4.3	306.4	167	201	142	130	164	39
	245	4.3	306.4	169	203	142	131	165	42
	255	4.3	306.4	173	208	142	132	168	47
	250	4.3	306.4	171	205	142	131	167	45

shaded - Preferred predictions.
* - Predictions determined along XLs 1 to 5 (see **Figure 1b,c** for cross line location)
W' = minimum (W, 1.4H).
Bold - Direct hydraulic connection to the surface is considered possible if A-Horizon prediction within 10 m of the surface.

Table 9B - Summary of Predicted Sub-Surface Fracturing Heights (A-Zone) above the Proposed LW 107 to 120

Longwall Panels	Cover Depth H (m)	Mining Height T (m)	Effective Panel Width W' (m)	Predicted Continuous (A Horizon) Fracture Heights (m)					Depth to A-Zone (m)
				Pi-Term Geology Model		Forster, 1995	Pi-Term Geometry Model		Geology Model
				mean	U95%CL	33T	mean	U95%CL	U95%CL
107	240	4.3	336	174	207	139	134	168	33
107	270	4.3	378	194	232	139	145	182	38
107	280	4.3	392	200	240	139	148	187	40
107	285	4.3	399	204	244	139	150	189	41
108	275	4.3	385	197	236	139	146	185	39
108	265	4.3	371	190	227	139	143	180	38
108	275	4.3	385	197	236	142	146	185	39
108	290	4.3	405	207	248	142	151	192	42
108	305	4.3	405	213	255	142	153	196	50
109	295	4.3	405	209	250	142	152	193	45
109	290	4.3	405	207	248	142	151	192	42
109	300	4.3	405	211	253	142	153	195	47
109	305	4.3	405	213	255	142	153	196	50
109	325	4.3	405	220	265	142	156	202	60
110	320	4.3	405	218	263	142	155	201	57
110	310	4.3	405	214	258	142	154	198	52
110	330	4.3	405	222	267	142	157	203	63
110	320	4.3	405	218	263	142	155	201	57
110	335	4.3	405	224	270	142	157	204	65
111	330	4.3	405	222	267	142	157	203	63
111	325	4.3	405	220	265	142	156	202	60
111	350	4.3	405	229	276	142	159	208	74
111	360	4.3	405	232	281	142	160	210	79
111	350	4.3	405	229	276	142	159	208	74
112	355	4.3	405	231	279	142	160	209	76
112	340	4.3	405	225	272	142	158	206	68
112	355	4.3	405	231	279	142	160	209	76
112	360	4.3	405	232	281	142	160	210	79
112	355	4.3	405	231	279	142	160	209	76
113	350	4.3	405	229	276	142	159	208	74
113	320	4.3	405	218	263	142	155	201	57
113	330	4.3	405	222	267	142	157	203	63
113	340	4.3	405	225	272	142	158	206	68
113	345	4.3	405	227	274	142	158	207	71
114	330	4.3	405	222	267	142	157	203	63
114	310	4.3	405	214	258	142	154	198	52
114	300	4.3	405	211	253	142	153	195	47
114	320	4.3	405	218	263	142	155	201	57
114	325	4.3	405	220	265	142	156	202	60
115	305	4.3	405	213	255	142	153	196	50
115	305	4.3	405	213	255	142	153	196	50
115	275	4.3	385	197	236	142	146	185	39
115	285	4.3	399	204	244	142	150	189	41
115	300	4.3	405	211	253	142	153	195	47

Table 9B (Cont…) - Summary of Predicted Sub-Surface Fracturing Heights (A-Zone) above the Proposed LW 107 to 120

Longwall Panels	Cover Depth H (m)	Mining Height T (m)	Effective Panel Width W' (m)	Predicted Continuous (A Horizon) Fracture Heights (m)					Depth to A-Zone (m)
				Pi-Term Geology Model		Forster, 1995	Pi-Term Geometry Model		Geology Model
				mean	*U95%CL*	*33T*	*mean*	*U95%CL*	*U95%CL*
116	270	4.3	378	194	232	142	145	182	38
116	270	4.3	378	194	232	142	145	182	38
116	245	4.3	343	177	211	142	136	170	34
116	255	4.3	357	184	219	142	139	175	36
116	280	4.3	392	200	240	142	148	187	40
117	230	4.3	322	167	199	142	131	163	31
117	240	4.3	336	174	207	142	134	168	33
117	225	4.3	315	163	195	142	129	160	30
117	225	4.3	315	163	195	142	129	160	30
117	245	4.3	343	177	211	142	136	170	34
118	200	4.3	280	146	174	142	120	148	26
118	205	4.3	287	150	178	142	122	150	27
118	205	4.3	287	150	178	142	122	150	27
118	210	4.3	294	153	183	142	123	153	27
118	225	4.3	315	163	195	142	129	160	30
119	190	4.3	266	139	166	142	116	143	24
119	200	4.3	280	146	174	142	120	148	26
119	210	4.3	294	153	183	142	123	153	27
120	180	4.3	252	133	158	142	112	137	22
120	190	4.3	266	139	166	142	116	143	24
120	205	4.3	287	150	178	142	122	150	27

shaded - Preferred predictions.
* - Predictions determined along XLs 1 to 5 (see **Figure 1b,c** for cross line location)
W' = minimum (W, 1.4H).
Bold - Direct hydraulic connection to the surface is considered possible if A-Horizon prediction within 10 m of the surface.

The Pi-Term Geology model predicts the highest A-Zone out of the three models assessed, with U95%CL values for each summarised in **Tables 9C** and **9D**. The next highest A-Zone predictions are indicated by the Geometry-only Pi-Term model or **Forster, 1995** models.

Table 9C - Summary of Sub-Surface Fracture Model Predictions

LW	Panel Width W (m)	Cover Depth H (m)	Effective Panel Width W' (m)	Mining Height T (m)	W/H	Predicted Maximum A-Zone Height above Longwall (m)		
						Geology Pi-Term	Geometry Pi-Term	Forster, 1995
101 - 106	306.5	165 - 255	231 - 306.5	3.3 - 3.4	1.20 - 1.86	144 - 208	128 - 168	88 - 139
107 - 120	405.4	180 - 360	252 - 408.9	3.4	1.13 - 2.25	158 - 281	137 - 210	90 - 142

Table 9D - Summary of Sub-Surface Fracture Model Predictions v. Key Mining Parameters

A-Zone Height Prediction Model	A/H	A/W'	A/T
Geology Pi-Term	0.78 - 0.88	0.61 - 0.69	34 - 65
Geometry Pi-Term	0.58 - 0.78	0.47 - 0.56	31 - 49
Forster, 1995	0.39 - 0.84	0.35 - 0.60	21 - 33

The predicted A-Zone based on the Geology PI-Term Model ranges from 78% to 88% of the cover depth; 0.61 to 0.69 times the effective panel width and 34 to 65 times the mining height.

The results indicates that the Geology Pi-Term Model is the most conservative of the three models assessed, with the height of A-Zone fracturing predicted to encroach within 21 m to 79 m below the surface. Based on this model then, it is considered 'unlikely' the A-Zone will extend up to the surface cracking zone (i.e. within 10 m below the surface) for the range of cover depths above LW 101 to 120.

9.3.8   Discontinuous Sub-Surface Fracture Height Predictions (B-Zone)

The predicted values for constrained discontinuous (B-Zone) sub-surface fracture heights above NM LW 101 to 106 are summarised in **Table 10A** with LW 107 to 120 in **Table 10B** for the two Pi-Term models presented earlier.

The *discontinuous* sub-surface fracture heights (A-Horizon) have been plotted against depth of rock cover in **Figure 19b** for LW 101 to 111 and **Figure 19c** for LW 112 to 120.

Table 10A - Summary of Predicted Sub-Surface Fracturing Heights (B-Zones) above the Proposed LW 101 to 106

Longwall Panels	Cover Depth, H (m)	Mining Height, T (m)	Effective Panel Width W' (m)	Predicted Discontinuous (B Horizon) Fracture Heights (m)				Depth to B-Zone from Surface, dB (m)	
				Pi-Term Geology Model		Pi-Term Geometry Model			
				mean	*U95%CL*	*mean*	*U95%CL*	*mean*	*U95%CL*
101	165	4.2	231.0	*183*	*206*	*169*	*192*	*-18*	*-41*
	160	4.2	224.0	*178*	*201*	*165*	*187*	*-18*	*-41*
	175	4.2	245.0	*192*	*217*	*178*	*202*	*-17*	*-42*
102	175	4.2	245.0	*192*	*217*	*178*	*202*	*-17*	*-42*
	180	4.2	252.0	*197*	*222*	*182*	*207*	*-17*	*-42*
	185	4.2	259.0	*201*	*227*	*186*	*212*	*-16*	*-42*
103	190	4.3	266.0	*207*	*234*	*191*	*218*	*-17*	*-44*
	195	4.3	273.0	*212*	*239*	*195*	*222*	*-17*	*-44*
	195	4.3	273.0	*212*	*239*	*195*	*222*	*-17*	*-44*
	200	4.3	280.0	*216*	*244*	*199*	*227*	*-16*	*-44*
104	180	4.3	252.0	*198*	*223*	*183*	*208*	*-18*	*-43*
	200	4.3	280.0	*216*	*244*	*199*	*227*	*-16*	*-44*
	210	4.3	294.0	*225*	*255*	*207*	*237*	*-15*	*-45*
	215	4.3	301.0	*230*	*260*	*211*	*242*	*-15*	*-45*
	215	4.3	301.0	*230*	*260*	*211*	*242*	*-15*	*-45*
105	200	4.3	280.0	*216*	*244*	*199*	*227*	*-16*	*-44*
	215	4.3	301.0	*230*	*260*	*211*	*242*	*-15*	*-45*
	225	4.3	306.5	*234*	*265*	*216*	*248*	*-9*	*-40*
	235	4.3	306.5	237	269	219	252	-2	-34
	235	4.3	306.5	237	269	219	252	-2	-34
106	220	4.3	306.5	233	264	215	246	-13	-44
	240	4.3	306.5	238	271	220	254	2	-31
	245	4.3	306.5	239	272	221	256	6	-27
	255	4.3	306.5	241	275	224	260	14	-20
	250	4.3	306.5	240	274	223	258	10	-24

* - Predictions determined along XLs 1 to 5 (see **Figure 1b,c** for cross line location); W' = minimum (W, 1.4H).
Italics - Discontinuous fracturing likely to interact with surface cracks as B-Horizon within 10 m of surface, resulting in surface flow re-routing.

Table 10B - Summary of Predicted Sub-Surface Fracturing Heights (B-Zone) above the Proposed LW 107 to 120

Longwall Panels	Cover Depth, H (m)	Mining Height, T (m)	Effective Panel Width W' (m)	Predicted Discontinuous (B Horizon) Fracture Heights (m)				Depth to B-Zone from Surface, dB (m)	
				Pi-Term Geology Model		Pi-Term Geometry Model			
				mean	*U95%CL*	*mean*	*U95%CL*	*mean*	*U95%CL*
107	240	4.3	336	*252*	*286*	*232*	*265*	*-12*	*-46*
107	270	4.3	378	*278*	*316*	*255*	*293*	*-8*	*-46*
107	280	4.3	392	*287*	*326*	*263*	*302*	*-7*	*-46*
107	285	4.3	399	*291*	*331*	*267*	*307*	*-6*	*-46*
108	275	4.3	385	*282*	*321*	*259*	*298*	*-7*	*-46*
108	265	4.3	371	*274*	*311*	*251*	*288*	*-9*	*-46*
108	275	4.3	385	*282*	*321*	*259*	*298*	*-7*	*-46*
108	290	4.3	405	*295*	*335*	*270*	*311*	*-5*	*-45*
108	305	4.3	405	*298*	*340*	*274*	*317*	*7*	*-35*
109	295	4.3	405	*296*	*337*	*272*	*313*	*-1*	*-42*
109	290	4.3	405	*295*	*335*	*270*	*311*	*-5*	*-45*
109	300	4.3	405	*297*	*338*	*273*	*315*	*3*	*-38*
109	305	4.3	405	*298*	*340*	*274*	*317*	*7*	*-35*
109	325	4.3	405	*302*	*346*	*279*	*325*	*23*	*-21*
110	320	4.3	405	*301*	*345*	*278*	*323*	*19*	*-25*
110	310	4.3	405	*299*	*342*	*275*	*319*	*11*	*-32*
110	330	4.3	405	*303*	*348*	*280*	*327*	*27*	*-18*
110	320	4.3	405	*301*	*345*	*278*	*323*	*19*	*-25*
110	335	4.3	405	*304*	*349*	*281*	*329*	*31*	*-14*
111	330	4.3	405	*303*	*348*	*280*	*327*	*27*	*-18*
111	325	4.3	405	*302*	*346*	*279*	*325*	*23*	*-21*
111	350	4.3	405	*307*	*354*	*285*	*334*	*43*	*-4*
111	360	4.3	405	*308*	*356*	*287*	*337*	*52*	*4*
111	350	4.3	405	*307*	*354*	*285*	*334*	*43*	*-4*
112	355	4.3	405	*308*	*355*	*286*	*336*	*47*	*0*
112	340	4.3	405	*305*	*351*	*283*	*330*	*35*	*-11*
112	355	4.3	405	*308*	*355*	*286*	*336*	*47*	*0*
112	360	4.3	405	*308*	*356*	*287*	*337*	*52*	*4*
112	355	4.3	405	*308*	*355*	*286*	*336*	*47*	*0*
113	350	4.3	405	*307*	*354*	*285*	*334*	*43*	*-4*
113	320	4.3	405	*301*	*345*	*278*	*323*	*19*	*-25*
113	330	4.3	405	*303*	*348*	*280*	*327*	*27*	*-18*
113	340	4.3	405	*305*	*351*	*283*	*330*	*35*	*-11*
113	345	4.3	405	*306*	*352*	*284*	*332*	*39*	*-7*
114	330	4.3	405	*303*	*348*	*280*	*327*	*27*	*-18*
114	310	4.3	405	*299*	*342*	*275*	*319*	*11*	*-32*
114	300	4.3	405	*297*	*338*	*273*	*315*	*3*	*-38*
114	320	4.3	405	*301*	*345*	*278*	*323*	*19*	*-25*
114	325	4.3	405	*302*	*346*	*279*	*325*	*23*	*-21*
115	305	4.3	405	*298*	*340*	*274*	*317*	*7*	*-35*
115	305	4.3	405	*298*	*340*	*274*	*317*	*7*	*-35*
115	275	4.3	385	*282*	*321*	*259*	*298*	*-7*	*-46*
115	285	4.3	399	*291*	*331*	*267*	*307*	*-6*	*-46*
115	300	4.3	405	*297*	*338*	*273*	*315*	*3*	*-38*

Table 10B (Cont…) - Summary of Predicted Sub-Surface Fracturing Heights (B-Zone) above the Proposed LW 107 to 120

Longwall Panels	Cover Depth H (m)	Mining Height T (m)	Effective Panel Width W' (m)	Predicted Discontinuous (B Horizon) Fracture Heights (m)				Depth to B-Zone from Surface, dB (m)	
				Pi-Term Geology Model		Pi-Term Geometry Model			
				mean	*U95%CL*	*mean*	*U95%CL*	*mean*	*U95%CL*
116	270	4.3	378	*278*	*316*	*255*	*293*	*-8*	*-46*
116	270	4.3	378	*278*	*316*	*255*	*293*	*-8*	*-46*
116	245	4.3	343	*256*	*291*	*236*	*270*	*-11*	*-46*
116	255	4.3	357	*265*	*301*	*243*	*279*	*-10*	*-46*
116	280	4.3	392	*287*	*326*	*263*	*302*	*-7*	*-46*
117	230	4.3	322	*243*	*275*	*224*	*256*	*-13*	*-45*
117	240	4.3	336	*252*	*286*	*232*	*265*	*-12*	*-46*
117	225	4.3	315	*239*	*270*	*220*	*251*	*-14*	*-45*
117	225	4.3	315	*239*	*270*	*220*	*251*	*-14*	*-45*
117	245	4.3	343	*256*	*291*	*236*	*270*	*-11*	*-46*
118	200	4.3	280	*216*	*244*	*199*	*227*	*-16*	*-44*
118	205	4.3	287	*221*	*249*	*203*	*232*	*-16*	*-44*
118	205	4.3	287	*221*	*249*	*203*	*232*	*-16*	*-44*
118	210	4.3	294	*225*	*255*	*207*	*237*	*-15*	*-45*
118	225	4.3	315	*239*	*270*	*220*	*251*	*-14*	*-45*
119	190	4.3	266	*207*	*234*	*191*	*218*	*-17*	*-44*
119	200	4.3	280	*216*	*244*	*199*	*227*	*-16*	*-44*
119	210	4.3	294	*225*	*255*	*207*	*237*	*-15*	*-45*
120	180	4.3	252	*198*	*223*	*183*	*208*	*-18*	*-43*
120	190	4.3	266	*207*	*234*	*191*	*218*	*-17*	*-44*
120	205	4.3	287	*221*	*249*	*203*	*232*	*-16*	*-44*

* - Predictions determined along XLs 1 to 5 (see **Figure 1b,c** for cross line location); W' = minimum (W, 1.4H).
Italics - Discontinuous fracturing likely to interact with surface cracks as B-Horizon within 10 m of surface, resulting in surface flow re-routing.

The Geology and Geometry Pi-Term models predict discontinuous sub-surface fracturing is likely to could interact with surface cracks (D-Zones) where cover depths are < 260 m above the 306 m wide panels and <360 m above the 405 m wide longwalls. Creek flows could be re-routed to below-surface pathways and re-surfacing down-stream of the mining extraction limits in these areas.

Discontinuous fracturing would be expected to occur above these limits and increase rock mass storage capacity and horizontal permeability without direct hydraulic connection to the workings.

The observation of stress trees above extracted longwalls to-date, indicates B-Zone interaction with tree root systems and a reduction in available moisture has in fact occurred at some locations to-date. The direct shearing impacts to tree roots are expected to decrease as cover depth increases however.

9.3.9 Rock Mass Permeability Changes

Rock mass permeability is unlikely to be affected outside a distance of 20 m from the panel extraction limits.

In regards to changes to rock mass permeability, **Forster, 1995** indicates that horizontal permeabilities in the Fractured Zone or A-Zone above longwall mines (see **Figure 18b**) could increase by 2 to 4 orders of magnitude (e.g. pre-mining $k_h = 10^{-9}$ to 10^{-10} m/s; post-mining $k_h = 10^{-7}$ to 10^{-6} m/s).

Vertical permeability in the A-Zone would be expected to be high between the transition boundary with the B-Zone where de-saturation is expected to occur. Re-saturation of the strata within the A-Zone and a decrease in permeability is usually assumed to occur with depth (towards the mine workings) by experienced ground water modellers.

In the B-Zone, only a slight increase in the vertical permeability would be expected, with horizontal permeability currently believed to increase between 10 and 100 times due to an increase in available void space and groundwater storage from discontinuous fracturing or bedding dilation (**Tammetta, 2014**).

9.3.10 Impact Management Strategies

Groundwater and surface aquifer impact studies should consider the above uncertainties in regards to surface and groundwater impacts. The practical options available for controlling sub-surface fracturing are limited to (in order of increasing impact to mining):

- Repair surface cracks when they occur.

- Decrease mining height longwall panel width to limit continuous fracture heights.

  Note: This option will require local subsidence and sub-surface monitoring data to make effective and reliable changes to the mining layout.

- Leave a barrier pillar beneath sensitive area or limit mining to first workings.

Installation of deep borehole piezometers and extensometers in the overburden above the first one or two panels would provide invaluable data on resolving a significant amount of the uncertainty associated with the available prediction models. Further discussion on the monitoring program may be found in **Section 10**.

9.4   Gradient Changes Along Creeks

9.4.1   Predicted Effects and Impacts

The surface topography overlying longwall blocks is 'gently' to moderately undulated, with slope angles generally being < 15°.

The likelihood of *en-masse* sliding (i.e. a landslip/landslide) of the surface terrain over basal siltstone beds tilted by subsidence has been assessed as barely credible, based on the landslide risk assessment terminology presented in **AGS, 2010**.

The potential for terrain adjustment due to erosion and deposition of soils after subsidence has also been broadly assessed below.

The final change in surface gradients after mining of LW101 to 111 is shown in **Figure 21a**, with LW112 to 120 shown in **Figure 21b**. The figures indicate that the surface gradients will be increased or decreased by 3.5% (typically +/- 2%).

The rate of soil erosion is expected to increase significantly in areas with exposed dispersive/reactive soils and slopes < 10° are expected to have low erosion rate increases, except for the creek channels, which would be expected to re-adjust to any changes in gradient.

Predicted final level and gradient changes along Pine Creek and Pine Creek Tributaries No.1 and 2 above the northern panels are shown in **Figures 22a,b** to **24a,b** respectively. The predicted subsidence effects to creeks above LW101 to LW111 for the 2009 EA and 2015 Modification are summarised in **Table 11A**.

Table 11A - Predicted Subsidence Effects to Creeks above Northern LW101 to 111

Creek Bed Gradient Change* (%)											
Pine Creek				Pine Creek Tributary 1				Pine Creek Tributary 2			
LW	2015 Mod	LW	2009 EA	LW	2015 Mod	LW	2009 EA	LW	2015 Mod	LW	2009 EA
101	-	1	-	101	-2.5/2.2	1	-0.2/1.4	101	-	1	-
102	-	2	-	102	-1.7/2.4	2	-1.4/0.3	102	-	2	-
103	-	3	-	103	-1.8/2.4	3	-1.4/1.5	103	-	3	-
104	-2.7/2.6	4	-2.6/2.5	104	-0.9/0.0	4	-2.0/2.0	104	-	4	-
105	-2.3/2.5	5	-2.3/2.4	105	-		-	105	-	5	-
106	-2.5/2.2	6	-2.0/2.1	106	-		-	106	-	6	-
107	-1.8/1.4	7,8	-2.1/1.6	107	-		-	107	-1.5/0.0	7,8	-1.3/1.3
108	-1.7/0.9	8,9	-1.7/1.8	108	-		-	108	-1.6/0.9	8,9	-1.1/1.3
109	-1.7/1.7	10,11	-1.8/1.6	109	-		-	109	-1.4/1.5	10,11	-1.1/1.2
110	-1.6/1.4	11,12	-1.6/1.7	110	-		-	110	-0.9/1.0	11,12	-1.2/0.9
111	-1.8/1.7	13	-1.5/1.7	111	-		-	111	-0.8/0.5	13	-0.8/0.9

* - Predictions are based on 'smooth' subsidence profiles and may be increased by 1.5 times due to discontinuous strata behaviour.

Predicted final level and gradient changes along Kurrajong Creek Tributary No.1 and Kurrajong Creek above the southern panels are shown in **Figures 25a,b** to **26a,b** respectively. The predicted subsidence effects to creeks above LW112 to LW120 for the 2009 EA and 2015 Modification are summarised in **Table 11B**.

Table 11B - Predicted Subsidence Effects to Creeks above Northern LW112 to 120

Creek Bed Gradient Change* (%)							
Kurrajong Creek Tributary 1				Kurrajong Creek			
LW	2015 Mod	LW	2009 EA	LW	2015 Mod	LW	2009 EA
112	-0.6/1.2	14	-0.5/1.2	112	-	14	-
113	-1.2/0.8	15,16	-1.2/1.2	113	-	15,16	-
114	-1.5/1.6	16,17	-1.1/1.2	114	-	16,17	-
115	-1.6/1.3	18,19	-1.4/1.7	115	-	18,19	-
116	-1.8/1.6	19,20	-1.9/1.7	116	-	19,20	-
117	-1.8/1.8	21,22	-2.0/2.0	117	-0.4/0.4	21	-0.4/0.7
118	-2.0/2.4	22,23	-2.0/2.2	118	-2.4/1.7	22	-2.3/1.8
119	-2.5/2.4	23,24	-2.3/1.9	119	-	23	-2.0/1.7
120	-1.2/2.4	25,26	-2.2/2.4	120	-	24,25,26	-

* - Predictions are based on 'smooth' subsidence profiles and may be increased by 1.5 times due to discontinuous strata behaviour.

Head-cuts would be expected to develop above chain pillars between the panels and on the side where gradients increase. Sediment would be expected to accumulate where gradients decrease. Therefore the proposed changes to the mining model and extended layout are likely to be minor along the subsided creeks.

9.4.2   Review of Predicted v. Measured Gradient Changes

Measured subsidence along Pine Creek (D-Line) and Pine Creek Tributary 1 (B-Line) reasonably matches the predicted subsidence and gradient changes as shown in **Table 11C, Figures 22a,b** and **23a,b**.

Table 11C - Predicted v. Measured Pine Creek Tributary 1 (B-Line) and Pine Creek (D-Line) Subsidence Effects

LW	Maximum Panel Subsidence (m)		Chain Pillar Subsidence (m)		Creek Bed Gradient Change (o)	
	Predicted	*Measured*	*Predicted*	*Measured*	*Predicted*	*Measured*
Pine Creek Tributary 1 (B-Line)						
101	2.55	2.459	0.11	0.09	-2.6 to +2.8	**-5.4** to +2.6
102	2.68	2.585	0.10	**0.235**	-2.6 to +1.4	-2.1 to **+1.7**
Pine Creek (D-Line)						
104	2.59	*0.34*	*0.21*	-	-2.7 to +2.6	*-0.5 to 0.5*

Bold - measured value exceeds predicted value; *italics* - subsidence incomplete

The gradient changes measured along Pine Creek Tributary 1 have exceeded the predicted values based on smooth profiles by -2.6% to +0.3%. The measured subsidence and gradients are likely to be due to discontinuous strata behaviour and unlikely to be representative of the gradient changes along the creek. No additional impacts to the creek have been detected by monitoring programs conducted to date.

9.4.3   Impact Management Strategies

To minimise the likelihood of slope instability from increased erosion due to cracking or changes to drainage patterns after extraction, the management strategy would include:

- surface slope displacement monitoring along subsidence cross lines (combined with general subsidence monitoring plans);

- infilling of surface cracking to prevent excessive ingress of runoff into the slopes;

- areas that are significantly affected by erosion after mining may need to be repaired and protected with mitigation works such as re-grading, installation of new contour banks and re-vegetation of exposed areas; and

- on-going review and appraisal of any significant changes to surface slopes such as cracking along ridges, increased erosion down slopes, foot slope seepages and drainage path adjustments observed after each longwall is extracted.

9.5   Ponding

9.5.1   Predicted Effects and Impacts

Surface slopes in the elevated areas between the creeks range between 0.9% and 7% typically (0.5$^\mathrm{o}$ to 4$^\mathrm{o}$), and indicate a net fall across the proposed longwall panels from 2.5 m to 10 m prior to mining. The predicted maximum panel subsidence of 2.75 m could therefore result in closed form depressions forming in the central areas of the panels and disrupt natural drainage pathways to the water courses.

Analysis of the pre and post-mining surface levels suggest that ponding is likely to develop near existing watercourses. Maximum potential ponding depths of between 0.1 and 2.6 m are estimated after LW 101 to 120 are completed. References to post-panel reports indicate that ponding locations and there extent have been consistent with the predicted ranges.

Pre-mining surface levels for the northern and southern longwalls are shown in **Figures 27a-d**. Post-mining surface level and pond locations are shown in **Figures 28a-d**.

The potential maximum ponding depths, affected area and volume above the proposed panels after mining have been updated with the re-calibrated prediction are summarised in **Table 13**.

Table 12 - Potential Worst-Case Ponding Assessment for LW 101 to 120

Location	Longwall	Pond No. (see Figures 28a-d)	Max Pond RL (AHD)	Max. Depth h (m)	Ponded Area Increase After Mining# (m²)	Ponded Volume Increase After Mining# (ML)
Pine Creek	103	103a	276.9	0.7	5,463	1.92
	104	104a	266.2	2.0	25,862	25.80
	105	105a	268.7	2.1	25,214	26.47
	106	106a	271.1	1.4	8,996	6.30
	107	107a	274.0	1.0	9,805	4.90
	108	108a	280.5	2.6	7,096	9.23
		108b	279.0	0.5	2,682	0.67
		108c	280.4	0.1	7,502	0.38
	109	109a	284.0	0.8	3,503	1.40
	110	110a	288.5	0.7	6,126	2.14
	111	111a	293.0	1.0	8,390	4.20
Pine Creek Tributary 1	101	101a	271.8	1.3	51,567	33.52
	102	102a	274.3	1.3	36,695	23.85
	103	103b	278.8	1.9	12,789	1.92
		103c	281.2	0.3	8,388	1.26
	104	104b	283.3	0.3	4,461	0.67
		104c	285.5	0.25	4,926	0.62
	105	105b	292.5	0.9	1,827	0.82
Pine Creek Tributary 2	108	108d	285	0.4	622	0.12
Kurrajong Creek Tributary 1	114	114a	308.3	0.3	5,623	0.84
	115	115a	301.5	0.5	3,659	0.92
	117	117a	290.0	1.0	6,871	0.34
		117b	298.0	0.7	4,923	1.72
	118	118a	285.5	1.5	4,034	3.03
	119	119a	282.0	2.0	11,580	11.58
	120	120a	279.0	2.0	33,956	33.96
Kurrajong Creek	118	118b	282.5	1.5	9,458	7.09
		118c	284.0	0.5	3,809	0.95

Pond Area = π BL/4 (ellipse); Pond Volume = Pond Area x h/2 (paraboloid);
- Pre-mining pond areas and volumes assumed to be nil; *italics* - ponding on different branch of Tributary 1.

The maximum pond depths for LW 101 to 120 range from 0.1 m to 2.6 m with pond volumes ranging from 0.12 ML to 33.96 ML. The majority of potential ponding areas will develop along the watercourses and are likely to remain in channel.

The previous ponded depths estimated in the 2009 EA ranged from 0.5 m to 1.5 m with no pond volumes provided. The increase in maximum subsidence from 2.44 m to 2.75 m appears to have also increased the predicted pond depth values. The potential surface water impacts associated with this predicted ponding are described in **WRM Water & Environment, 2015**.

It should also be noted that the actual ponding depths, areas and volumes would still depend upon several other factors, such as rain duration, surface cracking and effective percolation rates of the surface soils along the creeks.

9.5.2   Impact Management Strategies

Despite the increases in predicted ponding depths for the Modified mining layout, an appropriate management strategy would include the on-going review and an appraisal of changes to surface drainage paths and surface vegetation in areas of ponding development (if they occur) after each longwall is extracted (as occurs for the existing NM).

Based on the post-mining surface level predictions, consistent with the existing NM, it is assessed that channel earthworks may be required to re-establish drainage path ways along Pine Creek, Pine Creek No. 1 Tributary, Kurrajong Creek and Kurrajong Creek Tributary No. 1 after mining. This would be undertaken in accordance with the Land Management Plan (**EcoLogical, 2012**).

9.6   Valley Closure and Uplift

9.6.1   Predicted Effects and Impacts

Based on reference to **ACARP, 2002**, 'valley closure' (or opening) movements can be expected along cliffs and sides of deep valleys whenever longwalls are mined beneath them. Valley closure can also occur across broader drainage gullies where shallow surface rock is present.

When creeks and river valleys are subsided, the observed subsidence in the base of the creek or river is generally less than would normally be expected in flat terrain. This reduced subsidence is due to the floor rocks of a valley buckling upwards when subject to compressive stresses generated by surface deformation. This phenomenon is termed 'upsidence' and in most cases in the Newcastle and Southern NSW Coalfields, the observed upsidence has extended outside steep sided valleys and included the immediate cliff lines and the ground beyond them.

It should also be understood that valley closure and uplift movements are strongly dependent on the level of 'locked-in' horizontal stress immediately below the floor of the gullies and more importantly the bedding thickness of the floor strata (i.e. thin to medium bedded sandstone is more likely to buckle than thicker beds). The influence of the aspect ratio (i.e. valley width/depth) is also recognised as an important factor, with deep, narrow valleys having greater upsidence than broad, rounded ones, due to higher stress concentrations.

Measured closure movements along valley crests have ranged between 10 mm and 400 mm in the Southern NSW Coalfields, with measured upsidence movements (associated with the closure) also ranging between 10 mm and 400 mm. The impact of the movements range from imperceptible to moderate surface cracking in exposed bedrock on the floor of the valley (or gorge).

As the valleys across NM's mining lease are very broad between crests, and there is a lack of thick, massive beds of conglomerate and/or sandstone units along the creeks / valleys, the development of upsidence and closure along the creek beds above LW 101 to 120 is likely to be negligible.

If upsidence does occur, it may cause some minor, localised deviation of surface flows along ephemeral creek beds into sub-surface routes above the longwall panels. Failure and cracking of the near surface rocks due to tensile bending or compressive/shear strains will also contribute to the re-routing of surface flows. Re-routed surface flows would be expected to resurface downstream of the damaged area.

Survey measurements across Pine Creek Tributary 1 (Lines C and E-G) in October 2014 have indicated maximum closure of 148 mm between the 30 m wide creek bank crests at Line F, with compressive strain of 6.2 mm/m and uplift of 64 mm. Lines E and G did not detect any Valley Closure or Uplift movements in the creek above the chain pillars due to LW101 to 104. The measured movements are within the predicted range previously presented in the 2009 EA.

9.6.2 Impact Management Strategies

The impact of upsidence and valley bending effects along Pine Creek Tributary 1 have been monitored and managed as follows:

(i) Installation of survey lines along and across ephemeral drainage gullies and bank crests during and after longwall undermining. Combine surveys with visual inspections to locate damage (cracking, uplift).

(ii) Review predictions of upsidence and valley crest movements after each longwall.

(iii) Assess whether repairs (i.e. cementitious grouting or crushed rock) to cracking, as a result of upsidence or gully slope stabilisation works are required to minimise the likelihood of long-term degradation or risks to personnel and the general public.

At this stage, no damage to the creeks as a result of valley closure or uplift has been detected along Pine Creek Tributary No. 1. It is understood that the mine is proposing to reduce the amount of ground surveys with ALS for future longwalls.

Provided that there are visual inspections of the subsidence affected creeks, and several representative centrelines and crosslines to provide ground truthing and angle of draw data for the ALS surveys, it is not considered necessary to install survey lines along or across Pine Creek for LW106.

Further review of creek line monitoring requirements for the remaining longwalls will need to be based on observed impacts and detailed in the relevant Extraction Plans.

9.7 Far-Field Horizontal Displacements

9.7.1 Predicted Effects and Impacts

Horizontal movements due to longwall mining have been recorded at distances well outside of the angle of draw in the Newcastle, Southern and Western Coalfields (**Reid, 1998, Seedsman and Watson, 2001**). Horizontal movements recorded beyond the angle of draw are referred to as far-field horizontal displacements.

For example, at Cataract Dam in the Southern NSW Coalfield, **Reid, 1998**, reported horizontal movements of up to 25 mm when underground coal mining was about 1.5 km away. **Seedsman and Watson**, **2001** reported movements in the Newcastle Coalfield of around 20 mm at distances of approximately 220 m, for a cover depth ranging from 70 to 100 m and a panel width of 193 m, however, the results may have been due to GPS baseline accuracy limitations.

Based on a review of the above information, it is apparent that this phenomenon is strongly dependent on (i) cover depth, (ii) distance from the goaf edges, (iii) the maximum subsidence over the extracted area, (iv) topographic relief and (v) the horizontal stress field characteristics.

An empirical model for predicting Far-field displacement (FFDs) in the Newcastle Coalfield is presented in **Figure 29a**. The model indicates that measurable FFD movements (i.e. 20 mm) generally occur in relatively flat terrain for distances up to 3 to 4 times the cover depth.

The direction of the movement is generally towards the extracted area, but can vary due to the degree of regional horizontal stress adjustment around extracted area and the surface topography.

Far-field displacements (FFDs) generally only have the potential to damage long, linear features such as pipelines, bridges, dam walls and railway lines.

Overall, the far-field movements outside a distance equal to one cover depth from the longwall extraction limits are unlikely to generate significant strains or movement to cause cracking or damage to the surface (see **Figure 29b**).

9.7.2 Impact Management Strategies

Any surface features such as bridges or culverts within 5 times the cover depth (e.g. 800 m from the proposed longwalls on the eastern side of Stage 2) should be monitored for FFD movements during mining. It is understood that the Werris Creek Mungindi Railway and Kamilaroi Highway with their associated infrastructure are the only public utilities that exist to the east of the proposed modification area and are outside the 5 times cover depth range.

The deeper western side of the Modified mining layout may affect a larger area of up to 1.5 km away, however it is understood that there are no man-made infrastructure items within this range either.

It is therefore still considered unnecessary to develop a FFD Impact Management Plan unless the mine is required to confirm that the movements are negligible at selected points along the boundary of the NM mining lease and/or railway line bridges.

9.8 Aboriginal Cultural Heritage Sites

9.8.1 Predicted Effects and Impacts

The revised predictions of final subsidence, tilt, horizontal strain and surface gradient change for each listed Aboriginal cultural heritage site after the extraction of LW 101-120 are presented in **Table 13**. The locations of the sites are shown in **Figures 1d** and **2c**.

Table 13 - Predicted Worst-case Subsidence Effects at Aboriginal Cultural Heritage Sites

Site No	Type	Easting (MGA) (m)	Northing (MGA) (m)	LW #	Archaeological Significance	Final Subsidence (m)	Final Tilt (mm/m)	Final Gradient Change (%)	Horizontal Strain (mm/m)*	
									Final	Transient
1	AS	774380	6623220	107	Low	-2.773	2	-0.1	-5	3
2	IA	774460	6623260	107	Low	-2.393	18	0.5	-7	4
3	AS	774680	6623380	106	Low	-0.360	18	0.7	13	6
4	AS	774540	6623370	105	Low	-1.103	29	0.1	3	2
5	AS	775150	6622600	107	Low	-2.652	16	-1.0	-16	8
6	AS	775250	6623000	105	Low	-0.967	40	-1.1	10	5
7	AS	775170	6623200	105	Low	-2.751	5	0.2	-10	5
8	IA	775100	6623230	105	Low	-2.310	29	0.9	-17	9
9	IA	775000	6623380	105	Low	-0.140	3	0.2	14	7
10a	AS	775270	6623190	103	Low	-0.685	36	2.1	17	8
10b	**GG**	**775260**	**6623160**	**103**	**High**	**-0.906**	**41**	**2.1**	**13**	**6**
11	AS	775030	6623313	103	Low	-0.439	25	-0.5	18	9
12	AS	775640	6621690	103	Low	-0.647	33	1.4	17	8
13	AS	775700	6621640	102	Low	-2.322	29	1.9	-18	9
14	IA	775780	6621690	102	Low	-2.741	6	-0.3	-9	5
15	AS	775820	6621630	102	Low	-2.236	33	1.5	-20	10
16	AS	776130	6621700	102	Low	-2.654	6	-0.2	-9	5
17	IA	776180	6621690	101	Low	-1.898	44	2.2	-19	10
18	AS	776200	6621700	101	Low	-1.249	51	2.0	3	2
19	AS	776250	6621700	102	Low	-0.121	11	0.1	20	10
21	IA	776600	6621740	102	Low	-0.039	6	-0.2	11	5
22	AS	776050	6621620	102	Low	-2.583	12	0.4	-15	8
23	AS	776100	6621620	102	Low	-2.693	1	0.0	-2	1
24	AS	776130	6621450	102	Low	-2.574	12	-0.8	-16	8
25	IA	775980	6621270	103	Low	-1.414	46	3.1	-1	1
26	IA	776020	6621260	103	Low	-2.409	23	1.1	-20	10
27	AS	776010	6621200	103	Low	-2.250	30	2.0	-20	10
28	IA	775900	6621080	103	Low	-0.109	2	0.1	15	8
29	IA	775780	6620780	101	Low	-2.005	35	1.3	-14	7
30	AS	775690	6620800	101	Low	-2.645	10	0.1	-10	5
31	AS	775730	6620740	101	Low	-1.915	37	2.3	-12	6
32	AS	776250	6621480	104	Low	-0.086	2	0.0	18	9
33	AS	776250	6621510	104	Low	-0.085	3	0.1	18	9

Table 13 (Cont…) - Predicted Worst-case Subsidence Effects at Aboriginal Cultural Heritage Sites

Site No	Type	Easting (MGA) (m)	Northing (MGA) (m)	LW #	Archaeological Significance	Final Subsidence (m)	Final Tilt (mm/m)	Final Gradient Change (%)	Horizontal Strain (mm/m)*	
									Final	Transient
34	AS	776270	6621560	104	Low	-0.112	9	-0.2	19	10
35	AS	775710	6622970	104	Low	0.000	0	0.0	0	0
36	IA	775760	6623060	104	Low	0.000	0	0.0	0	0
37	IA	775640	6623290	104	Low	-0.269	23	1.5	24	12
38	**AS**	**775580**	**6623390**	**104**	**High**	**-2.157**	**38**	**2.1**	**-23**	**12**
39.1[1]	**AS**	**775660**	**6623460**	**104**	**High**	**-0.127**	**14**	**-0.8**	**18**	**9**
39.2	**AS**	**775680**	**6623480**	**104**	**High**	**-0.028**	**4**	**-0.3**	**8**	**4**
39.3	**AS**	**775680**	**6623520**	**104**	**High**	**-0.032**	**5**	**0.0**	**8**	**4**
39.4	**AS**	**775650**	**6623530**	**104**	**High**	**-0.279**	**24**	**0.8**	**24**	**12**
40	AS	775720	6623530	105	Low	0.000	0	0.0	1	0
41	AS	775630	6623220	102	Low	-0.394	30	-0.4	24	12
42	AS	775640	6623140	105	Low	-0.207	18	-1.2	19	10
43	**OCS**	**775080**	**6620610**	**FW**	**High**	**0.000**	**0**	**0.0**	**0**	**0**
44	IA	774191	6623362	107	Low	-0.338	11	0.4	8	4
45	IA	774225	6623326	107	Low	-0.729	21	1.4	7	3
46	IA	774223	6623302	107	Low	-0.720	21	1.4	7	3
47	AS	774254	6623273	107	Low	-1.257	27	1.7	2	1
48	AS	774286	6623232	107	Low	-1.881	26	-0.2	-4	2
49	AS	774321	6623231	107	Low	-2.398	18	0.3	-7	4
50	AS	774341	6623233	107	Low	-2.593	12	0.0	-7	3
51	AS	773932	6623550	108	Low	-2.778	1	0.0	-3	2
52	AS	773960	6623535	108	Low	-2.706	8	0.5	-7	4
53	AS	773936	6623490	108	Low	-2.786	2	0.1	-7	4
54	AS	774187	6623206	107	Low	-0.375	12	0.3	8	4
55	AS	776564	6620013	Solid	Low	0.000	0	0.0	0	0
56	AS	776577	6620029	Solid	Low	0.000	0	0.0	0	0
57	IA	776708	6620248	Solid	Low	0.000	0	0.0	0	0
58	AS	776629	6620197	Solid	Low	0.000	0	0.0	0	0
59	AS	776571	6620401	FW	Low	0.000	0	0.0	0	0
60	AS	776584	6620427	FW	Low	0.000	0	0.0	0	0
61	AS	776522	6620074	Solid	Low	0.000	0	0.0	0	0
62	AS	776495	6620031	Solid	Low	0.000	0	0.0	0	0
63	AS	776452	6620007	Solid	Low	0.000	0	0.0	0	0
64	IA	776439	6619986	Solid	Low	0.000	0	0.0	0	0
65	AS	776354	6619896	Solid	Low	-0.083	8	-0.5	9	5
66	AS	776268	6619979	120	Low	-1.812	36	-2.3	-10	5
67	AS	776269	6619975	120	Low	-1.784	36	-2.4	-10	5
68	IA	776360	6619836	Solid	Low	-0.044	5	0.1	6	3
69	AS	776353	6619843	Solid	Low	-0.074	7	0.3	9	4
70	AS	776393	6619862	Solid	Low	-0.004	1	0.0	1	1
71	AS	776453	6619769	Solid	Low	0.000	0	0.0	0	0
72	AS	776174	6619651	120	Low	-2.689	2	-0.1	-3	2
73	IA	776111	6619633	120	Low	-2.709	0	0.0	-1	0
74	AS	776035	6619560	120	Low	-2.553	12	0.2	-11	6
75	AS	776054	6619757	120	Low	-2.584	10	0.3	-10	5
76	AS	776129	6619772	120	Low	-2.710	0	0.0	0	0
77	IA	776069	6619787	120	Low	-2.647	6	0.1	-7	3

DgS

Table 13 (Cont…) - Predicted Worst-case Subsidence Effects at Aboriginal Cultural Heritage Sites

Site No	Type	Easting (MGA) (m)	Northing (MGA) (m)	LW #	Archaeological Significance	Final Subsidence (m)	Final Tilt (mm/m)	Final Gradient Change (%)	Horizontal Strain (mm/m)*	
									Final	Transient
78	AS	776021	6619792	120	Low	-2.144	28	0.8	-13	7
79	IA	776219	6619775	120	Low	-2.497	15	-0.9	-13	7
80	AS	776210	6619810	120	Low	-2.583	10	-0.6	-10	5
81	IA	774687	6619444	117	Low	-2.759	2	0.1	-4	2
82	AS	774400	6619174	116	Low	-0.275	7	0.1	9	4
83	AS	774312	6619099	116	Low	-1.381	27	1.7	1	0
84	AS	774282	6619053	116	Low	-1.878	25	1.4	-4	2
85	AS	774250	6619003	116	Low	-2.318	19	0.9	-6	3
86	AS	774230	6618998	116	Low	-2.531	13	0.5	-6	3
87	IA	774166	6618811	116	Low	-2.756	1	0.0	-6	3
88	AS	773570	6618800	115	Low	-1.566	25	-0.9	1	0
89	IA	773971	6619030	116	Low	-0.397	11	0.5	7	4
90	AS	774221	6619181	116	Low	-2.659	9	-0.1	-7	3
91	AS	774975	6619298	118	Low	-0.749	27	1.8	10	5
92	IA	774954	6619212	118	Low	-0.482	21	1.3	12	6
93	AS	774958	6619354	118	Low	-0.445	19	1.2	11	6
94	AS	774955	6619330	118	Low	-0.423	18	1.2	11	6
95	AS	774977	6619291	118	Low	-0.793	28	1.8	9	5
96	AS	774877	6619178	117	Low	-0.249	10	-0.5	9	5
97	IA	774783	6619064	117	Low	-1.617	29	-1.9	-3	2
98	AS	774742	6618977	117	Low	-2.242	21	-1.4	-8	4
99	AS	774697	6618941	117	Low	-2.643	8	-0.5	-6	3
100	AS	774878	6619099	117	Low	-0.214	8	0.4	9	5
101	IA	774980	6619194	118	Low	-0.965	32	-1.0	7	3
102	AS	775044	6619434	118	Low	-2.068	28	1.9	-9	5
103	AS	775195	6617782	118	Low	-1.855	36	-0.9	-11	6
104	AS	775220	6617682	118	Low	-1.062	39	-1.6	6	3
105	AS	775233	6618102	118	Low	-1.298	39	0.6	0	0
106	AS	775007	6616792	118	Low	-2.754	0	0.0	0	0
107	AS	775020	6616744	118	Low	-2.755	0	0.0	0	0
108	AS	775185	6616760	118	Low	-0.762	38	0.3	15	7
109	AS	775089	6616834	118	Low	-2.699	5	-0.2	-7	3
110	AS	775119	6616801	118	Low	-2.456	20	0.3	-17	8
111	AS	775217	6616803	118	Low	-0.211	17	-1.1	17	8
112	AS	775248	6616821	118	Low	-0.030	4	-0.2	6	3
113	AS	779082	6620856	Solid	Low	0.000	0	0.0	0	0
114	AS	779193	6620847	Solid	Low	0.000	0	0.0	0	0
115	IA	779096	6621008	Solid	Low	0.000	0	0.0	0	0
116	AS	779220	6621024	Solid	Low	0.000	0	0.0	0	0
117	IA	779002	6620852	Solid	Low	0.000	0	0.0	0	0
118	AS	778892	6620972	Solid	Low	0.000	0	0.0	0	0
119	AS	778845	6621031	Solid	Low	0.000	0	0.0	0	0
120	IA	778757	6621065	Solid	Low	0.000	0	0.0	0	0
121	AS	778646	6621082	Solid	Low	0.000	0	0.0	0	0
122	**GG**	**776000**	**6622361**	**102**	**High**	**-0.371**	**25**	**1.6**	**20**	**10**
123	**ST**	**774755**	**6623246**	**106**	**High**	**-2.111**	**31**	**0.2**	**-10**	**5**
124	IA	774207	6623420	107	Low	-0.442	15	0.6	8	4

Table 13 (Cont…) - Predicted Worst-case Subsidence Effects at Aboriginal Cultural Heritage Sites

Site No	Type	Easting (MGA) (m)	Northing (MGA) (m)	LW #	Archaeological Significance	Final Subsidence (m)	Final Tilt (mm/m)	Final Gradient Change (%)	Horizontal Strain (mm/m)*	
									Final	Transient
125	IA	774100	6623275	108	Low	-0.510	17	0.0	8	4
126	IA	773989	6623174	108	Low	-2.218	21	-1.2	-6	3
127	AS	773442	6623531	109	Low	-2.786	3	0.0	-9	4
128	IA	772435	6624670	111	Low	-1.515	23	-0.4	0	0
129	AS	772831	6623540	109	Low	-1.199	23	0.6	3	1
130	AS	773065	6621721	110	Low	-0.559	13	-0.9	6	3
131	IA	772841	6621434	110	Low	-2.753	7	0.0	-8	4
132	IA	773063	6621692	110	Low	-0.563	13	0.3	6	3
133	AS	775535	6623132	104	Low	-2.620	13	-0.3	-14	7
134	IA	775608	6623085	104	Low	-0.807	41	0.2	16	8
135	IA	775608	6623150	104	Low	-0.891	44	1.1	15	7

AS - Artefact Scatter; IA- Individual Artefact; GG - Grinding Groove; OCS - Open Camp Site; ST – Scarred Tree.

* - The sites may also be subject to transient phases of tensile and compressive strains of lower or higher magnitude than the final strains.

[1]   Note: Sites 39.1 to 39.4 determined to be a single site.

The Project Approval conditions require the sites of 'High' archaeological significance to be protected from mine subsidence related impact (including proposed remediation measures). The sites of 'High' archaeological significance include:

- two scattered artefact sites (No. 38 and 39) above LW104;

- two grinding groove sites (No. 10b and 122) which comprises grooves in separate sandstone floaters above LW103 and 102 respectively;

- an open camp site (No. 43) is located above the main access headings between the northern and southern longwalls (i.e. above First Workings); and

- one scarred tree (No. 123) above LW106.

The likelihood of cracking and/or erosion damage occurring at the sites was assessed in the 2009 EA using the impact parameter criteria shown in **Table 14**. The criteria consider the theoretical cracking limits of rock of 0.3 to 0.5 mm/m and the 'system' slackness or strain 'absorbing' properties of a jointed and weathered rock mass during subsidence deformation.

The lack of measured observed impact (i.e. surface cracking) due to measured strains of up to 1.5 mm/m at other mine sites in the Newcastle Coalfield is an example of the difference between theoretical and in-situ rock mass tensile cracking behaviour. The specific geotechnical characteristics of each site have been included for the Aboriginal Cultural Heritage Management Plan (ACHMP).

Based on discussions with the Aboriginal heritage consultant for the 2009 EA (refer **Archaeological Surveys & Reports, 2009**), the scattered artefact sites (No. 38 and 39) are susceptible to erosion from mine induced cracking and ponding impact. The grinding groove sites (No. 10b and No. 122) would also normally be considered susceptible to cracking damage, however, due to their apparent location on separate sandstone floaters, the likelihood of damage is significantly reduced.

The specific geotechnical characteristics of each site have been included for the ACHMP.

Table 14 – Impact Potential Criteria for Aboriginal Cultural Heritage Sites

Indicative Probabilities of Cracking Occurrence	Predicted 'Smooth Profile' Horizontal Strain (mm/m)	
	Tensile	**Compressive**
Very Unlikely (<5%)	<0.5	<2
Unlikely (5 - 10%)	0.5 - 1.5	2 – 3
Possible (10 - 25%)	1.5 - 2.5	3 – 5
Likely (>25%)	>2.5	>5
Indicative Probabilities of Erosion Occurrence	**Predicted Surface Gradient or Tilt Change**	
Very Unlikely (<5%)	<0.3% (<3 mm/m)	
Unlikely (5 - 10%)	0.3-1% (3 - 10 mm/m)	
Possible (10 - 25%)	1-3% (10 - 30 mm/m)	
Likely (>25%)	>3% (>30 mm/m)	

The 'Cracking Potential' is considered the primary damage potential indicator and includes the potential for artefact loss into the cracks. The 'Erosion Potential' is a secondary indicator of damage (i.e. the presence of erosion and sedimentation increases at a site may result in unacceptable long-term degradation of a site).

The results of the impact assessment are presented in **Table 15**.

Table 15 - Predicted Subsidence Impacts at Aboriginal Cultural Heritage Sites

Site No	Type	Archaeological Significance	Predicted Strain*		Predicted Gradient Change (%)	Site Cracking & Loss Potential		Site Erosion Potential
			Transient	Final		Transient	Final	
1	AS	Low	-5	3	-0.1	Likely	Likely	V.Unlikely
2	IA	Low	-7	4	0.5	Likely	Likely	Unlikely
3	AS	Low	13	6	0.7	Likely	Likely	Unlikely
4	AS	Low	3	2	0.1	Possible	Likely	V.Unlikely
5	AS	Low	-16	8	-1.0	Likely	Likely	V.Unlikely
6	AS	Low	10	5	-1.1	Likely	Likely	V.Unlikely
7	AS	Low	-10	5	0.2	Likely	Likely	V.Unlikely
8	IA	Low	-17	9	0.9	Likely	Likely	Unlikely
9	IA	Low	14	7	0.2	Likely	Likely	V.Unlikely
10a	AS	Low	17	8	2.1	Likely	Likely	Possible
10b	GG	High#	13	6	2.1	Unlikely	Unlikely	Unlikley
11	AS	Low	18	9	-0.5	Likely	Likely	V.Unlikely
12	AS	Low	17	8	1.4	Likely	Likely	Possible
13	AS	Low	-18	9	1.9	Likely	Likely	Possible
14	IA	Low	-9	5	-0.3	Likely	Likely	V.Unlikely
15	AS	Low	-20	10	1.5	Likely	Likely	Possible
16	AS	Low	-9	5	-0.2	Likely	Likely	V.Unlikely
17	IA	Low	-19	10	2.2	Likely	Likely	Possible
18	AS	Low	3	2	2.0	Possible	Likely	Possible
19	AS	Low	20	10	0.1	Likely	Likely	V.Unlikely
21	IA	Low	11	5	-0.2	Likely	Likely	V.Unlikely
22	AS	Low	-15	8	0.4	Likely	Likely	Unlikely
23	AS	Low	-2	1	0.0	Unlikely	Unlikely	V.Unlikely
24	AS	Low	-16	8	-0.8	Likely	Likely	V.Unlikely
25	IA	Low	-1	1	3.1	Unlikely	V.Unlikely	Likely
26	IA	Low	-20	10	1.1	Likely	Likely	Possible
27	AS	Low	-20	10	2.0	Likely	Likely	Possible
28	IA	Low	15	8	0.1	Likely	Likely	V.Unlikely
29	IA	Low	-14	7	1.3	Likely	Likely	Possible
30	AS	Low	-10	5	0.1	Likely	Likely	V.Unlikely
31	AS	Low	-12	6	2.3	Likely	Likely	Possible
32	AS	Low	18	9	0.0	Likely	Likely	V.Unlikely
33	AS	Low	18	9	0.1	Likely	Likely	V.Unlikely
34	AS	Low	19	10	-0.2	Likely	Likely	V.Unlikely
35	AS	Low	0	0	0.0	V.Unlikely	V.Unlikely	V.Unlikely
36	IA	Low	0	0	0.0	V.Unlikely	V.Unlikely	V.Unlikely
37	IA	Low	24	12	1.5	Likely	Likely	Possible
38	**AS**	**High**	**-23**	**12**	**2.1**	**Likely**	**Likely**	Unlikely
39.1	**AS**	**High**	**18**	**9**	**-0.8**	**Likely**	**Likely**	**V.Unlikely**
39.2	**AS**	**High**	**8**	**4**	**-0.3**	**Likely**	**Likely**	**V.Unlikely**
39.3	**AS**	**High**	**8**	**4**	**0.0**	**Likely**	**Likely**	**V.Unlikely**
39.4	**AS**	**High**	**24**	**12**	**0.8**	**Likely**	**Likely**	**Unlikely**
40	AS	Low	1	0	0.0	V.Unlikely	Unlikely	V.Unlikely
41	AS	Low	24	12	-0.4	Likely	Likely	V.Unlikely
42	AS	Low	19	10	-1.2	Likely	Likely	V.Unlikely
43	**OCS**	**High**	**0**	**0**	**0.0**	*V.Unlikely*	*V.Unlikely*	*V.Unlikely*
44	IA	Low	8	4	0.4	Likely	Likely	Unlikely

DgS

Table 15 (Cont…) - Predicted Subsidence Impacts at Aboriginal Cultural Heritage Sites

Site No	Type^	Archaeological Significance	Predicted Strain*		Predicted Gradient Change (%)	Site Cracking & Loss Potential		Site Erosion Potential
			Transient	Final		Transient	Final	
45	IA	Low	7	3	1.4	Likely	Likely	Possible
46	IA	Low	7	3	1.4	Likely	Likely	Possible
47	AS	Low	2	1	1.7	Unlikely	Possible	Possible
48	AS	Low	-4	2	-0.2	Possible	Possible	V.Unlikely
49	AS	Low	-7	4	0.3	Likely	Likely	Unlikely
50	AS	Low	-7	3	0.0	Likely	Likely	V.Unlikely
51	AS	Low	-3	2	0.0	Possible	Possible	V.Unlikely
52	AS	Low	-7	4	0.5	Likely	Likely	Unlikely
53	AS	Low	-7	4	0.1	Likely	Likely	V.Unlikely
54	AS	Low	8	4	0.3	Likely	Likely	V.Unlikely
55	AS	Low	0	0	0.0	V.Unlikely	V.Unlikely	V.Unlikely
56	AS	Low	0	0	0.0	V.Unlikely	V.Unlikely	V.Unlikely
57	IA	Low	0	0	0.0	V.Unlikely	V.Unlikely	V.Unlikely
58	AS	Low	0	0	0.0	V.Unlikely	V.Unlikely	V.Unlikely
59	AS	Low	0	0	0.0	V.Unlikely	V.Unlikely	V.Unlikely
60	AS	Low	0	0	0.0	V.Unlikely	V.Unlikely	V.Unlikely
61	AS	Low	0	0	0.0	V.Unlikely	V.Unlikely	V.Unlikely
62	AS	Low	0	0	0.0	V.Unlikely	V.Unlikely	V.Unlikely
63	AS	Low	0	0	0.0	V.Unlikely	V.Unlikely	V.Unlikely
64	IA	Low	0	0	0.0	V.Unlikely	V.Unlikely	V.Unlikely
65	AS	Low	9	5	-0.5	Likely	Likely	V.Unlikely
66	AS	Low	-10	5	-2.3	Likely	Likely	V.Unlikely
67	AS	Low	-10	5	-2.4	Likely	Likely	V.Unlikely
68	IA	Low	6	3	0.1	Likely	Likely	V.Unlikely
69	AS	Low	9	4	0.3	Likely	Likely	Unlikely
70	AS	Low	1	1	0.0	Unlikely	Unlikely	V.Unlikely
71	AS	Low	0	0	0.0	V.Unlikely	V.Unlikely	V.Unlikely
72	AS	Low	-3	2	-0.1	Possible	Possible	V.Unlikely
73	IA	Low	-1	0	0.0	V.Unlikely	V.Unlikely	V.Unlikely
74	AS	Low	-11	6	0.2	Likely	Likely	V.Unlikely
75	AS	Low	-10	5	0.3	Likely	Likely	V.Unlikely
76	AS	Low	0	0	0.0	V.Unlikely	V.Unlikely	V.Unlikely
77	IA	Low	-7	3	0.1	Likely	Likely	V.Unlikely
78	AS	Low	-13	7	0.8	Likely	Likely	Unlikely
79	IA	Low	-13	7	-0.9	Likely	Likely	V.Unlikely
80	AS	Low	-10	5	-0.6	Likely	Likely	V.Unlikely
81	IA	Low	-4	2	0.1	Possible	Possible	V.Unlikely
82	AS	Low	9	4	0.1	Likely	Likely	V.Unlikely
83	AS	Low	1	0	1.7	V.Unlikely	Unlikely	Possible
84	AS	Low	-4	2	1.4	Possible	Possible	Possible
85	AS	Low	-6	3	0.9	Likely	Likely	Unlikely
86	AS	Low	-6	3	0.5	Likely	Likely	Unlikely
87	IA	Low	-6	3	0.0	Likely	Likely	V.Unlikely
88	AS	Low	1	0	-0.9	V.Unlikely	Unlikely	V.Unlikely
89	IA	Low	7	4	0.5	Likely	Likely	Unlikely
90	AS	Low	-7	3	-0.1	Likely	Likely	V.Unlikely
91	AS	Low	10	5	1.8	Likely	Likely	Possible
92	IA	Low	12	6	1.3	Likely	Likely	Possible

DgS

Table 15 (Cont…) - Predicted Subsidence Impacts at Aboriginal Cultural Heritage Sites

Site No	Type^	Archaeological Significance	Predicted Strain*		Prdicted Gradient Change (%)	Site Cracking & Loss Potential		Site Erosion Potential
			Transient	Final		Transient	Final	
93	AS	Low	11	6	1.2	Likely	Likely	Possible
94	AS	Low	11	6	1.2	Likely	Likely	Possible
95	AS	Low	9	5	1.8	Likely	Likely	Possible
96	AS	Low	9	5	-0.5	Likely	Likely	V.Unlikely
97	IA	Low	-3	2	-1.9	Possible	Possible	V.Unlikely
98	AS	Low	-8	4	-1.4	Likely	Likely	V.Unlikely
99	AS	Low	-6	3	-0.5	Likely	Likely	V.Unlikely
100	AS	Low	9	5	0.4	Likely	Likely	Unlikely
101	IA	Low	7	3	-1.0	Likely	Likely	V.Unlikely
102	AS	Low	-9	5	1.9	Likely	Likely	Possible
103	AS	Low	-11	6	-0.9	Likely	Likely	V.Unlikely
104	AS	Low	6	3	-1.6	Likely	Likely	V.Unlikely
105	AS	Low	0	0	0.6	V.Unlikely	V.Unlikely	Unlikely
106	AS	Low	0	0	0.0	V.Unlikely	V.Unlikely	V.Unlikely
107	AS	Low	0	0	0.0	V.Unlikely	V.Unlikely	V.Unlikely
108	AS	Low	15	7	0.3	Likely	Likely	V.Unlikely
109	AS	Low	-7	3	-0.2	Likely	Likely	V.Unlikely
110	AS	Low	-17	8	0.3	Likely	Likely	V.Unlikely
111	AS	Low	17	8	-1.1	Likely	Likely	V.Unlikely
112	AS	Low	6	3	-0.2	Likely	Likely	V.Unlikely
113	AS	Low	0	0	0.0	V.Unlikely	V.Unlikely	V.Unlikely
114	AS	Low	0	0	0.0	V.Unlikely	V.Unlikely	V.Unlikely
115	IA	Low	0	0	0.0	V.Unlikely	V.Unlikely	V.Unlikely
116	AS	Low	0	0	0.0	V.Unlikely	V.Unlikely	V.Unlikely
117	IA	Low	0	0	0.0	V.Unlikely	V.Unlikely	V.Unlikely
118	AS	Low	0	0	0.0	V.Unlikely	V.Unlikely	V.Unlikely
119	AS	Low	0	0	0.0	V.Unlikely	V.Unlikely	V.Unlikely
120	IA	Low	0	0	0.0	V.Unlikely	V.Unlikely	V.Unlikely
121	AS	Low	0	0	0.0	V.Unlikely	V.Unlikely	V.Unlikely
122	GG	High#	20	10	1.6	Unlikely	Unlikely	Unlikely
123	ST	High	-10	5	0.2	Unlikely	Unlikely	V.Unlikely
124	IA	Low	8	4	0.6	Likely	Likely	Unlikely
125	IA	Low	8	4	0.0	Likely	Likely	V.Unlikely
126	IA	Low	-6	3	-1.2	Likely	Likely	V.Unlikely
127	AS	Low	-9	4	0.0	Likely	Likely	V.Unlikely
128	IA	Low	0	0	-0.4	V.Unlikely	V.Unlikely	V.Unlikely
129	AS	Low	3	1	0.6	Unlikely	Likely	Unlikely
130	AS	Low	6	3	-0.9	Likely	Likely	V.Unlikely
131	IA	Low	-8	4	0.0	Likely	Likely	V.Unlikely
132	IA	Low	6	3	0.3	Likely	Likely	Unlikely
133	AS	Low	-14	7	-0.3	Likely	Likely	V.Unlikely
134	IA	Low	16	8	0.2	Likely	Likely	V.Unlikely
135	IA	Low	15	7	1.1	Likely	Likely	Possible

AS - Artefact Scatter; IA- Individual Artefact; GG - Grinding Groove; OCS - Open Camp Site; ST – Scarred Tree.* - Tensile strain is positive; # - Grinding grooves are considered to be located on two sandstone 'floaters' in alluvial soils. This assumption has significant implications for impact management plan (see **9.8.2**).
Bold - Cracking likely to occur at site of 'high' Archaeological Significance; *italics* - no cracking is likely to occur at site of 'high' Archaeological Significance.

Based on the results in **Table 15**, the potential for cracking is 'likely' at the 'High' archaeologically significant Scattered Artefact site No. 38 to 39 after extraction of LW104. It is considered 'unlikely' that the cracking will result in direct damage to the artefacts themselves; however, they could be lost into cracks if they occur.

Cracking of the Grinding Groove Sites (No. 10b) due to LW105 is considered 'unlikely' because they are on sandstone 'floaters' in soil and not attached to bedrock. It is noted that similar 'floating' grinding grooves above LW102 and 103 (Site No. 122) were not impacted by cracking.

It is considered 'unlikely' that the Scarred Tree (with 'High' archaeological significance) will be damaged by surface cracking and tilting.

The possibility of erosion damage due to gradient increases is assessed for twenty-four artefact sites and the two grinding groove sites. It is understood that there have been no impacts to the sites as a result of subsidence effects above LW101 to LW104, however, the Registered Aboriginal Parties (RAPs) have raised the temporary salvage of artefacts as a management measure. This is yet to be approved in a revision to the sites ACHMP.

9.8.2   Impact Management Strategies

Impact management strategies for Aboriginal cultural heritage sites are presented in the ACHMP for the Narrabri Mine and have been developed in consultation with the RAPs. It is understood that the sites of 'high' Archaeological Significance are fenced off and will be remediated as necessary after mining LW 104 and 105.

9.9   Unsealed Gravel Access Roads and Tracks

9.9.1   Predicted Effects and Impacts

Based on the maximum final subsidence effect predictions, the gravel access roads above LW 101 to 120 are summarised in **Table 16** and shown in **Figure 2a**.

Table 16 – Maximum Final Subsidence Effect Predictions for Access Roads above LW 101 to 120

LW	Cover Depth (m)	Subsidence (m)	Tilt T_{max} (mm/m)	Tensile Strain (mm/m)	Compressive Strain (mm/m)
101-106	160 - 270	0.13 - 2.75	25 - 68	4 - 25	5 – 32
107 - 111	240 - 325	0.24 - 2.75	17 - 44	4 - 25	3 – 16
112 - 120	180 - 360	0.10 - 2.75	18 - 30	2 - 13	3 – 22

* - Subsidence range = Mean Tailgate Chain Pillar Subsidence to Maximum Panel Subsidence.

The unsealed gravel access roads and tracks are likely to be damaged by cracking and shearing in the tensile and compressive strain zones above the proposed longwall panels; see **Figure 15c** and **16c** for northern and southern panels respectively. Maximum tensile crack widths across or along roads are estimated to range between 20 mm and 250 mm. Surface 'steps' or humps due to compressive shear failures are estimated to range between 30 mm and

320 mm. Some sections of road may also require re-grading or drainage remediation works after subsidence development.

9.9.2   Impact Management Strategies

Appropriate impact management strategies relevant to EP development would include the following:

- Regular inspection (i.e. daily) and maintenance of the roads and access tracks during and after each longwall block is extracted.

- Repairs to road surface should be undertaken as required to allow safe passage for all vehicles.

- Local residents and/or site personnel working or passing through these areas should be informed of when and where the above subsidence effects may occur and temporary warning signs should be erected near the limits of actively subsiding areas.

Subsidence impacts may be assumed to start to occur within a 26.5^{o} angle of draw or 0.5 times the cover depth ahead of the retreating longwall face. Full subsidence development and impacts on the roads within an actively subsiding area is likely to be 90% complete when the longwall face has retreated a distance past the road of 1.5 times cover depth or a 56° angle of draw (see also **Section 9.10.2**).

9.10   Water Storage Dams and Soil Conservation (Contour) Banks

9.10.1   Predicted Effects and Impacts

A total of forty-one farm dams are shown to exist above LW 101 to 120 in **Figure 2a**. Several dams have already been subsided by LW101 to 104 but have not required remedial works to be implemented.

Non-engineered farm dams and water storages will be susceptible to surface cracking and tilting (i.e. storage level changes) due to mine subsidence. The tolerable tilt and strain values for the dams would depend upon the materials used, construction techniques, foundation type and likely repair costs to re-establish the dam's function and pre-mining storage capacity (if necessary).

The predicted worst-case subsidence deformations (subsidence, tilt and horizontal strain) at the dams within the limits of longwall extraction are based on **Figures 15a** to **16c**. A summary of likely subsidence effects at the dams above each longwall are summarised in **Table 17**.

Table 17 – Maximum Final Subsidence Effect Predictions for Dams* above LW 101 to 120

LW	No. Existing Dams	Cover Depth (m)	Subsidence (m)	Tilt T_{max} (mm/m)	Tensile Strain (mm/m)	Compressive Strain (mm/m)
102	4	175 - 188	0.11 - 2.69	41 - 68	8 - 22	10 – 29
103	2	195 - 200	0.12 - 2.75	39 - 64	7 - 18	9 – 24
104	2	160 - 215	0.11 - 2.75	36 - 56	6 - 22	8 – 27
105	4	200 - 235	0.12 - 2.75	31 - 63	5 - 17	7 – 22
106	5	220 - 255	0.20 - 2.75	26 - 53	4 - 14	5 – 18
107	2	240 - 285	0.28 - 2.75	23 - 44	4 - 13	5 – 13
108	2	265 - 305	0.34 - 2.75	24 - 36	3 - 10	4 – 13
110	1	310 - 335	0.44 - 2.75	18 - 30	3 - 8	3 – 10
111	1	325 - 360	0.30 - 2.75	17 - 28	2 - 7	3 – 8
116	2	245 - 280	0.23 - 2.75	23 - 43	4 - 12	5 – 16
117	2	225 - 245	0.19 - 2.75	28 - 48	5 - 14	6 – 18
118	4	200 - 225	0.11 - 2.75	32 - 54	6 - 18	8 – 22
119	4	190 - 210	0.14 - 2.75	35 - 59	7 - 20	8 – 25
120	6	180 - 205	0.10 - 2.75	35 - 62	7 - 21	9 – 27

* - Not all dams will be subject to maximum values shown. Refer to **Figures 15a** to **16c** for specific location predictions; * - Subsidence range = Mean Tailgate Chain Pillar Subsidence to Maximum Panel Subsidence.

The expected phases of tensile and compressive strain development may result in breaching of the dam walls or water losses through the floor of the dam storage area. Loss or increase of storage areas may also occur due to the predicted tilting. Maximum tensile crack widths across dam wall or storage areas are estimated to range between 20 mm and 250 mm. Surface 'steps' or humps due to compressive shear failures are estimated to range between 30 mm and 320 mm. Damage to windmills and fences near the dams and soil conservation (contour) banks may also occur and require repairing.

9.10.2 Impact Management Strategies

Appropriate impact management strategies and relevant EP issues would include the following:

(i)   The development of a suitable monitoring and response plan based on consultation with stakeholders and regulatory authorities, to ensure the impacts on the dams, windmills or fences do not result in unsafe conditions or loss of access to water during and after the effects of mining.

(ii)   Management of impacts would include maintaining the integrity of the dams and preventing potential downstream flooding or erosion damage and/or providing an alternate supply of water to the affected stakeholder, until the dams can be reinstated to pre-mining conditions (including re-filling the dams). Threats to public/personnel/ livestock safety should also be managed by good communication and keeping downstream areas clear until mining impacts to the dams are restored or controlled.

(iii)   Damage from subsidence (i.e. cracking and tilting) can manifest quickly after mining (i.e. within hours). The appropriate management plan will therefore need to consider the time required to respond to the impact in a controlled manner, when it occurs. It

will also be possible to identify the dams likely to be impacted significantly, based on their location above the mine panels and predicted subsidence contours.

(iv) Suitable responses to subsidence impacts would be to either (i) drain the dam storage area before subsidence occurs and repair the dam with an impermeable clay liner after mining, or (ii) monitor the dam wall during mining and place high capacity pumps on 24 hour stand-by during mining to draw down the storage area, if the walls are significantly weakened by subsidence development.

Subsidence impacts may be assumed to start to occur within a 26.5^o angle of draw or 0.5 times the cover depth ahead of the retreating longwall face. Full subsidence development and impacts on the dams within an actively subsiding area is likely to be 90% complete when the longwall face has retreated a distance past the road of 1.5 times cover depth.

Additional subsidence episodes may then occur at a subsided area when subsequent longwalls retreat past the site again, however the extra subsidence would be 'unlikely' to cause further cracking damage.

9.11   Property Fences, Livestock and Orchards

9.11.1   Predicted Effects and Impacts

The fence lines, orchards and grazing areas above longwalls 101 to 120 would be subject to the maximum predicted subsidence effects and cracking presented in **Table 18**.

Table 18 - Maximum Final Subsidence Effect Predictions for Fences and Orchards above LW 101 to 120

LW	No. of Existing Fences (orchards)	Cover Depth (m)	Subsidence* (m)	Tilt T_{max} (mm/m)	Tensile Strain (mm/m)	Compressive Strain (mm/m)
101	7	165 - 177	0.21 - 2.56	46 - 68	10 - 25	13 - 32
102	8	175 - 188	0.14 - 2.69	41 - 62	9 - 22	10 - 29
103	5	175 - 188	0.14 - 2.75	36 - 56	7 - 18	9 - 24
104	9	180 - 215	0.13 - 2.75	31 - 47	6 - 15	8 - 27
105	9 (2)	200 - 235	0.14 - 2.75	26 - 57	5 - 17	6 - 22
106	9	210 - 270	0.24 - 2.75	25 - 39	4 - 14	5 - 18
107-111	1 - 10	240 - 325	0.28 - 2.75	17 - 44	2 - 13	3 - 16
112-120	0 - 20	180 - 360	0.11 - 2.75	18 - 30	3 - 18	3 - 22

* - Subsidence range = Mean Tailgate Chain Pillar Subsidence to Maximum Panel Subsidence.

Impact to fences and orchards is likely to include the following:

- Straining and possibly tensile failure of fencing wire strands in tensile strain zones.

- Sagging of fencing wire strands and possibly loss of fence serviceability in compressive strain zones.

- Loss of gate function in either tensile or compressive strain zones.

- Tilting of fence, gate and strainer posts, leading to the outcomes mentioned above.

9.11.2 Impact Management Strategies

The impact of subsidence on the grazing of livestock would primarily require either the installation of temporary fencing or re-location of the livestock during repair of surface cracking and damaged fences. The location and suggested methods of repair to surface cracking is discussed further in **Section 9.2**.

9.12 Residential Dwellings and Machinery Sheds

9.12.1 Predicted Effects and Impacts

The existing buildings within the limits of LW 101 to 120 include residential dwellings (which would vacated prior to subsidence occurring), machinery sheds and water storage tanks (see **Figure 2a** for their location). The structures may be subject to between 50% and 100% of the subsidence effects presented in **Table 19**. All other existing buildings are located outside a 26.5^o angle of draw to the longwall panels and are unlikely to be impacted by subsidence effects.

Table 19- Maximum Final Subsidence Effect Predictions for Buildings above LW 101 to 120

LW	No. of Existing Buildings (tanks)	Cover Depth (m)	Subsidence* (m)	Tilt T_{max} (mm/m)	Tensile Strain (mm/m)	Compressive Strain (mm/m)
105	2 (1)	200 - 240	0.12 - 2.75	30 - 57	5 - 18	7 - 23
107	3 (7)	240 - 285	0.24 - 2.75	23 - 44	4 - 13	5 - 13
117	5 (4)	225 - 245	0.16 - 2.75	23 - 43	5 - 14	6 - 18
118	1 (1)	200 - 225	0.11 - 2.75	32 - 54	6 - 18	7 - 22

* - Subsidence range = Mean Tailgate Chain Pillar Subsidence to Maximum Panel Subsidence.

Based on **Holla & Barclay, 2000**, 'significant' damage to the existing buildings and tanks is likely where tilts > 7 mm/m and tensile and/or compressive strains > 4 mm/m. The severity of the damage will also be dependent on the type and geometry of each structure and whether localised 'humps' and 'troughs' develop over the goaf as it consolidates.

9.12.2   Impact Management Strategies

Based on the above, it may be assumed that all of the structures above the longwalls will require repair/demolishing after undermining occurs and that machinery sheds should be vacated before subsidence develops. It is noted that the dwellings would be vacated prior to subsidence occurring.

Mine subsidence (and possibly surface vibrations) will start to develop soon after a longwall retreats beneath the buildings and tanks. Mine subsidence movements would be expected to continue until the longwall face is 1 to 2 times the cover depth past the property; see **Figure 30**.

Subsidence movements would also be expected to 'start again' soon after the passing of subsequent longwall panels, albeit at decreasing rates and magnitudes. It is considered likely that primary subsidence movements will affect undermined properties for periods of 3 to 6 weeks after undermining, with residual subsidence occurring for periods of another 1 to 2 years after primary subsidence is complete (see **Glossary** for definitions of primary and residual subsidence).

An inspection of mine subsidence damaged structures should be made by qualified building consultants and any repair works to internal/externals cracking or re-levelling of damaged structures be implemented before allowing residents to move back into the dwellings. Alternatively, unoccupied, mine-owned dwellings may be demolished if necessary.

9.13   Utilities

9.13.1   Predicted Effects and Impacts

It is understood that the existing properties within the mining lease are connected to the following utilities:

- Telstra copper cabling (buried)

- Energy Australia domestic power supply (suspended 415V)

The Telstra line within LW 101 to 105 only goes to one company owned house with a company person as the tenant and the line has been disconnected. The mine has advised that assessment of the impact of the proposed longwalls on the line is not necessary at this stage.

There are fifteen timber power poles (P1 to 15) within the angle of draw above LW 101 - 105. The line provides power to the residence and machinery shed adjacent to the orchard above LW105. The poles are approximately 15 m high and 85 m apart on average (distances vary from 31 m to 132 m) as shown in **Figure 1**.

Some of the poles have been undermined by LW 101 to 103, with some prediction exceedances apparent. Worst-case predictions of final subsidence, tilt, strain and final tilt direction at each pole have been updated in **Table 20**.

The power poles would be subject to transient movements towards the retreating longwall face, and would generally start moving towards the north and then 'swing' around (up to 90 degrees in bearing) to their final positions after subsidence is fully developed. The poles would also be subject to tensile and compressive strains associated with the subsidence 'wave' as it passes underneath the poles. The transient tilts and strains are expected to range from 50% to 100% of the final values, and would be dependent on longwall face retreat rates.

Conductor clearances are estimated to be decreased by between 0.00 m and 1.87 m along the easement; see **Table 20**. The conductors are supported by relatively inflexible ceramic insulators that would probably not be able to tolerate the predicted pole movements. Sheaves and rollers have subsequently been installed to allow poles to move in accordance with the EEMP.

Table 20 - Worst-Case Final Subsidence Predictions for the Power Poles in the EP Area

Pole No.	Easting (MGA) (m)	Northing (MGA) (m)	Maximum Subsidence S_{max} (m)	Final Tilt[+] T_{max} (mm/m)	Final Tilt Direction (grid) (o)	Final Ground Strain[&] (mm/m)	Final HD* Base (mm)	HD^ Top (mm)	Maximum Conductor Clearance Loss[#] (m)	
									First	Final
1	776938	6620616	0.00	0	-	0	0	0	0.00	0.00
2	776621	6620675	0.00	0	292	0	0	0	-0.77	-0.77
3	776342	6620726	2.19	22	039	-10	346	670	-1.11	-1.96
4	776103	6620771	2.28	24	289	-12	381	739	-0.07	0.13
5	775879	6620812	0.11	2	272	12	27	52	-0.11	0.16
6	775620	6620860	1.19	41	093	4	659	1276	-0.91	-1.20
7	775365	6620907	2.72	7	091	-11	114	221	-1.25	-1.78
8	775110	6620954	1.72	39	273	-4	622	1206	0.00	0.00
9	775087	6621106	2.40	25	272	-12	398	772	0.01	0.00
10	775064	6621255	2.71	6	276	-13	92	179	na	na
11	775084	6620724	0.15	10	349	7	159	309	-0.01	-0.01
12	775058	6620496	0.00	0	-	0	0	0	0.00	0.00
13	775032	6620270	0.00	0	-	0	0	0	0.00	0.00
14	775011	6620083	0.00	0	-	0	0	0	0.00	0.00
15	774811	6619832	0.00	0	-	0	0	0	0.00	0.00

+ - Transient tilts due to travelling subsidence wave may be assumed to equal the final tilt magnitudes at a given location. Further analysis may be required if marginal conditions indicated.
& - Tension is positive. Transient strains may be assumed to equal to Final values.
* - HD Base = Absolute horizontal displacement of pole at ground level.
^ - HD top = Absolute horizontal displacement of pole at conductor level (assumed to be 15 m above the ground)
# - clearance loss at goaf edge between next pole and current pole.
Bold - Maximum clearance loss for the power line.

9.13.2   Impact Management Strategies

In addition to the EEMP developed for the power line that traverses LW101 to LW105, impact management strategies could also include:

(i)   Replacement of any damaged poles and/or mitigation works to conductors as mine subsidence develops. Flexible/roller-type conductor sheathing on the poles to control the conductor tension during/after mining impacts have already been implemented.

(ii)   Damage from subsidence (i.e. cracking and tilting) can manifest quickly after mining (i.e. within hours). The appropriate management plan will therefore need to consider the time required to respond to an impact exceedance if it occurs.

9.14   Narrabri Coal Mine Site and Other Infrastructure

9.14.1   Predicted Effects and Impacts

No damage or impacts are expected to the proposed mine site infrastructure, given it is located > 800 m east of the subsidence and strain zone (i.e. 0.5 times the cover depth of 160 m) and the far-field displacement zone (i.e. 5 times the cover depth of 160 m).

The Werris Creek Mungindi Railway and Kamilaroi Highway are both located > 1.9km to the east of the proposed longwalls 101 - 120 and it is therefore extremely unlikely that they will be affected by horizontal or vertical movements due to mine subsidence.

9.14.2   Impact Management Strategies

As measurable subsidence and horizontal displacement due to mining is 'very unlikely' to occur, it is suggested that environmental or 'confirmation' monitoring points are established at several accessible points adjacent to the western side of the railway line easement for before and after longwall panel monitoring of vertical and horizontal displacements (X, Y, Z).

10.0 Monitoring Program

10.1 Subsidence Development

The development of subsidence above a longwall panel generally consists of two phases that are defined as 'primary' and 'residual' subsidence.

Primary subsidence refers to the subsidence that is directly related to the retreating longwall face.

Residual subsidence, due to re-consolidation of goaf, represents approximately 5 to 10% of maximum final subsidence and will be on-going for several months to years after primary subsidence ceases.

Reference to **ACARP, 2003** indicates that measurable subsidence at a given location above the longwall panel centreline is likely to commence at a distance of about 50 to 100 m ahead of the retreating longwall face; accelerate up to rates from 50 to 300 mm/day when the face is 0.2 to 1 times the cover depth past the point; and decrease to < 0.020 m/week when the face is > 1.5 times the cover depth past the point (see **Figure 30**). Further subsidence is likely to develop due to compression of chain pillars when adjacent panels are subsequently mined.

10.2 Surface Monitoring

Surface monitoring to date has been conducted in relatively cleared grazing areas above the eastern portion of the NM. Future mining will be extended below natural bushland areas that would require extensive clearing to install survey monitoring lines.

It is therefore considered appropriate to reduce the number of ground based survey lines and rely more upon remote ALS monitoring techniques and existing access roads (instead of clearing new lines). It is not considered necessary to extend the creek lines any further if ground-truthed ALS information can be used instead to derive subsided profiles.

It is still considered necessary to measure cross line and panel starting end centreline angles of draw to the 20 mm subsidence contour due to the level accuracy limitations of the ALS results (which only has +/- 0.15 m level accuracy).

The following subsidence and strain-monitoring program is therefore suggested to provide adequate information to monitor and implement appropriate subsidence impact data for planning review and subsidence management purposes.

(i)   Extend the transverse subsidence line (Line A) across the subsequent panels 106 to 111 (on existing access tracks) to the middle of the next adjacent longwall panel before undermining occurs above the current panel or for a minimum distance equal to the cover depth.

(ii)   Install a longitudinal line extending in-bye and out-bye from the panel starting points where it is feasible (i.e. does not require excessive clearing) for a minimum distance equal to the cover depth.

(iii)   Install representative cross lines and end of panel centrelines as required for LW 112 to 120 where it is feasible (i.e. does not require excessive clearing) for a minimum istance equal to the cover depth).

(iv)   Complete ALS survey after each panel is completed.

The survey pegs should be spaced at a minimum of 10 m and a maximum of 15 m apart. A minimum of two baseline surveys of subsidence and strain is recommended before mine subsidence effects occur. Survey frequency will be dependent upon mine management requirements for subsidence development data in order to implement subsidence and mine operation management plans.

The suggested monitoring program also assumes that visual inspections and mapping of surface impacts will be conducted before, during, and after mining.

Subsidence and strains may be determined using total station techniques to determine 3-D coordinates, provided that the survey accuracy is suitable. Survey accuracy using EDM and traverse techniques from a terrestrial base line is normally expected to be +/- 2mm for level and +/- 7 mm for horizontal displacement (i.e. a strain measurement accuracy of +/- 0.7 mm/m over a 10 m bay-length).

Strain measurements using the steel tape method generally improve the accuracy to +/- 2mm (or 0.2 mm/m strain over 10 m) and would be the preferred method for measuring strain impacts on dams.

10.3   Sub-Surface Monitoring

It is noted that no deep borehole extensometer or piezometer instrumentation monitoring has been installed to directly monitor heights of groundwater level impacts at the NM. The assessment of HoF has therefore been necessarily conservative to ensure that performance criteria are not exceeded.

Typical monitoring of sub-surface fracture heights above longwall panels requires the direct measurement of vertical strata dilation between the surface - 10 m and the seam level + 50 m with deep borehole extensometers above the centre of a longwall panel. The instrument should also be installed at a distance greater than the panel width from the ends to avoid end effects.

Deep boreholes with multi-level vibrating wire piezometers may be installed to monitor groundwater impacts adjacent to the extensometers but upstream of the extraction limits or above the chain pillars between the panels.

Inspections and monitoring of underground workings stability, groundwater makes and goaf air entry should also be recorded and included with subsidence monitoring data.

DgS

11.0   Conclusions

The Modified mining layout would have six approved longwalls (LW 101 to 106) that would be 306.5 m wide, with 14 proposed longwalls (LW 107 to 120) that will be 408.9 m wide. The predicted subsidence effects and likely impacts for the proposed modification to the approved Narrabri Mine layout have been compared to the previously assessed predictions provided in the 2009 EA submission.

The cover depths vary from 160 m to 180 along the eastern side (LW 101 and 120) and from 340 m to 380 m along the western side of the mining area (LW 111 and 112). The mining height for the modified panels will be 4.3 m instead of 4.2 m as per the 2009 EA.

The subsidence prediction model used in the 2009 EA estimated a maximum subsidence of 2.44 m or 0.58T. Although the predicted values for LW 101 to 104 have been within 15% of the measured results, the model has now been adjusted to reflect the actual 95%CLs for subsequent panels as follows:

- Single Panel S_{max}/T increased from 0.58 to 0.60 for LW101 and 0.63 from LW102 to 120 (see **Figures 5a,b**).

- Final maximum panel S_{max}/T has been increased to 0.61T for LW101 and 0.64T for LW 102 to 120.

- Supercritical width appears to occur at 1.2H instead of 1.4H, based on measured tilts and strains to-date.

It is considered that the development of subsidence impacts would be not be affected by the spanning potential of the Garrawilla Volcanics, Basalt Sill or Digby Conglomerate units. Subsidence predictions have therefore only considered 'Low' SRP for the worst-case scenario. Revised subsidence profiles and contours have subsequently been derived for LW 101 to 120.

The key outcomes of the results of the study are presented below for the modified layout:

(i)   Final maximum panel subsidence is likely to range between 2.69 m and 2.75 m (64% of the mining height).

(ii)   Final maximum chain pillar subsidence is estimated to range between 0.11 m and 0.76 m above twin chain pillar widths ranging from 28 m to 36 m. The vertical stress acting on the pillars are estimated to range from 9.4 to 28.3 MPa with pillar FoS values of 3.20 to 1.09 estimated for a 3.5 m pillar height.

(iii)   Yielding of the chain pillars is not expected for the proposed mining layout (i.e. the predicted FoS values are > 1). However, strain-hardening of the pillars due to core confinement and goaf materials within the panels themselves would limit and result in eventual cessation of subsidence if overloading conditions were to occur.

(iv)   Maximum panel tilts are estimated to range from 17 to 46 mm/m for 'smooth' profile subsidence, with occasional tilts from 25 mm/m to 68 mm/m due to discontinuous strata behaviour (i.e. localised strata block rotations).

(v)   The maximum compressive strains are expected to range from 3 mm/m to 13 mm/m for 'smooth' profile subsidence, with strains ranging from 8 mm/m to 32 mm/m due to discontinuous strata behaviour (i.e. cracking).

(vi)   The maximum tensile strains are expected to range from 2 mm/m to 10 mm/m for 'smooth' profile subsidence, with strains ranging from 6 mm/m to 25 mm/m due to discontinuous strata behaviour (i.e. cracking).

The results presented in this study generally indicate changes in subsidence effect predictions between the EA and proposed mining layout Modification by approximately +/- 20%. The predicted increases in subsidence effect are unlikely to result in significantly higher impacts or environmental consequences, based on observed impacts to-date. Consequently, the Modification would not change the approved level of subsidence impact for the existing/approved underground mine layout.

It is noted that the height of continuous fracturing predicted using the 2014 Geology Pi-Term Model are 26 to 83 m higher than the EA Report indicated. The overall impact should therefore be re-assessed by the groundwater modelling consultant.

Consistent with previous studies, the results of this study indicate that the surface deformations due to the Modified mining layout are likely to cause the following impacts:

• Surface cracking within tensile strain zones and ranging in width from 20 mm to 250 mm at cover depths ranging from 360 m to 160 m, respectively.

• Surface shearing and uplift within compressive strain zones and ranging in from 30 mm to 330 mm at cover depths ranging from 360 m to 160 m, respectively.

   Note: The above crack widths are U95%CL values, which means that may be exceeded 5% of the time (by definition) due to adverse topographic or geological conditions. For example, it has been noted that in steep terrain around Newcastle, that the crack widths are increased (once they occur) in direct proportion to the measured tilts due to rigid body rotation of the subsided slope. Whilst this effect is unlikely to occur above LW 101-120, the predicted crack widths may be exceeded along the channel bank crests of the creeks and tributaries.

• Surface gradients are likely to increase or decrease by up to 3.5% (+/- 2°) along creeks, with occasional increases of up to approximately 5% (or 3°) (note that consistent with experience to date, higher values are likely to be due to discontinuous strata behaviour and unlikely to be representative of gradient changes along a creek).

• Potential ponding depths of 0.1 to 2.6 m may develop above several of the longwalls and creeks in the flatter areas of the site, based on post-mining contour predictions.

- Direct hydraulic connection to the surface, due to sub-surface fracturing above the panels, is considered unlikely to occur where cover depths are > 160 m.

- According to the **Ditton and Merrick, 2014** Pi-Term models, sub-surface aquifers within 144 m to 281 m above the proposed panels may be affected by direct hydraulic connection to the workings, and with significant long-term increases in vertical permeability. The predicted A-Zone (based on the Geology PI-Term Model) ranges from 78% to 88% of the cover depth; 0.61 to 0.69 times the effective panel width and 34 to 65 times the mining height.

- The results indicate that the Geology Pi-Term Model is the most conservative of the three models assessed, with the height of A-Zone fracturing predicted to encroach within 21 m to 79 m below the surface. Based on this model then, it is considered 'unlikely' that the A-Zone will extend up to the surface cracking zone (i.e. within 10 m below the surface) for the range of cover depths above LW 101 to 120.

- Discontinuous fracturing would be expected to occur above these limits and increase rock mass storage capacity and horizontal permeability by 10 to 100 times without direct hydraulic connection to the workings. Rock mass permeability is unlikely to increase significantly outside the limits of extraction.

- In-direct or discontinuous sub-surface fracturing could interact with surface cracks where cover depths are < 255 m. Creek flows could be re-routed to below-surface pathways and re-surfacing down-stream of the mining extraction limits in these areas due to this interaction. This behaviour usually only occurs where shallow surface rock is present and is unlikely to occur where deep soil profiles exist.

- General and localised slope instability along low-level hills is considered 'very unlikely' due to the predicted cracking and tilting above LW 101 - 120.

- Based on measured results along Pine Creek Tributary No. 1, the development of valley closure and associated uplift in valley floors and along creek beds is unlikely to exceed 150 mm.

- Stock watering dams are 'likely' to be damaged by mine induced cracking and/or shearing, resulting in dam wall breach or storage losses through the floor of the dam storage areas. Repairs to the dams and temporary supplies of water may be required. Windmills and fences around the dams could also be damaged and require repairs after mining.

- One-hundred and twenty nine scattered Aboriginal artefact sites of 'Low' archaeological significance plus six sites of 'High' archaeological significance, comprising two scattered artefact sites (No. 38 and 39), two semi-detached grinding groove sites (No. 10b and 122) and one scarred tree (No. 123) exist within the mine subsidence area for LW 101 to 120.

- It is assessed that the potential for cracking is 'Likely' at the 'High' archaeologically significant scattered artefact site No. 38 to 39 after extraction of LW104. It unlikely that

the cracking would result in direct damage to the artefacts themselves, however, they could be lost into cracks that occur.

- Cracking of the Grinding Groove Sites (No. 10b) due to LW105 is considered 'unlikely' because they are on sandstone 'floaters' in soil and not attached to bedrock. It is noted that similar 'floating' grinding grooves in a significant tensile strain zone above LW102 (Site No. 122) were not impacted by cracking.

- It is considered 'unlikely' that the scarred tree (with 'High' archaeological significance) will be damaged by surface cracking and tilting.

- There is a possibility of erosion damage due to gradient increases at twenty-four artefact sites; however, the presence of cracks also has the potential for artefact loss into the cracks.

- It is understood that there have been no impacts to the sites as a result of subsidence effects above LW101 to LW104, however, the Registered Aboriginal Parties (RAPs) have raised the temporary salvage of artefacts as a management measure. This is yet to be approved in a revision to the sites Aboriginal Cultural Heritage Management Plan (ACHMP).

- The various unsealed roads and tracks around the site are likely to be subject to cracking and shearing during mine subsidence development. The roads are likely to require maintenance and repair works after undermining occurs. Mine subsidence warning signs and possibly closure of the roads should be considered where public safety risks are identified.

- The impact of subsidence on fencing and the grazing of livestock would primarily require either the installation of temporary fencing or re-location of the livestock during repair of surface cracking and damaged fences. The location and suggested methods of repair to surface cracking is discussed further in **Section 9.2**.

- Vacant residential dwellings and machinery sheds are also likely to be significantly impacted during mining (i.e. 'Moderate' to 'Severe' impact rating in accordance with **AS2870:2011**).

  It is recommended that the dwellings and machinery sheds are vacated and all equipment/property of value removed before mining impacts. It is considered likely that subsidence movements will affect undermined properties for periods of at least 2 years after mining. Some of the structures will probably not be repairable after mining is completed.

- The fifteen power line and poles to the various residences and orchards within the mining lease will be subsided by above LW 101 to 105 by between 0.0 m and 2.72 m. The differential subsidence between subsided and non-subsided poles with chain pillars in between them may have conductor clearances decreased by up to 1.96 m or increased by up to 0.16 m.

- The poles will be affected by transient and final tilts towards the centre of the goaf of up to 41 mm/m. The ground strains at the poles are likely to range from +/- 12 mm/m. The predicted tilts and strains have the potential to damage the poles and ceramic conductor isolators. Flexible/roller-type conductor sheathing on the poles to control the conductor tension during/after mining impacts have already been implemented in accordance with the Essential Energy Management Plan (EEMP).

The above items will require further discussion with the stakeholders to enable an acceptable EP to be developed. A suggested program for monitoring subsidence, tilt and strain at the relevant locations has been provided for the purpose of implementing and reviewing the EP.

The use of ALS is considered an appropriate subsidence monitoring technique in lieu of some of the traditional ground based subsidence survey lines.

12.0   References

Archaeological Surveys & Reports, 2009. **Narrabri Coal Mine Stage 2 Longwall Project - Aboriginal Heritage Assessment** (Nov).

ACARP, 1998a. **Chain Pillar Design (Calibration of ALPS)**. Colwell, M., Mark, C.ACARP Report No. C6036 (October).

ACARP, 1998b. **ACARP Project No. C5024, Establishing the Strength of Rectangular and Irregular Pillars**.Galvin, J.M., Hebblewhite, B.K., Salamon, M.D.G., Lin, B.B.

ACARP, 2002. **Subsidence Impacts on River Valleys, Cliffs, Gorges and River Systems**. Project No. C9067, Waddington Kay & Associates, Report WKA110.

ACARP, 2003. **ACARP Project No. C10023, Review of Industry Subsidence Data in Relation to the Impact of Significant Variations in Overburden Lithology and Initial Assessment of Sub-Surface Fracturing on Groundwater**, Ditton, S. and Frith, R.C. Strata Engineering Report No. 00-181-ACR/1 (Sep).

ACARP, 2007. **Hydrological Response to Longwall Mining**. CSIRO Exploration & Mining. H. Guo, D. Adhikary, D. Gaveva. Report No. C14033 (October).

AGS, 2010. **Practice Note Guidelines for Landslide Risk Management 2010**.Australian Geomechanics Society.

AS2870, 2011. **Australian Standard - Residential Slabs and Footings**.

DgS, 2009. **Narrabri Coal Mine Stage 2 Longwall Project Mine Subsidence Predictions and Impact Assessment**. Ditton Geotechnical Services Pty Ltd. Report No. NAR-001/1 (August).

DgS, 2012. **Mine Subsidence Effect Predictions and Impact Assessment for the Proposed Longwalls 101 to 105 at the Narrabri Coal Mine, Narrabri**. DGS Report No. NAR-002/1 (15/02/2012).

DgS, 2015. **Mine Subsidence Assessment for the Proposed Addition of Longwall (LW) 106 to the Approved LW101 to LW105 Extraction Plan at the Narrabri Mine, Narrabri**. DGS Report No. NAR-002/2 (25/05/2015).

Ditton and Merrick, 2014. **A New Sub-Surface Fracture Height Prediction Model for Longwall Mines in the NSW Coalfields**. Presentation given at Australian Earth Sciences Convention, Newcastle (04/07/2014).

EcoLogical Australia Pty Ltd, 2012c**. Extraction Plan - Land Management Plan – Narrabri Mine**.

Forster, 1995. **Impact of Underground Coal Mining on the Hydrogeological Regime, Central Coast, NSW**. Forster, I. Published in Australian Geomechanics Society (AGS) Conference Proceedings (February), Engineering Geology of Newcastle – Gosford Region, University of Newcastle.

Holla & Barclay, 2000. **Mine Subsidence in the Southern Coalfield**. L.Holla and E.Barclay. Department of Minerals Resources (June).

Li *et al.,* 2006. **A Case Study on Longwall Mining Under the Tidal Waters of Lake Macquarie**. G. Li, I. Forster, M. Fellowes and A. Myors, 2006. Proceedings of Coal 2006 Conference, University of Wollongong.

NM, 2015. **Subsidence Management Status Report No. 9**. Narrabri Coal Operations Pty Ltd (13/04/15)

Pells *et al*, 1998. **Foundations on Sandstone and Shale in the Sydney Region**, Pells, P.J.N., Mostyn, G. and Walker, B.F..AustralianGeomechanics Journal.

Reid, 1998. **Horizontal Movements around Cataract Dam, Southern Coalfields**.Reid, P. Mine Subsidence Technological Society 4th Triennial Conference Proceedings. Newcastle, July 1998.

SCT, 2008. **Assessment of Longwall Panel Widths and Potential Hydraulic Connection to Bowmans Creek – Ashton Mine**. SCT Operations Pty Ltd Report to Ashton Coal, September.

Seedsman and Watson, 2001. **Sensitive Infrastructure and Horizontal Ground Movement at Newstan Colliery**. Seedsman, R. W. and Watson, G. Mine Subsidence Technological Society 5th Triennial Conference Proceedings, Maitland, August 2001.

SDPS, 2007. **Subsidence Deformation Prediction System - Quick Reference Guide and Working Examples**.Agioutantis, Z., Karmis, M. Department of Mining and Minerals Engineering, Virginia Polytechnic Institute and State University, Virginia.

Tammetta, 2014. **Estimation of the Change in Hydraulic Conductivity Above Mined Longwall Panels**. Paul Tammetta. Published in Vol 53, No. 1 - Groundwater Journal Jan-Feb 2015.

Vick, 2002. **Degrees of Belief: Subjective Probability and Engineering Judgement**. Vick, S.G., ASCE Press.

WRM, 2015. **Narrabri Mine Modification 5 - Surface Water Assessment**. WRM Water & Environment Pty Ltd.

APPENDIX A - Empirical Subsidence Prediction Model Details

DGS MODIFIED ACARP, 2003 EMPIRICAL SUBSIDENCE AND HEIGHT OF FRACTURING PREDICTION MODEL

A1   Introduction

This appendix provides a description of how subsidence and sub-surface fracturing develops above longwall panels and provides a summary of the empirical subsidence prediction models used in this study.

The **ACARP, 2003** model was originally developed by Strata Engineering (Australia) Pty Ltd under ACARP funding with the goal of providing the industry with a robust and reliable technique to utilise the significant amount of geological and testing information already gathered by mining companies.

Over the past six years the **ACARP, 2003** model has been used successfully by the model's author, Steven Ditton, at several longwall mines in the Newcastle, Hunter Valley, Western and Southern Coalfields of NSW and the Bowen Basin, Queensland.

Subsidence prediction work for Stage 1 of the Moolarben Coal Project in 2006 resulted in further external scrutinization of the model and the robustness of the methodology by an Independent Hearing and Assessment Panel (IHAP), which was set up to assess Environmental Impact Assessments for new coal mining projects by NSW Department of Planning (DoP).

The outcomes of the IHAP for Moolarben resulted in several refinements to the model, as requested by the independent subsidence expert, Emeritus Professor J M Galvin, UNSW School of Mining and Director of Galvin and Associates Pty Ltd.

The refinements generally included several technical adjustments and clarification of the terminology used to enable a better understanding of the model by the wider technical community.

Over the past 7 years, Ditton Geotechnical Services Pty Ltd (DgS) has modified the **ACARP, 2003** model to be able to use it to calibrate an influence function model (SDPS®) that was developed by the Polytechnical Institute for the US Coalfields. The SDPS® program allows a wider range of topographic and complex mining layouts (including longwall and pillar extraction panels) to be assessed.

This appendix summarises the **ACARP, 2003** model in its current format and explains the refinements made to the original model. Details of the **SDPS®** model itself are provided at the back of this appendix.

A2   Description of Subsidence Development Mechanisms above Longwalls

After the extraction of a single longwall panel, the immediate mine roof usually collapses into the void left in the seam. The overlying strata or overburden then sags down onto the collapsed material, resulting in settlement of the surface.

The maximum subsidence occurs in the middle of the extracted panel and is dependent on the mining height, panel width, cover depth, overburden strata strength and stiffness and bulking characteristics of the collapsed strata. For the case of single seam mining, maximum panel subsidence has not exceeded 60% of the mining height (T) in over 95% of the published cases for the Newcastle, and Southern Coalfields (refer **ACARP, 2003** and **Holla and Barclay, 2000**). For the 5% of cases, which did exceed 58%T, the maximum subsidence did not exceed 65%T (i.e. 2.7 m for a 4.2m mining height). The actual subsidence may also be lower than this value due to the spanning or bridging capability of the strata above the collapsed ground (or the goaf).

The combination of the above factors determines whether a single longwall panel will be *sub-critical, critical,* or *supercritical* in terms of maximum subsidence.

Sub-critical subsidence refers to panels that are narrow and deep enough for the overburden to bridge or 'arch' across the extracted panel regardless of geology. It is therefore termed 'deep arching' in the context of the subsidence model.

Beyond the *sub-critical* range, the overburden becomes *critical*, and is unable to develop deep arching behaviour. Spanning of the overburden is dependent on 'shallow beam' bending or Voussoir arching behaviour and the presence of massive, competent strata. Cracking or breakdown of the overburden strata may therefore start to develop above *critical* panel geometries as the spanning mechanism transitions from 'deep arching' to 'shallow beam' behaviour.

Supercritical panels refer to panel geometries that cause complete collapse of the overburden. In the case of super-critical panels, maximum panel subsidence does not usually continue to increase significantly with increasing panel width.

In the Newcastle Coalfields, *sub-critical* or (deep arching) behaviour generally occurs when the panel width (W) is <0.7 times the cover depth (H) and supercritical when W/H > 1.4. Critical behaviour usually occurs between W/H ratios of 0.7 and 1.4. In the deeper areas of the Southern Coalfield, critical subsidence behaviour may start to occur when W/H is > 0.5. As the cover depth averages at about 250 m in the Newcastle Coalfield and 450 m in the Southern Coalfield and both areas have massive strata units in the overburden, this indicates that the cover depth is likely to be a key factor when assessing subsidence.

The transition point from sub-critical to critical behaviour in a particular coalfield is also influenced by the 'bridging' capability of the strata if it can develop a spanning Voussoir Arch. In the Newcastle Coalfield, the commencement of critical panel behaviour can effectively increase up to W/H ratios of 0.9.

The maximum subsidence for sub-critical and critical panel widths is generally < 60% of the longwall extraction height (T) and could range between 5% and 40% T, depending on the thickness of massive sandstone or conglomerate strata.

The surface effect of extracting several adjacent longwall panels is dependent on the stiffness of the overburden and the chain pillars left between the panels. Invariably, 'extra' subsidence occurs above a previously extracted panel and is caused primarily by the compression of the chain pillars and adjacent strata between the extracted longwall panels.

A longwall chain pillar undergoes the majority of life-cycle compression when subject to double abutment loading (i.e. the formation of goaf on both sides of it, after two adjacent panels have been extracted). Surface survey data indicates that an extracted panel can affect the chain pillars between three or four previously extracted panels. The stiffness of the overburden and chain pillar system will determine the extent of load transfer to the preceding chain pillars. If the chain pillars go into yield, the load on the pillars will be mitigated to some extent by load transfer to adjacent fallen roof material or goaf.

The surface subsidence usually extends outside the limits of extraction for a certain distance (i.e. the angle of draw). The angle of draw distance is usually less than or equal to 0.5 to 0.7 times the depth of cover (or angles of draw to the vertical of 26.5^o to 35°) in the NSW and QLD Coalfields.

A3   ACARP Project Overview

The original **ACARP, 2003** model was originally developed for the Newcastle Coalfield to deal with the issue of making reliable subsidence predictions over longwall panels by using both geometrical and geological information.

The project was initially focused on the behaviour of massive sandstone and conglomerate strata in the Newcastle Coalfield, but has now been successfully used in other coalfields since development over the past six years. This has occurred naturally due to the expansion of the model's database with data from other coalfields and has resulted in generic refinements to the model to deal with the wider range of geometrical and geological conditions.

In regards to geometry, the subsidence above a series of longwalls is strongly influenced by the panel width, the cover depth, the extraction height and the stiffness of the interpanel pillars (i.e. the chain pillars) and immediate roof and floor strata.
In regards to geology, the presence of massive strata units, such as conglomerate and sandstone channels above longwall panels, has resulted in reduced subsidence compared to that measured over longwall panels with similar geometry and thinner strata units.

Geological structure, such as faults and dykes, can cause increases in subsidence due to their potential to adversely affect the spanning capability of the overburden.

During the original development of the model, a database of maximum single and multi longwall panel subsidence and associated massive strata units was compiled for the

Newcastle Coalfield. The database draws on subsidence data from over fifty longwall panels and covers a panel width to cover depth (W/H) ratio from 0.2 to 2.0 (cover depth ranges between 70 m and 351 m), as shown in **Figure A1**.

The original project database includes single seam longwall mining data from eleven collieries within the Newcastle Coalfield, as presented in **Table A1**.

Table A1 - Empirical Database Sources from Newcastle Coalfield

Colliery	Colliery	Colliery
Cooranbong	Lambton	Wyee
New Wallsend No. 2 (Gretley)	Teralba	
Moonee	Burwood	
Stockton Borehole	West Wallsend	
Newstan	John Darling	

The wide range of single longwall panel W/H ratios in the database was considered unique compared to the other Australian coalfields and enabled the study to focus on overburden and chain pillar behaviour effects separately.

Pillar extraction or multiple seam data was not used to produce the subsidence prediction curves, as it invariably makes the assessment of geological influences more difficult. Other NSW and QLD longwall and high pillar extraction mine data that have been added to the model database over the past seven years as shown in **Table A2**.

Table A2 - Empirical Longwall Database from Other Mines

Coalfield	Colliery	Colliery
Newcastle	West Wallsend	Newstan
	Mandalong	Chain Valley
Hunter Valley	United	Wollemi
	Austar	North Wambo
Southern	Berrima	Appin
	Elouera	Dendrobium
	Metropolitan	
Western	Springvale	Angus Place
	Ulan	
Queensland	Cook	Oaky Creek
	Moranbah North	

In summary, the key features of the **ACARP, 2003** model are that it:

- Is derived from a comprehensive database of measured subsidence, strain, tilt and curvature above longwalls in the Newcastle, Hunter Valley, Western and Southern Coalfields.

- Has been validated with measured subsidence profile data.

- Adds to the **DMR, 1987** model for the Newcastle Coalfield, as it addresses multiple panels and contains a significantly larger data base.

- Includes the effects of massive sandstone/conglomerate lithology on subsidence.

- Allows reliable predictions of maximum single panel subsidence, chain pillar subsidence, tilt, curvature, strain and the angle of draw within a 95% Confidence Limit.

- Enables 'greenfield' sites (i.e. where there is no subsidence data) to be assessed rapidly and accurately.

- Provides maximum subsidence predictions based on Upper 95% Confidence Limits (or 5% Probability of Exceedence limits), which in practice have rarely been exceeded.

- The confidence limits have been derived by the application of central limit theory and the likely normal distribution of residuals about lines of best fit or regression lines determined for the model database.

- Utilises historical information directly - predictions are based on actual data.

- Enables prediction of secondary tilt, curvature and strain magnitudes. Effects such as 'skewing' due to rapid surface terrain variations, surface 'hump' or step development and cracking can result in tilt, curvature and strain magnitudes significantly greater than predicted 'smooth' profile values.

  This issue has been addressed empirically by linking measured impact parameters with key mining geometry variables. Strain concentration factors and database confidence limits have been developed to estimate the likely range of subsidence impact parameters.

- Is amenable to subsidence contouring and allows the impacts on surface features to be assessed, including post-mining topography levels for watercourse impact assessment.

- Predictions of subsidence at specific locations can be done to provide an indication of likely subsidence magnitude; however, depending on the sensitivity of the feature, it may be prudent to adopt maximum predicted subsidence for a given panel.

- Incorporates an empirical model of sub-surface fracturing and far-field displacements.

  Note: Recent far-field horizontal displacement model work in the Newcastle Coalfield indicates the empirical model is conservative.

The following key input parameters are required to make subsidence predictions using the model:

- Panel Width (W)

- Cover Depth (H)

- Seam Working Height (T)

- Overburden lithology details, specifically the thickness and location of massive strata units (t, y).

- Chain Pillar Height (h), Width (w_{cp}) and Length (l) [solid dimensions]

- Roadway width (r)

The statistical inferences and estimates of the model uncertainty associated with the prediction methodology are presented in the following sections.

A4   Single Panel Subsidence Predictions

A4.1   Geometrical Factors

The major finding of the **ACARP, 2003** project in regards to mining geometry was that the historical relationship between subsidence and panel width to cover depth ratio (W/H) is not a constant for the range of cover depths (H) involved.

Figure A2.1 shows the range of maximum subsidence that can occur above longwall panels with similar mining geometries and a range of cover depths. The apparent differences between the DMR's Southern NSW and Newcastle Coalfield curves and laminated overburden theory (**Heasley, 2000**) also support the above finding.

For an overburden consisting of sedimentary rock layers or plates, **Heasley, 2000** applied laminated beam theory by **Salamon, 1989** to form the basis of the pseudo-numerical subsidence prediction program LAMODEL ("LAyered MODEL" of overburden) that has been found to have reasonable success in the US Coalfields.

According to LAMODEL theory, the maximum seam roof convergence (C_{max}) above a longwall panel of mining height (T), width (W) and cover depth (H), with an idealised overburden of uniform lamination thickness (t), Youngs Modulus (E), unit weight (γ) and Poisson's Ratio (v) is:

$C_{max} = [\sqrt{12(1-v^2)}]/t \, (\gamma H/E) \, (W^2/4)$ or T (whichever gives the lower value)

Several points can be made about this equation:

- The γH term represents the vertical stress acting on the plates at seam level and assumes spanning strata (i.e. sub-critical to critical panels).

- For completely collapsed strata, C_{max} may be assumed to equal T at seam level.

- The surface subsidence may then be estimated as the minimum of $0.5C_{max}$ and $0.6T$ for sub-critical/critical and supercritical panel geometries.

- In terms of traditional empirical models of estimating subsidence, the above equation indicates that the maximum single panel subsidence is a function of W^2/t and $\gamma H/E$ for sub-critical W/H ratios < 0.7 or T for super-critical W/H ratios >1.4. The influence of the panel width and mining height will therefore change with W/H.

Clamped elastic beam theory indicates that strata beam deflections, that are located at a distance y above the mine workings, are a function of $\gamma(H-y)/E$ and W^4/t^3 before cracking at the abutments and mid-span. The deflection of the beam will generate higher tensile stresses in the top of the beam at the abutments than in the bottom of the beam at mid-span. The cracking results in a transition from continuous elastic beam behaviour to a cracked beam of separate blocks or 'voussoirs' under simply supported loading conditions.

The Voussoir beam supports the load through the formation of a compressive arch, which develops as the individual blocks or Voussoirs rotate towards the goaf below it (i.e. the voussoirs cannot sustain tensile stresses, however, the deformed beam will span if the blocks have sufficient strength, stiffness and geometry. The elastic and Voussoir beam cases are shown in **Figure A2.2**.

If the rotated blocks are able to support the load, then the deflection of the cracked Voussoir beam is a function of $\gamma(H-y)/E$ and W^2/t, which is consistent with the laminated beam model theory; see **Figure A2.3**.

The **ACARP, 2003** model surmised that single panel subsidence normalised by mining height T, was a function of W/H, $\gamma H/E$ or H, W/t and y/H in accordance with Buckingham's Pi theory.

The first three parameters above are related to panel geometry (i.e. the panel width, W, cover depth, H, and mining height, T, whilst the last two parameters (strata unit thickness, t, and distance, y, to the unit above the workings) infer geological influences of massive strata units.

Based on the above equations, surface subsidence is expected to increase with increasing cover depth (H) for the same W/H ratio, and is primarily a function of the increasing panel width (W) as $S_{max} = f(W^2/H)$ according to beam theory. For constant single panel width (W), subsidence will therefore decrease with increasing cover depth (H). The subsidence data was subsequently separated into three cover depth categories of H = 100, 200 and 300 m +/-50 m and is presented in **Figures A3** to **A5**.

The influence of overburden lithology was found to be readily apparent once the database was filtered using the above cover depth ranges.

A4.2 Geological Factors

Once the first stage in the development of the subsidence prediction model had addressed the influence of cover depth the effect of "significant" overburden lithology above single longwall / miniwall panels could be addressed. **Figure A6** illustrates a physical model, showing the subsidence reducing effects of a massive strata unit.

Borehole data was used to derive the thickness and location of massive strata units considered to be critically important for surface subsidence prediction, for a given panel width and depth. The methodology takes into account the maximum massive strata unit thickness (t) at each location and the height to the base of the unit above the longwall panel (y).

The subsidence above a panel, given cover depth (H) and panel width (W) decreases significantly when a massive strata unit is thicker than a certain minimum limit value. The thickness is also reduced when the unit is closer to the surface. The strata unit is considered to have a 'high' subsidence reduction potential (SRP) when it exceeds a minimum thickness for a given y/H ratio, as shown in **Figures A7.1** to **A7.3** for each cover depth category.

For a thin strata unit located relatively close to a panel, the 'Subsidence Reduction Potential (SRP) will be 'low'. However, there is also an intermediate zone, where a single strata unit (or several thinner units) below the 'high' subsidence reduction thickness can result in a 'moderate' reduction in subsidence. A second limit line can therefore be drawn, which represents the threshold between 'moderate' and 'low' SRP.

It is considered that the 'high' SRP limit line represents the point between elastic and yielding behaviour of a spanning beam. The 'moderate' SRP limit line represents the point between yielding behaviour and collapse or failure of a spanning beam (which has been yielding).

The limit lines have been determined for the strata units located at various heights (y) above the workings in each depth category, as shown in **Figures A8** to **A10**.

A4.3 Summary of Model Concepts

The **ACARP, 2003** model introduces several new parameters, to improve the definition of various types of overburden behaviour and the associated mechanics.

As outlined in **Section A4.2**, the 'Subsidence Reduction Potential' (SRP) of massive or thickly bedded geological units above single longwall panels for the Newcastle Coalfield has been introduced to describe the influence that a geological unit may have on subsidence magnitudes. The massive geological units are defined in terms of 'high', 'moderate' or 'low' SRP.

Massive unit thickness, panel width, depth of cover and height of unit above the workings are considered to be key parameters for assessing overburden stiffness and spanning capability over a given panel width, controlling surface subsidence. A conceptual model for overburden behaviour is illustrated in **Figure A11**.

Variation in subsidence along the length of a panel may therefore be due to the geometry and / or SRP variation of geological units within the overburden.

For W/H ratios <0.7, the overburden spans across the extracted panel like a 'deep' beam or linear arch, whereby the mechanics of load transfer to the abutments is governed by axial compression along an approximately parabolic shaped line of thrust, see **Figure A12**.

For W/H ratios >0.7 the overburden geometry no longer allows axially compressive structural behaviour to dominate, as the natural line of thrust now lies outside of the overburden. Bending action due to subsequent block rotation occurs. Provided that the abutments are able to resist this rotation, flatter lines of thrust still develop within the overburden, but the structural action is now dominated by bending action. This type of overburden behaviour has been defined as 'shallow' beam behaviour, which in structural terms is fundamentally less stiff than 'deep' beam behaviour. This results in a significant increase in subsidence or sag across an extracted longwall panel (all other factors being equal), as shown **Figure A12**.

"Voussoir beam" or "fractured linear arch" theory can be used to explain both types of overburden behaviour, as deep seated or flatter arches develop in the strata in an attempt to balance the disturbing forces.

The database also indicates the presence of a 'Geometrical Transition Zone', whereby subsidence increases significantly, regardless of the SRP of the geological units, as shown in **Figure A13**. This behaviour occurs when panel width to cover height ratio (W/H) ranges from 0.6 to 0.9. This phenomenon can be simply explained as a point of significant shift in structural behaviour and the commencement of overburden breakdown.

The model therefore allows the user to determine the range of expected subsidence magnitudes and the location of geology related SRP and/or 'geometrical transition zones' along a panel. Identification of the transition zones is an important factor in assessing potential damage risks of differential subsidence to important infrastructure, buildings and natural surface features, such as rivers, lakes and cliff lines etc.

The 'strata unit location factor' (y/H) was developed to assist in assessing the behaviour of massive strata units above the workings. The y/H factor is a simple way to include the influence of the unit location above the workings in terms of the effective span of the unit and the stresses acting upon it.

The key elements of this factor and their influence on the behaviour of the strata unit are:

- y, the height of the beam above the workings, which determines the effective span of the beam, and

- H, cover depth over the workings, which exerts a strong influence on the stress environment and, hence, the propensity for buckling or compressive failure of the beam.

Essentially beam failure due to the action of increasing horizontal stress (i.e. crushing or buckling) appears more likely as y decreases and H increases. The ratio of y/H may therefore be used to differentiate between the SRP of a beam of similar thickness, but at varying heights above the workings. The model also demonstrates that as the depth of cover increases, a thicker beam is required to produce the same SRP above a given panel width. This phenomenon may also be simply due to greater vertical load acting upon the massive strata 'beam'.

A5   Multiple Longwall Panel Subsidence Prediction

A5.1   General

The effect of extracting several adjacent longwall panels is governed by the stiffness of the overburden and the chain pillars left between the panels. Invariably, 'extra' subsidence occurs above a previously extracted panel and is caused primarily by cracking of the overburden and the compression of the chain pillars and adjacent strata between the extracted longwall panels.

A conceptual model of subsidence mechanisms above adjacent longwall panels in a single seam is shown in **Figure A14**.

A5.2   Predicting Subsidence above Chain Pillars (ACARP, 2003 Model)

A chain pillar undergoes the majority of life-cycle compression when subject to double abutment loading (i.e. the formation of goaf on either side, after two adjacent panels have been extracted). Surface survey data indicates that an extracted panel can affect the chain pillars of up to three or four previously extracted panels. The stiffness of the overburden and chain pillar system will determine the extent of load transfer to preceding chain pillars.

Multiple-panel effects have therefore been included in the model by adding empirical estimates of surface subsidence over chain pillars to the maximum subsidence predictions for single panels.

The empirical model presented in **ACARP, 2003** for estimating the subsidence above a chain pillar, was based on the regression equation presented in **Figure A15**. The model compares the ratio of chain pillar subsidence (Sp) over the extraction height (T), to the width of the chain pillar divided by the cover depth multiplied by the total extracted width (1000w/W'H).

A regression analysis on the data indicates a strong exponential relationship for $1000wcp/W'H$ values up to 0.543. For values > 0.543, the relationship becomes constant.

$$S_p/T = 7.4044e{-}10.329F \ (R^2 = 0.92) \text{ for } F < 0.543, \text{ and}$$

$$S_p/T = 0.023 \text{ for } F > 0.543$$

where

F = 1000w/W'H

W' = The total extracted width which includes the width of the panels extracted on both sides of the subject chain pillar, and the width of the chain pillar itself (i.e. W' = W_i + w_i + W_{i+1}).

Note that the final subsidence for a longwall panel with several subsequent extracted panels was then determined empirically by adding 50% of the predicted chain pillar subsidence (S_p) to the single panel S_{max} estimate.
This approach however, did not include an abutment angle to estimate pillar loads, which are likely to vary significantly between sub-critical and supercritical panel layouts.

*The chain pillar model has now been amended to include better predictions of chain pillar load that are consistent with ALTS methodology (refer **ACARP, 1998a**) and has resulted in the modified version presented in Section A5.2.*

A5.2   Predicting Subsidence above Chain Pillars (DgS, 2008 Model)

After the **ACARP, 2003** model was published; further studies on chain pillar subsidence measurements were undertaken at several mine sites in the Western (Springvale, Angus Place and Ulan) and Southern Coalfields (Appin and Elouera). The measured subsidence above the chain pillars was significantly greater than the Newcastle Coalfield pillars and considered to be linked to the stress acting on the pillars and the longwall mining height.

Maximum subsidence above the chain pillars invariably occurred after the pillars were subject to double abutment loading conditions (i.e. goaf on both sides).

The **ACARP, 2003** model for estimating chain pillar subsidence was subsequently superseded by the pillar stress v. strain type approach presented in **Figure A16**. The chain pillar stress was estimated by assuming a design abutment angle of 21° for the pillar load, according to the methodology presented in **ACARP, 1998a** for sub-critical and supercritical longwall panels.

Prediction of subsidence above the chain pillars (S_p) was determined based on the following regression equation using the mining height, T and pillar stress, σ:

S_p/T = 0.238469/(1+$e^{-[(\sigma-25.5107)/7.74168]}$)   (R^2 = 0.833)

The uncertainty of the predictions was estimated by calculating the variance of the residuals about the regression lines and calculating 90% Confidence Limits for the database as follows:

90% CL S_p error = 0.048T

It was also considered necessary to test if the above stress v. strain type approach was adequate for reliable predictions, by comparing the subsidence outcomes with the pillar Factor of Safety; see **Figure A17**.

The strength of the chain pillars was estimated using the rectangular pillar strength formulae presented in **ACARP, 1998b**. The FoS was derived by dividing the pillar strength by the pillar load (i.e. stress).

Generally it has been found that significant surface subsidence above the chain pillar (i.e. 10 - 30% of pillar height) starts to occur when the pillar FoS is < 2. For FoS values greater than 2, subsidence above the pillars is virtually independent of FoS and the pillars generally perform elastically under load.

The database indicates that when the FoS is < 2, the stiffness of the pillar starts to decrease, due to the development of load induced fracturing within the pillar and surrounding strata. FoS values of < 2 represent pillar stresses that exceed 50% of the pillar strength. Laboratory testing of coal and sandstone samples also show sample 'softening' as the ultimate load carrying capacity of the sample is approached.

For pillars with FoS values < 1, the subsidence above the chain pillars tend to a maximum limit of approximately 25 to 30% of the mining height. This type of behaviour is expected for chain pillars that have width to height ratios w/h > 5, which is the point where 'strain hardening' deformation starts to develop with increased confinement of the 'pillar core'.

A5.3   Calculation of First and Final Subsidence for Multiple Longwall Panels

Multiple panel predictions can be made by adding the predicted single panel subsidence to a proportion of the chain pillar subsidence (including the residual subsidence) to estimate first and final subsidence above a given longwall panel.

The definition of first and final S_{max} is as follows:

First S_{max} =   the first maximum subsidence after the extraction of a longwall panel, including the effects of previously extracted longwall panels adjacent to the subject panel.

Final S_{max} =   the final maximum subsidence over an extracted longwall panel, after at least three more panels have been extracted, or when mining is completed.

In the Newcastle Coalfield, First and Final S_{max} values for a panel are predicted by adding 50% and 100% of the predicted subsidence over the chain pillars respectively (i.e. between the previous and current panel) less the goaf edge subsidence (see **Section A5**).

Residual subsidence above chain pillars and longwall blocks tends to occur after extraction due to (i) increased overburden loading on pillars and (ii) on-going goaf consolidation or creep effects. Based on the final chain pillar subsidence measurements presented in **Figure A16**, the residual movements can increase subsidence by a further 10 to 30%.

An example of measured multiple longwall subsidence behaviour is presented in **Figure A18**.

Final subsidence is normally estimated by assuming a further 20% of the chain pillar subsidence will occur. However, this may be increased or decreased, depending on local experience.

The prediction of first and final subsidence originally presented in **ACARP, 2003** involved the use of several empirical coefficients, which have proven to be difficult to apply in practice. The interested reader may refer to this methodology, however, the above method is considered easier to apply and likely to result in a similar outcome.

In summary, the mean values of the First S_{max} and Final S_{max} are calculated as:

$$\text{First } S_{max} = \text{Single } S_{max} + 0.5(S_{p(i-1)} - S_{goe(i-1)})$$

$$\text{Final } S_{max} = \text{First } S_{max} + 1.0(\text{Final } S_{p(i)} - \text{First } S_{goe(i)})$$

The U95% Confidence Limits or Credible Worst Case Values are then:

$$\text{U95\% First } S_{max} = \text{mean First } S_{max} + 1.64 (\text{U95\% } S_{max} \text{ error} + \text{U95\% } S_p \text{ error})^{1/2}.$$

$$\text{U95\% Final } S_{max} = \text{mean Final } S_{max} + 1.64 (\text{U95\% } S_{max} \text{ error} + \text{U95\% } S_p \text{ error})^{1/2}.$$

It should also be understood that the terms 'mean' and 'Upper 95% Confidence Limit' used in the model generally infer that the predicted maximum values will be exceeded by 50% and 5% respectively of the panels mined with similar geometry and geology etc.

Using lower probability of exceedence values (e.g. U99%CL) may be justified for particularly sensitive features, however, the magnitude of the maximum values does not usually increase significantly above the U95%CL values.

When local subsidence data is available for multiple longwall panels, the relationship between the multiple and single panel subsidence predictions can be determined as follows:

$$\text{First } S_{max} = \text{Single } S_{max} + 0.5b(S_{p(i-1)} - S_{goe(i-1)})$$

$$\text{Final } S_{max} = \text{First } S_{max} + b(\text{Final } S_{p(i)} - \text{First } S_{goe(i)})$$

The 'b' factor may be estimated from measured subsidence profiles, and allows the load transfer effect between the goaf and the chain pillars to be included in the model if necessary.

It has been observed at deeper NSW Coalfield Mines (i.e. the Western and Southern Coalfields) where the proportion of subsidence over the chain pillars to be added to the single panel subsidence decreased when the cover depth exceeded 350 m.

A6 Subsidence Profile and Impact Parameter Predictions

Part of the **ACARP, 2003** project included the development of several models to predict the maximum panel deformation parameters and surface profiles associated with subsidence. The following models were developed:

- panel goaf edge or rib subsidence,

- angle of draw,

- maximum transverse and longitudinal tilt, curvature and strain,

- the locations of the above parameters over the longwall panel for the purposes of subsidence profile development, and

- heights of continuous and discontinuous fracturing above the longwall, based on measured surface tensile strains and fracture limit horizons over extracted panels (see **Section A7** for details).

A conceptual model of surface deformation profiles that develop above longwall panels is given in **Figure A19**.

All of the above subsidence parameters have been statistically linked to key geometrical parameters such as the cover depth (H), panel width (W), working height (T) and chain pillar width (w_{cp}) and shown in **Figures A20** to **A27**.

A summary of all the empirical model relationships between the key subsidence profile parameters that were developed in **ACARP, 2003** and DgS are presented in **Table A3**.

Table A3 - Summary of Subsidence Impact Parameter Prediction Models Developed from ACARP, 2003

Parameter	Regression Equation and +/- 90% Confidence Limits or Upper95% CL	Coefficient of Determination (R^2)	Figure No.
Subsidence Reduction Potential (SRP) of Strata Unit in Overburden with thickness t, panel width, W and location factor, y/H above workings for Cover Depth Category	**High** SRP t for a given panel W plots above line for given strata unit y/H. **Moderate** SRP t plots between High SRP line and next y/H line below it. **Low** SRP t plots below Moderate SRP limit line.	N/A - curve location determined by successful re-prediction of >90% of cases I databases	**Figure A8** for H<150m; **Figure A9** for H< 250m; **Figure A10** for H< 350m
Single Maximum Longwall Panel Subsidence (Single S_{max}) for Assessed Strata Unit SRP of Low, Moderate or High	Upper and Lower bound prediction lines for a given SRP are used to estimate range of S_{max}/T for a given Panel W/H. Average of limit lines value is mean Single S_{max} value +/- 0.03T for W/H < 0.6; +/- 0.1T for 0.6<W/H<0.9; +/-0.05T for W/H>0.9	N/A - curve location determined by successful re-prediction of >90% of cases I databases	**Figure A3** for H<150m; **Figure A4** for H< 250m; **Figure A5** for H< 350m
Chain Pillar Subsidence, S_p (m)	Mean $S_p/T = 0.238469/(1+e^{-[(\sigma DAL-25.5107)/7.74168]})$ +/- 0.048T	$R^2 = 0.833$	**Figure A16**
Goaf Edge Subsidence	Mean $S_{goe}/S_{max} = 0.0722(W/H)^{-2.557}$ U95%CL $S_{goe}/S_{max} = 0.0719(W/H)^{-1.9465}$	$R^2 = 0.82$	**Figure A20**
Angle of Draw	Mean AoD = $7.646Ln(S_{goe})+32.259$ U95%CL = Mean AoD + 8.7°	$R^2 = 0.56$	**Figure A21**
Maximum Tilt T_{max} (mm/m)	$T_{max} = 1.1925(S_{max}/W')^{1.3955}$ +/- 0.4T_{max} (W' = lesser of W and 1.4H)	$R^2 = 0.94$	**Figure A22**
Maximum Convex Curvature C_{max} (km^{-1})	Mean $C_{max} = 15.60(S_{max}/W'^2)$ +/- 0.5Mean	$R^2 = 0.79$	**Figure A23**
Maximum Concave Curvature C_{min} (km^{-1})	Mean $C_{min} = 19.79(S_{max}/W'^2)$ +/- 0.5Mean	$R^2 = 0.79$	**Figure A24**
Maximum Tensile Strain E_{max} (mm/m)	Mean 'smooth' $E_{max} = 5.2C_{max}$ +/- 0.5 Mean Mean 'Cracked' $E_{max} = 14.4C_{max}$	$R^2 = 0.72$ $R^2 = 0.32$	**Figure A25**
Maximum Compressive E_{min} (mm/m)	Mean $E_{max} = 5.2(C_{min})$ +/- 0.5 Mean Mean 'Cracked' $E_{min} = 14.4C_{min}$	$R^2 = 0.72$ $R^2 = 0.32$	**Figure A25**
Critical Panel Width	$W_{crit} = 1.4H$ where H = cover depth	N/A	**ACARP, 2003**

Table A3 (Continued) - Summary of Subsidence Impact Parameter Prediction Models Developed from ACARP, 2003

Subsidence at Inflexion Point or Maximum Tilt S_{Tmax}	Mean S_{Tmax}/S_{max} = -0.0925(W/H)+0.7356 +/- 0.2	R^2 = 0.5	**ACARP, 2003**
Distance to Inflexion Point, d/H	d/H = 0.2425Ln(W/H) + 0.3097	R^2 = 0.73	**Figure A27**
Distance to Peak Tensile Strain (mm/m)	d_t/H = 0.1643Ln(W/H) + 0.2203 for W/H >0.6; d_t/H = 0.2425Ln(W/H) + 0.2387 for W/H <0.6;	R^2 = 0.28	**Figure A27**
Distance to Peak Compressive Strain (mm/m)	d_c/H = 0.3409Ln(W/H) + 0.3996 for W/H >0.6; d_c/H = 0.2425Ln(W/H) + 0.3767 for W/H <0.6	R^2 = 0.59	**Figure A27**

* - If H within 25 m of depth category boundary, then average result with overlying or underlying depth category value.

- Centreline profile parameters are not presented here (refer to **ACARP, 2003**).

A7   Subsidence Profile Predictions above Longwall Panels

Predicted 'smooth' subsidence profiles above single and multiple longwall panels have been determined based on cubic spline curve interpolation through seven key points along the subsidence trough (i.e. maximum in-panel subsidence, inflexion point, maximum tensile and compressive strain, goaf edge subsidence, subsidence over chain pillars and 20 mm subsidence or angle of draw limit).

The locations of these points have been determined empirically, based on regression relationships between the variables and the geometry of the panels (see **Table A3**). Both transverse and longitudinal profiles have been derived in this manner.

First and second derivatives of the fitted spline curves provide 'smooth' or continuous subsidence profiles and values for tilt and curvature. Horizontal displacement and strain profiles were derived by multiplying the tilt and curvature profiles by an empirically derived constant associated with the bending surface beam thickness (based on the linear regression relationship between the variables, as discussed in **ACARP, 2003**).

An allowance for the possible horizontal shift in the location of the inflexion point (within the 95% Confidence Limits of the database) has also been considered, for predictions ofsubsidence at features located over the goaf or extracted area.

DgS

A8   Subsidence Contour Predictions above Longwall Panels

Subsidence contours can be derived with geostatistical kriging techniques over a 10 m square grid using Surfer 10® software and the empirically derived subsidence profiles along cross lines, centre lines and corner lines around the ends of the longwall panels. Vertical 'slices' may taken through the contours to (i) determine subsidence profiles along creeks or infrastructure, and (ii) assess the likely impacts on the relevant surface features.

A8.1   Subsidence Contours

Subsidence contour predictions have been made in this study using SPDS®, which is an influence function based model that firstly calculates seam convergence and pillar displacements empirically around the workings. The influence of an extracted element of coal is transmitted to the surface via a 3-D influence function, which also takes varying topography into account.

The model is usually calibrated to measured maximum subsidence values by adjusting key parameters such as influence angles and inflexion point location from extracted panel sides.

A8.2   Tilt and Curvature Contours

The predicted principal tilt and curvature contours were derived using the calculus module of the Surfer10® program and the predicted subsidence contours from the SPDS® runs. The subsidence contours were based on a 10 m grid.

Principal tilts (i.e. surface gradient or slope) were calculated by taking the first derivative of the subsidence contours in x and y directions as follows:

$$T_p = [(\partial s/\partial x)^2 + (\partial s/\partial y)^2]^{0.5}$$

where ∂s = subsidence increment over distances ∂x and ∂y
            along x and y axes.

Principal curvatures (i.e. rate of change in slope or surface bending) were calculated by taking the second derivative of the subsidence contours in x and y directions as follows:

$$C_p = [(\partial^2 s/\partial x^2)(\partial s/\partial x)^2 + 2(\partial^2 s/\partial x \partial y)(\partial s/\partial x)(\partial s/\partial y) + (\partial^2 s/\partial y^2)(\partial s/\partial y)^2]/pq^{2/3}$$

where $p = (\partial s/\partial x)^2 + (\partial s/\partial y)^2$ and $q = 1+p$

A8.3   Strain

Before predictions of strain can be made, the relationship between the measured curvatures and strain must be understood. As discussed in **NERDDP, 1993b** and **ACARP, 2003**, structural and geometrical analysis theories indicate that strain is linearly proportional to the curvature of an elastic, isotropic bending 'beam'; see **Figure A28**. This proportionality actually represents the depth to the neutral axis of the beam, or in other words, half the beam

thickness. **NERDDP, 1993b** studies returned strain over curvature ratios ranging between 6 and 11 m for NSW and Queensland Coalfields. Near surface lithology strata unit thickness and jointing therefore dictate the magnitude of the proportionality constant between curvature and strain.

ACARP, 2003 continued with this approach and introduced the concept of secondary curvature and strain concentration factors due to cracking. The peak strain / curvature ratio for 'smooth' subsidence profiles in the Newcastle Coalfield was assessed to equal 5.2 m (mean) and 7.8 m (U95%CL) with the possibility that surface cracking could increasing the 'smooth-profile' strains to 10 or 15 times the curvature. The above values may also be affected by the thickness of near surface geology.

Reference to **DMR, 1987** also suggests a curvature to strain multiplier of 10 for high pillar extraction and longwall panels in the Newcastle Coalfield.

Attempts by others to reduce the variability in strain and curvature data by introducing additional parameters, such as the radius of influence, r, by **Karmis et al, 1987** and cover depth, H, by **Holla and Barclay, 2000**, appear to have achieved moderate success in the coalfields in which they were applied. However, when these models were applied to the Newcastle Coalfield data presented in **ACARP, 2003**, the results did not appear to improve things unfortunately; see **Figures A29.1** and **A29.2**.

It is therefore considered that the variability in behaviour is probably due to other parameters, which are very difficult to measure (such as the thickness and flexural, buckling and shear strengths of the near surface strata).

Provided that the likelihood of cracking can be ascertained from the strain predictions, then appropriate subsidence management plans can still be implemented.

A9   Prediction Of Subsidence Impact Parameters And Uncertainty Using Regression Analysis Techniques

A9.1   Regression Analysis

Key impact parameters have been predicted using normalised longwall subsidence data from the Newcastle Coalfield. This approach allows a reasonable assessment of the uncertainty involved using statistical regression techniques. A linear or non-linear regression line has been fitted to the database for each impact parameter, normalised to easily measured parameters, such as maximum subsidence, panel width and cover depth. The quality or significance of the regression line is influenced by the following parameters:

    (i)   the size of the database,

    (ii)   the presence of outliers, and

    (iii)   the physical relationship between the key parameters.

The regression curves were reviewed carefully, as such curves can be (i) affected by outliers, and (ii) misleading, in that by adopting a mathematical relationship which gives the best fit (i.e. R^2) the curves are controlled by the database and may not reflect the true underlying physical dependencies or mechanisms that the data represents.

These issues are inherent in all prediction modelling techniques because, for example, all models must be calibrated to field observations to validate their use for prediction or back analysis purposes.

The regression techniques presented in the **ACARP, 2003** was done by firstly assessing conceptual models of the mechanics and key parameter dependencies (based on established solid mechanics and structural analysis theories), before generating the regression equations.

Several outliers in the model databases were excluded in the final regression equations, but only when a reasonable explanation could be given for each anomaly (i.e. multiple seam subsidence, geological faults / dykes and surface cracking effects).

The regression equations in **ACARP, 2003** have R^2 (i.e. Coefficients of Determination) values generally greater than 50%; indicating that the relationships between the variables are significant. For cases where the R^2 values are < 50%, the regression lines are almost horizontal (i.e. the parameter doesn't change significantly over the range of the database), and the use of the regression line will be close to the mean of the database anyway.

A9.2   Prediction Model Uncertainty

The level of uncertainty in the model predictions has been assessed using statistical analysis of the residuals or differences between the measured data and regression lines (i.e. lines of best fit). The *Standard Error* of the prediction has been derived from the residuals, which has then been multiplied by the appropriate 'z' or 't' statistic for the assumed normal probability distribution to define Upper (and Lower) Confidence Limits.

The residual population errors for the single panel subsidence model are shown in **Figure A30**.

The empirical database therefore allows an assessment of variance and standard error such that the required subsidence parameter's mean and upper 95% Confidence Limit (Credible Worst Case) values can be determined for a given mining geometry and geology.

Provided there are (i) more than 10 data points in the data sets covering the range of the prediction cases, and (ii) the impact parameter and independent variables have an established physical relationship based on solid or structural mechanics theories, then it is considered unlikely that the regression lines will be significantly biased away from the underlying physical relationship between the variables by any limitations of the data set.

On-going review of each of the regression equations over the past six years by DgS has not required significant adjustment of the equations to include new measured data points. The

regression equations derived are also amenable to spreadsheet calculation and program automation.

It is also important to make the distinction between the terms confidence *limit* and confidence *interval*. The Credible Worst Case terminology used in the model is **not** the upper limit of the 95% Confidence **Interval** - which would encompass 95% of the data. Since the lower 95% Confidence Limit is rarely used in practice, it was considered appropriate to adopt the 5% Probability of Exceedence values instead (this by definition represents the upper limit of the **90% Confidence Interval**).

Further, the term *Upper 95% Confidence Limit* used in the **ACARP, 2003** model is considered acceptable in the context of 'one-tailed' probability distribution limits (i.e. the Lower 95% Confidence Limit is generally of little practical interest).

A10   Subsidence Model Validation Studies

A10.1 Model Development

The **ACARP, 2003** model was developed so that it could re-predict > 90% of the database on which it is based. Validation studies also included comparison of measured and predicted subsidence, tilt and strain profiles above several longwall panel crosslines and centrelines. Examples of predicted and measured profiles above multiple panels for the Newcastle Coalfield are shown in **Figures A31** to **A34** using the **ACARP, 2003** model. Subsequent predictions v. measured subsidence profiles are presented in **Figures A35** to **A38** using the updated version of the model discussed herein.

DgS is usually required to review predicted v. measured subsidence profiles after the completion of a longwall panel and report the results to mines and government departments. Over the past nine years, the model has usually over predicted measured subsidence, with the data falling somewhere between the mean and U95%CL values. Prediction exceedances have occurred less than 5% of the time and where the assessment of the overburden SRP was found to be incorrect.

The predictions of curvature and strain, however, are generally problematic due to the common effects of discontinuous or cracking behaviour (i.e. lithological variation and cracking), resulting in measured strains that can be two to four times greater than predicted 'smooth' profile strains. This issue is discussed further in **Section A10.2**.

A10.2 Field Testing of Strain Predictions

Strain and curvature concentrations can increase 'smooth' profile strains by 2 to 4 times in the Newcastle Coalfield, when the panel width to cover depth ratio (W/H) exceeds 0.8 or radius of curvature is less than 2 km, see **ACARP, 2003**.

Where cracking occurs, measured strains will be highly dependent on the bay-length. Rock exposures with widely spaced or adversely orientated jointing can also result in much larger crack widths than for a location with deep soil profiles.

For example, a measured strain of 3 to 6 mm/m along a cross line above a longwall panel in the Newcastle Coalfield caused several cracks in soil that ranged in width from 10 mm to 30 mm and a single 100 mm wide crack in a sandstone rock exposure with medium strength and widely spaced jointing, see **Figure A39**.

At the moment, it is not possible to predict the magnitude of strains from 'smooth profile' models confidently, however, it is possible to make reasonable predictions that strains > 2 mm/m will cause cracking within the tensile strain zones. Shearing and buckling is also likely to occur within the compressive zones above a longwall with shallow surface rock.

Overall, strains and cracking can be managed effectively by assuming cracks will occur within the limits of a longwall panel and may need to be repaired after each panel is completed.

A11   Sub-Surface Fracturing Model

A11.1   Sub-Surface Fracturing Zones

The caving and subsidence development processes above a longwall panel usually result in sub-surface fracturing and shearing of sedimentary strata in the overburden, according to **Peng and Chiang, 1984** (see **Figure A40a**) and **Whittaker and Reddish, 1989** (see **Figure A40b**). The height of fracturing (HoF) is dependent on mining geometry and overburden geology.

International and Australian research on longwall mining interaction with groundwater systems indicates that the overburden may be divided into essentially four or five zones of surface and subsurface fracturing. The zones are defined in **Table A4** (in descending order):

Table A4 - Sub-Surface Fracture Zone Summary

Zone Type	Zone	Fracture and Groundwater Response Description	Typical Vertical Strain (mm/m)
Surface Cracking Zone (un-constrained)	D	Vertical cracking due to horizontal strains extending to maximum depths of 10 - 15 m. Surface waters may be diverted below affected area and resurface downstream where interaction with B & C Zones occur.	<3
Elastic Deformation Zone (dilated bedding & constrained)	C	Generally unaffected by strains with some bedding parting dilation. Horizontal strains constrained by overlying/underlying strata. Groundwater levels may be lowered temporarily due to new storage volume in voids between beds, but likely to recover at a rate dependant on climate. Elastic Zone may not be present if B or A Zones extend up to Surface Zone.	<3
Discontinuous Fracture Zone (dilated bedding & constrained)	B	Minor vertical cracking due to bending that do not extend through strata units. Increased bedding parting dilation and similar groundwater response to Zone C. Some groundwater leakage may occur to B Zone, however, losses likely to be recharged by surface hydro-geological system.	<8
Continuous Fracture Zone (unconstrained)	A	Major vertical cracking due to bending that pass through strata units and allow a direct hydraulic connection to workings below. Full depressurisation of groundwater occurs in the Zone that may recover in the long term once mining is completed.	>8
Caved (included in the A-Zone)	A	Caved strata up to 3 to 5 x Mining Height above the workings. Collapsed roof bulks in volume to provide some support to overlying strata.	>80

The characteristics of each HoF zone are further described below:

Starting from the seam level, the **Caved Zone** (included in the **A-Zone**) refers to the immediate mine workings roof above the extracted panel, which has collapsed into the void left after the coal seam has been extracted. The Caved Zone usually extends for 3 to 5 times the mining height, T, above the roof of the mine workings due to bulking factors of 1.3 to 1.5, and sometimes from 10 to 15T if the strata have low bulking properties (e.g. bulking factors of 1.10 to 1.15). Thinly bedded and laminated strata are likely to have lower bulking factors than thickly bedded or massive units within the Caved Zone.

The **Continuous Fracture Zone (A-Zone)** has been affected by a high degree of bending deformation, resulting in significant fracturing and bedding parting separation and shearing of the rock mass. Vertical tensile strains range from -10 to 140 mm/m with strata dilation in excess of 1 m. Compressive strains tend to develop at horizontal bedding separations after initial fracturing and overlying strata deflections occur resulting in re-compaction of the goaf and disturbed strata.

Continuous sub-surface fracturing refers to the zone of cracking above a longwall panel that is likely to result in a direct flow-path or hydraulic connection to the workings. All groundwater (or surface waters) within this Zone would be expected to drain vertically into the mine workings goaf.

The **Strata Dilation Zone (B-Zone)** refers to the section of overburden immediately above the A-Zone that has also been deformed by bending action, but to a lesser degree than the A-Zone. The B-Zone will have bedding parting separations and discontinuous fractures through bending strata units due to vertical strains ranging from -2 to 8 mm/m and strata dilation from 30 mm to 400 mm, depending on the panel width. An increase to horizontal rock mass permeability (hydraulic conductivity) is expected in the B-Zone with groundwater flowing horizontally into dilated strata.

Only minor vertical permeability increases are expected in the B-Zone due to alternating horizontal tensile and compression zones associated with Voussoir Beam action above the A-Zone. It is noted in **Whittaker and Reddish, 1989**, that some groundwater leakage from the B-Zone to the A-Zone is possible due to limited crack or joint interaction between the zones.

Overall, the majority of the B-Zone is considered to be a 'constrained' and 'dilated' zone with low connectivity potential to the mine workings. The B-Zone therefore represents a sub-surface fracturing zone that causes temporary groundwater system disturbance.

The **Elastic Deformation Zone (C-Zone)** is located above the B Zone and is the zone where the strata may have suffered minor bending and disturbance. Impacts include horizontal shearing and minor bed separations or dilation of up to 30 mm due to vertical tensile strains between 1 and 2 mm/m. The bedding separations may result in minor increases to horizontal hydraulic conductivity and negligible changes to vertical hydraulic conductivity. Groundwater system disturbance is expected to be negligible in this zone.

The development of the Elastic Deformation Zone (C-Zone) will depend on the mining geometry and the presence of spanning strata. The C-Zone is probably only likely to develop above critical to sub-critical mining geometries (i.e. W/H < 1.4) but may also be present above super-critical panels also if favourable geological conditions exist.

The strata in the B and C-Zones are also likely to be in compression due to natural arch formation (above sub-critical and critical panels). The arch will also act as barrier to vertical drainage of groundwater despite the presence of naturally occurring vertical joints in the rock mass. Low permeability strata such as claystone, tuff and mudstone will also limit rock mass 'gaps' and further retard vertical flow rates through these zones.

In the absence of significant geological structure (i.e. faults and dykes), the overall effect on the surface groundwater system due to leakage through the B and C-Zones will be minimal, with re-charging of groundwater losses likely to occur from the surface hydrological system. The presence of significant geological structure may increase the drainage rates through these strata zones however. Monitoring of mine groundwater makes v. rainfall - runoff data will determine the rate of leakage that is occurring through these zones.

The **Surface Cracking Zone (D-Zone)** includes the vertical cracking due to horizontal tensile and compressive strains caused by mine subsidence deformation. The D-Zone may extend to depths ranging from 5 m to 20 m (typically < 15 m) in the Newcastle Coalfield, and is dependent on near-surface geology and surface topography.

For mine design purposes, typical D-Zone depths in relatively flat terrain may be assumed to range from 10 m to 12 m (i.e. < 15m). *Note: **Forster and Enever, 1992** adopted a D-Zone thickness of <15 m based on data from Wyee and Cooranbong Collieries, and included it in the minimum cover depth formula of 45T+10 m for designing supercritical panels below tidal waters of Lake Macquarie in the Newcastle Coalfields.*

A11.2   Impact on Rock Mass Permeability

In regards to changes to rock mass permeability, **Forster, 1995** indicates that horizontal permeabilities in the fractured zones above longwall mines could increase by 2 to 4 orders of magnitude (e.g. pre-mining $k_h = 10^{-9}$ to 10^{-10} m/s; post-mining $k_h = 10^{-7}$ to 10^{-6} m/s).

Vertical permeability's could not be measured directly from the boreholes but could be inferred by assuming complete pressure loss in the 'A Zone', where direct hydraulic connection to the workings occurs. Only a slight increase in the 'B zone' or indirect / discontinuous fracturing develops (mainly due to increase in storage capacity) from bedding parting separation. It is possible that minor vertical flows will occur from B zone into A zone (and workings) as well.

Discontinuous fracturing would be expected to increase rock mass storage capacity and horizontal permeability without direct hydraulic connection to the workings. Rock mass permeability is unlikely to increase significantly outside the limits of extraction.

A11.3 Mine Design Criteria for Sub-Surface Fracture Height Control

When designing mining layouts for sub-surface fracture control, the A-Zone is the most significant in regards to groundwater and surface water interaction as it represents the region of broken ground whereby a hydraulic connection to the mine workings will most certainly occur.

The B-Zone is probably just as important as it represents the transition zone between the continuously fractured ground and elastic deformation or surface zones. The B-Zone also includes strata which are confined and where bedding parting separations (i.e. dilations) occur in the sagging rock mass above the caved and broken strata units in the A-Zone.

The C-Zone has been deformed as well, but not to the same extent as the B-Zone.

Note: It is difficult to define the boundary between the B and C-Zones without vertical strain measurements from extensometers. Both zones are considered to be 'constrained' and 'dilated' and will act as an effective barrier between the A-Zone and near surface groundwater and surface watercourses.

The formation and thickness of the HoF Zones will firstly be dependent on the 'criticality' of the proposed longwall panel. The same terms used for subsidence prediction are also referred to below and are based on the ratio between panel width (W) and the cover depth (H):

- Subcritical refers to panels with W/H < 0.7;

- Critical refers to panels with W/H > 0.7 and < 1.4; and

- Supercritical refers to panels with W/H > 1.4.

Several case studies have been referred to below which consider super-critical and sub-critical panel geometries separately due to their fundamental differences in spanning behaviour.

Conceptual models of the A and B-Zones above supercritical panels are presented in **Whittaker & Reddish, 1998** and are based on physical modelling results. **Forster and Enever, 1992** indicated similar strata zoning from field monitoring (**Figure A40c**) above supercritical, total pillar extraction panels in the Lake Macquarie Area of the Newcastle Coalfield.

A conceptual model that includes the B and C-Zones was presented in **ACARP, 2007** (**Figure A40d**) for sub-critical mining geometries in the Western Coalfield. A similar sub-surface fracture zoning is also suggested by **Mark, 2007** (**Figure A40e**) for the US Coalfields and **Kendorski, 1993** for the UK Coalfields (**Figure A40f**).

From the above conceptual height of fracturing models, several simple empirical models have been developed over the years to estimate the thicknesses of the A, B and C-Zones for the purpose of avoiding groundwater and surface water connectivity with underground mines.

The suite of HoF prediction models that probably represent the state-of-the-art are summarised in the following sections.

A11.3.1   Wardell, 1975, Reynolds, 1977 and Singh and Kendorski, 1981

Wardell, 1975 recommended a minimum rock cover depth of 50T - Surface Zone thickness above total extraction or longwall panels when mining under tidal waters in the Newcastle Coalfield. The minimum cover depth (H) was based on a maximum horizontal tensile strain limit of 7.5 mm/m and the Newcastle Holla curves. It is noted that a maximum horizontal tensile strain of 10 mm/m has been specified in the UK when mining below permanent waters.

Wardell has also recommended a minimum cover depth of 60T (which included a Surface Zone thickness ranging from 12 m to 15 m) for mining below stored waters with longwalls in the Southern Coalfield.

The Wardell Guidelines recommended that panel widths should be limited to <0.4H to maximize the thickness of the Constrained Zone (i.e. B and C-Zones) beneath tidal waters. **Reynolds, 1977** recommended 0.33H for maximum panel widths at depths more than 120 m below the reservoirs in the Southern Coalfield.

The height of continuous fracturing was not estimated in the Wardell Guidelines, but probably assumed to be significantly lower than 50T - the 15 m thick surface cracking zone. **Holla, 1991** noted that the 60T value is dependent on the S_{max} and K ratio (and hence W/H ratio) and should not be applied blindly to all mining geometries.

Singh and Kendorski, 1981 adopted a general height of A-Zone Fracturing of $56T^{0.5}$ based on a review of international case studies with a minimum Constrained plus Surface Zone thickness of 45 m for mudstone and 57 m for sandstone strata conditions when mining below tidal waters. The model recognizes that fracturing may extend further through massive strata than thinly bedded units due to their propensity to carry greater load.

A11.3.2   Whittaker and Reddish Physical Model, 1989

It is considered that the published physical modeling work in **Whittaker and Reddish, 1989** provides valuable insight into the mechanics of sub-surface fracturing over longwall panels. The outcomes included specific guidelines (over and above such work as the Wardell, 1975 Guidelines) for the prevention of inundation of mine workings beneath surface and sub-surface water bodies.

The **Whittaker and Reddish, 1989** height of fracturing model was developed in response to the water ingress problems associated with early longwall extraction at the Wistow Mine in Selby, UK. The longwall panel was located at 350 m depth and experienced groundwater inflows of 121 to 136 litres/sec when sub-surface fracturing intersected a limestone aquifer 77 m above the seam.

The physical model is a scaled down version of the real-world, and therefore requires compatible material strength properties (i.e. plaster) to generate fracturing from the laboratory-sized void widths and mining heights being simulated. The pattern of cracking and heights of fracturing observed should therefore not be dismissed because of the materials used to create the model.

The Whittaker and Reddish model identifies two distinct zones of fracturing above super-critical width extractions (continuous A-Zone and discontinuous B-Zone fracturing) and indicates the height of each is a function of maximum tensile strain at the surface. As such, its use is also based upon being able to make credible subsidence and strain predictions. The mechanical concepts of the model are shown in **Figure A40b**.

The definition of the 'continuous' height of fracturing refers to the height in which a zone of direct hydraulic connection for groundwater inflows to the mine workings develops (i.e. the A-Zone).

The definition of the extent of 'discontinuous' height of fracturing refers to the height at which the horizontal permeability increases as a result of strata de-lamination and incomplete fracturing through the strata beds (i.e. the B-Zone). Minor occurrences of direct connection of fractures to the workings is considered possible, but will depend on the geology (e.g. the presence of persistent vertical structure such as faults and dykes).
The outcomes of the modeling work resulted in two logarithmic type curves that relate the surface horizontal strain to the measured A and B fracture heights normalized to the cover depth (see **Figure A40b**).

The physical modeling work that was completed to derive the prediction curves is summarised below:

- The physical model was constructed from multiple 1.25 cm thick layers of coloured sand and plaster with sawdust bond breakers placed between each successive layer. Based on a real world/model ratio of 92, the model layers represented 1.15 m thick layers in the real world. The model was initially devoid of vertical joints or cracks.

- The scale and mechanical properties of the model satisfied dimensional analysis and similitude laws. *Note: This aspect of mechanical models is very important, as overburden strength properties will not fracture if they are too high for the model's mining geometry.*

- The plaster layers for the model were equivalent to a rock mass with a density of 2.35 t/m^3, a UCS of 10.94 MPa and Youngs Modulus, E, of 984 MPa.

- The model was used to simulate the overburden behaviour of a panel with a W/H ratio of 1.31 and a progressively increasing working height range that commenced at 1.2 m and finished at 10.8 m. The advancing longwall face was simulated by removing timber blocks at the base of the model in 1.2 m to 2.0 m lift stages.

- The extent or heights of 'continuous' and 'discontinuous' fracturing above the longwall 'face' were measured and plotted with the associated peak tensile strain predictions at the surface. The subsidence and strains were measured from a grid and calculated using the method provided in the **UK Subsidence Engineers Handbook, 1975**.

- The fracturing path progressed up at an inward angle of approximately 18° to 19° from the solid rib and increased towards the centre of the panel higher up into the strata. Continuous fracturing occurred in the cantilever bending zone close to the rib-side only, as fracturing in the overburden above the middle portion of the panel tended to 'close' and did not appear to represent an area where groundwater inflows into the workings would eventuate.

- Surface cracks extended down from the surface for a depth up to 7.5 m.

- Other similar models were also prepared and used to demonstrate the "ability of strong overburden at the surface to cause bridging of the strata in this manner is dependent upon the strength and general competence of the rocks near to the surface, in addition to the width of the extracted region."

- Any groundwater inflow conditions were therefore considered to be "mainly associated with the longwall rib-side fracture zone [or tensile strain zone]" above longwall panels.

The findings above are considered reasonable for super-critical longwall geometries where panel widths are greater than the critical width (i.e. 1.2 - 1.4H) and the height of fracturing is likely to be controlled primarily by the mining height and strata properties.

Using the analytical model equations derived in **Section A11.4.2**, the progression of the height of continuous fracturing was back analysed by DgS using the maximum compressive beam stress for spanning strata units under full loading conditions (Equation 1) and goaf supported strata units (Equation 2):

$$\sigma_c = 0.75\gamma(H - A)(W - 2A\tan\theta)^2/t_i^2 \qquad \text{(Lower Beam)} \qquad (1)$$

$$\sigma_c = 4\Delta Et_i/(W - 2A\tan\theta)^2 \qquad \text{(Upper Beams)} \qquad (2)$$

It was noted that the goaf did not 'bulk' in the model, resulting in no reduction in subsidence between the seam and surface (i.e. $S_{max} = T$) and measured surface strain/curvature ratio indicated $\Delta = 0.5T$ over the effective span, $W_i = W - 2y\tan\theta$ above the goaf.

The results of the model are summarized in **Table A5** below:

Table A5 - Physical Model Results Summary for the Height of Continuous Fracturing Development above a Supercritical Longwall Panel

Lift No	Mining Height T (m)	S_{max} (m)	E_{max} (mm/m)	A (m)	Effective Beam Span W_i (m)	Measured Beam Curvature in Spanning Strata (km^{-1})	Measured Effective Beam Thickness t_i (m)	Stress in Lowest Beam after Lift & Prior to Collapse (MPa)	Stress in Spanning Unit above Goaf (MPa)	Predicted Minimum Beam Thickness Required to Span Goaf (m)
1	1.2	1.2	7.6	23.96	137.55	0.51	105 (47.9)	12.0	4.82	**56.7**
2	2.4	2.4	15.3	43.26	120.77	0.66	81 (38.6)	12.5	7.81	**43.6**
3	4.2	4.2	26.8	67.38	107.25	1.46	62 (24.1)	17.3	6.55	*26.6*
4	6.0	6.0	38.2	85.60	90.36	2.94	38 (18.2) (9.1)	13.8	10.10	*10.8*
5	8.4	8.4	53.5	99.57	77.60	5.58	19.4 (14) (7)	19.2	7.45	*5.6*
6	10.8	10.8	68.8	105.0	67.81	9.39	5.4 (2.7)	12.5	-	*3.0*

W_i = Effective Span above mine workings at A-Zone Limit Horizon (W - 2Atanθ).
(9.1) - Bedding thickness halved as bedding sheared under load > it's shear strength during test.
Bold - stress limited to UCS based on full cover load (Equation 1).
italics - stress limited to UCS based on deflecting strata curvature (Equation 2).
UCS = 10.94 MPa; E = 984 MPa; θ=19.3°.

The measured strata unit thickness (t_i) required to span the goaf voids and limit the height of continuous fracturing (A) after each successive lift were back-analysed using the measured A-Zone heights and Equation (2); see **Figure A40g**. The minimum beam thickness required to span the goaf was also estimated based on the two analytical model Equations (1) and (2) and compared to the measured beam thickness at the A-Horizon in **Figure A40h**.

Several further salient points are apparent from the results as follows:

- After extraction of the panel, all of the spanning units deflected under gravity loading until the tensile, shear and compressive stresses in some of the rock mass bedding units were exceeded.

- It was apparent from the modelling data that the overburden above each mining stage resulted in the beam shearing into two or three separate beams, with the lower beam collapsing and the upper beam(s) left to span the void. It is noted that the maximum shear stress acting on the initial beam would have developed on the bedding surface near the middle of the beam section, so it would be expected to shear or slip there first.

- If the strata unit separated from the overlying rock mass, it either collapsed into the void below (if the stress exceeded the UCS of the beam) or it was thick enough to span under its own self weight. The sagging beam units were also supported by the underlying goaf to some degree.

- The rock mass units caved up into the overburden at an angle of break (θ) and effectively reduced the span of overlying units to $W_i = W - 2y\tan(\theta)$. The potential load acting on the strata units also decreased linearly with the reduction in overlying cover.

- The height of continuous fracturing (i.e. the A-Zone) was defined as the point where the overlying strata were spanning the cracked and collapsed strata below it.

- The A-Zone height increased after the mining height T was increased, with no change to panel width or cover depth.

- The strata units continued to deflect after each incremental increase in mining height, with the lower units collapsing when the UCS of the beam was exceeded. In some of the lifts, it is apparent that the spanning strata units sheared into units that were approximately half the thickness of the original spanning beam. The beam stress was also subsequently decreased if shearing occurred. Estimates of shear stress at mid-beam thickness exceeded the shear strength of the strata unit (or bedding plane surface) in these instances, assuming a friction angle of 20° along the bedding planes.

- The spanning strata lost stiffness when their thickness was decreased, resulting in further deflection (and stress acting in the beam).

- Collapsed strata units provided support to the sagging strata above and ultimately controlled the deflection of the overlying units.

- The A/T ratio ranged from 20 to 10 as the mining height increased from 1.2 m to 10.8 m. For real world mining heights of 2.4 m to 6 m, the A/T ranged from 18 to 14.

Further discussion on the analytical height of fracturing models for real world conditions is presented in **Section A11.4.2**.

A11.3.3   Forster and Enever, 1992

A comprehensive monitoring program above two supercritical pillar extraction and one longwall panel in the Great Northern Seam was presented in **Forster and Enever, 1992**.

The outcomes of the work was to recommend a reduction in the minimum rock cover limit required to extract coal beneath Lake Macquarie to 45T + 10 m, and was based on borehole piezometric and rock mass permeability testing before and after total extraction mining. The 10 m was not added to account for the surface cracking zone, but to allow for localized depressions that could reduce the rock cover thickness to < 45T. The surface cracking zone of <15 m was therefore included in the 45T+10 m criterion.

The height of continuous fracture zone was assessed to have ranged between 21T and 33T above the mine workings. The thickness of the Constrained Zone was defined as being dependent on the cover depth, but should be > 12T + 10 m below tidal waters.

The thickness of the 'Constrained Zone' above the 'Fractured Zone' was also considered to have greater importance in regards to providing a groundwater drainage path barrier than the tensile strain limit of 7.5 mm/m set by **Wardell, 1975**. It was considered that the thickness of the Constrained Zone and the presence of low permeability lithologies, such as mudstone and claystone, were more likely to influence the performance of the strata barrier above the A-Zone than putting a limit on surface strain. The strain limit criterion has subsequently been left out of sub-aqueous mine design criteria in NSW Coalfields.

A11.3.4   ACARP, 2006

This report reviews the impacts of shallow longwall mining on the groundwater systems based on fieldwork conducted in the Hunter Valley, NSW (Beltana Mine) and Bowen Basin, Queensland (Gregory Crinum Mine).

The **ACARP, 2006** report suggests that continuous cracking is likely to occur through the strata beams within the Fractured Zone defined by an "angle of break" of 12° to the vertical and extending inwardly from the rib-sides. International research suggests a range between 10° and 15°.

A complementary set of fractures would also be expected to develop further inside the panel on the undersides of the bending units where full subsidence develops in the strata. The angle to full subsidence ranges from 25° to the vertical according to **ACARP, 2006** and from 32° to 45° in **Li and Cairns, 2000**.

Back analysis of the angles of break suggest that surface to seam cracking could theoretically reach the surface above panels that are wide enough to prevent the opposing cantilevering abutments to interact together and limit fracturing. For a panel width of 200 m, this would occur where cover depths are < 370 m to 470 m (due to angles of break of 12° to 15°). It is also noted that the inferred height of fracturing is very sensitive to the assumed angle of break.

Note: The panel geometry discussed is actually still in the sub-critical range (i.e. W/H < 0.7) and it is considered by DgS that theoretical fracturing to the surface can only occur in the critical to supercritical panel width range.

ACARP, 2006 also notes an absence of surface to seam fracturing connection or groundwater inflows in the literature, where sub-aqueous mining has occurred below a depth of cover of 120 m to 160 m (for assumed critical to super-critical panel widths). The reason for this phenomenon is considered to be related to the observation that cracked and rotated blocks may still interact and provide low permeability regions in the zones of compressive strain above and below tensile cracking in the deflected beams. It was assessed that the reduction in effective span due to the cantilever effect over the ribs and increase in support that develops to overlying strata units may also allow strata units as thin as 10 m or so span across the fractured zone.

The report concluded that the height of continuous fracturing is therefore likely to be controlled by either spanning strata units or units that are not spanning which are thick enough to stop fracturing occurring right through the unit.

In the case of the non-spanning strata mechanism, **ACARP, 2006** did not have the resources available to fully evaluate what the minimum strata thickness range is likely to be in order to limit the continuous fracturing height.

Note: A similar conclusion was reached by DgS after a case by case review by DgS of supercritical longwall geometries in the NSW Coalfields in this study. It is also considered likely that this phenomenon would require the compressive stress in the deformed rock mass units to exceed their unconfined compressive strength for complete break-through to occur. However, it is also apparent that the presence of thin strata units that deform predominately in shear along slipping bedding partings, can also limit vertical cracking developing to the surface cracking zones.

A11.3.5 MSEC, 2011 and SCT, 2001

The MSEC and SCT models are based on several published case-studies for mining impacts in the NSW Coalfields and their own internal analytical and numerical modeling results. The 'heights of fracturing' are predicted based on longwall and total pillar extraction panel widths and indicate maximum values ranging from 1W to 1.5W (SCT) and 1.374 (W-30) (MSEC). The database of 'observed heights of fracturing' and the above panel width models are presented in **Figure A40i**.

Based on a review by DgS of the database from which the MSEC and SCT models are derived, and extensometer and vertical strain measurements at other mines, it is apparent that the models include cases of both A and B-Zone fracture heights (see **Figure A40j** and **Section 11.4** for further details). DgS concludes that the MSEC and SCT 'height of fracturing' models are probably conservative.

It is also apparent that there are three reported cases in the database which indicate 'fracturing through to the surface' has occurred (LW1 at Invincible, LW11 at Angus Place and LWE1 at South Bulga). A review of the extensometer data published by **Holla, 1991** for the Invincible case study, DgS concurs with the assessment that continuous fracturing has probably extended to the surface cracking zone (or to within 10 m below the surface). No data is available for the latter two cases, however, based on the above discussion, it is considered possible that surface to seam connectivity of the B-Zone (and not the A-Zone) occurred at these sites (further discussion on these sites are included in the following sections).

A11.3.6 Bulli Seam PAC, 2010

The NSW Government Planning and Assessment Commission (PAC) for the Bulli Seam Project Application in 2010 identified several apparent deficiencies in the commonly used 'height of sub-surface fracturing' models as follows:

- It is apparent that the prediction models based on panel width only indicated significantly greater sub-surface fracture heights than the models based on mining height.

- The panel width only-based models did not distinguish between continuous and discontinuous fracture heights.

- The authors and reviewers of the prediction models all recognize the deficiencies in the height of fracturing models that are based solely on panel width or mining height. They also indicate that more thorough analysis is probably required to determine a 'more definitive' function that relates the height of connective cracking to the mining geometry.

Based on the PAC report and review of available published data the following comments are made by DgS:

- The data on which the Panel Width-Only models are based are likely to include both A and B type fracturing zones (hence the review of MSEC and SCT database presented in **Figures A40i** & **A40j**).

- The Panel Width only models appear to have been developed mainly from data obtained at deep, sub-critical mines of the Southern and Western Coalfields.

- The height of fracturing is considered unlikely to extend further up into the strata once the critical panel width is reached (for a given mining height) and no further deformation of the overburden can occur.

- The behaviour of the overburden is more likely to be influenced by panel width for sub-critical panels and mining height for supercritical panels.

A11.3.7 State of the Art Summary and Gap Analysis for Alternative Models

In summary, the literature review outcomes indicate the following:

- The A-Zone is assessed to range from 21T to 33T above supercritical panels and up to 43T above critical and sub-critical panels. The B and C-Zone thicknesses will generally depend on the cover depth less the A-Zone Horizon estimate.

- The models that are based on the longwall panel widths only indicate maximum 'heights of fracturing' that range from 1.0W to 1.5W (SCT) and 1.374(W-30). These models however, probably include both A and B-Zone fracture heights in some instances and are therefore likely to be conservative.

- It is apparent that the published height of fracturing models based on mining height alone varies significantly for supercritical, critical and sub-critical mining geometries. The A-Zone could (and does) extend higher up into the overburden above sub-critical

panel geometries as the fracturing due to strata deformation is also influenced by the panel width.

- It is also reasonable to assume that the maximum height of the A-Zone will probably occur above the centre of a sub-critical longwall panel with a naturally spanning catenary arch.

- Surface drilling investigations above subsided longwall panels in NSW and QLD have found the maximum height of fracturing is in fact 'dome-shaped' and develops somewhere between the point of maximum tensile strain and the centre of the panels.

- In order to distinguish between A and B-Zones it is considered best-practice to install borehole extensometers and multiple-piezometers (deep and shallow) above longwall panels and measure the various fracture and dilated zones based on anchor displacements, vertical strain and the short to medium term impacts to established groundwater regimes.

- When longwall mining beneath lakes and sensitive groundwater aquifers, it is essential that the mining geometry be controlled to provide an effective B/C-Zone or Constrained Zone thickness to minimise the potential for connective cracking to develop up to the feature. The presence of geological structure should also be considered as it may act as a potential groundwater conduit between the A and B-Zones.

- Based on **Forster and Enever, 1992**, the minimum Constrained Zone (B/C Zone) thickness above the Fractured A-Zone should be >12T + 10 m and include the surface cracking zone thickness of <15 m beneath Lake Macquarie. The minimum B/C Zone thickness does not include weathered material and/or alluvial sediments.

- For cases where permanent water bodies do not exist, but surface to seam hydraulic connection is not desirable, it is recommended that the continuous height of fracturing zone should not encroach within the surface cracking zone (ie. A minimum of 10 m to 12 m below the surface should be assumed generally, but may need to be increased up to 20 m for steep topography affects).

- As mentioned earlier, the height of A-Zone fracturing is strongly dependant on the presence of the bridging capability of massive conglomerate or sandstone units above a given panel. Therefore, estimating the height of A and B-Zone fracturing also requires a review of the overburden lithology and the presence of geological structure.

- It is also apparent from a case by case review, that the height of fracturing may be controlled by strata that is not actually spanning, but may be thick enough or flexible enough to stop fracturing occurring right through the strata unit. For this scenario, it is considered the height of fracturing will be controlled by (i) the thickness and/or flexibility of the strata unit relative to the panel width and its location above the workings, (ii) the thickness of compressible goaf material that will induce curvature in

the overlying strata units as the goaf is compressed, and (iii) the presence of confined, semi-impermeable strata units such as mudstone and claystone in the B and C-Zones that will swell in the presence of groundwater and effectively seal off small width cracks.

- For the case of sub-critical panels, the maximum non-spanning strata height and load acting on the goaf may be limited by the 'natural' or catenary arch that can form across the mined void width. It is noted that the A-Zone has not intersected the surface above any of the 13 sub-critical longwall panels in the NSW Coalfields.

- For super-critical panels however, the height of fracturing could theoretically reach the surface and the maximum load acting on the goaf will probably equal the cover depth. It is noted that the A-Zone has not intersected the surface above critical and supercritical panels at 17 out of 20 longwalls (85%) in NSW and Queensland Coalfields.

- Near surface geology will affect the potential for surface cracking to intersect the sub-surface fractures above supercritical longwall panels. Based on physical modelling results and mine site case studies, thinner and weaker strata units may actually reduce the likelihood of cracking zone interconnection compared to thicker and stronger units.

- Subsidence effect data (i.e. Horizontal strain/curvature ratios or K Factors) also suggest that the near surface strata will behave like a beam with a thickness equal to twice this ratio or the observed cracking depths (i.e. the depth to the neutral axis of bending). For the Newcastle Coalfield, the effective beam thickness ranges from 10 m to 30 m (i.e. K Factors of 5 to 15). The Western and Southern Coalfields have effective beam thickness ranges from 30 m to 60 m (i.e. K Factors of 15 to 30).

Based on the HoF prediction model review, it was considered necessary in this study to:

(i)   review and expand the database of continuous and discontinuous cracking to include a representative range of mining geometries on which to base the empirical models on;

(ii)   update and re-evaluate the **ACARP, 2003** models;

(iii)   attempt to develop further subsurface fracturing models that included the panel width, mining height, cover depth and lithology (effective strata unit thicknesses and their properties).

(iv)   provide a clearer definition of the surface cracking depth (D-Zone).

A11.4   Expansion of the Database and Review of Sub-Surface Fracturing Prediction Models Presented in ACARP, 2003

A recent review of the **ACARP, 2003** database and the inclusion of new HoF data has recently been undertaken by DgS in 2012 and 2013 for various projects in the Newcastle/Lake Macquarie and Hunter Valley Coalfields. The up-dated database is presented in **Table A6.1** and includes a greater number of cases where A and B-Zone fracture heights have been determined from borehole extensometer <u>and</u> piezometeric data collected over a reasonable period of time (i.e. > 12 months after mining impacts). Surface and groundwater interaction may also be established by other means in the absence of piezometers and extensometer results (e.g. mine water make increases several days or weeks (instead of months) after rainfall events, would indicate direct hydraulic connection to the surface).

The measured coalfield data base presented in **ACARP, 2003** was based mainly on a dataset of post-mining drilling data to estimate heights of fracturing for the A and B-Zones (except for the **Forster and Enever, 1992** data). The updated model database now includes further extensometer and/or piezometric data from the Southern, Western and Hunter Valley Coalfields in NSW, including Newcastle (West Wallsend, Mandalong, Wyee, Cooranbong, Teralba), Lower Hunter Valley (Abel, Austar, Ellalong); the Upper Hunter Valley (Homestead, Ashton, South Bulga), Southern Coalfield (Berrima, Metropolitan, Kemira, Belambi West, West Cliff, Tahmoor, Dendrobium, Appin) and the Western Coalfield (Springvale, Invincible). Two cases for Queensland (Oaky Creek and Crinum) were also included in the database.

Based on a review of published extensometer results presented in **Holla, 1991**, **Frith, 2006, MSEC, 2011** and **ACARP, 2007**, it is assessed that there are six cases in the database presented in **MSEC, 2011** that appear to include the A and B-Zones and four cases whereby the 'height of fracturing' are claimed to have reached the surface at distances above the workings of 21T (Homestead Mine, LWs 9/9A), 39T (Invincible Colliery, LW1), 57T (South Bulga, LWE1) and 106T (Angus Place, LW11).

In order to use the height of fracturing data presented in **MSEC, 2011** with the **ACARP, 2003** data, it was necessary to identify the likely A-Zone cases and B-Zone cases based on the following fracture zoning criteria:

(i)   A-Zones are likely to have vertical strains > 20 mm/m and large strata dilations > 200 mm; and

(ii)   B-Zones are likely to have vertical strains of < 8 mm/m and strata dilations < 200 mm, based on measured values for cases with piezometer-established B-Zone strains measured at other mines.

Note: it does not necessarily follow that uniform vertical strains throughout the strata mean the height of continuous fracturing is likely to have reached the surface. The uniform strains may also be due to strata bedding dilations if strains are < 8 mm/m. Rock mechanics theory also indicates that a vertical tensile strain of 8 - 9 mm/m will induce a horizontal tensile strain of 2 - 3 mm/m in the rock mass due to

Poisson's ratio effect. The theoretical strain to fracture a joint-free sample of rock is 0.3 to 0.6 mm/m. It has been observed in the field that existing joints and bedding in the rock mass allow it to 'absorb' higher levels of tensile strain before developing fresh cracks at around 2 - 3 mm/m. The use of the proposed vertical strain of 8 mm/m is therefore considered to be a reasonable indicator that fresh cracking is likely to occur in the rock mass.

The following cases were changed from A to B-Zone fracturing horizons or reinterpreted by DgS based on the above criteria:

- Tahmoor LW3 (extensometer interpretation by **Holla & Buizen, 1991**)
- Westcliff / Endeavour Drift BH3 (post-mining bore interpretation by **MSEC, 2006**)
- Angus Place LW11 (fractures to surface interpreted by **Kay, 1990**)
- Springvale LW411 (extensometer & piezometer interpretation by **CSIRO, 2007**)
- Springvale LW409 (piezometer interpretation by **CSIRO, 2007**)
- Ellalong LW2 (extensometer interpretation by **Holla, 1986**)

The height of continuous fracturing for LWE1 at South Bulga (**SCT, 2000**) has been assumed to extend to within 10 m of the surface and into the surface cracking zone as the extensometer or piezometric data is not available to review at this stage.

The assessment in **Kay, 1990** that the height of fracturing above LW11 at Angus Place extended to the surface was well above previous ranges (106T) measured at the mine to-date. Further discussions by the mine with the author recently indicates that a 100 m high cliff face probably affected the overburdens spanning capability, resulting in a greater than normal level of subsidence and near surface cracking. Although the surface flows in the creeks may have been re-routed into near surface cracks at the time, it is not likely that a surface to seam connection occurred.

It has also been decided to remove two case study points (Central and Southern German Creek Mines) from the original **ACARP, 2003** data base as they appear to be much lower than other cases with similar geology and geometry and were based on drilling data only.

The results of the database review and re-assignment of A- to B-Zones are shown in **Figure A40j** with the reinterpreted values summarised in **Table 6.1.** A summary of several representative extensometer results that were used to review the published heights of fracturing data presented in **Table A6.1** are provided in **Table A6.2**.

The expanded database presented in **Table A6.1** has subsequently been used to (i) update the strain and curvature index-based models presented in **ACARP, 2003** and (ii) develop more technically concise models that allow variations in geology and geometry to be assessed in each coalfield. The results are presented in the following sections.

Table A6.1 - Updated HoF Model Database for Australian Coalfields

Site	Panels	Mine	Seam	W (m)	H (m)	W/H	T (m)	A (m)	B (m)	A/T	t^ (m)	y^ (m)	Unit SRP*	ACARP 2003 Model Predictions U95% CL S$_{max}$ (m)	U95% CL E$_{max}$ (mm/m)
1	MW508	Bellambi W.	Bulli	110	421	0.26	2.50	92	-	37	100	90	High	0.30	2
2	LW10	Metropolitan	Bulli	140	460	0.30	3.40	130	-	38	100	130	High	0.29	3
3	LW1-4	South Coast	Bulli	110	325	0.34	2.50	85	-	34	100	85	High	0.24	3
4	LW6	Kemira	Wong.	117	335	0.35	2.75	98	-	36	100	98	High	0.16	2
5	LW20	Metropolitan	Bulli	163	450	0.36	3.40	100	-	29	100	100	High	0.34	2
6	LWA1	Austar	Greta	159	417	0.38	6.00	*87*	277	15	100	80	High	0.56	4
7	LW514	Bellambi W.	Bulli	150	400	0.38	2.70	90	-	33	100	90	High	0.29	2
8	LW28	Appin	Bulli	200	500	0.40	2.30	90	-	39	120	90	*High*	0.27	1
9	*LW2*	*Ellalong*	*Greta*	*150*	*368*	*0.41*	*3.50*	*113*	*210*	*32*	*100*	*113*	*High*	*0.40*	*3*
10	*LW3*	*Tahmoor*	*Bulli*	*180*	*424*	*0.42*	*2.18*	-	*204*	-	*100*	*100*	*High*	*0.29*	*2*
11	LW9	Teralba	YW	150	350	0.43	2.70	*110*	150	41	34	110	High	0.32	2
12	*TE*	*West Cliff*	*Bulli*	*200*	*446*	*0.45*	*2.50*	*101*	*245*	*40*	*100*	*101*	*High*	*0.30*	*1*
13	TE	Berrima	Wong.	120	176	0.68	2.3	76	112	33	100	76	High	0.50	3
14	*LW409*	*Springvale*	*Lithgow*	*265*	*385*	*0.69*	*3.25*	*133*	*254*	*41*	*55*	*133*	High	*0.6*	*3*
15	LW9	Mandalong	WW	160	220	0.73	4.50	-	-	-	30	160	High	0.5	3
16	***LW11***	***Angus Place***	***Lithgow***	***211***	***263***	***0.80***	***2.47***	-	***253***	-	***100***	***253***	**High**	***0.5***	***3***
17	*411*	*Springvale*	*Lithgow*	*315*	*368*	*0.86*	*3.25*	*139*	*288*	*43*	*55*	*139*	High	*0.68*	*5*
18	LW5	Mandalong	WW	160	179	0.89	3.70	118	154	32	25	83	*Mod*	1.38	3
19	LW5	Dendrobium	Wong.	245	255	0.96	3.75	123	-	33	80	123	High	1.25	5
20	LW1	Wyee	Fassifern	216	206	1.05	3.44	126	-	37	30	126	High	1.09	5
21	**LW1**	**Invincible**	**Lithgow**	**145**	**116**	**1.25**	**2.70**	**106**	***111***	**39**	**15**	**106**	**Low**	**1.62**	**16**
22	TE1	Abel	U. Don.	120	95	1.26	2.55	45	*75*	20	15	41	Low	1.51	22
23	LWs	Ashton	Pikes Gully	216	154	1.40	2.55	82	*130*	32	30	82	Low	1.5	15
24	LW40	WWC	WBH	179	113	1.58	3.80	80	*108*	21	20	80	Low	2.28	21
25	**LWE1**	**Sth Bulga**	**Whybrow**	**259**	**155**	**1.67**	**2.55**	**145**	**150**	**57**	**20**	**145**	**Low**	**1.53**	**8**
26	LW41	WWC	WBH	179	105	1.70	3.80	72	100	19	20	72	Low	2.28	24
27	LW9	Crinum	Lillyvale	280	155	1.81	3.50	85	*150*	24	35	105	High	1.82	8
28	LW39	WWC	WBH	179	97	1.84	3.90	68	92	17	20	68	Low	2.18	25
29	TE-3D	Wyee North	GN	355	185	1.92	1.90	63	*143*	33	50	63	High	1.14	4
30	TE-355	Wyee North	GN	355	180	1.97	1.90	40	-	21	50	40	High	1.14	4
31	Panel2	Abel	U. Don	150	76	1.97	1.88	45	71	24	15	33	Low	1.13	23
32	TE-Nth B	Cooranbong	G.N	150	75	2.00	2.80	58	*70*	21	20	58	Low	1.68	33
33	LW1	Oaky Ck	German Ck.	205	95	2.16	3.20	55	*90*	17	30	55	Low	1.92	25
34	**LW9/9a**	**Homestead**	**Whybrow**	**200**	**80**	**2.50**	**3.40**	**75**	**75**	**23**	**15**	**65**	**Low**	**1.98**	**29**

- = not available; **bold** - surface to seam fracturing assessed by others; *italics* - Continuous Fracture Zone heights (A-Zone) was originally reported by others and included the Discontinuous Fracture and Dilated Zone (B-Zone). A and B- Zone height of the B-Zone heights were re-assessed by DgS based on a review of available measured vertical strains and piezometric data (see **Figure A40i and A40j**); No shade - Sub-critical panels (W/H<0.7); Light grey shade - Critical panels (0.7<W/H<1.4); Grey shade - Supercritical panels (W/H>1.4).
* - SRP = Subsidence Reduction Potential for strata unit with thickness t and distance y above the workings. The SRP may be due to spanning or bulking behavior over the range of W/H and is also considered to be an indicator of whether a strata unit will limit the height of continuous fracturing; ^ - likely values assessed from borehole and subsidence data; Wong. = Wongawilli; YW= Young Wallsend; WW = West Wallarah; U. Don = Upper Donaldson; WBH = West Borehole; GN - Great Northern.

Table A6.2 - Summary of Measured A, B, C & D Zone Strains in Extensometers*

Parameter	Underground Coal Mines									
	Angus Place$		West Wallsend				Abel^			
Panel No.	LW11		LW39		LW40		Panel 1		Panel 2	
Cover Depth H (m)	211		97		113		95		76	
Panel Width W (m)	263		179		179		120		150	
W/H	0.8		1.84		1.58		1.26		2.0	
Mining Height, T	2.5		3.8		3.9		2.1		2.1	
Fracture Zone	Dilation (mm)	Strains# (mm/m)	Dilation (mm)	Strains# (mm/m)	Dilation (mm)	Strains# (mm/m)	Dilation (mm)	Strains# (mm/m)	Dilation (mm)	Strains# (mm/m)
D-Zone	-	*3 - 5*	-	*25*	-	*24*	-	*24*	-	*23*
C-Zone	-	**-**	-	**-**	-	**-**	-	**-**	-	**-**
B-Zone	~60 - 120	**5 - 6**	8 - 17	**1 - 2**	25 - 50	**5 - 8**	14 - 19	**1 - 2**	<20	**-1 - 0**
A-Zone	~1000	**100**	234 - 957	**115 - 139**	390 - 769	**39 - 77**	279 - 1289	**28 - 129**	158 - 185	**16 - 19**

Parameter	Mandalong		Austar		Ellalong	Invincible	Tahmoor
Panel No.	LW5		LWA1		LW2	LW1	LW3
Cover Depth H (m)	179		453		368	116	424
Panel Width W (m)	160		159		150	145	180
W/H	0.89		0.35		0.41	1.25	0.42
Mining Height, T	3.7		6.0		3.5	1.26	2.2
Fracture Zone	Dilation (mm)	Strains# (mm/m)	Dilation (mm)	Strains# (mm/m)	Strains# (mm/m)	Strains# (mm/m)	Strains# (mm/m)
D-Zone	-	*5*	-	*3*	*3*	*10*	*1*
C-Zone	<20	**<1**	<10	**<1**	**<1**	**-**	**<1**
B-Zone	19 - 29	**2 - 5**	24 - 133	**1 - 7**	**1 - 5**	**<5**	**1 - 4**
A-Zone	73 - 672	**80**	222 - 1177	**11 - 59**	**>10**	**10 - 75**	**N/A**

* - A, B & C-Zone strains are vertical and approximately 3 to 4 times the horizontal strain due to Poisson's ratio effect; *italics* - D-Zone strains are horizontal.

- tensile strains are positive. Negative strains or compression develops after full subsidence occurs and goaf compresses under load from sagging overburden strata; ^ - Effective mining height for total pillar extraction (Te = 0.85T); $ - Strain data not available and quoted from published literature.

Table A6.2 (Cont…) - Summary of Measured A, B, C & D Zone Strains in Extensometers*

Parameter	Underground Coal Mine			
	Springvale			
Panel No.	LW411		LW412	
Cover Depth H (m)	368		400	
Panel Width W (m)	315		315	
W/H	0.90		0.79	
Mining Height, T	3.25		3.25	
Fracture Zone	Dilation (mm)	Strains[#] (mm/m)	Dilation (mm)	Strains[#] (mm/m)
D-Zone	-	*3*	-	*3*
C-Zone	<42	<5	<33	<5
B-Zone	39 - 410	4 - 10 (**17**)	2 - 505	4 - 8 (**25**)
A-Zone	194 - 1441	14 - 42	174 - 1571	5 - 42

* - A, B & C-Zone strains are vertical and approximately 3 to 4 times the horizontal strain due to Poisson's ratio effect; *italics* - D-Zone strains are horizontal.

- tensile strains are positive. Negative strains or compression develops after full subsidence occurs.

^ - Effective mining height for total pillar extraction (Te = 0.85T).

bold - measure strain near the top of the B-Zone where a bedding separation occurred. Piezometer data indicates the height of continuous fracturing is further below this point.

A11.4.1 Updated Tensile Strain Model

The physical model presented in **Whittaker and Reddish, 1989** related the ratio of the height of continuous and discontinuous fracturing (A and B) above longwall panels over cover depth (H) with the maximum tensile strain (E_{max}) at the surface due to mine subsidence. Actual drilling data over extracted longwall panel goaf was subsequently used to define a real-world relationship between these variables at several Australian Coalfield mines in **ACARP, 2003**.

The additional data presented in **Table A6.1** has been added to the original database and the regression equations have been revised below:

{A-Line} Mean A/H $= 0.180 \, Ln(E_{max}) + 0.1405, \quad R^2 = 0.70$

U95%CL A/H* $= 0.180 \, Ln(E_{max}) + 0.3742.$

{B-Line} Mean B/H $= 0.146 \, Ln(E_{max}) + 0.5315, \quad R^2 = 0.47$

U95%CL B/H* $= 0.146 \, Ln(E_{max}) + 0.8426.$

* - Maximum A/H and B/H = 1.

where

A, B = height above workings to A and B-Zone horizons,
H = cover depth,

E_{max} = the maximum predicted tensile strain for a 'smooth' subsidence profile.

The new tensile strain model is presented in **Figure A41a** and has a much stronger fit to the new database for the A-Zone than the **ACARP, 2003** model, with only a slight improvement for the B-Zone horizon. The R^2 value for the logarithmic regression curve fitted to the revised A-Zone data was previously 0.44 and is now 0.70. The R^2 value for the B-Zone was previously 0.46 and is now 0.47.

The measured database model still appears to indicate a similar height of fracturing trend to the **Whittaker and Reddish, 1989** physical model. However, as was concluded in **ACARP, 2003**, the predicted heights of 'continuous' and 'discontinuous' fracturing in the real world were again higher for a given tensile strain at the surface, and probably due to the influence of jointing in the rock mass (compared to none in the physical model).

The real world database indicates that the tensile strain probably needs to be >32 mm/m for surface to seam connection to occur, and is approximately 50% of the physical model value of 60 mm/m. It should also be noted that if connective cracking is likely to extend into the Surface Cracking Zone (a depth of 10~15 m below the surface), then the maximum tensile strain for surface to seam connection reduces to 25 mm/m. It is assessed however, that the predicted strains are also dependent on surface crack width development and should therefore not be used to assess surface to seam connectivity directly without considering the near surface B and C-Zone lithologies.

Considering the potential difficulties with predicting strains after the onset of cracking, it is still assessed that it is unlikely that the tensile strain-based model will be reliable. **ACARP, 2003** attempted to modify the strain-based model to a curvature-based approach. The resulting regression equations however, did not improve the correlation between the adopted variables (i.e. both methods had R^2 values of 0.44). The curvature-based model of height of sub-surface fracture prediction was subsequently revised with the expanded model database in **Section A11.4.2** to see if the regression equations could be improved upon.

A11.4.2   Updated Overburden Curvature Index Model

The Overburden Curvature Index or S_{max}/W'^2 term was introduced in **ACARP, 2003** in an attempt to provide a readily measurable field parameter that would not be compromised as much by surface strain concentration effects (i.e. cracking). The logarithmic regression lines were re-derived using the expanded database to give new predictions of the mean and U95%CL values for both A and B-Zones as follows:

{A-Line} Mean A/H $= 0.198\,Ln(S_{max}/W'^2) + 1.1518$, $R^2 = 0.66$

U95%CL A/H* $= 0.198\,Ln(S_{max}/W'^2) + 1.3915$.

{B-Line} Mean B/H $= 0.152\,Ln(S_{max}/W'^2) + 1.3265$, $R^2 = 0.52$;

U95%CL B/H* $= 0.152\,Ln(S_{max}/W'^2) + 1.5928$.

          * - Maximum A/H and B/H = 1.

where

    A, B   = height above workings to A and B Horizons,

    H   = cover depth (m).

    S_{max}/W'^2 = Overburden Curvature Index,

    W'   = lesser of W and 1.4H

Note: It is reasonable to assume the effective mining width (W') and height of fracturing (A/B) will be limited beyond the point where the maximum subsidence or strata deformation has been reached above supercritical mining geometries (i.e. W/H > 1.4).

The revised regression results are shown in **Figure A41b**.

Despite the apparent improvement in the regression equations, the same apparent differences still remain between the Australian height of fracturing database and the UK physical modelling results. One obvious difference is that the UK physical model represents a supercritical case study where the panel width and cover depth was constant (i.e. W/H = 1.34). The Australian database however, has a significant range of sub-critical, critical and super-critical panel geometries and further investigation of this difference is therefore required (see **Section A11.4.4**).

A11.4.3   Influence of Lithology on Sub-Surface Fracture Heights

An assessment was made in **ACARP, 2003** on whether massive lithology had the potential to control or limit the height of fracturing above a longwall panel. The expanded model database presented in **Table A6.1** still indicates that it does, with the A-Horizon likely to have coincided with the base of the massive strata units in 17 out of 21 cases with 'Moderate' to 'High' SRP strata units.

The potential for massive strata units to mitigate the height of continuous fracturing above the workings should therefore not be ignored where subsidence magnitudes and HoF are clearly being controlled by spanning strata.

Overall, the HoF results suggest that the presence of massive sandstone or conglomerate lithology can control the height of hydraulic fracturing due to their spanning capability or thickness generally. However, as has been observed at Mandalong and Springvale Mines, the presence of geological structure (faults, dykes, seam rolls and shear zone or joint swarms) has resulted in a weakening of the overburden by the tectonic activity and there has been increased subsidence due to the breakdown of massive sandstone / conglomerate into several thinner units and (ii) increased shearing and tensile stress acting on the discontinuities has resulted in groundwater conduits developing deeper into the overburden.

It is therefore usually recommended that a mine undertake a sub-surface fracture-monitoring program which includes a combination of borehole extensometer and piezometer measurements during extraction in non-sensitive areas of the mining lease. Mitigation strategies for longwall mining are generally limited to (i) reducing the extraction height, (ii) decreasing the panel width and (iii) panel location adjustment. On-going monitoring of

surface alluvium and near surface rock mass aquifers is also undertaken with standpipe piezometers to check the post-mining integrity of ground water dependent ecosystems (GDE) and surface water systems generally.

A11.4.4 Height of Fracturing Angle Model, DgS 2012

Due to the currently held belief in the Australian mining industry that the sub-surface fracture heights are strongly influenced by panel width and mining height, an alternative model was developed by DgS in 2012 using a different approach to analysing the UK model data presented in **ACARP, 2003**.

Predictions of the heights of continuous and discontinuous fracturing (the A and B-Zone horizons) were re-analysed using the panel width, the mining height and a simple parabolic profile formula to estimate A and B-Zone fracture heights from a calibrated abutment angle at seam level (θ_A and θ_B) as follows:

- Continuous Fracture Zone Height, $A = W'/(4\tan(\theta_A))$

- Discontinuous Fracture Zone Height, $B = W'/(4\tan(\theta_B))$

where,

W' = Effective Panel width or minimum of W and 1.4H.

θ_A = abutment angle to estimate height of A-Zone

θ_B = abutment angle to estimate height of B-Zone

When the UK model's fracture height data is plotted as a height of fracturing angle (estimated from an assumed parabolic fracturing profile between rib abutments), a strong correlation is apparent between the mining height for a given panel width and cover depth (W/H = 1.34); see **Figures A41c** and **A41d** for A and B-Zone Horizons respectively.

The regression analysis indicates the following fracture height angles (in degrees) apply for estimating A and B-Zone fracture heights in the real world:

$\theta_A = 41.617T^{-0.467}$ (mean) and $25.083T^{-0.401}$ (lower 95%CL)

$\theta_B = 21.806T^{-0.233}$ (mean) and $17.295T^{-0.238}$ (lower 95%CL)

Real world fracture height data measured with piezometers and borehole extensometers indicates a similar trend as the physical model results, although there is more scatter in the data that is probably due to both mining geometry (W/H) and geological variability.

The UK physical model assessed mining heights of 1.2 m to 10.8 m, and generated fracture height angles at the abutments ranging from 55° to 18° for the A-Zone and from 37° to 18° for

the B-Zone horizon. The fracture height angle tends to follow a decaying power law as the mining height increases.

For real-world mining heights of 1.9 m to 6.0 m (median of 3.0 m), the calibrated fracture height angles range from 34° to 18° for the A-Zone, and from 22° to 13° for the B-Zone. One A-Zone case had a fracture height angle of 58° due to the apparent 'truncating' effect of a 40 m thick conglomerate strata unit 40 m to 60 m above a supercritical panel in the Great Northern Seam (Wyee Colliery's North-3D Panel).

As was found in the strain and curvature-based model's, the presence of pre-existing jointing in the rock mass is likely to have contributed to greater fracture heights determined from the field data compared to the laboratory model.

The effect of massive strata units is apparent in the database (see **Figure A41c**) and further measurements are necessary to develop a more discerning prediction model that allows 'Low' and 'High' SRP strata to be assessed separately using this model. The height of fracturing model proposed at the time was considered likely to be conservative for greenfields sites if based on the lower bound fracture height angles and to give upper bound fracture height predictions.

Further review of sub-critical, critical and supercritical panel case studies in 2013 has found that the A and B-Zone fracture height angle model could also be further divided into sub-critical, critical and supercritical panel geometries (see **Figure A41e** and **A41f**) as follows:

$\theta_A = 32.448T^{-0.241}$ for the mean fracture height angle.

Upper 95%Confidence limits for the A-Zone were estimated by reducing the mean angle by 5°, 7° and 10° for supercritical, critical and sub-critical longwalls respectively.

$\theta_B = 31.5T^{-0.373}$ for the mean fracture height angle for supercritical panels
$\quad\quad = 25.4T^{-0.373}$ for the mean fracture height angle for critical/sub-critical panels

Upper 95%Confidence limits for the B-Zone were estimated by reducing the mean angle by 3.5^o, 7° and 7° for supercritical, critical and sub-critical longwalls respectively.

The review outcomes suggest that heights of subsurface fracturing appear to increase above sub-critical panels for a given mining height, but are also likely to be due to the panel width and changes in macro-scale structural behaviour of the overburden as well.

Whilst the trend from sub-critical to supercritical panel geometries appears reasonably consistent across the abutment angle model database (with a few cases where thick strata has clearly limited the fracture heights) it is noted that the predicted heights of fracturing are highly sensitive to the selected value of theta. It was therefore considered that a new modelling approach based on Dimensional Analysis and Buckingham's Pi-Theorem would be

needed to reasonably establish definitive relationships between the key variables over a broader range of mining geometries and geological conditions.

A11.5   Alternative Sub-surface Fracture Model Development

Starting with the influence of mining height (T) on the height of A-Zone fracturing, if we firstly consider a supercritical panel of a given width (W) and cover depth (H), **Whittaker and Reddish, 1989** and **Singh & Kendorski, 1991** each demonstrated that the height of continuous fracturing (A) will increase with the square root of the mining height, $T^{\sim 0.5}$, or a power rule of the form $A = aT^b$, as shown in **Figure A41g**. It is apparent that the database of real-world fracture heights with W/H range from 0.3 to 2.22 has greater scatter than the UK model curve for supercritical panel geometry, and therefore indicates that other factors such as the panel width and geology should probably be considered. The apparent under prediction of A-Zone fracture heights by the **Forster and Enever, 1992** model, also supports this view.

If the fracture heights are plotted against panel width (W) only, a similar 'scattered' outcome results as shown in **Figure A41h**. The conservative nature of the height of fracturing models presented by SCT and MSEC is also demonstrated in the figure and suggests that both A and B-Zones are included in their models.

A slightly improved regression analysis results if A is plotted against W/H in **Figure A41i** or when normalized to the panel width (A/W) and is plotted against T in **Figure A41j** for sub-critical, critical and super-critical panel geometries.

Based on these plots, it is clear that consideration needs to be given to the structural behavior of the overburden across the full range of mining geometries, its constituent strata units (or 'beams') and the influence of mining height, T on the development of fracture heights above longwall panels.

A11.5.1   Strata Behaviour Mechanisms that Influence Fracture Heights above Longwalls

Based on structural analysis theories, a conceptual model of the macro-scale and micro-scale mechanisms of sub-surface fracture height development are described below and shown graphically in **Figure A42a**:

Macro-Scale Mechanisms:

- For sub-critical panels, a natural catenary will probably form and transfer the weight of the top half to 2/3 of the overburden to the abutments. The strata below the arch will be subject to sagging or bending forces caused by the void formation. Depending on the span and thickness of individual strata units, the strata in the immediate roof will bend, separate, crack and ultimately cave into the extracted coal void (see *Micro-scale Mechanisms* below).

- Natural catenary arching action infers that the spanning overburden can remain entirely in compression and there is an absence of tensile and shear or 'bending'

stresses. Subsidence data indicates that catenary arching stops occurring once W/H exceeds 0.7.

- Once W/H exceeds 0.7, the overburden will still attempt to span, however, the geometry of the arch will be too shallow for a catenary arch to develop, resulting in bending and cracking of the rock mass.

- The load will still be able to be carried over the void by the overburden, provided the rock mass has adequate strength and stiffness to resist the applied bending moments and shear and tensile stresses (along with increased compressive stresses from inward strata block rotation). This type of behaviour is known as Voussoir or 'cracked beam' behaviour, and is basically a flatter, but a less stiff version of a catenary arch.

- Shallow arching or Voussoir beam action will continue across the panel until it can no longer support the span or weight of the shallow arch. This is usually assumed to have occurred once W/H reaches 1.2 to 1.4H. The weight of the overburden will then be fully supported by the goaf beyond this point and subsidence will be a function of the mining height and cover depth or goaf load.

- The above macro-mechanisms will influence the behavior of the overburden strata units and subsequent development of the sub-surface fracture heights as follows:

Micro-scale Mechanisms:

- Soon after the coal seam is extracted from beneath the overburden, its constituent 'beams' in the immediate roof will generally deflect and behave elastically until the tensile and shear stresses within the rock mass units exceed the material and/or bedding parting strength of the units.

- The strata units will subsequently crack at the abutments and mid-span and the confinement will be partially lost. The cracked beam segments will then rotate inwardly and create a shallow compression arch within the beams (Voussoir action) that may or may not support the load.

- The cracks in the beams at this stage are likely to be discontinuous, with the beam continuing to behave pseudo-elastically with zones of compressive stress above and below the tensile cracks.

- The beam will continue to span and deflect under the applied loading until the compressive strength of the beam is reached, where the beam will then either collapse into the available void, or yield and load the previously failed strata units and goaf below it.

- Based on the physical model results presented in **Whittaker and Reddish, 1989**, the beams may also shear into two or three thinner units before the lower units ultimately crush if their UCSs are exceeded. Bending beam theory indicates that the maximum

shear stress will occur at mid-beam thickness. The beams are therefore likely to break down into half their thickness units each time shearing occurs along bedding partings.

- The goaf will compress and cause further overlying strata units to deflect, shear and crack. The goaf load will continue to increase as cracking continues up into the strata.

- The curvature induced in the beams will probably not cause complete fracture to develop through the beam until the compressive strength of the beam materials is reached. The induced curvature will therefore be a function of the stiffness of the goaf, the stiffness (and thickness) of the deflecting beam and the load acting on it.

- The goaf stiffness will initially be a function of the mining height and the bulking properties of the collapsed roof materials. The goaf stiffness will also increase as the load acting upon it increases (i.e. strain hardening behavior).

- The goaf load will be a function of the rock mass density and effective height of rock above it. The effective goaf load height is likely to be somewhere between the height to the underside of the spanning arch (above sub-critical and critical panels) and the full cover depth. Full load spanning of strata units above supercritical panel geometries are unlikely to occur and full cover depth load may be assumed to act upon the goaf.

A11.5.2   Analytical Height of Fracturing Model

An analytical model of how sub-surface fracturing develops in the overburden is described below in an attempt to define the likely relationships between the mining geometry and overburden as described in the previous section.

Initial Conditions - Elastic Beam Response to Longwall Mining

The maximum horizontal tensile stress before fracturing (σ_t) in a beam of thickness (t) with an effective span of W_i at a distance (y) above the workings will be:

$$\sigma_t = 6M/t^2 = 3\gamma(H-y)W_i^2/4t^2$$

where

M = surcharge load x span^2 /12 = $\gamma D W_i^2/12 = \gamma(H-y)\ W_i^2/12$

γ = unit weight of the rock mass

D = the depth to the base of the spanning beam (or H-y)

The equation shows that the tensile stress in a stack of beams will be greatest near the roof of the mine workings and then decrease linearly towards the surface. The effective span W_i of the beam will decrease as a function of the angle of break of the collapsing strata in the

Caving Zone. The angles of break (θ) are likely to range between 12° and 19° according to the literature and underground observations.

Elastic Beam Cracking and Voussoir Beam Development

The fracturing will continue to progress higher up into the strata until a beam of a certain critical thickness is reached that can either span the distance between the naturally occurring abutments or is thick enough not to fracture right through the beam after it has failed. It is also important to note that the angle of break is not the same as the height of fracturing angles (θ_A and θ_B) discussed in **Section A11.3.4**, as the latter angles were back-calculated from measured heights of continuous fracturing and assumed parabolic fracture limit profiles.

As discussed earlier, the cracking of the strata will lead to the development of Voussoir arching or 'cracked beam' behaviour. The stability of the Voussoir beam will depend upon the compressive stress (σ_c) developed in the beam of thickness (t) that is located a distance, y, above the workings with an effective span (W_i) as follows:

$$\sigma_c = \gamma(H'-y)W_i^2/(4nt^2(1-0.667n))$$

where

      n = the proportion of the beam t in compression and may be determined iteratively by minimizing σ_c as the arch shortens under load and develops a new equilibrium (and provided the stress remains in the elastic region or is less than the UCS). Voussoir analysis results based on the method presented in **Diedrichs and Kaiser, 1999**, indicate that 'n' can range from 0.5 and 0.75 in spanning beams, and will be closer to 0.5 when beam crush conditions are reached.

      W_i = W - 2ytanθ = effective span of the bending beam at distance, y above the mine workings.

      H' = Effective Goaf Load Height, H' or Cover Depth, H.

Voussoir Beam Crushing and Height of Continuous Fracturing

It follows then, that the height of continuous fracturing, A, is likely to develop up to the point where the beam crushes or σ_c = UCS and infers the following relationship exists at the point where the beam starts to yield or crush:

$$UCS = \gamma(H'- A)(W-2Atan\theta)^2/(4nt^2(1-0.667n))$$

$$= 0.75\gamma(H'- A)(W-2Atan\theta)^2/t^2 \qquad\qquad (1)$$

where

      θ = the angle of break that subtended to vertical from the rib side and ranges from 12° - 19° based on subsidence data and underground observations.

H'- A = thickness of rock supported by the beam and may decrease to t (the beam thickness) if the strata beds shear and dilate during subsidence development.

n = 0.5 (conservative).

Equation (1) indicates that the height of A-Zone fracturing is likely to be a <u>cubic function</u> that is dependent on the following variables:

- Panel width, W

- Effective Goaf Load Height, H' or Cover Depth, H.

- Thickness, location and strength and stiffness of the strata units within the overburden (t, y, UCS, E)

- Angle of break, $\tan\theta$

<u>Stresses in Overlying Beams Supported by Collapsed/Fractured Beams</u>

It is noted that Equation (1) ignores the presence of collapsed and fractured material within the A-Zone itself. The formation of the goaf will provide support to overlying fractured units, but also influence the magnitude of curvature and bending stress in the overlying beams as the goaf is compacted and the beams deflect. The curvature of the overlying 'beams' (p_i) may be estimated as follows:

$$p_i = 8\Delta/(y+W_i)^2 = 8(S_{max})/(y+W_i)^2 = 8(\varepsilon_g \, 4T)/(y+W_i)^2 = 32(\sigma_g/E_g)T/(y+Wi)2$$
$$= 32(\gamma H'/E_g)T/(y+W_i)^2$$

where
Δ = mid-span deflection of beam with an effective span, $W_i = W - 2y\tan\theta$.
ε_g = vertical strain of goaf with thickness of 4T (T+3T) and a bulking factor of 1.3.
σ_g = maximum vertical stress acting on the goaf = $\gamma H'$.
H' = effective goaf load height = minimum of H and W'/(4$\tan\theta$)).
E_g = stiffness of the goaf, which is likely to be a function of H, W, T and t.

From the estimated curvature of the strata units above the compacting goaf, the bending stress in the beam may be estimated as follows:

$$\sigma_c = 2M/(Znt) = 2p_i \, E't^3/[12(nt^2(1-0.667n))] = 16(\gamma H)T \, t \, E'/(E_g(A+W_i^2)) \qquad (2)$$

where

E' = rock mass Young's Modulus = 100 - 300UCS (depending on rock mass Geological Strength Index (**Hoek & Diderichs, 2006**));

n = 0.5 for beam at the yield point (i.e. σ_c = UCS)

As before, if σ_c exceeds the UCS, the cracking may extend right through the beam and the height of fracturing, A, may then continue to develop up to the next strata unit. The following relationship will therefore exist at the A horizon:

$$\sigma_c = UCS = 16(\gamma H')T \, t \, E' \, / \, E_g \, (W+A(1-2\tan\theta))^2$$

Overall, the equations represent the physical relationships for either spanning strata (Equation (1)) or non-spanning strata (Equation (2) that are of sufficient thickness to limit fracture continuation through it for a given UCS and mining geometry. As discussed in the following sections, the goaf modulus is likely to be dependent on the mining geometry (W, T and H').

The above equation indicates a complex system with a significant number of independent variables that will influence the height of fracturing outcomes.

Considering the complexity of the above equation and uncertainty in regards to assigning the rock mass and goaf properties, the physical relationship between the variables may also be assessed practically with Dimensional Analysis, a commonly used tool by hydraulics engineers (see **Section A11.5.3**).

A11.5.3   Dimensional Analysis and Buckingham's Pi Theory

According to **Vennard and Street, 1982**, Dimensional Analysis is "the mathematics of dimensions of quantities" built on Fourier's 1882 "principle of dimensional homogeneity". The underlying principle states that "an equation expressing a physical relationship between quantities must be dimensionally homogeneous" i.e. the dimensions of each side of the equation must be the same. It is a valuable means of determining physical relationships between variables in complex systems that defy analytical solution and must be solved by empirical means (i.e. observation, intuition or experiment).

Buckingham's Pi-theory accomplishes this by the formation of dimensionless groups of independent variables that are measureable in the field. For the theory to work, the Pi-terms together must represent all of the three fundamental or primary dimensions of Mass (M), Distance (L) and Time (T), be independent of each other, and not break down into further dimensionless groups.

Buckingham's Pi theory states that in order to determine the physical relationship between a set of 'n' independent parameters in a complex system, it follows that n-3 dimensionless parameters (known as Pi-terms) will be required to reasonably define the dependent variable.

The final equations obtained are in the form of:

$$\pi_1 = f \, (\pi_2, \pi_3 \ldots \pi_{n-3}) \text{ or } f'(\pi_1, \pi_2 \ldots \pi_{n-3}) = 0$$

From the previous analytical equations derived in **Section A11.5.2**, it is assessed that up to 10 variables may influence the height of Continuous Fracturing (A) and Discontinuous Fracturing (B) as follows:

$A, B = f(W, H, T, t, \rho, UCS, E, E_g, \tan\theta)$

The above variables may then be expressed as a combination of products and powers:

$A, B = aW^b H^c T^d t^e UCS^f, \rho^g E^h E_g^i \tan\theta^j$

Seven dimensionless Pi-terms will therefore be necessary to describe the relationships between ten variables identified in a system driven by horizontal and vertical stress, panel width, cover depth, mining height, rock mass density, rock mass strength and stiffness, goaf stiffness, caving angle or angle of break and the location of competent or relatively thick strata units in the overburden.

Notes:
1. The y term may be ignored as it corresponds with the dependent variable (A or B).
2. The goaf modulus (E_g) and caving angle (θ) are considered to be dependent on the mining geometry and may therefore be precluded from the regression analysis.
3. The beam thickness, t refers to the thickness likely to exist just above the fracture height location (t is the most difficult of the parameters to assess, as the strata units may 'break down' into thinner units during subsidence development. The assignment of the appropriate t value therefore requires engineering judgment and analysis that includes a review of borehole logs and rock mass properties with extensometer and piezometer data (if available).

The first step in the analysis is to select a suitable set of recurring variables that cannot themselves be formed into a dimensionless group and can be used to represent one or more of the fundamental dimensions. The recurring variable set selected included the panel width, W, rock mass strength, UCS, and density, ρ, and were used to express the fundamental variables as follows:

Length, L: W;   Mass, M: ρW^3;   Time, T: $\rho^{0.5} W / UCS^{0.5}$

The dimensionless π terms for the remaining independent variables were then assessed using the recurring variable set as follows:

π_1: $A \cdot L^{-1} = A/W$ (Height of Fracturing Term)

π_2: $H \cdot L^{-1} = H/W$ (Goaf Load Index Term)

π_3: $T \cdot L^{-1} = T/W$ (Strata Curvature Index Term)

π_4: $t \cdot L^{-1} = t/W$ (Strata Unit Thickness Term)

π_5: $E \cdot M^{-1} L^1 T^2 = E/UCS$ (Strata Unit Stiffness Term)
which gives:

$A/W = a (H'/W)^b (T/W)^c (t/W)^d (E/UCS)^e$

The constants and powers for each Pi-term can now be determined using measured values in the field and non-linear regression techniques.

If we assume for the moment that the last π term representing the ratio of rock mass stiffness over strength for all cases in the database will be constant (E is typically 250 to 300 times the UCS), then the full equation of dimensionless π terms may be simplified as follows:

$$A/W = a \ (H/W)^b \ (T/W)^c \ (t/W)^d \text{ and } B/W = e \ (H'/W)^f \ (T/W)^g \ (t/W)^h$$

The form of the dimensionless π term equations will be explained in the following sections.

Note: Some of the published literature recommends that the super-critical panel width W' = 1.4H should be used instead of the Panel Width, W, for estimating the height of fracturing above super-critical panels. This is because it was argued that the height of fracturing would probably not continue to develop higher into the strata once the overburden had reached the critical width and had already completely failed. The author agrees with this view and considers the height of continuous fracturing beyond this point would then be controlled by the mining height, cover depth (or goaf load) and geological conditions only.

A11.5.4 Pi-Term Model for Predicting Height of Continuous Fracturing (A) above Longwalls based Mining Geometry Only (i.e. Geometry Model)

For the purposes of demonstrating that height of fracturing prediction models need to consider the influence of geology, a regression analysis was completed without the strata unit thickness Pi-term (t'/W') included. Based on the empirical database presented in **Table A6.1**, the statistics software XLSTAT® was used to complete a multi-nonlinear regression analyses on the first three Pi-terms defined earlier as follows:

$$\underline{\text{Mean } A/W' = 2.215 \ (H/W')^{0.271}(T/W')^{0.372}} \qquad R^2 = 0.61 \ \& \ r.m.s.e. = 0.12W' \ (21\%)$$

$$\underline{\text{U95\% } A/W' = \text{Mean } A/W' + a}$$

where   a = 0.16 for subcritical panels; 0.16 - 0.085(W/H - 0.7) for critical panels; and 0.10 for supercritical panels.

W' = Effective Panel Width = minimum of W and 1.4H.

T = Mining Height.

Re-arranging the above equation in terms of A gives:

$$\underline{A = 2.215W'^{0.357}H^{0.271} T^{0.372}} \qquad +/- aW'$$

The regression results suggest that the height of continuous fracturing (A) will increase with effective panel width (W'), the cover depth or goaf load (H) and the mining height (T) all raised to powers ranging from 0.27 to 0.37.

The above equation(s) may be used to estimate A-Zone fracture heights in the absence of specific geological information (i.e. borehole data). The predicted v. measured outcomes using the "geometry" Pi-terms only model are presented in **Figures A42b** to **A42d**.

The plots indicate that the 'geometry only' Pi-term model is likely to provide reasonably conservative predictions, provided that the geology is not too dissimilar to the conditions that were present for the given mining geometry. For cases where the geology is significantly different above a proposed mining geometry, the above equation may underestimate or overestimate the fracture heights by a significant amount.

The development of a Pi-term model that considers the influence of overburden geology is subsequently addressed in **Section A11.5.5**.

A11.5.5   Pi-Term Model for Predicting Height of Continuous Fracturing (A) above Longwalls with the Geology Pi-Term Included

The presence of massive strata units such as sandstone, conglomerate and igneous rock that may span the fractured strata in the A-Zone is likely to limit the potential range of continuous fracture height development above the mine workings. Based on the analytical models (Equations (1) and (2)), the minimum thickness required to span the A-Zone or limit its development will depend on a number of factors, including span, thickness and rock mass axial and diametric strength. The minimum strata unit thickness required to span the A-Zone may be estimated using empirical and analytical methods, and are described in **Sections A11.5.6** and **A11.5.7** respectively.

If no obvious strata unit thickness is present in the overburden, then it will be necessary to adopt an appropriate minimum value based on subsidence data and typical or atypical geological conditions. The minimum effective t' values are also defined in **Section A11.5.6**.

Based on the empirical database presented in **Table A6.1**, the statistics software XLSTAT[®] was used to complete a multi-nonlinear regression analyses on the first four Pi-terms defined earlier as follows:

$$\underline{\text{Mean A/W' = 1.52 (H/W')}^{0.535}\text{(T/W')}^{0.464}\text{(t'/W')}^{-0.4}} \qquad R^2 = 0.81 \ \& \ rmse = 0.09W'(15\%)$$

$$\underline{\text{U95\% A/W' = Mean A/W' + a}}$$

where   a = 0.15 for subcritical panels; 0.15 - 0.0714(W/H - 0.7) for critical panels; and 0.10 for supercritical panels.
H = cover depth = the maximum potential goaf load height.
W' = effective panel width = minimum of W and 1.4H.
T = mining height.
t' = effective strata unit thickness; see **Sections A11.5.6**.

Re-arranging the above equation in terms of A, gives:

$$\underline{A = 1.52W'^{0.4}H^{0.535}T^{0.464}t'^{-0.4}} \qquad +/- \ aW'$$

The regression results indicate that the height of continuous fracturing (A) will increase with effective panel width (W'), the cover depth or goaf load (H) and mining height (T), all raised to powers ranging from to 0.4, 0.54 and 0.46 respectively and decrease with effective strata unit thickness (t') raised to the power of -0.4. The form of the power rule equation requires the powers to sum to unity to achieve dimensional consistency. The back-analysed powers are also similar in magnitude to the analytical models previously discussed.

A11.5.6 **Effective Strata Unit Thickness Estimates for the Geology Pi-Term Model using Empirical Modelling Techniques**

In order to calibrate the geological Pi-term model, it was necessary to use back-analysis techniques to estimate the likely strata unit thicknesses that existed immediately above the measured heights of continuous fracturing for a given mining geometry.

One of the difficulties in estimating the effective strata thickness from borehole data is the uncertainty in regards to the response of the 'bedded' strata under bending forces and whether they will break down into thinner units.

For example, a 33 to 40 m thick unit of Munmorah Conglomerate existed 80 m above LW5 at the Mandalong Mine and extensometer data measured the beam shearing into 15 m and 20 m thick units, which reduced the effective thickness of the conglomerate beam by approximately 50% (i.e. 15 m to 20 m). The height of continuous fracturing was estimated to occur at 118 m or near the top of the conglomerate, based on piezometer data.

Other longwalls with similar geometry at Mandalong did not break down into thinner units (based on measured subsidence data). The presence of a seam roll and thrust fault to the near the panel was identified in the mine workings and indicates that the strata may have been significantly 'worked' and weakened by tectonic activity prior to mining. It is suggested that assessments in greenfields sites should consider the outcome of massive units shearing into two beams for worst-case geological condition scenarios.

Initial values of t' were therefore estimated from borehole log and extensometer data to derive the general form of the equation presented in **Section A11.5.5**. The resulting regression equation indicated the strata unit thickness should be raised to a power of -0.4 to -0.5. A single iteration was then required to re-define the coefficients and remaining Pi-term powers. The results of the analysis are summarized in **Table A6.3a** and **Figure A42e**.

The results indicate that the back-analysed (or measured) t' values ranged between 18 m and 80 m (median of 46 m) for the *sub-critical* panels; from 8.5 m to 42 m (median of 25 m) for the *critical* panels and between 6 m and 34 m (median of 23 m) for the *supercritical* panel geometries. The measured t' values for the deeper panels appear to be generally thicker than the panels at lower depth of cover in areas with similar geological conditions (i.e. massive sandstones and conglomerate units capable of spanning the longwall voids were present in both cases). Further review of the geomechanical properties of the overburden is necessary to increase our understanding of this phenomenon.

Table A6.3a - Effective Strata Unit Thicknesses (t') Back Analysed from HoF Model Database for Australian Coalfields

Site	Panels	Mine	W (m)	H (m)	W/H	A (m)	Back Analysed t' (m)	Bore log t_log (m)	t_max 95% goaf span probability	Rock Mass Conditions (see TA6.3b)	t_min from subsidence data (m)	Effective Strata unit thickness* t' (m)
1	MW508	Bellambi W.	110	421	0.26	92	36.5	100	49	Normal	30	49
2	LW10	Metropolitan	140	460	0.30	130	31.5	100	49	Normal	30	49
3	LW1-4	South Coast	110	325	0.34	85	31.5	100	41	Normal	20	41
4	LW6	Kemira	117	335	0.35	98	27	100	40	Normal	20	40
5	LW20	Metropolitan	163	450	0.36	100	68	100	70	Normal	30	70
6	LWA1	Austar	159	417	0.38	*87*	160	100	78	Normal	30	78
7	LW514	Bellambi W.	150	400	0.38	90	54	100	64	Normal	30	64
8	LW28	Appin	200	500	0.40	90	80	120	103	Normal	40	103
9	LW2	Ellalong	150	368	0.41	113	37	100	49	Normal	30	49
10	LW3	Tahmoor	180	424	0.42	-	60	100	74	Normal	30	74
11	LW9	Teralba	150	350	0.43	*110*	27	34	48	Normal	30	30
12	TE	West Cliff	200	446	0.45	*101*	57	100	85	Normal	30	85
13	TE	Berima	120	176	0.68	*76*	18	100	29	Normal	20	29
14	LW409	Springvale	265	384	0.69	*133*	42	55	78	Normal	32	32
15	LW9(11)	Mandalong	160	220	0.73	-	30	30	25	Normal	20	25
16	LW11	Angus Place	211	263	0.80	-	30	100	26	Normal	10	26
17	411	Springvale	315	368	0.86	139	42	55	86	Normal	32	32
18	LW5	Mandalong	160	179	0.89	118	14.5	25	37	Normal	20	20
19	LW5	Dendrobium	245	255	0.96	123	32	80	55	Normal	20	55
20	LW1	Wyee	216	206	1.05	126	18.2	30	39	Normal	20	20
21	**LW1**	**Invincible**	**145**	**116**	**1.25**	**96**	**8.5**	**15**	19	**Adverse**	**10**	**10**
22	TE 1	Abel	120	95	1.26	45	18	15	29	Normal	15	15
23	LWs	Ashton	216	154	1.40	82	25.5	30	44	Normal	15	15
24	LW40	WWD	179	113	1.58	80	21	20	25	Normal	20	20
25	**LWE1**	**Sth Bulga**	**259**	**155**	**1.67**	**145**	**6.2**	**15**	28	**Adverse**	**10**	**10**
26	LW41	WWD	179	105	1.70	72	23	20	24	Normal	20	20
27	LW9	Crinum	280	155	1.81	85	34	35	36	Normal	20	20
28	LW39	WWD	179	97	1.84	68	22.5	20	22	Normal	20	20
29	TE (3D)	Wyee North	355	185	1.92	63	54	50	78	Normal	20	20
30	TE(LW4)	Wyee North	355	180	1.97	40	>54	50	109	Normal	20	20
31	TE	Abel	150	76	1.97	45	15.5	15	26	Normal	15	15
32	TE(NthB)	Cooranbong	150	75	2.00	58	12.5	20	16	Normal	20	16
33	LW1	Oaky ck	205	95	2.16	55	29	30	25	Normal	15	25
34	**LW9/9a**	**Homestead**	**200**	**80**	**2.50**	**70**	**11**	**15**	16	**Normal**	**15**	**15**

W' = minimum (W, 1.4H); t_{min} - minimum beam thickness values at A-Horizon based on subsidence and borehole extensometer data; t' = effective beam thickness above A-Zone derived from back analysis techniques; * - t' is selected by consideration of t_{log}, t_{max} and t_{min} (see text below).

Bold - surface to seam fracturing reported by others; *italics* - Continuous Fracture Zone heights (A-Zone) was originally reported and included the Discontinuous Fracture and Dilated Zone (B-Zone). The A and B- Zone heights were re-assessed by DgS based on a review of available measured vertical strains and piezometric data (see **Figure A40i and A40j**).

In order to be able to make credible height of continuous fracturing predictions at a 'green fields' site based on borehole data alone, it was necessary to identify strata unit thicknesses that <u>did</u> and <u>did not</u> stop the height of fracturing.

To do this, the effective strata unit thicknesses from the database that appeared to have stopped the height of fracturing were normalized to the effective panel width (t'/W') and plotted against the unit's location factor (y/H); see **Figure A42f**. A similar exercise was completed for the strata units that did not stop the height of fracturing development, and are plotted on the above figure as well.

The two strata thickness categories were subsequently used in a logistic regression analysis to define the probabilistic power line equation below to indicate whether a strata unit is likely to span the goaf and limit the development of the height of fracturing at a given horizon above the workings:

$$P(i=1)=50\% \text{ for } t_{max} = W'[0.035(y/H)^{-1.3}]$$

where
i = 1 for a spanning unit, and

$P(i=1)=50\%$ for t_{max} refers to a 50% probability that a beam of a given thickness will span the fractured zone at a given location in the overburden.

A similar exercise was completed in order to define for the 95% probability of spanning equation:

$$P(i=1)=95\% \text{ for } t_{max} = W'[0.12(y/H)^{-0.85}]$$

where
i = 1 for a spanning unit, and

$P(i=1)=95\%$ for t_{max} refers to a 95% probability that a beam of a given thickness will span the fractured zone at a given location in the overburden.

The two above equations above are shown in **Figure A42f** with the database of 'goaf spanning' and 'non-goaf spanning' units.

For conservative or worst-case height of fracturing prediction, subsidence data was also reviewed to indicate the minimum effective beam thickness values (t_{min}) when massive strata units are not obviously present to span and limit the height of the A-Zone.

For this scenario, it is considered that t_{min} is likely to equal twice the measured peak surface strain to curvature ratios or twice the depth of observed cracking (whichever is the greater). For the Newcastle and Hunter Coalfields, a t_{min} range from 15 m to 20 m is indicated from subsidence monitoring data, with a t' range from 30 m to 40 m indicated for the Western and Southern Coalfields.

The t_{min} values for the likely cover depths are provided in **Table A6.3b**.

Table A6.3b - Minimum Effective Strata Thickness Based on Subsidence Data for Normal and Adverse Rock Mass Conditions in Australian Coalfields

Cover Depth H (m)	Minimum Effective t_{min}					
	Normal*					Adverse**
	Southern	Western	Newcastle/ Greta	Tomago/Hunter Valley/Narrabri	Bowen Basin	All Coalfields
>450	40	-	-	30	30	15
350 - 450	40	40	30	20	20	15
250 - 350	20	20	20	20	20	10
150 - 250	20	20	20	15	15	10
<150	20	15	20	15	15	10

* - Normal conditions refer to rock mass behaviour that is unlikely to be adversely affected by geological structure or atypical rock mass conditions (e.g. deep weathering or a lack of low permeability units in the B-Zone).

** - Adverse are likely to be affected by geological structure or atypical rock mass conditions (see definition above).

Validation of the model involved the application of the following algorithm to check that the predicted beam thickness values (t') from the available borehole data (t_{log}) were consistent with the back-analysed results and the maximum (t_{max}) and minimum thicknesses (t_{min}) derived from borehole and subsidence data that is required to span the goaf:

- If $t_{log} > t_{max \text{ (for 95\% spanning probability)}}$ then t' = $t_{max \text{ (for 95\% spanning probability)}}$

  (so as not to bias the database above the required t' to span the goaf at a given horizon);

- If $t_{log} < t_{max \text{ for 95\% spanning probability}}$ then t' = $t_{min \text{ based on subsidence data}}$

  (see below).

A summary of the back analysis v. predicted effective strata unit thickness presented in **Table A6.3a** are compared graphically in **Figure A42g**. It is assessed that the proposed algorithm to estimate the likely strata unit thickness for the Pi-Term model is reasonable to give an R^2 value of 0.8 and root mean square area of 15%.

The predicted v. measured outcomes using the "Geology" Pi-term model are presented in **Figures A42h** to **A42j**. Further validation of the Geology Pi-term model outcomes are presented in **Sections A11.5.7** and **A11.5.8**.

A11.5.7   Analytical Models of Goaf Spanning Strata Unit Thickness

The minimum thicknesses of the strata units required to limit the height of continuous fracturing have also been estimated analytically for the following scenarios:

(i)   Strata units that can support the full overburden load.

(ii) Single goaf spanning units, which are single strata units that have sheared / dilated away from the overlying rock mass but are able to support their own weight and span any partial voids immediately below.

For Scenario (i) the minimum strata unit thickness to fully support the overburden above it was assessed using Voussoir Beam theory presented in **Diedrichs and Kaiser, 1999**. For a factor of safety against crushing of 2:

$$t_{min, \, full} = \sqrt{(1.5\gamma(H-y)(W-2y\tan\theta)^2/UCS)}$$

For Scenario (ii) the minimum strata unit thickness to support its self-weight only was also assessed using Voussoir Beam theory presented in **Diedrichs and Kaiser, 1999**. For a factor of safety against crushing of 2:

$$t_{min, \, single} = 1.5\gamma(W-2y\tan\theta)^2/UCS$$

Note: The above equations were derived from Equation (1) and assume that the compression arch forms within 50% of the beam thickness (conservative).

Back analysis of the database indicated the angle of break increases with W/H and ranges from $\theta = 12^o$ for sub-critical panels and 19.3^o for supercritical panels. The following equations give the best fit to the geology model presented in **Section A11.5**:

$\theta = 12^o$ or W/H <0.45
$\theta = 9.63^o + 4.42(W/H) + 1.8(W/H)^2$ for 0.45 < W/H < 1.4
$\theta = 19.3^o$ for W/H > 1.4

Published laboratory UCS testing data on sandstone / conglomerate / igneous core samples from each coalfield were adopted as shown in **Table A6.4**.

A summary of the analytical goaf spanning equation results and back analysed strata unit thicknesses and beam stresses are presented in **Table A6.4**. It is considered that the minimum beam stress will govern the loading/spanning scenario for a given mining geometry. The results again demonstrate the complexity of how the fracture zone heights develop and the difficulties involved with using analytical or numerical techniques v. empirical methods.

The analytical beam thicknesses estimated for the goaf spanning scenarios are also plotted in **Figure A42f**. It is apparent the minimum thicknesses determined for the full rock mass loading case scenario and single spanning unit scenario generally plot above and below the logistic regression line for a 50% Probability of Spanning respectively. This would suggest that the Scenario (i) model is more likely to reflect the loading behaviour of the rock mass compared to Scenario (ii) (assuming the rock mass properties adopted are reasonable).

The predicted v. observed A values for the proposed Geology Pi-term model are presented in **Figures A42f** and **Figure A42g** respectively. The residual errors reasonably follow a normal probability distribution about the regression curve according to Central Limit Theory in statistics (see **Figure A42h**).

Table A6.4 - Minimum Strata Unit Thicknesses Required for Spanning the Goaf based on Analytical Models of the Overburden

Site	Panels	Mine	W (m)	H (m)	W_i	UCS (MPa)	t (m)	y (m)	y/H	Back analysed t, (m)	Full Load t_{min} (m)	Single Beam t_{min} (m)	Full Beam Load Stress (MPa)	Goaf Supported Beam Stress (MPa)
1	MW508	Bellambi W.	110	421	71	70	100	90	0.21	36.5	30	3	23	72
2	LW10	Metropolitan	140	460	85	70	100	130	0.28	31.5	36	4	45	49
3	LW1-4	South Coast	110	325	74	70	100	85	0.26	31.5	26	3	25	66
4	LW6	Kemira	117	335	75	70	100	98	0.29	27	27	3	35	52
5	LW20	Metropolitan	163	450	120	70	100	100	0.22	68	52	8	21	100
6	LWA1	Austar	159	417	122	70	100	80	0.19	160	51	8	18	208
7	LW514	Bellambi W.	150	400	112	70	100	90	0.23	54	46	7	25	75
8	LW28	Appin	200	500	162	70	120	90	0.18	80	76	14	31	61
9	LW2	Ellalong	150	368	102	70	100	113	0.31	37	38	6	36	59
10	LW3	Tahmoor	180	424	180	70	100	100	0.24	60	75	17	72	85
11	LW9	Teralba	150	350	103	70	34	110	0.31	27	37	6	66	34
12	TE	West Cliff	200	446	157	70	100	101	0.23	57	68	13	49	45
13	TE	Berima	120	176	84	70	100	76	0.43	18	19	4	40	34
14	LW409	Springvale	265	384	201	70	55	133	0.27	78	74	22	108	26
15	LW9(11)	Mandalong	160	220	160	67	30	160	0.73	30	29	14	-	-
16	LW11	Angus Place	211	263	211	70	100	*253*	0.96	30	15	24	-	-
17	411	Springvale	315	368	242	70	100	139	0.38	42	85	31	142	20
18	LW5	Mandalong	160	179	97	67	25	83	0.46	14.5	18	5	51	23
19	LW5	Dendrobium	245	255	177	70	80	123	0.48	32	47	17	75	28
20	LW1	Wyee	216	206	143	70	30	126	0.61	18.2	30	11	92	18
21	**LW1**	**Invincible**	**145**	**116**	**83**	**70**	**15**	**106**	**0.91**	8.5	9	**4**	36	15
22	TE 1	Abel	120	95	91	30	15	41	0.43	18	23	10	24	20
23	LWs	Ashton	216	154	158	30	30	82	0.53	25.5	47	31	52	10
24	LW40	WWD	179	113	102	30	20	80	0.71	21	21	13	15	22
25	**LWE1**	**Sth Bulga**	**259**	**155**	**115**	**30**	**20**	**145**	**0.94**	6.2	13	**17**	65	2
26	LW41	WWD	179	105	97	30	20	72	0.69	23	20	12	11	28
27	LW9	Crinum	280	155	157	130	35	105	0.68	34	22	7	28	79
28	LW39	WWD	179	97	88	30	20	68	0.70	22.5	17	10	8	32
29	TE (3D)	Wyee North	355	185	215	70	50	63	0.34	54	55	25	36	28
30	TE(LW4)	Wyee North	355	180	224	70	50	40	0.22	<u>156</u>	61	27	37	34
31	TE	Abel	150	76	75	30	15	33	0.43	15.5	15	7	14	18
32	TE(NthB)	Cooranbong	150	75	64	67	20	58	0.77	12.5	8	2	8	47
33	LW1	Oaky ck	205	95	94	30	30	55	0.58	29	21	11	8	37
34	**LW9/9a**	**Homestead**	**200**	**80**	63	**30**	**15**	**65**	**0.81**	11	8	5	6	18

W' = minimum (W, 1.4H); t_{min} - minimum beam thickness values at A-Horizon based on subsidence and borehole extensometer data; t' = effective beam thickness above A-Zone derived from back analysis techniques;
Bold - surface to seam fracturing reported by others;
<u>Underlined</u> - Conservative estimate of t' returned.
italics - Continuous Fracture Zone heights (A-Zone) was originally reported and included the Discontinuous Fracture and Dilated Zone (B-Zone). The A and B- Zone heights were re-assessed by DgS based on a review of available measured vertical strains and piezometric data (see **Figure A40i** and **A40j**).

A11.5.8   Pi-Term Model for Predicting Heights of Discontinuous Fracturing (B) Above Longwalls using Geometry Pi-Terms Only (Geometry Model)

Based on the empirical database presented in **Table A6.1**, the statistics software XLSTAT$^{\circledR}$ was used to complete a multi-nonlinear regression analysis as follows for estimating the height of the dilated B-Zone :

$$\underline{\text{Mean B/W'} = 1.621 \, (H'/W')^{0.55}(T/W')^{0.175}} \qquad R^2 = 0.86 \ \& \ \text{rsme} = 0.12W' \ (13\%)$$

$$\text{U95\% B/W'} = \text{Mean B/W'} + b$$

where b = 0.16 for subcritical panels, 0.16-0.085(W/H-0.7) for critical panels and 0.10 for supercritical panels.

H' = Goaf Load Height = H

W' = Effective Panel Width = minimum of W and 1.4H.

T = Mining Height.

Re-arranging the above equation in terms of B gives:

$$\underline{B = 1.621 \, W'^{0.275}H^{0.55}T^{0.175}} \quad +/- \ bW'$$

The predicted v. observed B/W' and B' values are presented in **Figure A42k** and **Figure A42l** respectively. The residual errors follow a normal probability distribution about the regression curve as expected according to Central Limit Theory in statistics (see **Figure A42m**). The regression indicates a relatively weaker relationship exists between the height of B-Zone fracturing and the mining height compared to the A-Zone relationship.

A11.5.9   Pi-Term Model for Predicting Heights of Discontinuous Fracturing (B) Above Longwalls using the Geology Pi-Term

Based on the empirical database presented in **Table A6.1**, the statistics software XLSTAT$^{\circledR}$ was used to complete a multi-nonlinear regression analysis as follows for estimating the height of the dilated B-Zone :

$$\underline{\text{Mean B/W'} = 1.873 \, (H'/W')^{0.635}(T/W')^{0.257}(t'/W')^{-0.097}} \quad R^2 = 0.86 \ \& \ \text{rmse} = 0.13W'(15\%)$$

$$\underline{\text{U95\% B/W'} = \text{Mean B/W'} + b}$$

where b = 0.15 for subcritical panels; 0.15-0.0714(W/H-0.7) for critical panels and 0.10 for supercritical panels.

H' = Goaf Load Height = H

W' = Effective Panel Width = minimum of W and 1.4H.

T = Mining Height.

t' = Effective strata unit thickness; see **Section A11.5.6**.

Re-arranging the above equation in terms of B gives:

$$\underline{B = 1.873 \ W'^{0.205} \ H^{0.635} T^{0.257} \ t'^{\ -0.097}} \qquad +/- \ bW'$$

The predicted v. observed B/W' and B' values are presented in **Figure A42n** and **Figure A42o** respectively. The residual errors follow a normal probability distribution about the regression curve as expected according to Central Limit Theory in statistics (see **Figure A42p**). The regression indicates a relatively weaker relationship exists between the height of B-Zone fracturing, the mining height and strata unit thickness compared to the A-Zone relationship.

A11.5.10 Pi-Term Model Validation

Validation of the proposed Pi-Term model has been completed as follows:

  (i)   A review of the range of independent variables within the database to check if the model is likely to be biased towards a particular parameter or mining geometry.

  (ii) Comparison of predicted v. measured A and B-Horizons for each model to check model reliability.

  (iii) Sensitivity analysis of the model to the assumed input parameters (based on method applied in **Hydrosimulations, 2013**).

  (iv) Comparison of model results with other models over a representative range of mining geometries and overburden geologies.

(i)   Database Variable Review

In regards to the data base, the following parameters from **Table A6.1** were plotted against the W/H ratio in **Figures A43a** to **43d** to test for sample bias:

- Panel Width (W)

- Cover Depth (H)

- Mining Height (T)

- Height of A-Zone Fracturing (A)

- Height of B-Zone Fracturing/Strata Dilation (B)

It is assessed that the database has sufficient coverage in regards to panel width, cover depth and mining height to reliably estimate HoF Zones above sub-critical to super-critical panels with W/H values ranging from 0.3 to 2.2.

(ii)   Model Reliability

In regards to prediction model reliability, the minimum effective strata unit thickness assessed for each site has used to estimate the height of A and B-Zones and the residual areas subjected to a Normality test. The distributions of model residual errors should follow the Central Limit theorem for regression analysis. That is, a normal distribution of errors would be expected to occur about the regression line of 'best-fit'. If the regression lines are deemed to meet this requirement, the assessment of predicted confidence limits will then be possible. It would then be expected that < 5% of measured values would exceed the predicted U95%CL values on average.

The regression results for the A-Zone Geological model are summarised in **Table A6.5** and **Figure A42j**. The results demonstrate the model errors satisfy normality tests with 61% of the measured values below the predicted mean values and 97% of the measured values below the Upper 95%CL predictions. A slightly lower reliability outcome was achieved for the Geometry Model for the B-Zone with 55% of measured values below the mean and 90% below the U95%CL (see **Table A6.6**).

It is therefore considered that the reliability of the Pi-Term geology model is acceptable for worst-case estimates of A-Zone fracture heights at new or existing coal mines in Australia until local performance data either confirms or supersedes it.

The results for the B-Zone geology model checks also indicate the model errors satisfy normality tests as shown in **Figure A42p** and are summarised in **Table A6.7**. The proposed mean and U95%CL model satisfactorily over predicts 52% and 95% of the measured B-Zone data (i.e. within 5% of the expected values). A slightly lower reliability outcome was achieved for the Geometry Model for the B-Zone (see **Table A6.8**).

Overall, it is considered that the reliability of both the Pi-Term Models is acceptable for estimates of B-Zone discontinuous fracture height assessments at new or existing coal mines in the NSW Coalfields and should be confirmed or re-calibrated with local measurement data.

The above results indicate that the model is likely to provide reasonably conservative estimates of the height of continuous fracturing for the full range of mining geometries, based on the effective panel width, effective goaf load height (cover depth), mining height and effective strata unit thickness in the A or B-Zones.

Table A6.5 - Summary of Measured v. Predicted Height of Continuous Fracture A-Zones for the Geology Model

Site	Panel	Mine	Panel Width W (m)	Cover Depth H (m)	W/H	Mining Height T (m)	Predicted t' (m)	Predicted A (m) mean	Predicted A (m) U95%CL	Measured A (m)	Pass = 1; Fail = 0 m	Pass = 1; Fail = 0 U95
1	MW508	Bellambi W	110	421	0.26	2.50	49	82	98	**92**	0	1
2	LW10	Metropolitan	140	460	0.30	3.40	49	109	130	**130**	0	1
3	LW1-4	South Coast	110	325	0.34	2.50	41	76	93	**85**	0	1
4	LW6	Kemira	117	335	0.35	2.75	40	84	102	**98**	0	1
5	LW20	Metropolitan	163	450	0.36	3.40	70	99	124	**100**	0	1
6	LWA1	Austar	159	417	0.38	6.00	78	118	142	*87*	1	1
7	LW514	Bellambi W	150	400	0.38	2.70	64	84	106	**90**	0	1
8	LW28	Appin	200	500	0.40	2.30	103	81	111	**90**	0	1
9	LW2	Ellalong	150	368	0.41	3.50	49	101	123	**113**	0	1
10	LW3	Tahmoor	180	424	0.42	2.18	74	80	107	**-**	-	-
11	LW9	Teralba	150	350	0.43	2.70	30	106	128	*110*	0	1
12	TE	West Cliff	200	446	0.45	2.50	85	86	116	*101*	0	1
13	TE-SW1	Berrima	120	176	0.68	2.3	29	63	81	*76*	0	1
14	LW409	Springvale	265	384	0.69	3.25	32	148	188	**133**	0	1
15	LW9	Mandalong	160	220	0.73	4.50	25	115	139	**-**	-	-
16	LW11	Angus Place	211	263	0.80	2.47	16	129	159	**-**	-	-
17	411	Springvale	315	368	0.86	3.25	32	156	199	**139**	0	1
18	LW5	Mandalong	160	179	0.89	3.70	20	103	125	**118**	0	1
19	LW5	Dendrobium	245	255	0.96	3.75	55	100	132	**123**	0	1
20	LW1	Wyee	216	206	1.05	3.44	20	121	148	**126**	0	1
21	*LW1*	*Invincible*	*145*	*116*	*1.25*	*2.70*	*15*	90	106	*96*	**0**	1
22	TE1	Abel	120	95	1.26	2.30	15	59	72	**45**	1	1
23	LWs	Ashton	216	154	1.40	2.55	15	101	123	**82**	1	1
24	LW40	WWD	179	113	1.58	3.80	20	81	97	**80**	1	1
25	*LWE1*	*South Bulga*	*259*	*155*	*1.67*	*2.55*	*15*	120	142	*145*	**0**	**0**
26	LW41	WWD	179	105	1.70	3.80	20	76	91	**72**	1	1
27	LW9	Crinum	280	155	1.81	3.50	20	105	127	**85**	1	1
28	LW39	WWD	179	97	1.84	3.90	20	71	85	**68**	1	1
29	TE-3D	Wyee North	355	185	1.92	1.90	20	60	86	**63**	0	1
30	TE-355	Wyee North	355	180	1.97	1.90	20	59	84	**40**	1	1
31	Panel2	Abel	150	76	1.97	1.88	15	45	56	**45**	1	1
32	TE - North B	Cooranbong	150	75	2.00	2.80	16	53	64	**58**	0	1
33	LW1	Oaky Ck	205	95	2.16	3.20	25	58	71	**55**	1	1
34	*LW9/9a*	*Homestead*	*200*	*80*	*2.50*	*3.30*	*15*	62	73	*70*	0	1
									Percentage of Measured < Predicted Value		39	97

italics - Surface to seam connection reported by authors.

Table A6.6 - Summary of Measured v. Predicted Height of Continuous Fracture A-Zones for the Geometry Model

Site	Panel	Mine	Panel Width W (m)	Cover Depth H (m)	W/H	Mining Height T (m)	Predicted A (m)		Measured A (m)	Pass = 1; Fail = 0	
							mean	U95%CL		m	U95
1	MW508	Bellambi W	110	421	0.26	2.50	86	103	**92**	0	1
2	LW10	Metropolitan	140	460	0.30	3.40	107	130	**130**	0	1
3	LW1-4	South Coast	110	325	0.34	2.50	80	98	**85**	0	1
4	LW6	Kemira	117	335	0.35	2.75	85	104	**98**	0	1
5	LW20	Metropolitan	163	450	0.36	3.40	113	139	**100**	1	1
6	LWA1	Austar	159	417	0.38	6.00	135	161	*87*	1	1
7	LW514	Bellambi W	150	400	0.38	2.70	97	121	**90**	1	1
8	LW28	Appin	200	500	0.40	2.30	108	140	**90**	1	1
9	LW2	Ellalong	150	368	0.41	3.50	105	129	**113**	0	1
10	LW3	Tahmoor	180	424	0.42	2.18	97	126	**-**	-	-
11	LW9	Teralba	150	350	0.43	2.70	94	118	*110*	0	1
12	TE	West Cliff	200	446	0.45	2.50	108	140	*101*	1	1
13	TE	Berrima	120	176	0.68	2.3	68	87	*76*	0	1
14	LW409	Springvale	265	384	0.69	3.25	126	169	**133**	0	1
15	LW9	Mandalong	160	220	0.73	4.50	102	128	**-**	-	-
16	LW11	Angus Place	211	263	0.80	2.47	95	127	**-**	-	-
17	411	Springvale	315	368	0.86	3.25	133	179	**139**	0	1
18	LW5	Mandalong	160	179	0.89	3.70	90	113	**118**	0	0
19	LW5	Dendrobium	245	255	0.96	3.75	116	150	**123**	0	1
20	LW1	Wyee	216	206	1.05	3.44	101	129	**126**	0	1
21	*LW1*	*Invincible*	*145*	*116*	*1.25*	*2.70*	69	85	**96**	**0**	**0**
22	TE1	Abel	120	95	1.26	2.30	57	71	**45**	1	1
23	LWs	Ashton	216	154	1.40	2.55	84	105	**82**	1	1
24	LW40	WWD	179	113	1.58	3.80	80	105	**80**	0	1
25	*LWE1*	*South Bulga*	*259*	*155*	*1.67*	*2.55*	84	119	**145**	**0**	**0**
26	LW41	WWD	179	105	1.70	3.80	76	100	**72**	1	1
27	LW9	Crinum	280	155	1.81	3.50	95	129	**85**	1	1
28	LW39	WWD	179	97	1.84	3.90	73	95	**68**	1	1
29	TE-3D	Wyee North	355	185	1.92	1.90	84	126	**63**	1	1
30	TE-355	Wyee North	355	180	1.97	1.90	83	123	**40**	1	1
31	Panel2	Abel	150	76	1.97	1.88	48	65	**45**	1	1
32	TE-NthB	Cooranbong	150	75	2.00	2.80	55	72	**58**	0	1
33	LW1	Oaky Ck	205	95	2.16	3.20	67	88	**55**	1	1
34	*LW9/9a*	*Homestead*	*200*	*80*	*2.50*	*3.30*	61	79	*70*	0	1
								Percentage of Measured < Predicted Value		45	90

italics - Surface to seam connection reported by authors.

Table A6.7 - Summary of Measured v. Predicted Height of Dilated B-Zones for the Geology Model

Site	Panel	Mine	Panel Width W (m)	Cover Depth H (m)	W/H	Mining Height T (m)	t' (m)	Predicted B (m) mean	Predicted B (m) U95%CL	Measured B (m)	Pass = 1; Fail = 0 m	Pass = 1; Fail = 0 U95
1	MW508	Bellambi West	110	421	0.26	2.50	49	198	214	-	-	-
2	LW10	Metropolitan	140	460	0.30	3.40	49	238	259	-	-	-
3	LW1 to 4	South Coast	110	325	0.34	2.50	41	170	187	-	-	-
4	LW6	Kemira	117	335	0.35	2.75	40	181	198	-	-	-
5	LW20	Metropolitan	163	450	0.36	3.40	70	234	258	-	-	-
6	LWA1	Austar	159	417	0.38	6.00	78	254	278	277	0	1
7	LW514	Bellambi West	150	400	0.38	2.70	64	203	225	-	-	-
8	LW28	Appin	200	500	0.40	2.30	103	227	257	-	-	-
9	LW2	Ellalong	150	368	0.41	3.50	49	211	233	210	1	1
10	LW3	Tahmoor	180	424	0.42	2.18	74	204	231	204	0	1
11	LW9	Teralba	150	350	0.43	2.70	30	200	223	150	1	1
12	TE	West Cliff	200	446	0.45	2.50	85	220	250	245	0	1
13	TE SW1	Berrima	120	176	0.68	2.3	29	119	137	112	1	1
14	LW409	Springvale	265	384	0.69	3.25	32	249	289	254	0	1
15	LW9	Mandalong	160	220	0.73	4.50	25			-	-	-
16	LW11	Angus Place	211	263	0.80	2.47	16	177	208	253	0	0
17	411	Springvale	315	368	0.86	3.25	32	251	295	288	0	1
18	LW5	Mandalong	160	179	0.89	3.70	20	150	171	154	0	1
19	LW5	Dendrobium	245	255	0.96	3.75	55	186	218	-	-	-
20	LW1	Wyee	216	206	1.05	3.44	20	171	198	-	-	-
21	LW1	Invincible	145	116	1.25	2.70	10	110	116	111	0	1
22	TE1	Abel	120	95	1.26	2.30	15	86	95	75	1	1
23	LWs	Ashton	216	154	1.40	2.55	15	135	154	130	1	1
24	LW40	WWD	179	113	1.58	3.80	20	112	113	108	1	1
25	LWE1	South Bulga	259	155	1.67	2.55	10	141	155	150	0	1
26	LW41	WWD	179	105	1.70	3.80	20	100	105	100	1	1
27	LW9	Crinum	280	155	1.81	3.50	20	143	155	150	0	1
28	LW39	WWD	179	97	1.84	3.90	20	92	97	92	0	1
29	TE-3D	Wyee North	355	185	1.92	1.90	60	128	154	143	0	1
30	TE-355	Wyee North (LW4)	355	180	1.97	1.90	60	125	150	-	-	-
31	Panel2	Abel	150	76	1.97	1.88	15	69	76	71	0	1
32	TE-North B	Cooranbong	150	75	2.00	2.80	16	70	75	70	1	1
33	LW1	Oaky Ck	205	95	2.16	3.20	25	91	95	90	1	1
34	LW9/9a	Homestead	200	80	2.50	3.30	15	75	80	75	1	1
									Percentage of Measured < Predicted Value		43	96

Table A6.8 - Summary of Measured v. Predicted Height of Dilated B-Zones for the Geometry Model

Site	Panel	Mine	Panel Width W (m)	Cover Depth H (m)	W/H	Mining Height T (m)	Predicted B (m) mean	Predicted B (m) U95%CL	Measured B (m)	Pass = 1; Fail = 0 m	Pass = 1; Fail = 0 U95
1	MW508	Bellambi West	110	421	0.26	2.50	192	210	**-**	-	-
2	LW10	Metropolitan	140	460	0.30	3.40	228	250	**-**	-	
3	LW1 to 4	South Coast	110	325	0.34	2.50	167	184	**-**	-	-
4	LW6	Kemira	117	335	0.35	2.75	175	194	**-**	-	-
5	LW20	Metropolitan	163	450	0.36	3.40	235	261	**-**	-	-
6	LWA1	Austar	159	417	0.38	6.00	247	272	**277**	0	0
7	LW514	Bellambi West	150	400	0.38	2.70	206	230	**-**	-	-
8	LW28	Appin	200	500	0.40	2.30	246	278	**-**	-	-
9	LW2	Ellalong	150	368	0.41	3.50	206	230	**210**	0	1
10	LW3	Tahmoor	180	424	0.42	2.18	216	245	**204**	1	1
11	LW9	Teralba	150	350	0.43	2.70	192	216	**150**	1	1
12	TE	West Cliff	200	446	0.45	2.50	234	266	*245*	0	1
13	TE SW1	Berrima	120	176	0.68	2.3	120	139	**112**	1	1
14	LW409	Springvale	265	384	0.69	3.25	244	286	*254*	0	1
15	LW9	Mandalong	160	220	0.73	4.50	165	191	**-**	-	-
16	LW11	Angus Place	211	263	0.80	2.47	177	209	*253*	0	0
17	411	Springvale	315	368	0.86	3.25	250	296	**288**	0	1
18	LW5	Mandalong	160	179	0.89	3.70	143	166	**154**	0	1
19	LW5	Dendrobium	245	255	0.96	3.75	195	229	**-**	-	-
20	LW1	Wyee	216	206	1.05	3.44	165	193	**-**	-	-
21	LW1	Invincible	145	116	1.25	2.70	104	116	*111*	0	1
22	TE1	Abel	120	95	1.26	2.30	86	95	*75*	1	1
23	LWs	Ashton	216	154	1.40	2.55	134	154	*130*	1	1
24	LW40	WWD	179	113	1.58	3.80	111	113	*108*	1	1
25	LWE1	South Bulga	259	155	1.67	2.55	134	155	**150**	0	1
26	LW41	WWD	179	105	1.70	3.80	104	105	**100**	1	1
27	LW9	Crinum	280	155	1.81	3.50	142	155	*150*	0	1
28	LW39	WWD	179	97	1.84	3.90	92	97	**92**	0	1
29	TE-3D	Wyee North	355	185	1.92	1.90	148	174	*143*	1	1
30	TE-355	Wyee North (LW4)	355	180	1.97	1.90	144	170	-	-	-
31	Panel2	Abel	150	76	1.97	1.88	71	76	**71**	0	1
32	TE-North B	Cooranbong	150	75	2.00	2.80	70	75	*70*	1	1
33	LW1	Oaky Ck	205	95	2.16	3.20	93	95	*90*	1	1
34	LW9/9a	Homestead	200	80	2.50	3.30	75	80	**75**	1	1
								Percentage of Measured < Predicted Value		**48**	**91**

(iv)   Parameter Sensitivities

A review of the sensitivity of the Pi-Term Models has been completed in **Merrick, 2014** and demonstrates that the model is not overly sensitive to changes to the input parameters, W, H and T. The influence of the effective strata thickness t' has a greater impact on the height of fracturing for values < 20 m than the cases with t' > 20 m. This is not surprising as the spanning capabilities of the strata units will probably decrease rapidly below this thickness range as it corresponds with the point where the bending beam stress starts to exceed the UCS of the rock mass.

The model variable sensitivity charts are presented in **Figures A43e** to **A43h**.

(v)   Comparison with other models

Three critical cases were identified in the analysis where the A-Zone extended to within 10 m of the surface (Invincible, South Bulga, and Homestead Mines) with a minimum t' value of 10 m assumed. Adopting a minimum beam thickness of 10 m will generally indicate the maximum likely height of continuous fracturing for all cases in the database (see **Figure A42g**).

For completeness, four case studies have been selected from the sub-critical, critical and supercritical panel geometries and plotted with varying panel widths in **Figures A43i** to **A43l** to demonstrate the sensitivity of the models to changes in mining geometry. Several sub-surface fracture height models (**Foster, 1995; SCT, 2008; ACARP, 2007** and **Tammetta, 2013**) that have been referred to by OEH and PACs during recent project approval applications are also plotted with the Pi-term model results. It is apparent that the models are based on a smaller number of key variables and some were developed from data in a particular coalfield only. The application of the models in other coalfields with significantly different geological conditions and mining geometries are considered to have resulted in a larger range of 'error' compared to the Pi-term models.

Finally, the width-based models also do not consider the effect of cover depth or mining height and assume the A-Zone will continue to increase above *supercritical* panel geometries. This usually means that surface to seam connectivity will always be predicted for critical and supercritical panel widths. It is noted that only 2 or 3 cases out of 14 (15% - 20%) or 1 in 5 supercritical longwalls have resulted in surface to seam connectivity; see **Figure 43m**.

This outcome suggests that other factors such as cover depth, mining height and geological conditions should also be considered than just the panel width alone when estimating heights of fracturing above longwall panels.

A11.5.11 Definition of Surface Cracking Zone

During the development of the Pi-term model it has also been necessary to better define the surface cracking zone depth. The depth of the surface cracking zone has been estimated from subsidence data, surface crack observations and published measurements as follows:

- The literature review findings presented in **Section A11.3** indicate that surface cracking depths above longwalls are likely to be < 15 m generally.

- The Mean and median strain/curvature ratios of 5.3 m and 7.4 m mentioned earlier in Section derived from subsidence data measurements for Newcastle Coalfield (see **Figures A43n** and **A43o**) indicates the *average surface cracking depth*. The ratio is considered to be a direct measurement of the depth to the neutral axis of bending where tensile strains cross over to compressive strain. This also suggests near surface strata beam thicknesses are twice the depth to the neutral axis of bending or 11 m to 15 m. It is apparent that these values are consistent with near surface beam thicknesses assumed in the Pi-Term Geology Model.

- Borehole measurement devices measured depths of cracking at the base of sandstone valleys in the Southern Coalfield of up to 12 m after mine subsidence effects (refer **Mills, 2007**).

- Measured crack depths of up to 20 m have been measured along the crests of steep slopes above LW41 (ref to **RCA, 2013**).

Based on the above information, it is assessed that the following conservative crack depths presented in **Table A6.9** may be assumed when assessing surface to seam connectivity potential above longwalls beneath varying topography:

Table A6.9 - Suggested Maximum Cracking Depths for Impact Assessment

Location and Topography	Surface Cracking Depth (m)
	Newcastle/Hunter Valley - Southern/Western Coalfield
Flat Terrain with Moderate Slopes up to 18°	7.5 - 12
Bases of Valleys	12 - 15
Low side of panel beneath steep slopes > 18° (not valley floor)	3.5 - 5
Crests or high side of panel beneath steep slopes > 18°	15 - 20

A11.5.12 Summary

The geometry and geology Pi-term models presented in **Section A11.5** for estimating the A-Zone and B-Zone fracture horizons are generally consistent with the prevailing view that the panel width, cover depth and mining height will have the greatest influence on fracture development heights above longwall panels. The Pi-term models for A and B-Zone Fracture

Heights are also generally consistent with **Whittaker and Reddish, 1990**, **Singh & Kendorski, 1991** and the analytical models presented earlier.

The spanning or non-spanning capability of strata units in the overburden cannot be ignored however, when assessing the potential fracturing heights above a longwall panel. Where local extensometer and piezometric data are available, the influence of spanning strata may be used to calibrate the Geology Pi-term model to a given site.

Predictions based on the up-dated Strain, Overburden Curvature Index and Fracture Height Angle Models are still also considered relevant and will provide similar, if not more conservative outcomes. These models may be used to provide a range of predictions at a greenfields site for risk assessment purposes. It should be understood however, that only the Geology Pi-term model will allow the influence of strata unit thickness or local site geology to be included directly in the predictions of sub-surface fracture height.

It should be understood that the vagaries of the rock mass do not usually allow the strata unit thickness term to be assessed directly from borehole data without back analysis of overburden performance measurements. The database presented in this appendix has been used to derive a minimum beam thickness of 10 m to estimate worst-case heights of fracturing for adverse rock mass conditions. A thickness of 15 m to 20 m corresponds to the minimum beam thicknesses assessed from surface strain and curvature measurements (and a cracking depth of 7.5 m to 10 m).

Subsequent measurements of continuous heights of fracturing may require a thinner strata unit thickness to be used to calibrate the model. At this stage, there are three cases in the database that have been reported to have fractured through to the surface, which required a beam thickness of 6 to 11 m to match the Pi-term model exactly and intersect the surface cracking zone (or D-Zone). One of the cases (South Bulga LWE1) however, may have included the B-Zone in the interpretation of the 'height of fracturing' at the time it was assessed.

It is assessed that the assumptions that the height of fracturing will be limited when either:

- critical panel widths exceed 1.4H;

- spanning strata exists that can bridge the fractured zone or the presence of plastic, low strength strata that tends to shear along bedding partings when deformed through bending action, rather than crack vertically, may also limit continuous cracking heights.

All of these outcomes are intuitively correct and correlate well with observed behaviour across sub-critical to supercritical mining geometries. It is also noted that the strata unit thickness term enables all of the database and subsequent regression equations to be used with a reasonable level of confidence, such that the predicted worst-case values will not be unduly biased by the database itself. The geology Pi-term t'/W' was back analysed for each of the 34 case studies to give an exact fit between the predicted and measured fracture heights. The set of measured t' values were correlated with the predicted t' with a high R^2 of 0.9. The

predicted v. measured heights of continuous fracturing were also correlated and returned an R^2 value of 0.8, which is also a good fit.

For estimates of HoF above partial pillar extraction panels, the HoF zones may be based on the effective mining height, T_e (if remnant pillars are likely to fail) or the maximum span between stable remnant pillars.

The use of the Pi-term models for multi-seam mining environments will also require consideration of the interburden thicknesses and cumulative effects of the A-Zones if they likely to intersect overlying longwall goafs. The multi-seam affect may be estimated for an overlying seam by converting the multi-seam subsidence increase to an effective mining height.

A12   Far-Field Displacements and Strain Predictions

A12.1 Background

The term far-field displacements (FFD) generally refer to the horizontal surface movements that occur outside the vertical subsidence limit or angle of draw to an extracted pillar panel or longwall block. It is currently understood that FFDs are a phenomenon caused by the reduction of horizontal stress when collapse of overburden rock (i.e. goafing) occurs above an extracted area. There also appears to be a strong correlation between the FFDs and the surface subsidence magnitude (which is also an indicator of horizontal stress relief). A conceptual model of the mechanics of FFDs is presented in **Figure A44a**.

Horizontal stress in rock is normally greater than the vertical stress at a given depth of cover; it has been 'locked' into the strata by tectonic movements and over-consolidation pressures (i.e. stress). Over-consolidation stresses occur in sedimentary rock after uplift and erosion over millennia has gradually removed the overlying material since the time of formation. Tectonic induced stress usually results in strong directional bias between the major and minor principal stress magnitudes, with variation due to stiffness of the lithological units as well (refer to **Nemcik et al, 2005**, **Pells, 2004**, **McQueen, 2004, Enever, 1999** and **Walker, 2004**).

It is considered that both of the abovementioned horizontal stress development mechanisms are likely to be present in the near surface rocks in the western area of the Newcastle Coalfield.

FFD's have only recently become an issue in the Newcastle Coalfield because of adverse surface impact experiences in the Southern Coalfield (e.g. horizontal movements of around 25 mm have been measured over 1.5 km away from extracted longwall panels on a concrete dam wall. No cracking damage occurred to the dam wall because of these movements however).

The strains associated with FFDs are usually very low, however, there is one case in the Southern Coalfield where a bridge was subject to lateral shearing of approximately 50 mm along the river bed axis.

To-date, it is understood that there are no precedents in the Newcastle Coalfield where similar FFD effects (measured or inferred via damage) have occurred around longwalls or total extraction panels. Horizontal movements have been measured outside the angle of draw limits from mine workings however, albeit at smaller distances and magnitudes (eg. 20 mm of horizontal movement has been measured in undulating terrain at 250 m from one longwall block where the cover depth was 135 m).

The horizontal stress in the Newcastle Coal Measures has been measured at several locations along the F3 Freeway to the west of Wyong and Newcastle (**Lohe and Dean-Jones, 1995**). The magnitude of the measured horizontal stress indicates that it is relatively high, with magnitudes that are 1.5 to >5 times the vertical stress, in relatively flat or moderately undulated terrain.

The major principal horizontal stress is usually orientated N to NE in the Western Newcastle Coalfield, but it can be re-orientated parallel to the axis of a ridge due to natural weathering processes near the surface (which cause lateral unloading towards the gullies); refer to **Lohe and Dean Jones, 1995**.

A12.2   In-situ Stress Field

Reference to stress measurement data in **Lohe and Dean-Jones, 1995** indicates that the 'shallow' (ie < 100 m below the surface) regional stress field in the undulating terrain along the eastern and eastern sides of Lake Macquarie is likely to have its major principal horizontal stress > 5 x vertical stress (and assuming horizontal stress is zero at the surface). Deeper strata at depths > 150 m is likely to have its major principal horizontal stress <2 x vertical stress.

The stress data from the above reference was measured using over-coring / HI-Cell techniques and is presented in Table A4.

Table A6 - Horizontal Stress Field Measurements in Newcastle Coalfield Relevant to Tasman

Location	Depth (m)	In-situ Stress Measurements*			
		Major Sigma 1 (MPa)	Minor Sigma 2 (MPa)	Vertical Sigma 3 (MPa)	Sigma1+/ Sigma 3
Wakefield	24	10.4	0.42	0.6	17.3
Wallsend Borehole	100	13.3	9.7	2.5	5.3
West Wallsend No. 2	190	27.4	20.3	4.75	5.8
Kangy Angy	70	11.8	4.2	1.75	6.7
Moonee	90	11.7	8.3	2.25	5.2
West Wallsend	170	6.4	n/a	4.25	1.5
Ellalong	320	6.5	4.6	8.0	0.8

* - All measurements in medium strength sandstone.
+ - ratio assumes horizontal stress is zero at the surface (which is not always correct).

The shallow stress data is plotted in **Figure A44b** and indicates that the major principal horizontal stress could be as high as 6 MPa at the surface (unless weathered rock and soil is present) with the Major and Minor Principal Horizontal stresses equal to approximately 4 times the vertical stress for depths up to 250 m.

This high Sigma 1 reading, however, may be associated with a sandstone / conglomerate ridgeline and not typical for the areas away from ridgelines (although a residual 'surface' horizontal stress range from 1.5 to 6.5 MPa has also been assessed for the Sydney Metropolitan area in **McQueen, 1999** and **Pells, 2002**).

Another commonly used assumption in the NSW Coalfields is that the major principal horizontal stress is approximately 2 x the vertical stress and the minor principal horizontal stress is 1.4 ~ 1.5 x the vertical stress (or the Major Principal Horizontal Stress is 1.33~1.4 x the Minor Principal Horizontal Stress). It is also acknowledged that the horizontal stress in the

Newcastle and Sydney areas can be 4 to 5 times the vertical stress, based on shallow rock mass data at depths < 50 m; refer to **Lohe and Dean Jones, 1995**. The sources of this stress field imbalance has been explained in **Enever, 1999**, **Pells, 2002** and **Fell *et al*, 1992** as being due to:

(i)   the 'over consolidation' ratio; where the vertical pressure due to ancient surface at the time of consolidation has since been eroded away, leaving a 'locked' in horizontal stress component in today's sedimentary rock mass. The OCR can be shown to decrease exponentially with depth and is equal in all directions at a given point.

(ii)   Tectonic strain; where crustal plate movements apply a strain to the rock mass and the resultant stress is dependent on the stiffness of the individual beds and direction of movement.

(iii)   Geological structure (faults/dykes); where discontinuities can change the magnitude and orientations of the regional stress field significantly.

(iv)   Topographic relief (ridges/valleys/gorges); where the magnitude and direction of the regional stress field can vary due to geometric affects.

The influence of underground mining can also result in changes (both increases and decreases) in horizontal and vertical stress field magnitudes as the rock mass adjusts to a new equilibrium state.

Based on the measured stress conditions, the horizontal stress magnitudes may be estimated based on the equations presented in **Nemcik et al, 2005**:

$$\sigma_H = K\sigma_v + E\varepsilon = \sigma_v\left[(\upsilon/1-\upsilon)OCR\right] + E\varepsilon$$

$$\sigma_h = f(\sigma_H) \text{ and } \sigma_v = 0.025H \text{ (MPa)}$$

where,

σ_H = Major Horizontal Principal Stress;

σ_h = Minor Horizontal Principal Stress;

σ_v = Vertical Stress;

υ = Poisson's Ratio (normally ranges between 0.15 and 0.4 in coal measure rocks);

$(\upsilon/1-\upsilon)$ = Horizontal to vertical stress ratio factor (K_o) due to Poisson's Ratio effect on its own;

OCR = The over-consolidation ratio, which relates vertical pre-consolidation pressure (σ_{vo}) with current vertical pressure (σ_v) as follows, OCR = σ_{vo}/σ_v = H_o/H.

(*Note: This is an additional term that has been introduced by DgS, and has been mentioned (but not derived) in* **Pells, 2002** *and calculated in* **Fell et al, 1992**).

E = Young's Modulus for rock-mass unit;

ε = Tectonic Stress Factor (TSF) or Tectonic Strain.

Due to the wide range of horizontal stress values noted in the literature, it is recommended that the horizontal stress magnitudes be measured in-situ at several lithological horizons before high extraction mining commences.

Based on the apparent complexity and large variation between the interpretations of published stress field data, it was considered necessary to conduct a sensitivity analysis on the stress field profiles during the calibration of Map-3D® using the flat terrain data (see **Section A12.3** for details).

Total horizontal displacement measurements outside the ends and corners of several longwall panels in the Newcastle Coalfield (Newstan and West Wallsend Collieries), have been plotted against distance from the panel goaf edge / cover depth at the panel; refer to **Figure A45**.

Curves of best fit have been fitted to identify data trends from various locations from the ends and corners of the panels (note: the movements outside the corners of a longwall are typically smaller than the panel ends). The data has been obtained using GPS / EDM traverse techniques with quoted accuracy limits of +/- 7 to 10 mm.

The data in **Figure A45** has also been normalised to maximum measured subsidence (S_{max}) above a given panel and is presented in **Figure A46**. It is considered that presenting the data in this format allows all of the available data to be used appropriately to make subsequent FFD predictions.

The data presented in **Figures A47** was measured from the sides of several longwall panels using in-line, steel tape measurements. This method is considered more accurate than the EDM techniques, however, they do not capture all of the displacement. The measured values have subsequently been adjusted to absolute movements, based on the EDM measurements presented in **Figures A45** and **A46**.

A combined graph of normalised total displacement data from the ends and sides of the longwall panels is presented in **Figure A48** with worst-case design curves from ends, corners and sides of a longwall panel for flat terrain conditions.

The empirical models may be used for calibrating the numerical models input parameters when proposed mining layouts and topographical conditions are considered to be well outside the available database (see **DgS, 2007**).

A12.3 Numerical Far-Field Displacement Modelling

The numerical modelling program Map-3D® has been applied at several mines in the Newcastle Coalfield to-date for the purposes of estimating FFD movements. The model was chosen mainly due to its suitability for modelling large-scale rock masses.

The program is a 3-dimensional elastic, isotropic, boundary-element model, which essentially starts with an infinite solid space and calculates the effects of excavations, geological structure, varying material types, and free-surfaces on the regional stresses and strains. Further details about the software can be found at the Map-3D® web site.

The model is firstly calibrated to measured displacement data for a given mining geometry, regional horizontal stress field and surface topography. The Young's Modulus or stiffness of the overburden is then adjusted above an extracted panel (or panels) and assumed caving zone until a reasonable match is achieved.

Although the empirical models indicate that subsidence is a key parameter for predicting FFDs, numerical modelling of horizontal stress relief effects does not require the subsidence above the panels to be matched (by the model) because the extraction of coal and subsequent goafing behaviour can be calibrated to measured far-field displacements instead. Therefore, the modelling outcomes are not linked to the modelled subsidence directly.

Non-linearity can be introduced into the model to analyse the effects of fault planes and bedding using displacement-discontinuity elements with normal and shear stiffness and Mohr-Coulomb friction and cohesive strength properties.

Multiple mining stages and irregular topography can also be defined to enable mechanistic extrapolation of existing empirical databases with a reasonable degree of confidence.

An example of a predicted far-field displacement pattern around a high extraction pillar panel mine is presented in **Figure A49**.

A12.5 Empirical Strain Prediction Model

Strain measurements from the side of several longwall panels from West Wallsend and Newstan Collieries and were also normalised to maximum panel subsidence. The data are presented in **Figure A50**.

Several curves are shown with the data in the above figure, one is the best-fit or mean curve and two are upper limit confidence limit curves for the data (U95%CL and U99%CL). The confidence limit curves have been defined using weighted non-linear statistical techniques and the residual errors about the mean curve.

A13   References

ACARP, 1998a. **Chain Pillar Design (Calibration of ALPS)**. ACARP Project No. C6036, Colwell, M. Colwell Geotechnical Services.

ACARP, 1998b, **Project No. C5024, Establishing the Strength of Rectangular and Irregular Pillars**. J.M.Galvin, B.K. Hebblewhite, M.D.G. Salamon and B.B.Lin. School of Mining, UNSW.

ACARP, 2003. **Review of Industry Subsidence Data in Relation to the Impact of Significant Variations in Overburden Lithology and Initial Assessment of Sub-Surface Fracturing on Groundwater**. ACARP Project No. C10023. S. Ditton and R. Frith, Strata Engineering Report No. 00-181-ACR/1.

ACARP, 2006. **Techniques to Predict and Measure Subsidence & its Impacts on the Groundwater Regime above Shallow Longwalls**. ACARP Project No. C23920 Report by Seedsman Geotechnics Pty Ltd and Geoterra Pty Ltd (March).

ACARP, 2007. **Hydrological Response to Longwall Mining**. CSIRO Exploration & Mining. H. Guo, D. Adhikary, D. Gaveva. Report No. C14033 (October).

Bulli Seam PAC, 2010. **Bulli Seam Operations Review Report**. NSW Government Planning Assessment Commission (10 July).

Colwell,1993. **Water Inflow Investigation for a Longwall Operation**. M. Colwell. Published in Queensland Coal Geology Groups Conference Proceedings, New Developments in Coal Geology, Brisbane.

Diedrichs and Kaiser, 1999. **Stability of Large Excavations in Laminated Hard Rock Masses: the Voussoir Analogue Revisited**. M.S. Diedrichs and P.K. Kaiser. International Journal of Rock Mechanics and Mining Sciences 36.

DgS, 2007. **Prediction of Far-Field Displacements Due to Pillar Extraction or Longwall Mining in Mountainous Terrain**. S. Ditton. Proceedings of the 7th Triennial MSTS Conference on Mine Subsidence, University of Wollongong (November 26-27)

DMR, 1987. **Mining Subsidence in NSW: 2. Surface Subsidence Prediction in the Newcastle Coalfield**. L. Holla. Department of Minerals Resources (June).

Enever, 1999. **Near Surface In-situ Stress and its Counterpart at Depth in the Sydney Metropolitan Area**. Enever, J.R. Published in Australian Geomechanics Society (AGS) Conference Proceedings of the 8th Annual Conference on Geomechanics, Hobart.

Fell *et al*, 1992. **Geotechnical Engineering of Embankment Dams**. Fell, R., MacGregor, P. and Stapledon, D.A.A. Balkema.

Forster and Enever, 1992. **Hydrogeological Response of Overburden Strata to Underground Mining, Central Coast, NSW**. I.R. Forster (Pacific Power) and J. Enever (CSIRO).

Forster, 1995. **Impact of Underground Coal Mining on the Hydrogeological Regime, Central Coast, NSW**. I.R. Forster. Published in Australian Geomechanics Society (AGS) Conference Proceedings (February), Engineering Geology of Newcastle – Gosford Region, University of Newcastle.

Frith, 2006. **Geotechnical Assessment of Overburden Fracturing Related to the Bulli Seam Extraction along the Line of the Proposed Endeavour Drift**. Frith Consulting Pty Ltd. Internal Report to BHP Billiton (October).

Holla, 1991. **Some Aspects of Strata Movement relating to Mining Under Water Bodies in NSW, Australia**. L. Holla. Published proceedings of 4th Int. Water Congress, Ljubljana, Slovenia, Yugoslavia (September).

Holla and Barclay, 2000. **Mine Subsidence in the Southern Coalfield**. L.Holla and E.Barclay. Department of Minerals Resources (June).

Karmis, et al, 1987. **Surface Deformation Characteristics Above Undermined Areas: Experiences from the Eastern United States Coalfields**. M. Karmis, A. Jarosz, P. Schilizzi & Z. Agioutantis. Published in Civil Engineering Transactions Journal, Institution of Engineers, Australia.

Kendorski, F.S., 1993. **Effect of High Extraction Coal Mining on Surface and Ground Water**. Proceedings of the 12th Conference on Ground Control in Mining, Morgantown, WV.

Li and Cairns, 2000. **Strata control experiences in longwall mining over old mine workings**. Li, G. and Cairns, R. AJM 3rd Annual Longwall Mining Summit, Yeppoon.

Lohe and Dean-Jones, 1995. **Structural Geology of the Newcastle-Gosford Region**. E.M. Lohe and G.L. Dean-Jones. Published in Australian Geomechanics Society (AGS) Conference Proceedings (February), Engineering Geology of Newcastle - Gosford Region, University of Newcastle.

McQueen, 2004. **In-situ Rock Stress and Its Effect in Tunnels and Deep Excavations in Sydney**. McQueen. L.B. Article presented in Australian Geomechnics Journal Vol 39. No. 3 (September).

MSEC, 2011. **Review of Under Surface and Groundwater Resources at Shallow Depths of Cover for the Proposed LWs 41 to 50, West Wallsend Colliery**. MSEC Report No. 519 (Rev A) - August.

Nemcik et al, 2005. **Statistical Analysis of Underground Stress Measurements in Australian Coal Mines**. Nemcik, J., Gale, W. and Mills, K. Published in proceedings of the Bowen Basin Geology Symposium.

Pells, 2002. **Developments in the Design of Tunnels and Caverns in the Triassic Rocks of the Sydney Region**. International Journal of Rock Mechanics and Mining Sciences No. 39. Pells, P.J.N.

Pells, 2004. **Substance and Mass Properties for the Design of Engineering Structures in the Hawkesbury Sandstone**. Article presented in Australian Geomechnics Journal Vol 39. No. 3 (September).

Peng and Chiang, 1984. **Longwall Mining**. S.S. Peng & H.S. Chiang. Wiley.

RCA, 2013. **End of Panel Longwall 41, Surface Subsidence Mapping Report, West Wallsend Colliery**. Robert Carr and Associates Pty Ltd. *Report Pending*.

Reynolds, 1977. **Coal Mining Under Stored Water**. Report on an Inquiry into Coal Mining Under or in the Vicinity of Stored Waters of the Nepean, Avon, Cordeaux, Cataract and Woronora Reservoirs, NSW for the NSW Government.

SCT, 2001. **Geotechnical Assessment for the Dendrobium Project**. SCT Operations Pty Ltd Report No. DEN1950 (5th June).

SCT, 2008. **Assessment of Longwall Panel Widths and Potential Hydraulic Connection to Bowmans Creek – Ashton Mine**. SCT Operations Pty Ltd Report to Ashton Coal, September.

Seedsman, 2010. **Calibrated Parameters for the Prediction of Subsidence at Mandalong Mine**. R.W. Seedsman. Coal Operators' Conference, University of Wollongong (February).

Singh and Kendorski, 1981. **Strata Disturbance Prediction for Mining Beneath Surface Water and Waste Empoundments**. M.M. Singh and F.S Kendorski. First Conference in Ground Control in Mining, West Virginia University, 76-89.

Tammetta, 2013. **Estimation of the Height of Complete Groundwater Drainage Above Mined Longwall Panels**. Paul Tammetta. Paper published in Groundwater Journal (Vol 51, No. 5, Sep-Oct 2013).

Walker, 2004. **Stress Relief on Hillsides and Hillside Excavations**. Walker, B.F. Article presented in Australian Geomechnics Journal Vol 39. No. 3 (September).

Wardell, 1975. **Mining Under Tidal Waters**. Wardell and Partners Report prepared for NSW Government.

Whittaker & Reddish, 1989. **Subsidence, Occurrence, Prediction and Control**. B. N. Whittaker and D.J. Reddish. Department of Mining Engineering, University of Nottingham, UK.

Project Database and DMR Subsidence Prediction Curves for Single Longwall Panels in Newcastle Coalfield

DMR (Southern Coalfield Upper Limit Curve)
H = 189 - 490 m

DMR (Newcastle Coalfield Upper Limit Curve)
H = 80 - 220 m

W/H

Smax/T
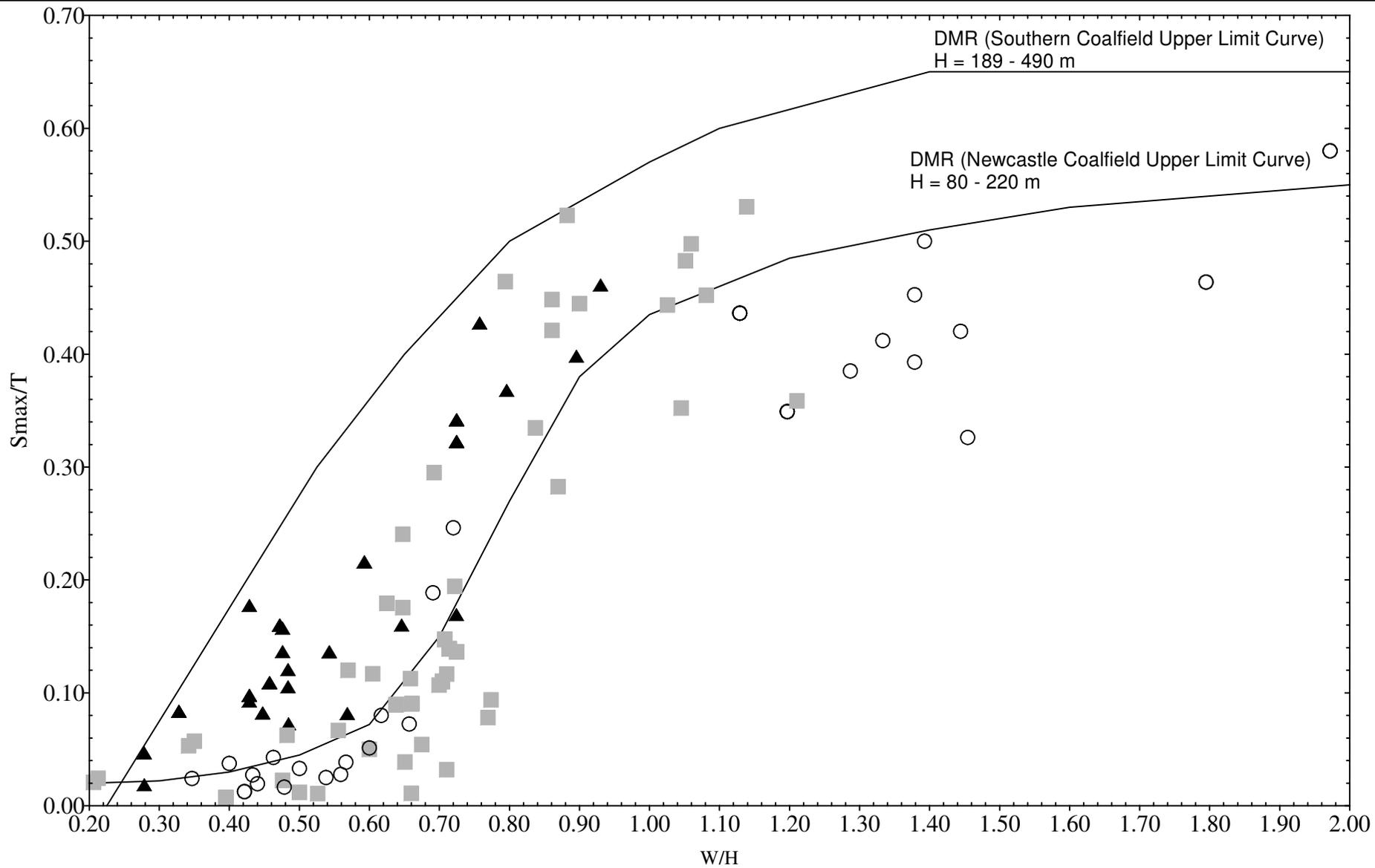
LEGEND
Cover Depth, H (m)

○ H = 70m to H = 151m
■ H = 151m to H = 251m
▲ H = 251m to H = 350m

DgS

Ditton Geotechnical
Services Pty Ltd

Engineer:	S.Ditton	Client:	Adapted from ACARP, 2003
Drawn:	S.Ditton		
Date:	08.06.08	Title:	Project Database and DMR Subsidence Prediction Curves for Single Longwall Panels in Newcastle Coalfield
Scale:	NTS		Figure No: A1

Project Database for Single Longwall Panels in Newcastle Coalfield showing Cover Depth for Each Point

Continuous
or clamped
elastic beam
in overburden
with horizontal
stress.

Simply supported beam
analogy for cracked beam
analysis

Bending stress   Horizontal stress
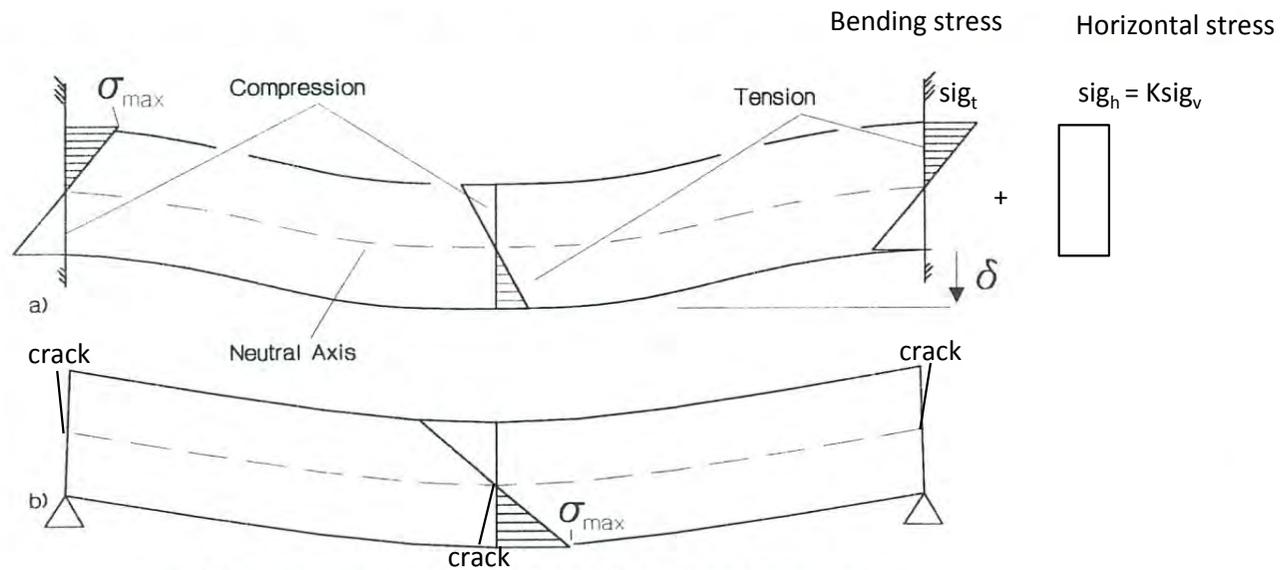
Fig. 4. Elastic beam with (a) fixed ends and (b) simple (pin) supports.

Note: Elastic beam cracks if $sig_t + sig_h > 0$, where tensile stress is positive.

Ref: Diedrichs & Kaiser, 1999

DgS Ditton Geotechnical Services Pty Ltd	Engineer:	S.Ditton	Client:	Adapted from ACARP, 2003		
	Drawn:	S.Ditton				
	Date:	03.06.13	Title:	Internal Compressive Stress Arch Geometry		
	Scale:	NTS			Figure No:	A2.2

Initial Geometry

a)

T

$\dfrac{L}{2}$

$\dfrac{NT}{3}$

$Z_O = t(1-2N/3)$

$\dfrac{\gamma TS}{2}$

$\dfrac{S}{4}$

$\dfrac{S}{2}$

Deformed Geometry

b)

$\delta = Z_o - Z$

NT

$\dfrac{L - \Delta L}{2}$

$Z = \sqrt{(3S/8)(8Z_o{}^2 - \Delta L)}$

F

f_{max}

$\Delta L = L f_{max}(2/9 + N/3)$
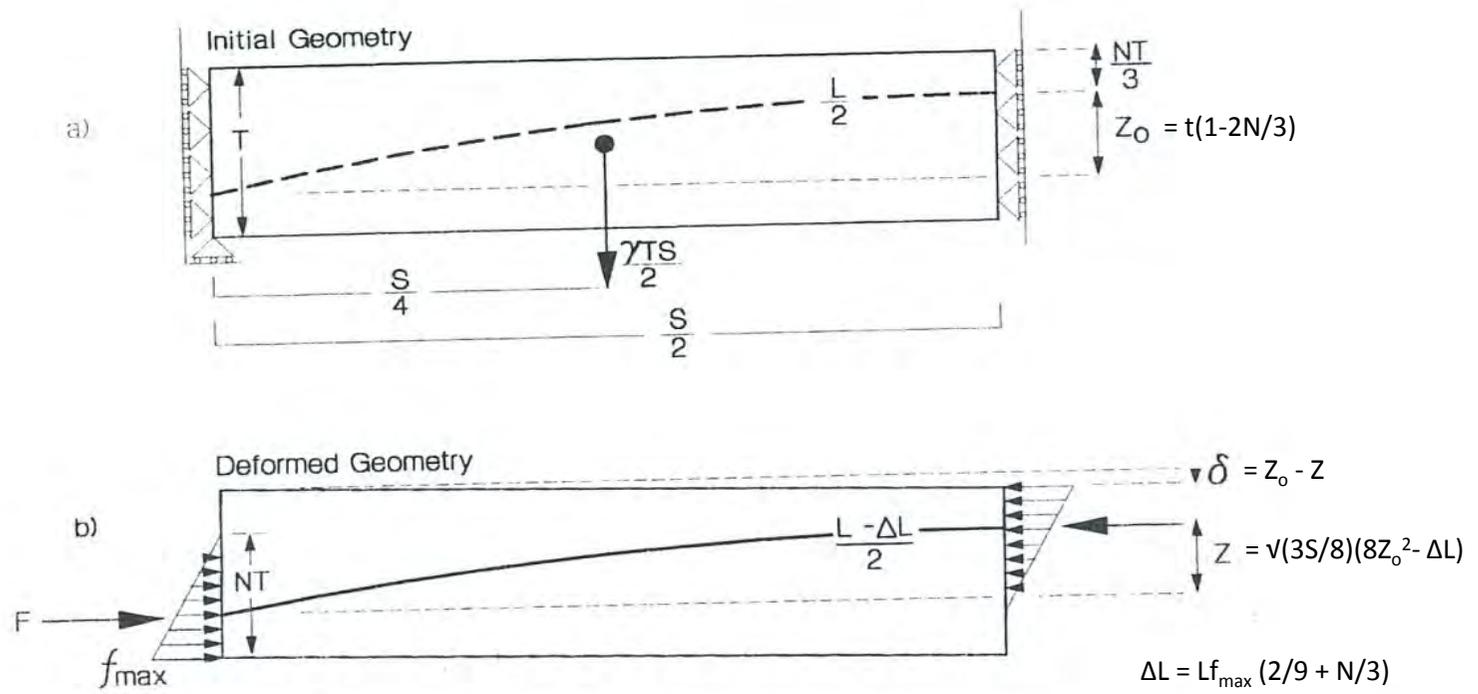
Fig. 5. Voussoir beam (half-span shown) and nomenclature.

Ref: Diedrichs & Kaiser, 1999

DgS **Ditton Geotechnical Services Pty Ltd**	Engineer:	S.Ditton	Client:	Adapted from ACARP, 2003		
	Drawn:	S.Ditton				
	Date:	03.06.13	Title:	Internal Compressive Stress Arch Development in Simply Supported Beam (i.e. Voussoir Beam Analogy)		
	Scale:	NTS	Scale:	NTS	Figure No:	A2.3
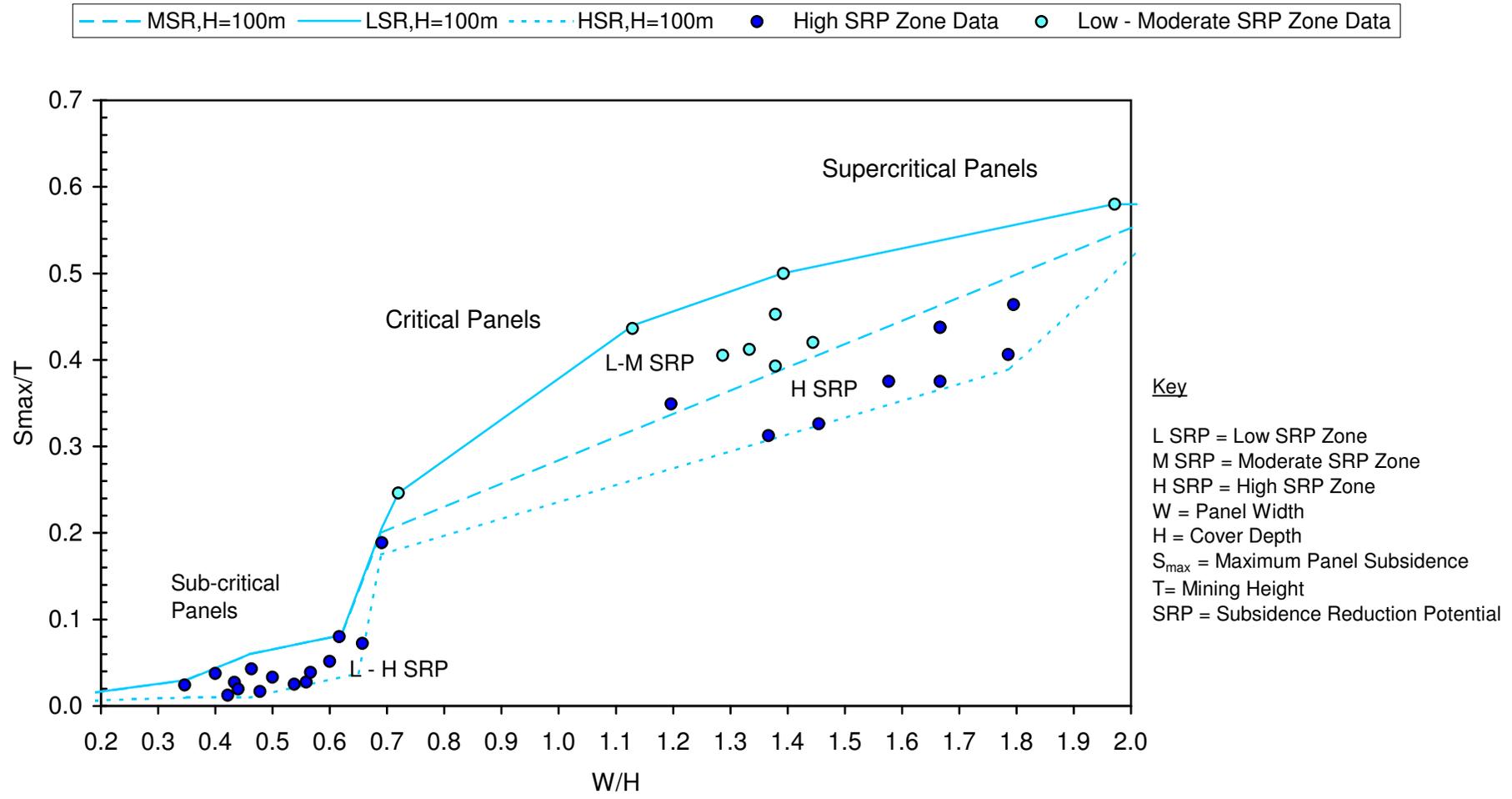
Note: No SRP distinguishment for panels with W/H<0.65

	Engineer:	S.Ditton	Client:	Adapted from ACARP, 2003
DgS	Drawn:	S.Ditton		
	Date:	08.08.08	Title:	Empirical Model for Predicting Subsidence Above Panels with Cover Depths
Ditton Geotechnical				Between 50 and 150 m and Low to High SRP Zones
Services Pty Ltd	Scale:	NTS		Figure No:	A3

Chart labels:
- MSR,H=100m
- LSR,H=100m
- HSR,H=100m
- High SRP Zone Data
- Low - Moderate SRP Zone Data

Y-axis: Smax/T (0.0 to 0.7)
X-axis: W/H (0.2 to 2.0)

Chart annotations:
- Supercritical Panels
- Critical Panels
- L-M SRP
- H SRP
- Sub-critical Panels
- L - H SRP

Key
L SRP = Low SRP Zone
M SRP = Moderate SRP Zone
H SRP = High SRP Zone
W = Panel Width
H = Cover Depth
S_{max} = Maximum Panel Subsidence
T= Mining Height
SRP = Subsidence Reduction Potential

Legend:
- .... HSR,H=200m
- – – – MSR,H=200m
- ——— LSR,H=200m
- **– · – · HSR(L),H=200m**
- ◆ High SRP Zone Data
- ◆ Moderate SRP Data
- ◇ Low SRP Data

Chart axes: Y-axis = Smax/T (0.0 to 0.7), X-axis = W/H (0.2 to 2.0)

Chart annotations:
- Sub-critical Panels
- Critical Panels
- Super-critical Panels
- L SRP
- M SRP
- H SRP

Key

L SRP = Low SRP Zone
M SRP = Moderate SRP Zone
H SRP = High SRP Zone
W = Panel Width
H = Cover Depth
S_{max} = Maximum Panel Subsidence
T = Mining Height
SRP = Subsidence Reduction Potential

Engineer:	S.Ditton	Client:	Adapted from ACARP, 2003
Drawn:	S.Ditton		
Date:	08.08.08	Title:	Empirical Model for Predicting Subsidence Above Panels with Cover Depths
			Between 250 and 350 m and Low to High SRP Zones
Ditton Geotechnical Services Pty Ltd		Scale:	NTS

DgS

Ditton Geotechnical Services Pty Ltd

Figure No: A4

Key

L SRP = Low SRP Zone
M SRP = Moderate SRP Zone
H SRP = High SRP Zone
W = Panel Width
H = Cover Depth
S_{max} = Maximum Panel Subsidence
T= Mining Height
SRP = Subsidence Reduction Potential

DgS	Engineer:	S.Ditton	Client:	Adapted from ACARP, 2003		
	Drawn:	S.Ditton				
Ditton Geotechnical Services Pty Ltd	Date:	08.08.08	Title:	Empirical Model for Predicting Subsidence Above Panels with Cover Depths Between 250 and 350 m and Low to High SRP Zones		
	Scale:	NTS			Figure No:	A5

SPANNING MASSIVE STRATA UNIT

Fractured Zone

Caved Zone

Extracted LW Panel

Physical model of caved strata above longwall extraction with strong overburden. Mining data: h = 84m; w = 118m; M = 4m.

DgS	Engineer:	S.Ditton	Client:	Adapted from ACARP, 2003		
	Drawn:	S.Ditton				
	Date:	08.08.08	Title:	Physical Overburden Model Showing the Subsidence Reducing Effect of		
Ditton Geotechnical				a Massive Strata Unit At the Surface		
Services Pty Ltd	Scale:	NTS			Figure No:	A6

Figure No: A7.1

DgS	Engineer:	S.Ditton	Client: Extract from ACARP, 2003
	Drawn:	S.Ditton	
	Date:	08.08.08	Title: Project Database of Maximum Strata Unit Thickness and SRP Threshold Limit Lines for H=50 m to 150 m
	Ditton Geotechnical Services Pty Ltd		
	Scale:	NTS	Figure No: A7.1

Figure caption / title block:

		Client:	Extract from ACARP, 2003
DgS	Engineer: S.Ditton		
	Drawn: S.Ditton		
	Date: 08.08.08	Title:	Project Database of Maximum Strata Unit Thickness and SRP Threshold Limit Lines for
	Ditton Geotechnical		H=150 m to 250 m
	Services Pty Ltd	Scale: NTS	Figure No: A7.2

Chart labels:

DATABASE RANGE
H = Cover Depth (m) = 151m to 250m
W = Panel Width (m) = 34m to 230m
t = Maximum Strata Unit Thickness (m) = <1m to 86m
y = Height of Base of Strata Unit Above Workings (m) = 5m to 205m

High SRP for datapoints that plot above the threshold limit lines - Moderate to Low SRP for data points below the lines

Y-axis: Maximum Strata Unit Thickness, t (m)
X-axis: Panel Width, W (m)

High SRP (y/H = 0.0)
High SRP (y/H = 0.2), Moderate SRP (y/H = 0.0)
High SRP (y/H = 0.3), Moderate SRP (y/H = 0.2)
High SRP (y/H = 0.5), Moderate SRP (y/H = 0.3)
Moderate SRP (y/H = 0.5)

LEGEND
Label = Strata Unit Location Factor, y/H

Subsidence Reduction Potential (SRP)

Low
Moderate
High

DATABASE RANGE
H = Cover Depth (m) = 251 to 350m
W = Panel Width (m) = 78 to 240m
t = Maximum Strata Unit Thickness (m) = <1m to 86m
y = Height of Base of Strata Unit Above Workings (m) = 14m to 305m

High SRP for datapoints that plot above the threshold limit lines - Moderate to Low SRP for data points below the lines

High SRP (y/H = 0.0)
High SRP (y/H = 0.2), Moderate SRP (y/H = 0.0)
High SRP (y/H = 0.3), Moderate SRP (y/H = 0.2)
High SRP (y/H = 0.8)
Moderate SRP (y/H = 0.3)
Moderate SRP (y/H = 0.8)

Maximum Strata Unit Thickness, t (m)

Panel Width, W (m)

LEGEND
Label = Strata Unit Location Factor, y/H

Subsidence Reduction Potential (SRP)

△ Low
▲ Moderate
▲ High

Engineer:	S.Ditton	Client: Extract from ACARP, 2003
Drawn:	S.Ditton	
Date:	08.08.08	Title: Project Database of Maximum Strata Unit Thickness and SRP Threshold Limit Lines for H=250 m to 350 m
Ditton Geotechnical Services Pty Ltd		Scale: NTS

DgS
Ditton Geotechnical Services Pty Ltd

Figure No: A7.3

Legend: y/H = 0.0 (H=100m) — y/H = 0.2 (H=100m) — y/H = 0.5 (H=100m) — y/H = 0.9 (H=100m)

X-axis: Panel Width, W (m)
Y-axis: Massive Strata Unit Thickness, t (m)

Engineer:	S.Ditton	Client: Adapted from ACARP, 2003
Drawn:	S.Ditton	
Date:	08.08.08	Title: Empirical Model for Predicting Subsidence Reduction Potential Above Panels with Cover Depths Between 50 and 150 m
Ditton Geotechnical Services Pty Ltd		Scale: NTS

DgS

Figure No: A8

Legend:
— y/H = 0.0 (H=200m) — — y/H = 0.2 (H=200m) · · · y/H = 0.3 (H=200m) — · — y/H = 0.5 (H=200m)

Y-axis: Massive Strata Unit Thickness, t (m)

X-axis: Panel Width, W (m)

Engineer:	S.Ditton	Client:	Adapted from ACARP, 2003
Drawn:	S.Ditton		
Date:	08.08.08	Title:	Empirical Model for Predicting Subsidence Reduction Potential Above Panels with Cover Depths Between 150 and 250 m
Ditton Geotechnical Services Pty Ltd			
		Scale:	NTS	Figure No:	A9

DgS
Ditton Geotechnical Services Pty Ltd

Legend:
— y/H = 0.0 (H=300m) — — y/H = 0.2 (H=300m) · · · y/H = 0.3 (H=300m) — · — y/H = 0.8 (H=300m)

Y-axis: Massive Strata Unit Thickness, t (m)

X-axis: Panel Width, W (m)

Engineer:	S.Ditton	Client: Adapted from ACARP, 2003
Drawn:	S.Ditton	
Date:	08.08.08	Title: Empirical Model for Predicting Subsidence Reduction Potential Above Panels with
DgS Ditton Geotechnical Services Pty Ltd		Cover Depths Between 250 and 350 m
		Scale: NTS
		Figure No: A10

Maximum Surface Subsidence, S_{max}

'SPANNING' ZONE

Side Abutment Load

Massive Unit Surcharge

Side Abutment Load

Cover Depth, H

Massive Unit of thickness, t

Effective Massive Unit Span

'FRACTURED' ZONE

Massive Unit Location above Workings, y

ϕ Caving Angle

'CAVING' ZONE

Working Height, T

Panel Width, W

DgS	Engineer:	S.Ditton	Client:	Adapted from ACARP, 2003		
	Drawn:	S.Ditton				
	Date:	08.08.08	Title:	Overburden with Massive Strata Unit Behaviour Concept Model and Key Parameter Definitions		
Ditton Geotechnical Services Pty Ltd						
			Scale:	NTS	Figure No:	A11

DEEP 'BEAM' BEHAVIOUR
(W/H < 0.7)

Geometrical ➡

SHALLOW 'BEAM' BEHAVIOUR
(W/H > 0.7)

AXIAL ACTION OR
DEEP 'ARCHING' DOMINATES
SMALL BENDING ZONE

BENDING ACTION DOMINATES AS
DEEP ARCHING NOT POSSIBLE
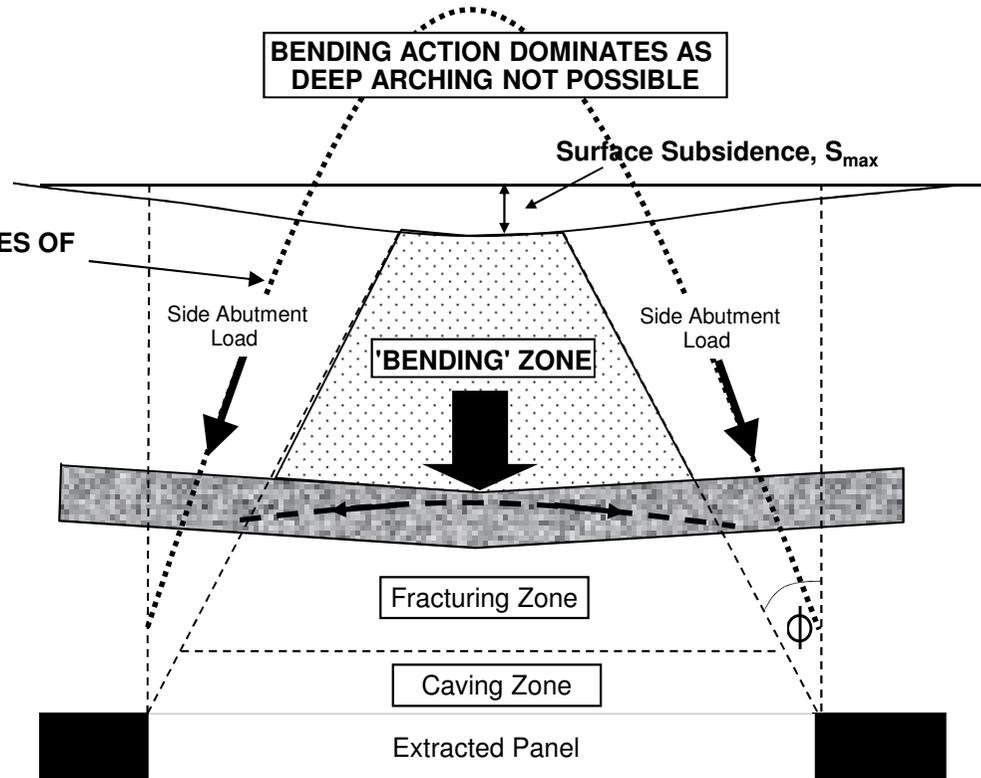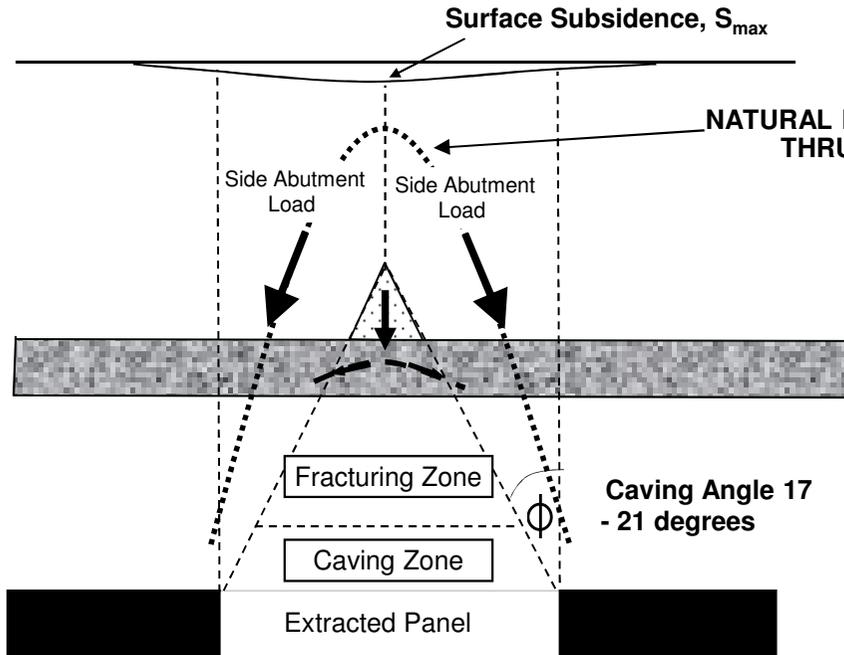
Surface Subsidence, S_{max}

Surface Subsidence, S_{max}

NATURAL LINES OF
THRUST

Side Abutment Load

Side Abutment Load

Side Abutment Load

Side Abutment Load

'BENDING' ZONE

Fracturing Zone

Caving Angle 17
- 21 degrees

ϕ

Fracturing Zone

ϕ

Caving Zone

Caving Zone

Extracted Panel

Extracted Panel

DgS	Engineer:	S.Ditton	Client:	Adapted from ACARP, 2003		
	Drawn:	S.Ditton				
	Date:	08.08.08	Title:	Overburden with Massive Strata Units Behaviour Concept Models of Beam Action Types		
Ditton Geotechnical				for Subcritical and Supercritical Longwall Panels		
Services Pty Ltd	Scale:	NTS			Figure No:	A12

Sub-Critical
Panel
or

'Deep' Beam
Behaviour

Critical
Panel
or

'Shallow' Beam
Behaviour

Super-Critical
Panel
Behaviour

S_{max}/T

0.58

SRP Range For
Cover Depth, H

Increasing H for
constant W/H Effect

Low SRP Curve

Moderate SRP Curve

High SRP Curve

Geometrical Transition

H=300m.

H=200m

H=100m

Decreasing
Geological SRP
Effect

0.6

0.9

W/H

1.4 to 2.0

DgS	Engineer:	S.Ditton	Client:	Adapted from ACARP, 2003		
	Drawn:	S.Ditton				
	Date:	08.08.08	Title:	Geomechnical and Geological Effects of Overburden Behaviour on Maximum Subsidence		
Ditton Geotechnical				for Single Panels		
Services Pty Ltd	Scale:	NTS			Figure No:	A13

Chain Pillar Subsidence

Single $S_{max(i)}$

Final $S_{max(i)}$ = First $S_{max(i)}$ + ($S_{p(i)}$-S_{ge})

$S_{p(i-1)}$

$S_{p(i)}$

Subsidence trough

Chain pillars subject to double abutment loading conditions
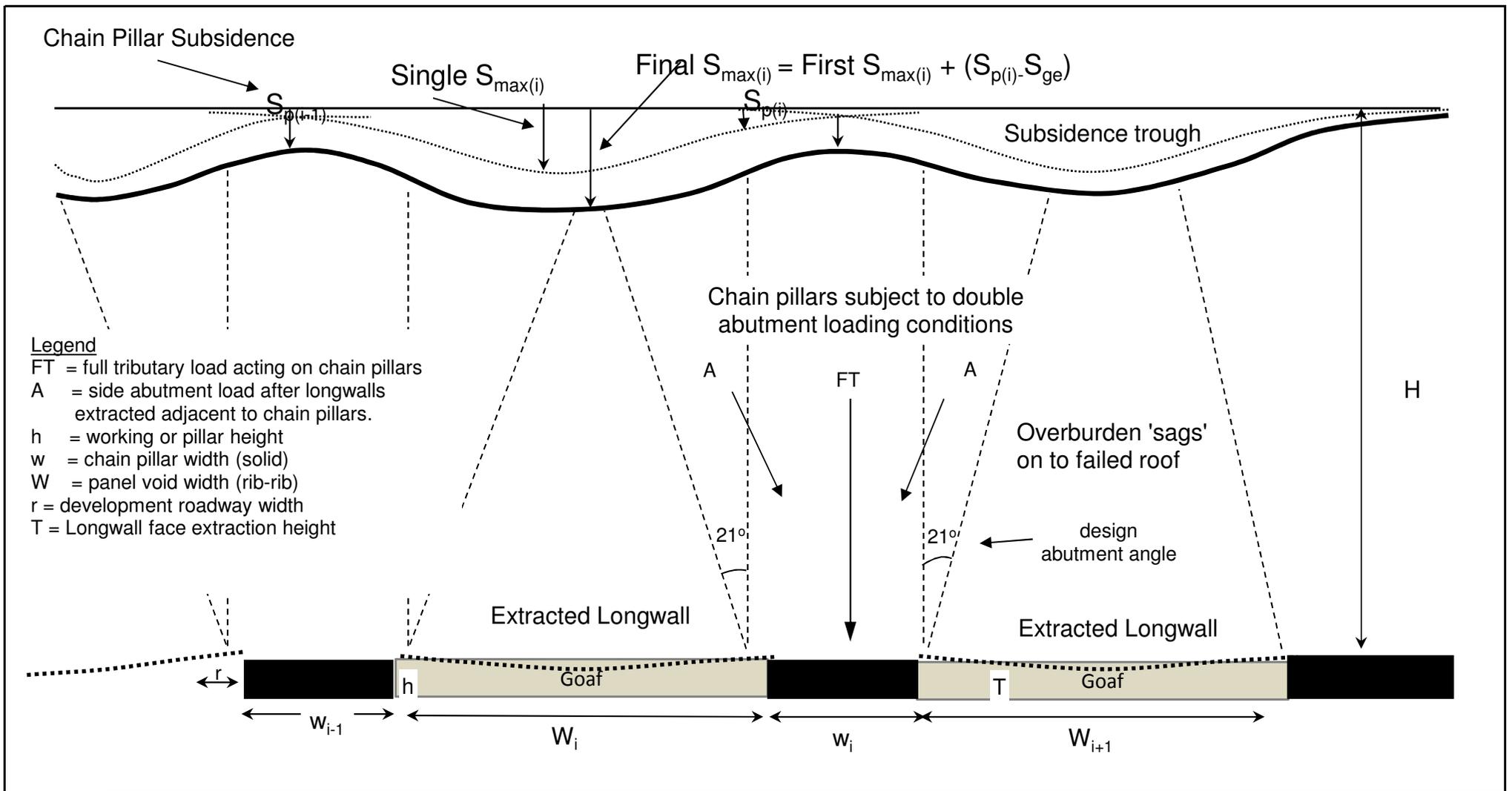
Legend
FT = full tributary load acting on chain pillars
A = side abutment load after longwalls extracted adjacent to chain pillars.
h = working or pillar height
w = chain pillar width (solid)
W = panel void width (rib-rib)
r = development roadway width
T = Longwall face extraction height

A

FT

A

H

Overburden 'sags' on to failed roof

$21°$

$21°$

design abutment angle

Extracted Longwall

Extracted Longwall

r

h

Goaf

T

Goaf

w_{i-1}

W_i

w_i

W_{i+1}

DgS	Engineer:	S.Ditton	Client:	Adapted from ACARP, 2003		
	Drawn:	S.Ditton				
	Date:	19.07.12	Title:	Multiple Longwall Panel Subsidence Mechanism Concepts		
Ditton Geotechnical Services Pty Ltd						
	Scale:	NTS			Figure No:	A14

Maximum $S_p/T = 0.58$

95% UCL Line for F<0.385 (Mean +/- 0.13)

$S_p/T = 7.4044e^{-10.329F}$
$R^2 = 0.917$

95% UCL Line for 0.385<F<0.543 (Mean +/- 0.030)

95% UCL Line for F>0.53 (Mean +/- 0.023)

Mean = 0.025
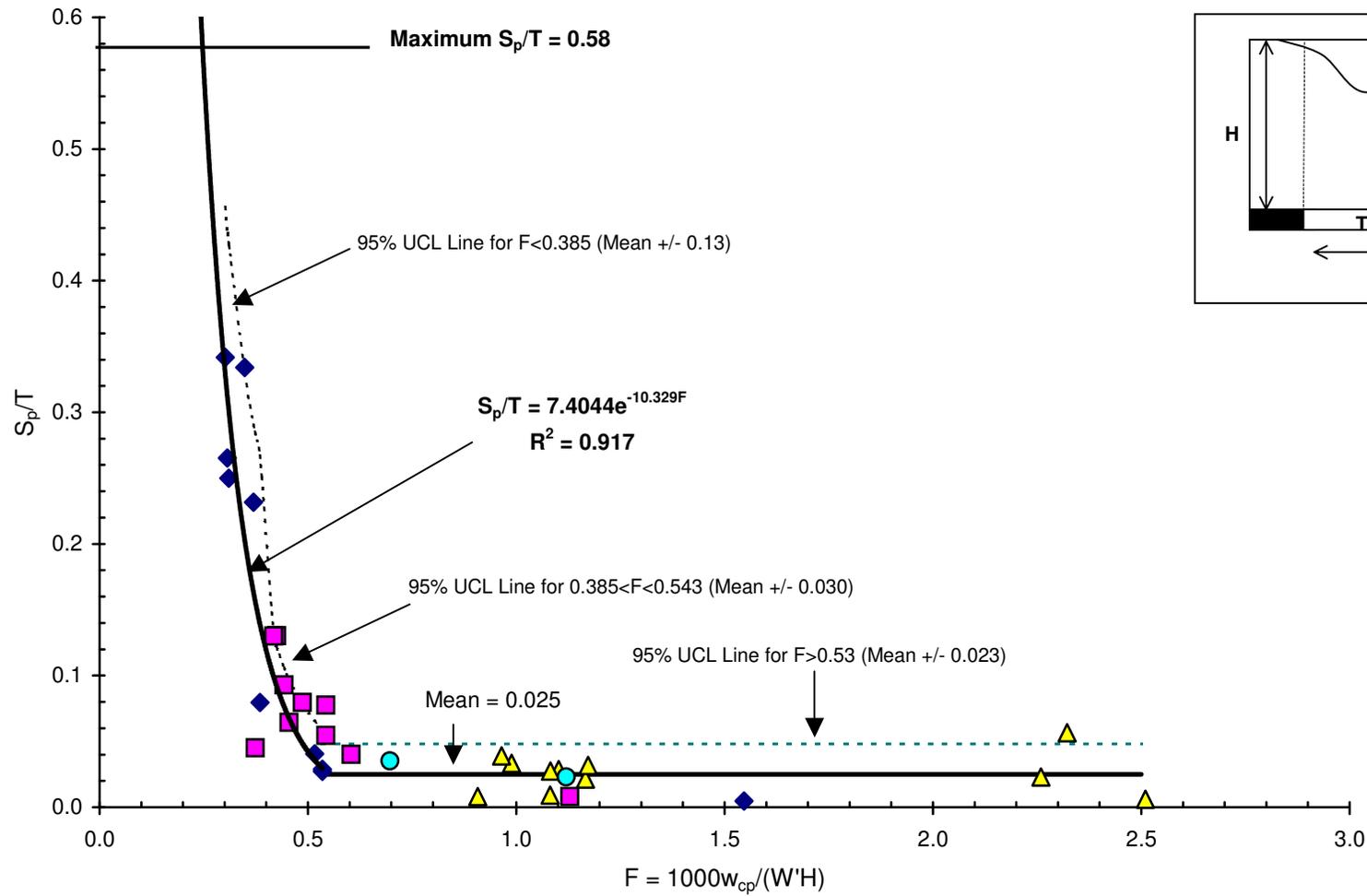
◆ West Wallsend(LWs11-23)
△ Gretley (MWs1-62)
■ Newstan (LWs 5-17)
○ Cooranbong (LWs 1-6)

S_p/T

$F = 1000w_{cp}/(W'H)$

DgS	Engineer:	S.Ditton
	Drawn:	S.Ditton
	Date:	08.08.08
Ditton Geotechnical Services Pty Ltd		

Client:	Extract from ACARP, 2003
Title:	2003 Empirical Model for Predicting Subsidence above Chain Pillars Subject to Double Abutment Loading
Scale:	NTS

Figure No: A15

Figure A16

	Engineer:	S.Ditton	Client:	Adapted from ACARP, 2003
DgS	Drawn:	S.Ditton		
	Date:	08.08.08	Title:	2008 Empirical Model (DgS) for Predicting Subsidence above Chain Pillars Subject to Double
Ditton Geotechnical				Abutment Loading
Services Pty Ltd	Scale:	NTS		Figure No: A16

Figure A17: Empirical DgS, 2008 Model Data of 1/FoS v. Subsidence above Chain Pillars Subject to Double Abutment Loading

Measured Multiple Longwall Panel Subsidence in Newcastle Coalfield

Engineer:	S.Ditton
Drawn:	S.Ditton
Date:	08.08.08

DgS
Ditton Geotechnical
Services Pty Ltd

Client:	Adapted from ACARP, 2003
Title:	Measured Multiple Longwall Panel Subsidence in Newcastle Coalfield
Scale:	NTS
Figure No:	A18

Chart legend:
- 12-Feb-99
- 19-Aug-99
- 18-Feb-00
- 01-Sep-00
- 14-Mar-01

LW19 Completed 29/01/99
LW20 Completed 26/07/99
LW21 Completed 08/02/00
LW22 Completed 14/09/00
LW23 Completed 08/01/01

Subsidence (m)

Chainage (m)

VERTICAL DISPLACEMENT PARAMETER PROFILES

HORIZONTAL DISPLACEMENT PARAMETER PROFILES

Tilt

T_{max}

HD_{max}

Horizontal Displacement (towards panel centreline)

Convex Curvature

$+ C_{max}$

$+ E_{max}$

Tensile Strain

DEFORMED SURFACE

d

Concave Curvature

$- C_{max}$

$- E_{max}$

0.6

Inflexion Point

Depth of Cover, H

Compressive Strain

Angle of Draw

Abutment Angle

S_{max}

Solid

Chain Pillar

EXTRACTED LONGWALL PANEL

Chain Pillar

Solid

Gate Roadways

Panel Width W

Extracted Seam Thickness, T

	DgS	Engineer:	S.Ditton	Client:	Extract from ACARP, 2003		
		Drawn:	S.Ditton				
		Date:	08.08.08	Title:	Mine Subsidence Trough Deformation Parameters		
	Ditton Geotechnical				(adapted from Holla, 1987)		
	Services Pty Ltd	Scale:	NTS			Figure No:	A19

Figure A20: Empirical Model for Goaf Edge Subsidence Prediction Above Longwall Panels

Legend:
- ◆ Measured LW Panel Side Data (Newcastle Coalfield)
- U95%CL
- Power (Measured LW Panel Side Data (Newcastle Coalfield))

$U95\%\ S_{side}/S_{max} = 0.1719\ (W/H)^{-1.9465}$

$Mean = 0.0722x^{-2.557}$
$R^2 = 0.8215$

Y-axis: Panel Side Subsidence/Maximum Panel Subsidence (S_{side}/S_{max})

X-axis: W/H

Engineer:	S.Ditton	Client:	Adapted from ACARP, 2003
Drawn:	S.Ditton		
Date:	08.08.08	Title:	Empirical Model for Goaf Edge Subsidence Prediction Above Longwall Panels
		Scale:	NTS

DgS
Ditton Geotechnical Services Pty Ltd

Figure No: A20

Empirical Prediction Model for Longwall Panel Angle of Draw

DgS	Engineer:	S.Ditton	Client:	Extracted from ACARP, 2003
	Drawn:	S.Ditton		
	Date:	08.08.08	Title:	Empirical Prediction Model for Longwall Panel Angle of Draw
Ditton Geotechnical Services Pty Ltd	Scale:	NTS		Figure No: A21

$y = 1.1925x^{1.3955}$
$R^2 = 0.9428$

95% UCL (Mean + 0.4Mean)

95% LCL (Mean - 0.4Mean)

Tmax(mm/m)

Smax/W (mm/m)

Engineer:	S.Ditton	Client:	Extract from ACARP, 2003
Drawn:	S.Ditton		
Date:	08.08.08	Title:	Empirical Model for Maximum Panel Tilt Prediction Above Longwall Panels
Scale:	NTS		Figure No: A22

DgS

Ditton Geotechnical
Services Pty Ltd

Legend: ■ Convex (Tensile) □ Failed Cases

'Discontinuous' Cmax = 1.3548Ln(Smax/W'^{2}) + 5.8671
R^2 = 0.9994

'Smooth' Cmax = 15.603(S_{max}/W^2)
R^2 = 0.7925

95% UCL (1.5Mean)

95% LCL (0.5Mean)

Y-axis: Convex Curvature, C_{max} (km^{-1})

X-axis: S_{max}/(W^2) (mm/m^2))

DgS	Engineer:	S.Ditton
	Drawn:	S.Ditton
	Date:	08.08.08
Ditton Geotechnical		
Services Pty Ltd	Scale:	NTS

Client:	Extract from ACARP, 2003
Title:	Empirical Model for Maximum Panel Convex Curvature Prediction Above Longwall Panels for Smooth and Discontinuous Profiles
	Figure No: A23

Empirical Model for Maximum Panel Concave Curvature Prediction Above Longwall Panels for Smooth and Discontinuous Profiles

Legend: ▲ Smooth Profile   △ Failed Cases   ━ ━ Log. (Failed Cases)

X-axis: $S_{max}/(W^2)$ (mm/m2)

Y-axis: Concave Curvature, C_{min} (km^{-1})

Discontinuous $C_{max} = 1.7071 Ln(S_{max}/W^2) + 7.0267$
$R^2 = 0.857$

'Smooth' $C_{min} = 19.79(S_{max}/W^2)$
$R^2 = 0.7946$

95% UCL (1.5Mean)

95% LCL (0.5Mean)

Engineer:	S.Ditton	Client:	Extract from ACARP, 2003
Drawn:	S.Ditton		
Date:	08.08.08	Title:	Empirical Model for Maximum Panel Concave Curvature Prediction Above Longwall Panels
Ditton Geotechnical			for Smooth and Discontinuous Profiles
Services Pty Ltd		Scale:	NTS	Figure No:	A24

DgS

Ditton Geotechnical Services Pty Ltd

Empirical Model for Maximum Panel Strain Prediction Above Longwall Panels for Smooth and Cracked Profiles

DgS	Engineer:	S.Ditton	Client:	Extract from ACARP, 2003
	Drawn:	S.Ditton		
	Date:	08.08.08	Title:	Empirical Model for Maximum Panel Strain Prediction Above Longwall Panels
Ditton Geotechnical Services Pty Ltd				for Smooth and Cracked Profiles
	Scale:	NTS		Figure No: A25

$S_{Tmax}/S_{max} = -0.0925(W/H) + 0.7356$

$R^2 = 0.0482$

mean = 0.67

STmax/Smax

W/H

Engineer:	S.Ditton	Client:	Extract from ACARP, 2003		
Drawn:	S.Ditton				
Date:	08.08.08	Title:	Empirical Model for Subsidence at Maximum Tilt Above Longwall Panels		
Ditton Geotechnical Services Pty Ltd					
		Scale:	NTS	Figure No:	A26

DgS

Legend:
- ◆ Inflexion Point
- ■ Maximum Convex Curvature
- ▲ Maximum Concave Curvature
- — — Log. (Maximum Concave Curvature)
- —— Log. (Inflexion Point)
- — — Log. (Maximum Convex Curvature)

Sub-critical Panels

Critical Panels

Super-critical Panels

$y = 0.245Ln(x) + 0.3767$ for W/H <0.6

$y = 0.245Ln(x) + 0.2387$ for W/H<0.6

$y = 0.3409Ln(x) + 0.3996$
$R^2 = 0.59$

$y = 0.2425Ln(x) + 0.3097$
$R^2 = 0.73$

$y = 0.1643Ln(x) + 0.2203$
$R^2 = 0.28$

di/H

W/H

Key
d= inflexion point distance from solid rib
dc=compressive strain peak distance from solid rib
dt=tensile strain peak from solid rib

DgS	Engineer:	S.Ditton	Client:	Adapted from ACARP, 2003
Ditton Geotechnical Services Pty Ltd	Drawn:	S.Ditton		
	Date:	08.08.08	Title:	Empirical Model for Predicting the Location of Inflexion Point, Maximum Tensile and Compressive Strain Peaks due to Longwall Panel Subsidence in the Newcastle Coalfield
	Scale:	NTS		Figure No: A27

EXTENSION SIDE
OF BEAM

NEUTRAL AXIS $\cdots\cdots$

d_n

COMPRESSION SIDE
OF BEAM

Origin

Strain E = (mm/m)
Curvature C = km-1

$E = C \times d_n$

Average
dn = 5.2 m
for database

R = Radius of curvature
or the curvature, C = 1/R
(km^{-1})

DgS	Engineer:	S.Ditton	Client:	Extract from ACARP, 2003	
	Drawn:	S.Ditton			
	Date:	08.08.08	Title:	Bending Beam Theory for Strain Prediction	
	Ditton Geotechnical			from Curvature Measurements	
	Services Pty Ltd		Scale:		Figure No: A28

Legend: ◆ Tensile Strain Data ▲ Compressive Strain Data ▬ Linear (Tensile Strain Data)

Y-axis: Emax (mm/m)

X-axis: Cmax.r (m/km)

$y = 0.1437x$
$R^2 = 0.3559$

inflexion point

z   d

H

beta

beta = influence angle
r = influence radius = d + z
tan(beta) = H/r
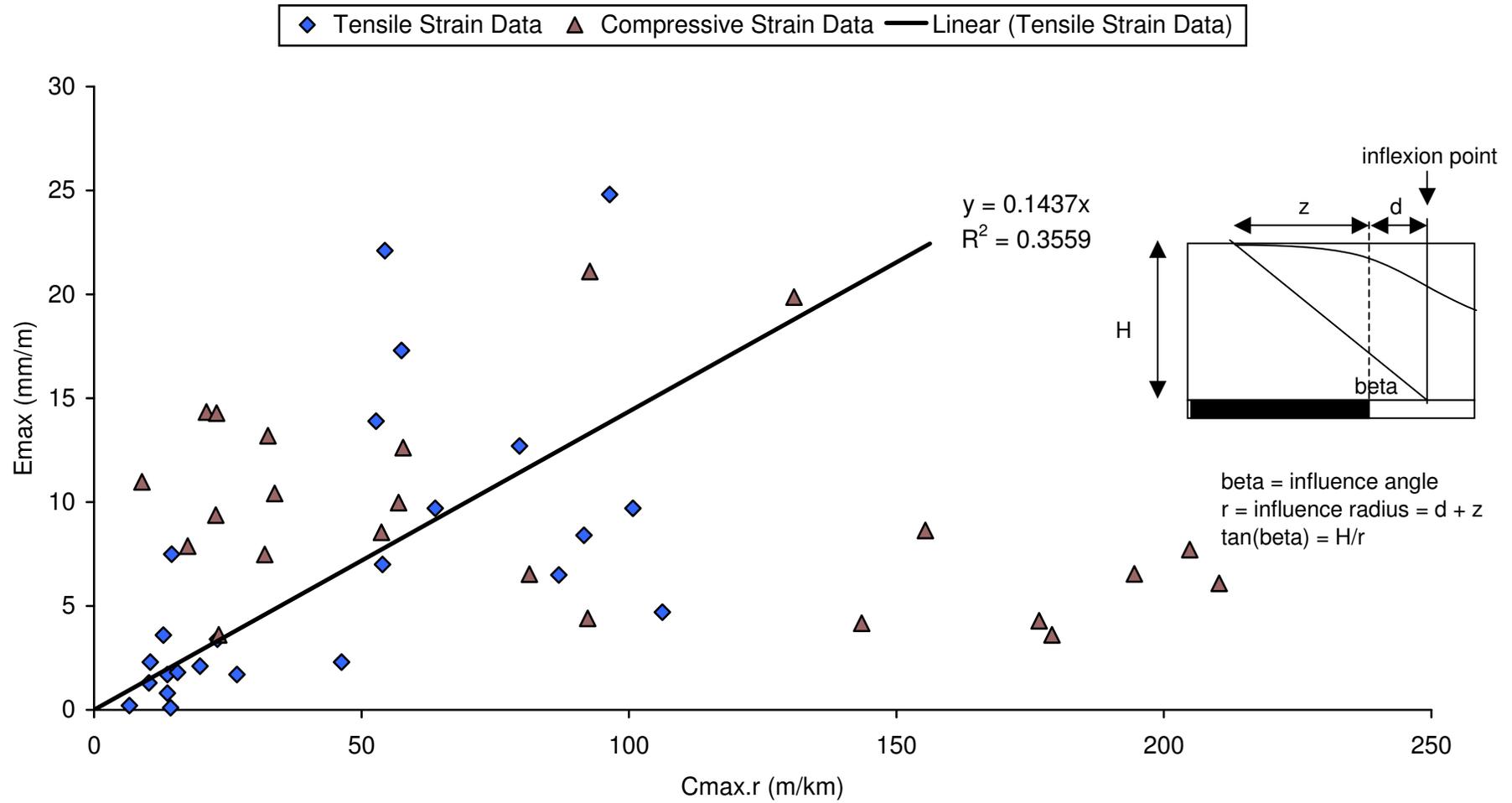
DgS	Engineer:	S.Ditton	Client:	Karmis, 1987 Adapted for ACARP, 2003		
	Drawn:	S.Ditton				
Ditton Geotechnical Services Pty Ltd	Date:	08.08.08	Title:	Empirical Model Recommended by Karmis et al, 1987 for Predicting Strain from Curvature Above Longwall Panels in Newcastle Coalfield		
			Scale:	NTS	Figure No:	A29.1

Legend: ◆ Tensile Strain Data —— Linear (Tensile Strain Data)

$y = 13.632x$
$R^2 = 0.279$

Y-axis: [Absolute] H.C$_{max}$ (m/km)

X-axis: [Absolute] Maximum Strain E$_{max}$ (mm/m)

Notes:
1. H = Cover depth
2. Tensile and compressive strains included
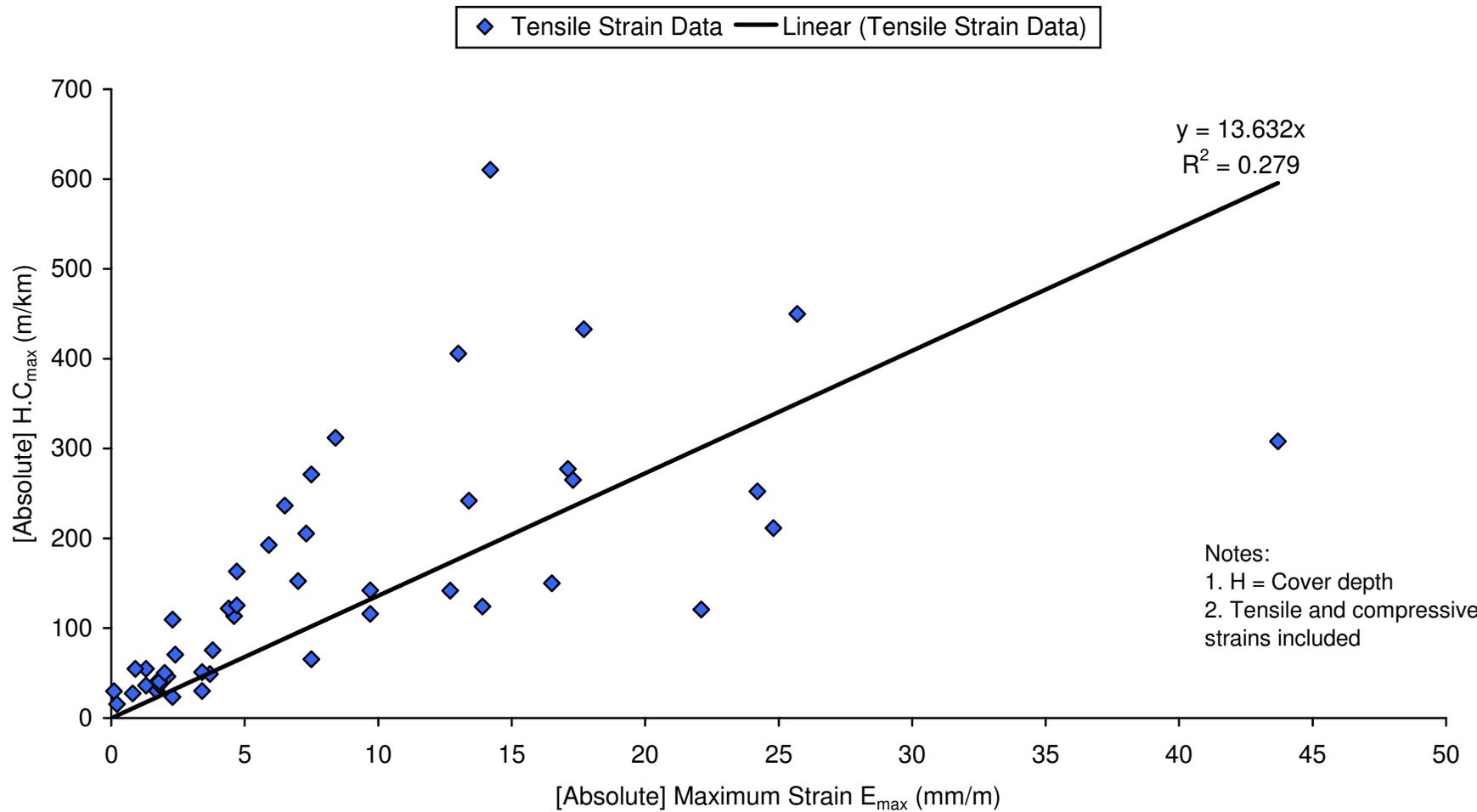
Engineer:	S.Ditton	Client:	Holla and Barclay, 2000 Adapted for ACARP, 2003
Drawn:	S.Ditton		
Date:	08.08.08	Title:	Empirical Model Recommended by Holla and Barclay, 2000 for Predicting Curvature from Maximum Strain Above Longwall Panels in the Newcastle Coalfield
Scale:	NTS		Figure No: A29.2

DgS

Ditton Geotechnical Services Pty Ltd

Engineer:	S.Ditton	Client:	Extract from ACARP, 2003		
Drawn:	S.Ditton				
Date:	08.08.08	Title:	Residual Errors of Database for Single Panel Prediction Model above Longwalls		
Ditton Geotechnical			in the Newcastle Coalfield		
Services Pty Ltd		Scale:	NTS	Figure No:	A30

DgS — Ditton Geotechnical Services Pty Ltd

Plot axes: Residual Model E_{rrors}/T (m/m) vs W/H

95%UCL = +0.101T
95%UCL = +0.030T
95%UCL = +0.05T
95%LCL = -0.030T
95%LCL = -0.05T
95%LCL = -0.101T

Legend:
- W/H<0.6
- 0.6<W/H>0.9
- W/H >0.9

Legend: Measured (19/03/97) — Predicted — DMR Newcastle — Conglomerate Thickness

Data point annotations on chart:
- -0.385
- -0.836
- -1.269
- -2.248

HIGH SRP

LOW-MOD SRP

Geometric Transition in Low-Moderate SRP Area

W/H > 0.8   **W/H < 0.8**

LW 9 Completed 27/02/97

Subsidence (m) — vertical axis left
Conglomerate Unit Thickness (m) — vertical axis right

Chainage (m)

H =160 - 190m, W = 135m, T = 4.3m, y = 7 - 15m

Engineer:	S.Ditton	Client:
Drawn:	S.Ditton	
Date:	08.08.08	Title:

DgS

Ditton Geotechnical Services Pty Ltd

Client: Extract from ACARP, 2003

Title: Predicted v. Measured Centreline Subsidence Profiles for a Newcastle Coalfield Longwall with Massive Conglomerate Strata and Sub-Critical to Supercritical Transition

Scale: NTS

Figure No: A31

Legend: Measured LW1 · Predicted LW1 · Measured LW1+2 · Predicted LW1+2

Engineer:	S.Ditton	Client:	Extract from ACARP, 2003		
Drawn:	S.Ditton				
Date:	08.08.08	Title:	Predicted v. Measured Crossline Subsidence Profiles for a Newcastle Coalfield Longwall Mine		
Ditton Geotechnical Services Pty Ltd					
		Scale:	NTS		Figure No:	A32

DgS
Ditton Geotechnical Services Pty Ltd

Title: Predicted v. Measured Crossline Tilt Profiles for a Newcastle Coalfield Longwall Mine

Engineer:	S.Ditton
Drawn:	S.Ditton
Date:	08.08.08

Ditton Geotechnical
Services Pty Ltd

Client: Extract from ACARP, 2003

Title: Predicted v. Measured Crossline Tilt Profiles for a Newcastle Coalfield Longwall Mine

Scale: NTS

Figure No: A33

Predicted v. Measured Crossline Strain Profiles for a Newcastle Coalfield Longwall Mine

Engineer:	S.Ditton	Client:	Extract from ACARP, 2003
Drawn:	S.Ditton		
Date:	08.08.08	Title:	Predicted v. Measured Crossline Strain Profiles for a Newcastle Coalfield Longwall Mine
Ditton Geotechnical Services Pty Ltd			
		Scale:	NTS
			Figure No: A34

DgS

Legend:
- Predicted (Mean)
- Predicted (U95%CL)
- Measured (31/07/08)

Y-axis: Subsidence (m)
X-axis: Chain (m)

LW34   LW35

Engineer:	S.Ditton	Client:	DgS, 2008 Modified ACARP, 2003 Model Outcomes
Drawn:	S.Ditton		
Date:	07.09.08	Title:	Predicted v. Measured Crossline Subsidence Profiles for a Newcastle Coalfield Longwall
Ditton Geotechnical			Longwall Panel
Services Pty Ltd		Scale:	NTS

DgS
Ditton Geotechnical Services Pty Ltd

Figure No: A35

Predicted v. Measured Crossline Tilt Profiles for a Newcastle Coalfield Longwall Mine

DgS	Engineer:	S.Ditton	Client: DgS, 2008 Modified ACARP, 2003 Model Outcomes
	Drawn:	S.Ditton	
	Date:	07.09.08	Title: Predicted v. Measured Crossline Tilt Profiles for a Newcastle Coalfield Longwall Mine
Ditton Geotechnical Services Pty Ltd	Scale:	NTS	Figure No: A36

Predicted (mean)
Predicted (U95%CL)
Measured (31/07/08)

LW34

LW35

Curvature (km^{-1})

Chain (m)

Engineer:	S.Ditton	Client:	DgS, 2008 Modified ACARP, 2003 Model Outcomes		
Drawn:	S.Ditton				
Date:	07.09.08	Title:	Predicted v. Measured Crossline Curvature Profiles for a Newcastle Coalfield Longwall Mine		
Scale:	NTS			Figure No:	A37

DgS

Ditton Geotechnical
Services Pty Ltd

Predicted v. Measured Crossline Strain Profiles for a Newcastle Coalfield Longwall Mine

Legend:
- Predicted (mean)
- Predicted (U95%CL)
- Measured (31/07/08)

topographic induced anomaly (?)

LW34   LW35

Strain (mm/m) vs Chain (m)

Engineer:	S.Ditton	
Drawn:	S.Ditton	
Date:	08.09.08	

DgS

Ditton Geotechnical Services Pty Ltd

Client:	DgS, 2008 Modified ACARP, 2003 Model Outcomes
Title:	Predicted v. Measured Crossline Strain Profiles for a Newcastle Coalfield Longwall Mine
Scale:	NTS

Figure No: A38

100 mm wide
crack in 10 m bay-length

Strain Concentration Factor Calculation
for 10 m Baylength^

- Measured crack width = 100 mm.
- Measured crack depth >5 m
- Location = 27 m from solid rib.
  Smax = 1.4 m.
- Cover depth, H = 180 m.
- LW panel width, W= 175 m.
  (W/H = 0.97)
- Measured curvature,
  C = 1.15 km-1
  (radius of 867 m)
- Measured strain over 10 m,
  E = 5.8 mm/m*
- Concentrated strain = crack
  width/bay-length = 100/10 = 10
mm/m.

Therefore, concentrated strain =
10/5.8 = 1.7 x uniform strain.

*- peak strains measured 10 m to
south of crack at same distance from
rib.
^ - It is likely that strain concentration
includes strain from adjacent 'bays'.

DgS Ditton Geotechnical Services Pty Ltd	Engineer:	S.Ditton	Client: Adapted from ACARP, 2003
	Drawn:	S.Ditton	
	Date:	08.08.08	Title: Example of Strain Concentration Effect Above Longwall with Shallow Surface Rock
	Scale:	NTS	Figure No: A39

Surface Cracking
(Tensile Strain Zone)

Surface Cracking
(Shearing/buckling in
Compressive Strain Zone)

Surface Cracking
(Tensile Strain Zone)

Surface cracking

Continuous deformation zone

Fractured zone

Caved zone

Collapsed strata
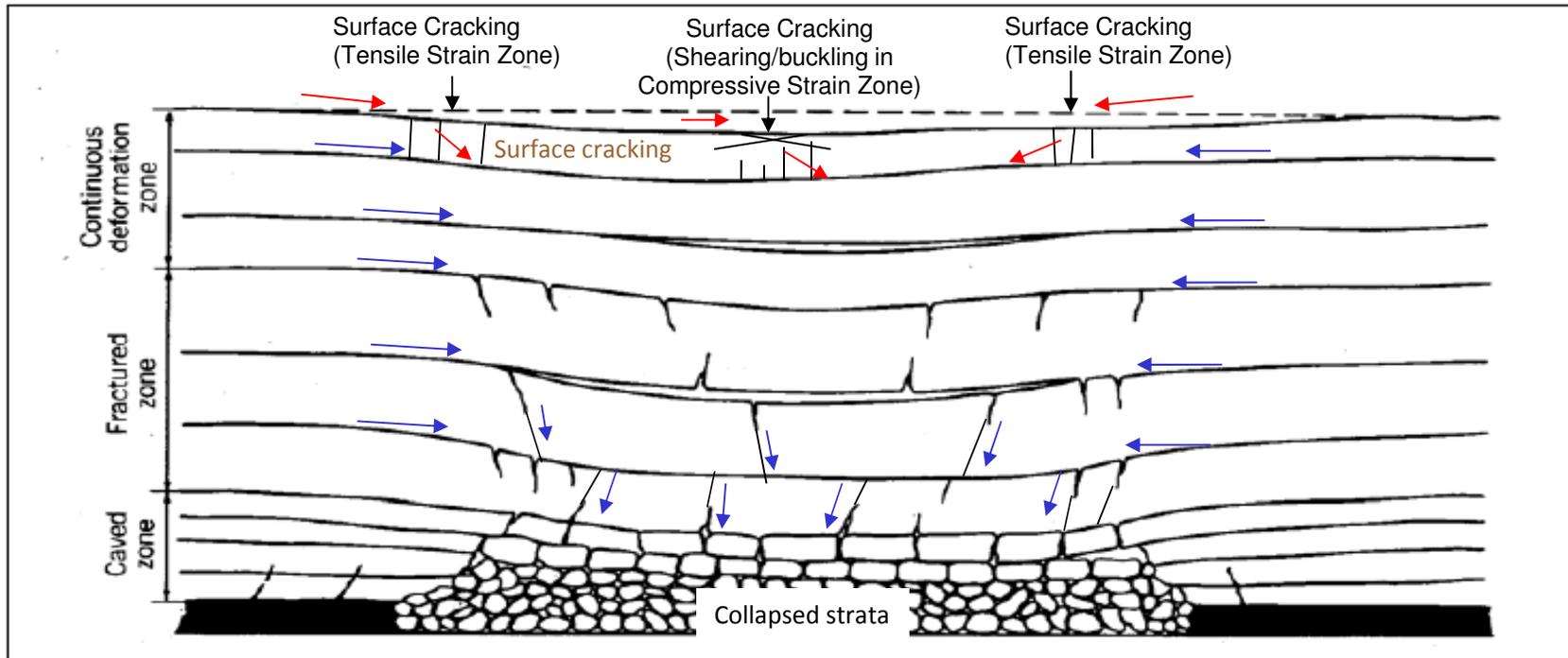
Zones in the Overburden According to Peng and Chiang (1984)

Key

→ Surface water flow path   → Sub-surface water flow path

DgS	Engineer:	S.Ditton	Client:	Appendix A
	Drawn:	S.Ditton		
	Date:	23.11.12	Title:	Schematic Model of Overburden Fracture Zones Above Longwall Panels
	Ditton Geotechnical			
	Services Pty Ltd		Scale: NTS	Figure No: A40a

Extent of major fractures from mining horizon towards surface (% h)

100% — At surface

80 —

60 —

B

A

40 —

20 —

0 — Mining horizon

0   10   20   30   40   50   60   70

+E

h

B

A

critical extraction

A: direct connection of cracks with extraction horizon
B: possible connection of cracks with extraction horizon

Predicted maximum tensile strain (+E), mm/m
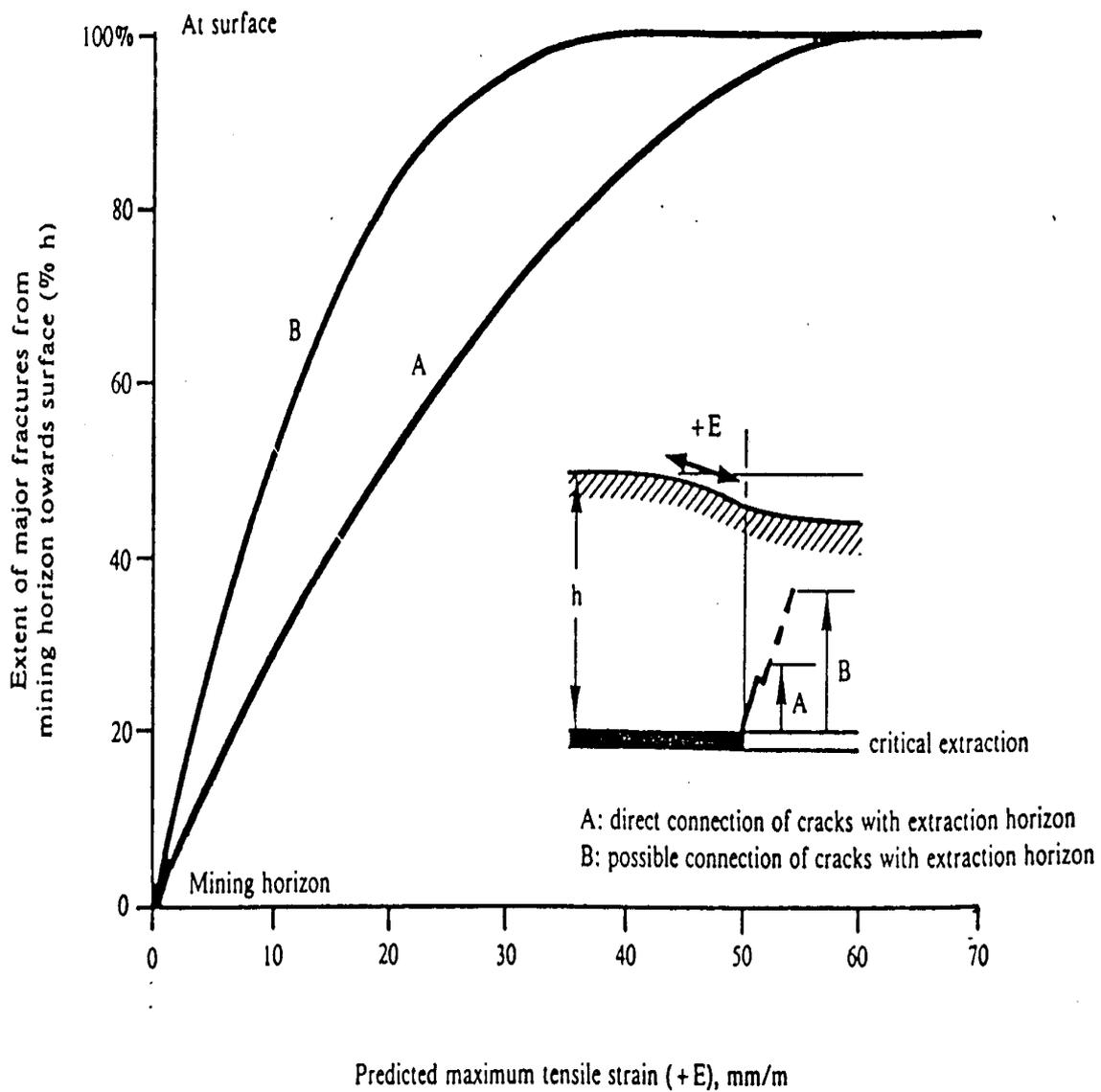
DgS	Engineer:	S.Ditton	Client:	Extract from ACARP, 2003		
	Drawn:	S.Ditton				
	Date:	30.04.07	Title:	Enpirically Based Sub-Surface Fracturing Model		
	Ditton Geotechnical			Presented in Whittaker & Reddish, 1989		
	Services Pty Ltd		Scale:	NTS	Figure No:	A40b

Rib Area | Goaf Area | Rib Area

ground surface

'D' Zone

Surface Zone

Variable - mostly not detected due to presence of weathered surface layer or alluvial deposits. Surface effects only noted in areas with small depth of cover

'C' Zone

Constrained Zone*

'B' Zone

Dilated with no vertical cracks
Thickness varies depending on depth of cover and/or spanning massive strata

Dilated with some vertical cracks

Interface possibly forms at plane of weakness (Vales Point Seam)

Fractured Zone

'A' Zone

21t -33t depends on depth of cover and geological factors

Caved Zone   **'A' Zone**

<10t (probably about 5t)

Extracted coal seam - thickness = t

Zones in the Overburden according to Forster (1995)

* - Constrained Zone generally means B-Zone, but may include C-Zone , depending on W/H ratio and geology

DgS	Engineer:	S.Ditton	Client:	Appendix A		
	Drawn:	S.Ditton				
	Date:	23.11.12	Title:	Schematic Model of Overburden Fracture Zones in **Forster, 1995** Model		
	Ditton Geotechnical			(based on Piezometric Data Above High Extraction Panels in the Newcastle Coalfield)		
	Services Pty Ltd		Scale:	NTS	Figure No:	A40c

Figure H (top diagram)

Average permeability $= \sqrt[3]{(K_x \times K_y \times K_z)}$ Change in permeability $(CP_{avg}) = \left(\dfrac{K_{avg}^{new}}{K_{avg}^{original}}\right)$

Surface zone   Vertical Strain = 0.08 % CP_{avg} = 5 - 30

Vertical strain = 0.11 % with minimal bed separation and fractures CP_{avg} = 3 - 5

Elastic zone with possible bed separations

Elastic strain limit in uniaxial compression <0.13 % ; it would be higher under triaxial stress state

75m

Transition

Vertical strain = 0.19 % possibly with some bed separations and minor fractures CP_{avg} = 5 - 10

Constrained zone with multiple bed separations

105m

Moderate aquifer interference (interference decreasing)
(Change in permeability decreasing)

Transition

Fracture zone 106 m CP_{avg} = 20 - 1000   Vertical strain > 0.98 %

Blue line indicates three separation zones within the fracture zone and black line indicates average deformation gradient

Extensive aquifer interference

Transition 24 m CP_{avg} = 1000 - 2000

Caving zone 9 m

(Vertical strain > 3 %)

Direction of permeability increase

Depth, m — 0, 50, 100, 150, 200, 250, 300, 350, 400

Vertical displacement, mm — 0, 500, 1000, 1500, 2000, 2500, 3000

Figure H. Hydrogeological response model for Springvale Colliery

Figure I (bottom diagram)

Surface zone   y = 95 - 105T   D <15 m deep

D - Zone   Increase of up to 10 times in vertical permeability

C - Zone   Increase of 3 to 5 times in average overall permeability   vertical strain = 1 -2mm/m

Elastic zone (≈20t-23t)

y = 75-78T

Transition zone

B - Zone   Increase of up to 2 times in vertical and 5 to 10 times in average overall permeability   vertical strain = 2 - 8 mm/m

Constrained zone (≈32t-35t)

Cover Depth H=350 m

y = 43T

Transition zone

Fracture zone (≈33t)

A - Zone   vertical strain > 10 mm/m   Connective Cracking   vertical strain > 30 mm/m

y = 10T

Transition zone (≈7t)

y = 3T

Caving zone (≈3t)

Increasing permeability

Permeability increasing

Increase of up to 50 times in vertical and 2000 times in average overall permeability (extensive aquifer interference) (≈43t)

y

Extraction height = t =3.25m

Roadway width = w   W=315 m

(≈8w)   Roadway induced damage zones

Not to scale

Figure I. A schematic representation of the hydrogeological response model of Springvale Colliery

ACARP Project C14033 Hydrogeological Response to Longwall Mining   xviii

DgS	Engineer:	S.Ditton	Client:	Appendix A
	Drawn:	S.Ditton		
	Date:	23.11.12	Title:	Schematic Model of Overburden Fracture Zones **in ACARP, 2007**
	Ditton Geotechnical Services Pty Ltd		Scale:		Figure No: A40d

Figure 6 is a conceptual model that illustrates the type of damage that can be expected within the overburden due to subsidence above a full-extraction panel. Five broad zones can be identified [Singh and Kendorski 1981; Peng and Chiang 1984; Kendorski 1993, 2006]:

1. The *complete caving zone*, in which the roof rock is completely disrupted as it falls into the gob, normally extends two to four times the extracted seam height (h).
2. The *partial caving zone,* in which the beds are completely fractured but never lose contact with one another, extends up to 6–10 h.
3. The *fracture zone,* within which the subsidence strains are great enough to cause new fracturing in the rock and create direct hydraulic connections to the lower seam. The top of this zone can be as high as 24 h above the lower seam.
4. The *dilated zone,* where the permeability is enhanced but little new fracturing is created, extends up to 60 h.
5. The *confined zone,* where subsidence normally causes no change in strata properties other than occasional bed slippage. This zone extends from the top of the dilated zone to about 50 ft below the surface.

6. D - Zone (<15 m)

5. C - Zone

4. B - Zone

3. A - Zone

1, 2. A - Zone
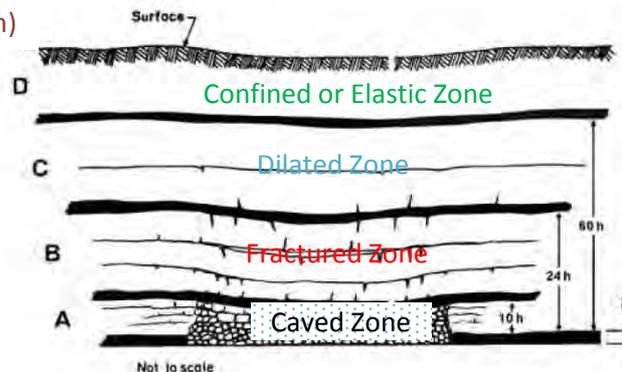
Figure 6.—Overburden response to full-extraction mining: (A) caving zones, (B) fracture zone, (C) dilated zone, and (D) confined zone.

The dimensions of these zones vary from panel to panel because of differences in geology and panel geometry. The implication of this model for multiple-seam mining is that when the interburden thickness exceeds approximately 6–10 times the lower seam thickness, the upper seam should be largely intact, although the roof may be fractured or otherwise damaged.

Note: Equivalent **ACARP, 2007** model zones A to D also shown down the left side.

DgS	Engineer:	S.Ditton	Client:	Appendix A	
	Drawn:	S.Ditton			
	Date:	03.06.13	Title:	Model of Overburden Fracture Zones above	
	Ditton Geotechnical			US Longwall Mines According to Mark, 2007	
	Services Pty Ltd		Scale:		Figure No:	A40e

Zone and Thickness Ranges
(based on Mining Height, T)

SURFACE DISTURBANCES
CLOSE OR FILL IN
2 YRS OR LESS

SURFACE
DISTURBANCE
15 m

SURFACE
WATER

GROUND SURFACE

SURFACE WATER
DRAINS INTO SURFACE
DISTURBANCE ZONE

WATER BELOW SURFACE
DISTURBANCE ZONE IS
UNAFFECTED

CONSTRAINED AND
UNAFFECTED ZONE
60T to H-15 m

WELL
TEMPORARILY
DRY

WELL

WELL

AQUIFER

DILATED ZONE
24 - 30T to 60T

TEMPORARILY
INTERMITTENT

WELL

WATER IN THIS ZONE
GOES INTO STORAGE
IN DILATED ROCK MASS

TEMPORARY DROP RECOVERS
AS STORAGE IS FILLED OR
DILATION CLOSES AS MINE
PASSES THROUGH AND BEYOND

AQUIFER

FRACTURED ZONE
6 - 10T to 24 -30T

WATER IN THIS ZONE
DRAINS TO THE MINE

CAVED ZONE
6 - 10T

WATER INTRUSION

CAVED ZONE

WHAT WE THINK MINERS AND
HYDROGEOLOGISTS BOTH SAW

- GROUNDWATER
FLOW PATH

DgS	Engineer:	S.Ditton	Client:	Appendix A
	Drawn:	S.Ditton		
	Date:	03.06.13	Title:	Model of Overburden Fracture Zones above
	Ditton Geotechnical			UK Longwall Mines According to Kendorski, 1993
	Services Pty Ltd		Scale:		Figure No:	A40f

Interpreted Beam Stress in Spanning Units of Physical Model of Laminated Overburden above a Longwall

DgS	Engineer:	S.Ditton
	Drawn:	S.Ditton
	Date:	07.06.13
Ditton Geotechnical Services Pty Ltd		

Client:	Review of Height of Fracturing Data
Title:	Interpreted Beam Stress in Spanning Units of Physical Model of Laminated Overburden above a Longwall
Scale:	NTS

Figure No: A40g

Note: Caving Angle , θ = 19.3°

Ref: Data from Whittaker & Reddish, 1989

Engineer:	S.Ditton	Client:	Review of Height of Fracturing Data		
Drawn:	S.Ditton				
Date:	07.06.13	Title:	Analytical v. Physical HoF Model Mimimum Beam Thickness Required to Span the Continuous Fracture Zone		
DgS Ditton Geotechnical Services Pty Ltd					
		Scale:	NTS	Figure No:	A40h

Figure showing Observed Fracture Heights (m) versus Panel width, W (m).

Plotted data points and annotations:

- W = panel width
- H = depth of cover
- MSEC (2006) Endeavour Drift BH3 W=250 H=505 post mining bore
- Holla & Buizen (1991) Tahmoor LW3 W=180 H=424 exto
- Kay (1990) Angus Place LW11 W=211 H=263 (fractures to surface)
- Holla (1986) Ellalong W=150 H=395 exto
- Holla & Buizen (1990) Invincible W=135 H=170 exto (fractures to surface)
- MSEC (2008) Metrop LW10 W=140 H=460 post mining bore & piezo
- Morton (1975/6) Kemira LW6 W=117.348 H=335 piezo
- Forster (1997) Cooranbong Nth B Panel W=105 H=75 piezo
- SE (2003) Southern QLD LW603 W=200 H=142
- SE (2003) Central QLD LW301 W=205 H=132
- Mills (2000) Sth Bulga LWE1 W=250 H=155 exto (fractures to surface)
- Holla & Buizen (1990) Wyee LW1 W=216 H=206 exto
- Forster (1995) Wyee Nth 3D Panel W=170 H=185 piezo
- SE (2003) Oaky Creek QLD LW1 W=205 H=95
- Forster (1996) Wyee LW4 W=245 H=207 piezo
- CSIRO (2007) Springvale SPR39 W=315 H=330 exto & piezo
- CSIRO (2007) Springvale SPR32 W=260 H=370 exto & piezo

Lines: 1.5 x W, MSEC model 1.374(W-20), 1 x W

Ref: MSEC, 2011

Engineer:	S.Ditton	Client:	Review of Height of Fracturing Data		
Drawn:	S.Ditton				
Date:	07.06.13	Title:	Observed Fracture Height Models presented by SCT and MSEC		
Ditton Geotechnical Services Pty Ltd					
		Scale:	NTS	Figure No:	A40i

DgS

Figure: Review of Observed Fracture Height Models presented by SCT and MSEC v. Whittaker & Reddish Sub-Surface Fracture Model Zoning

W = panel width
H = depth of cover

Chart axes: Observed Fracture Heights (m) [vertical, 0–400] vs Panel width, W (m) [horizontal, 0–400]

Lines: 1.5 x W; MSEC model 1.374(W-30); 1 x W

Data points and labels:

- MSEC (2006) Endeavour Drift BH3 W=250 H=505 post mining bore — B
- Holla & Buizen (1991) Tahmoor LW3 W=180 H=424 exto
- Kay (1990) Angus Place LW11 W=211 H=263 (fractures to surface) — B
- CSIRO (2007) Springvale SPR39 W=315 H=330 exto & piezo — B
- Holla (1986) Ellalong W=150 H=395 exto — B
- CSIRO (2007) Springvale SPR32 W=260 H=370 exto & piezo — B
- Holla & Buizen (1990) Invincible W=135 H=170 exto (fractures to surface) — B
- Mills (2000) Sth Bulga LWE1 W=250 H=155 exto (fractures to surface) — A
- Holla & Buizen (1990) Wyee LW1 W=216 H=206 exto — A
- MSEC (2008) Metrop LW10 W=140 H=460 post mining bore & piezo — A
- Forster (1995) Wyee Nth 3D Panel W=170 H=185 piezo — A
- Morton (1975/6) Kemira LW6 W=117.348 H=335 piezo — A
- SE (2003) Oaky Creek QLD LW1 W=205 H=95 — A
- Forster (1996) Wyee LW4 W=245 H=207 piezo — A
- Forster (1997) Cooranbong Nth B Panel W=105 H=75 piezo — A
- SE (2003) Southern QLD LW603 W=200 H=142 — X
- SE (2003) Central QLD LW301 W=205 H=132 — X

Key

A: A-Zone Horizon

B: B-Zone Horizon

X: In-conclusive data

Ref: MSEC, 2011

Engineer:	S.Ditton	Client:	Review of Height of Fracturing Data
Drawn:	S.Ditton		
Date:	07.06.13	Title:	Review of Observed Fracture Height Models presented by SCT and MSEC v. Whittaker & Reddish Sub-Surface Fracture Model Zoning
Ditton Geotechnical Services Pty Ltd			
		Scale:	NTS

DgS — Ditton Geotechnical Services Pty Ltd

Figure No: A40j

Continuous and Discontinuous Sub-Surface Fracture Height Model above Longwalls using Surface Tensile Strains as the Key Indicator

Engineer:	S.Ditton
Drawn:	S.Ditton
Date:	18.11.12
Ditton Geotechnical Services Pty Ltd	

Client: Updated Whittaker and Reddish Model presented in ACARP, 2003

Title: Continuous and Discontinuous Sub-Surface Fracture Height Model above Longwalls using Surface Tensile Strains as the Key Indicator

Scale: NTS

Figure No: A41a

DgS

Continuous and Discontinuous Sub-Surface Fracture Heights above Longwalls (based on ACARP, 2003)

Engineer:	S.Ditton	
Drawn:	S.Ditton	
Date:	03.12.12	

Ditton Geotechnical Services Pty Ltd

Client: Updated from ACARP, 2003

Title: Continuous and Discontinuous Sub-Surface Fracture Heights above Longwalls (based on ACARP, 2003)

Scale: NTS

Figure No: A41b

Notes:
1. UK Physical Model based on constant W and H (W/H = 1.34)
2. Real world data indicates increased fracture heights for a given mining geometry and likely to be due to influences of lithology and jointing (i.e. geology).
3. Vertical permeability within the A horizon likely to increase by 1 to 2 orders of magnitude with hydraulic connection to workings likely.

Legend:
- ○ Measured Field Data
- ○ Measured Field Data (High SRP Cases)
- —— Power (UK Physical Model)
- ◆ UK Physical Model
- —— Power (Measured Field Data)
- – – Power (Measured Field Data (Lower Bound))

UK Model Theta = $59.7905T^{-0.5297}$
$R^2 = 0.9897$

Mean thetaA = $41.617T^{-0.467}$

Lower Bound thetaA = $25.083T^{-0.401}$

W' = min (W, 1.4H)

X-axis: Extraction Height (m)
Y-axis: Effective Caving Angle to Maximum Height of Continuous Fracturing (o)

Engineer:	S.Ditton
Drawn:	S.Ditton
Date:	15.11.12

DgS

Ditton Geotechnical Services Pty Ltd

Client:	Modified from ACARP, 2003 (DgS,2012)
Title:	Alternative ACARP, 2003 A-Zone Sub-Surface Fracture Height Model based on Panel Width and Mining Height as Key Parameters
Scale:	NTS
Figure No:	A41c

Effective Caving Angle to Maximum Height of Discontinuous Fracturing (B) (o)

Legend: UK Physical Model · NSW B Data · Power (NSW B Data) · Power (B Zone (Lower Limit))

Notes:
1. UK Physical Model based on constant W and H (W/H = 1.34)
2. Real world data based on piezometer & extensometer measurements and indicates increased fracture heights for a given mining geometry. The variation in the data is likely to be due to influences of panel width, lithology and jointing (i.e. geology).
3. Minor leakage is possible from B into A Zones.

Discontinuous Fracture Zone Height, B = W'/(4tan(theta (B))

Continuous Fracture Zone Height, A = W'/(4tan(theta (A))

Mean Model Theta (B) = $35.8237T^{-0.3304}$
$R^2 = 0.9043$

Mean thetaB = $21.806T^{-0.233}$

Lower Bound thetaB = $17.295T^{-0.238}$

theta (A)   theta (B)

W' = min (W, 1.4H)

Extraction Height T (m)

Engineer:	S.Ditton	Client: Modified from ACARP, 2003 (DgS,2012)
Drawn:	S.Ditton	
Date:	15.11.12	Title: Alternative ACARP, 2003 B-Zone Sub-Surface Fracture Height Model based on Panel Width and Mining Height as Key Parameters
DgS Ditton Geotechnical Services Pty Ltd		
		Scale: NTS
		Figure No: A41d

Predicted Height of Continuous Fracturing Based on HoF Angle and Mining Height

Legend:
- Field data (Supercritical Panels; W/H>1.4)
- Field Data (Critical Panels; 0.7<W/H<1.4)
- Field Data (Sub-Critical Panels; W/H<0.7)
- UK Physical Model (W=137.6m)

Notes:

1. UK Physical Model based on constant W and H (W/H = 1.34) and scaled material properties.

2. Real world data indicates greater fracture heights for a given mining geometry and likely to be due to influences of lithology and jointing (i.e. geology).

3. Vertical permeability within the A-Zone likely to increase by 1 to 2 orders of magnitude with hydraulic connection to workings.

Continuous Fracture Zone Height A = W/4tan(theta (A))

UK Model Theta = $60T^{-0.5297}$
$R^2 = 0.9897$

Mean $\theta_A = 32.448T^{-0.241}$

mean - 5°
mean - 7°
mean - 10°

$y = 23.282x^{-0.409}$

Lower 95%CL supercritical $\theta_A = 27.643T^{-0.3}$
Lower 95%CL critical $\theta_A = 25.875T^{-0.336}$
Lower 95%CL sub-critical $\theta_A = 23.282T^{-0.409}$

Y-axis: Abutment Angle for Height of Continuous Fracturing (o)
X-axis: Extraction Height (m)

Engineer:	S.Ditton	Client:	Modified from ACARP, 2003
Drawn:	S.Ditton		
Date:	10.06.13	Title:	Predicted Height of Continuous Fracturing Based on HoF Angle and Mining Height
Ditton Geotechnical Services Pty Ltd			
		Scale:	NTS	Figure No:	A41e

DgS

UK Physical Model ■ **Field Data (Supercritical Panels)** ● **Field Data (Critical Panels)** ▲ **Field Data (Sub-critical Panels)**

Notes:
1. UK Physical Model based on constant W and H (W/H = 1.34)
2. Real world data based on piezometer & extensometer measurements and indicates increased
fracture heights for a given mining geometry. The variation in the data is likely to be due to influences of panel width,
lithology and jointing (i.e. geology).
3. Minor leakage is possible from lower B-Zone into the A Zone.

Discontinuous Fracture Zone Height, B = W'/(4tan(theta (B))

Mean UK Model Theta (B) = $35.8237T^{-0.3304}$
$R^2 = 0.9043$

theta (A)   theta (B)

W' = min (W, 1.4H)

Mean Super-critical Theta B = $31.5T^{-0.373}$
Mean Critical/Sub-critical Theta B = $25.427T^{-0.373}$
(and Lower 95%CL Supercritical)

Lower 95%CL Critical/Subcritical Theta B = $20.172T^{-0.658}$

Effective Caving Angle to Maximum Height of Discontinuous Fracturing (B) (o)

Extraction Height T (m)

Engineer:	S.Ditton	Client:	Modified from ACARP, 2003		
Drawn:	S.Ditton				
Date:	10.06.13	Title:	Predicted Height of Discontinuous Fracturing Based on Measured Heights of Discontinuous Fracture Angles and Mining Height		
Ditton Geotechnical					
Services Pty Ltd		Scale:	NTS	Figure No:	A41f

DgS
Ditton Geotechnical Services Pty Ltd

Legend:
- ◆ Predicted UK (Kendorski, 1993)
- ◆ UK Physical Model, 1989
- ■ Measured Australian Data (Sub-critical Cases)
- ● Measured Australian Data (Critical Panel Cases)
- ▲ Measured Australian Data (Supercritical Cases)
- – – Forster,1995 (21T)
- – · – Forster, 1995 (33T)
- —— Power (Predicted UK (Kendorski, 1993))
- – – Power (UK Model Regression)

Data base Summary:

T - 1.9 m to 6.0 m
H - 75 m to 500 m
W - 110 m to 355 m
W/H - 0.30 to 2.22

$A = 56T^{0.5}$

$A = 27T^{0.59}$

Note: UK Physical Model based on W/H = 1.31

A-Zone Height (m)

Mining Height, T(m)

Engineer:	S.Ditton	Client:	Review of Height of Fracturing Data	
Drawn:	S.Ditton			
Date:	07.06.13	Title:	Continuous UK Fracture Height Models based on Mining Height Only v. Measured Australian Database	
		Scale:	NTS	Figure No: A41g

DgS

Ditton Geotechnical
Services Pty Ltd

Figure: Continuous Australian Fracture Height Model based on Panel Width Only Database

Legend: A-Zone Horizon Data, B-Zone Horizon Data, SCT (HoF=W), SCT (HoF=1.5W), MSEC (HoF=1.374(W-30)), Surface

Data base Summary:

T - 1.9 m to 6.0 m
H - 75 m to 500 m
W - 110 m to 355 m
W/H - 0.30 to 2.22

Maximimum A = 145 m (South Bulga)
Minimum A = 40 m (Wyee North)

Y-axis: A or B Height of Fracturing (m)
X-axis: W

Engineer:	S.Ditton	Client:	Review of Height of Fracturing Data		
Drawn:	S.Ditton				
Date:	07.06.13	Title:	Continuous Australian Fracture Height Model based on Panel Width Only		
Ditton Geotechnical Services Pty Ltd			Database		
		Scale:	NTS	Figure No:	A41h

DgS

Figure: Continuous Australian Fracture Height Model based on A normalised to Panel Width with Influence of Mining Height Included

Legend:
- ◆ All Data (T = 1.7 m to 6.0m)
- ■ UK Physical Model (T = 1.2 m to 6.0 m)
- ○ Outliers
- — Power (All Data (T = 1.7 m to 6.0m))

Y-axis: A/W (0.0 to 1.4)
X-axis: W/H (0.0 to 3.0)

Data labels (All Data): T=3.4, T=1.7, T=6.0, T=2.5, T=2.3, T=2.7, T=3.4, T=2.7, T=2.5, T=3.5, T=2.5, T=3.3, T=3.4, T=3.5, T=1.9, T=2.7, T=2.6m, T=2.6, T=3.8, T=3.8, T=3.2, T=3.8, T=2.8, T=3.3, T=1.9, T=1.9, 0.35

Outlier: T=3.7 ○ Angus Place LW7

UK Physical Model: T=6.0m, T=4.2m, T=2.4m, T=1.2m

Data base Summary
T : 1.9 m to 6.0 m
H : 75 m to 500 m
W : 110 m to 355 m
W/H : 0.30 to 2.22
A/W : 0.27 - 0.93

$A/W = 0.4815(W/H)^{-0.364}$
$R^2 = 0.606$

DgS	Engineer:	S.Ditton
	Drawn:	S.Ditton
	Date:	07.06.13
Ditton Geotechnical Services Pty Ltd		

Client:	Review of Height of Fracturing Data
Title:	Continuous Australian Fracture Height Model based on A normalised to Panel Width with Influence of Mining Height Included
Scale:	NTS

Figure No: A41i

Figure A41j — Continuous Australian Fracture Height Model based on A normalised to Panel Width v. Mining Height

Legend:
- Subcritical Panels
- Critical Panels
- Supercritical Panels
- UK Physical Model (Supercritical)
- Power (Subcritical Panels)
- Power (Critical Panels)
- Power (Supercritical Panels)
- Power (UK Physical Model (Supercritical))

$A/W = 0.58T^{0.16}$
$R^2 = 0.05$

$A/W = 0.23T^{0.74}$
$R^2 = 0.39$

$A/W = 0.13T^{0.90}$
$R^2 = 0.30$

$A/W = 0.15T^{0.80}$
$R^2 = 1.00$

Data base Summary:

T - 1.9 m to 6.0 m
H - 75 m to 500 m
W - 110 m to 355 m
W/H - 0.30 to 2.22

Axis labels:
- Y-axis: A/W
- X-axis: Mining Height T (m)

DgS	Engineer:	S.Ditton	Client:	Review of Height of Fracturing Data
	Drawn:	S.Ditton		
Ditton Geotechnical Services Pty Ltd	Date:	07.06.13	Title:	Continuous Australian Fracture Height Model based on A normalised to Panel Width v. Mining Height
	Scale:	NTS		Figure No: A41j

Key:

= Continuous fractures

Δ = strata deflects (and cracks) as goaf compresses under load γH' where H' = W'/4tanθ to H

Cover Depth, H

Maximum Goaf Load Height H' = H to W'/4tanθ

Zone B

Zone A

t2

Sagging beam of thickness, t2 limits Zone A

Fractured beam of thickness, t1 cracked through

Stable Natural Arch thrust line

Zone A

t1

Δ

Goaf

4-6T
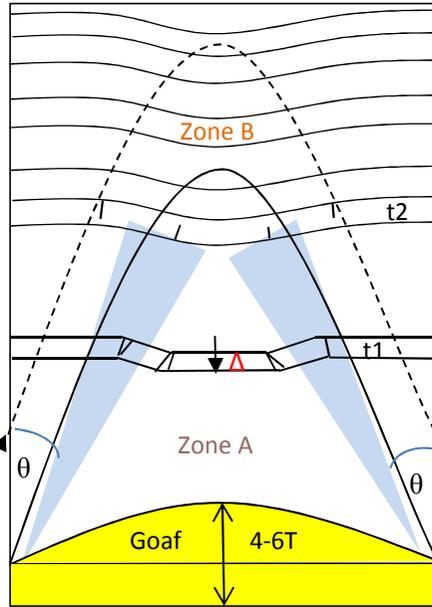
Mining Height, T

Sub-critical Panel Width, W
(W/H <0.7)

Fractured beam of thickness, t3 limits Zone A

Zone B

Zone A   Zone A

t3

Δ   Δ

Maximum Goaf Load Height, H' = H

Goaf

4-6T

Stable Natural Arch can't form

θ   θ   θ
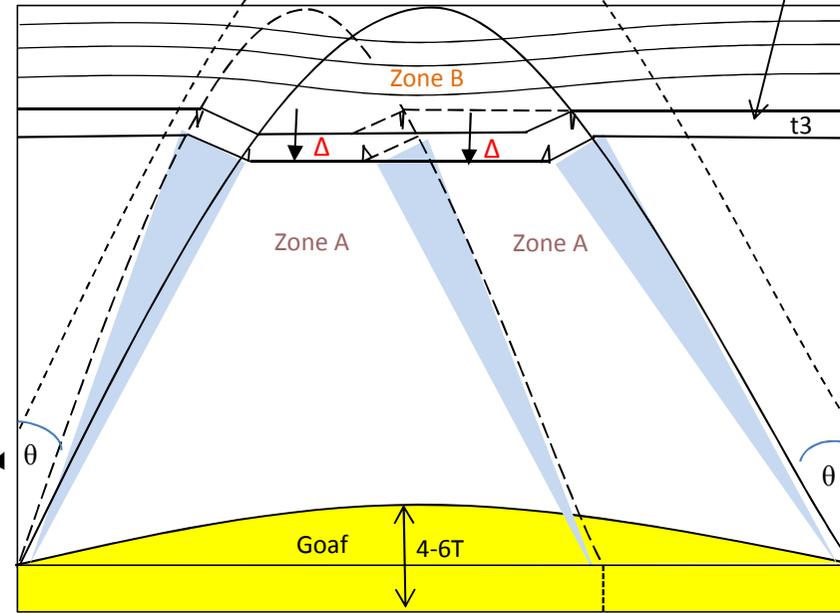
Super-critical Panel Width, W'=1.4H

Super-critical Panel Width, W
(W/H > 1.4)

Engineer:	S.Ditton	Client:	Review of Height of Fracturing Data		
Drawn:	S.Ditton				
Date:	26.08.13	Title:	Conceptual Model for Development of Height of Continuous Fracturing Zone for a range of Longwall Panel Geometries		
DgS Ditton Geotechnical Services Pty Ltd					
		Scale:	NTS	Figure No:	A42a

Mine Geometry Only PI-Term Model

PI-Term Equation of best-fit (mean):

$A/W' = 2.215(H/W')^{0.271}(T/W')^{0.372}$ ($R^2 = 0.61$ & rsme=0.12W' (21%))

and by re-arrangement:

$\underline{A = 2.215W'^{0.357}H^{0.271}T^{0.372}}$

Measured A/W' (y-axis)

Predicted A/W' (x-axis)

DgS	Engineer:	S.Ditton	Client:	Review of Height of Fracturing Data		
	Drawn:	S.Ditton				
	Date:	01.05.14	Title:	Results of Non-Linear Regession Analysis: Predicted v. Measured Value Analysis		
	Ditton Geotechnical			for Height of A-Zone Fracturing for the Geometry PI-Term Model		
	Services Pty Ltd		Scale:	NTS	Figure No:	A42b

Note: Surface to seam connection cases labelled

Legend: Predicted Geometry PI-Term (mean +/- 90%CI) ● Measured A △ Cover Depth ── Power (Predicted Geometry PI-Term (mean +/- 90%CI)) - - - -

Y-axis: Height of Continuous Sub-surface Fracturing, A (m)

X-axis: Panel W/H

Labels on chart: Invincible, South Bulga, Homestead

Engineer:	S.Ditton	Client:	Review of Height of Fracturing Data		
Drawn:	S.Ditton				
Date:	01.05.14	Title:	Results of Non-Linear Regession Error analysis for Geometry PI-Terms Only Height of		
Ditton Geotechnical			A-Zone Prediction Model (Geology Pi-Term Not Included)		
Services Pty Ltd		Scale:	NTS	Figure No:	A42c

DgS

Histograms

Cumulative distributions

Legend: Regression Errors — Normal(-0.002,0.114)
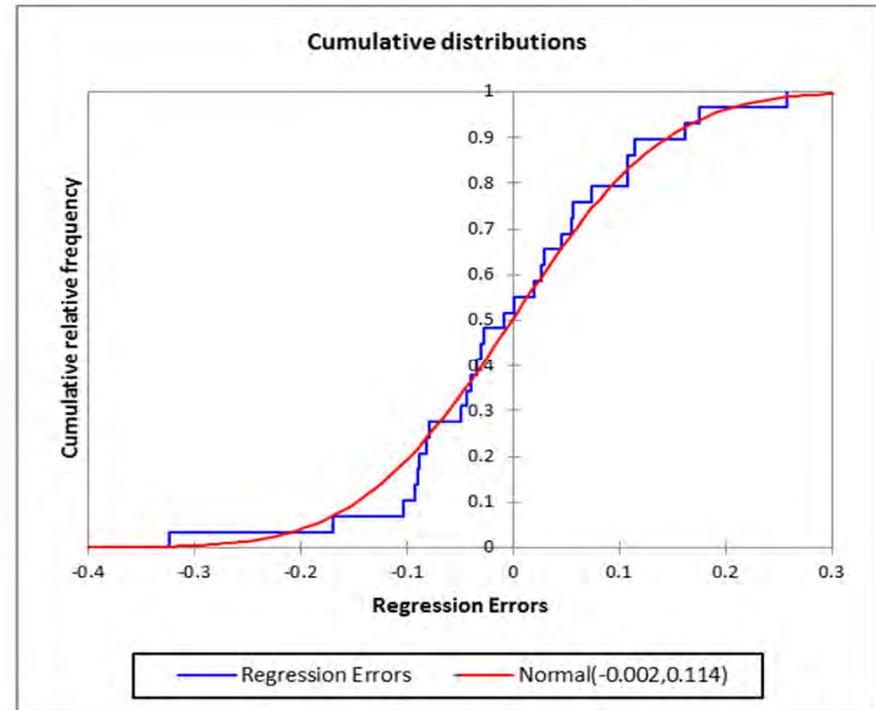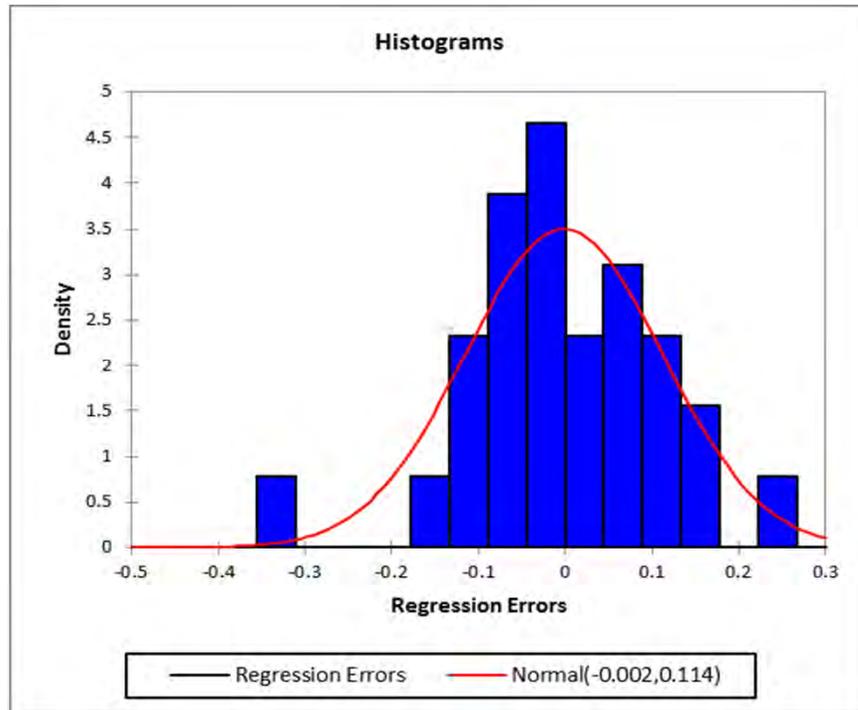
Kolmogorov-Smirnov test:

D	0.117
p-value	0.798
alpha	0.05

Test interpretation:
H0: The sample follows a Normal distribution
Ha: The sample does not follow a Normal distribution
As the computed p-value is greater than the significance level alpha=0.05, one cannot reject the null hypothesis H0.
The risk to reject the null hypothesis H0 while it is true is 79.75%.

DgS	Engineer:	S.Ditton	Client:	Review of Height of Fracturing Data
	Drawn:	S.Ditton		
	Date:	01.05.14	Title:	Results of Non-Linear Regession Error analysis for Geometry Pi-Term Height of A-Zone
	Ditton Geotechnical			Prediction Model: Regression Error Normal Distribution Test
	Services Pty Ltd		Scale:	NTS

Figure No: A42d

Results of Back-analysis of Effective Strata Units required to Match the Observed A-Zone Heights above Longwall Panel Goafs using the Geology Pi-Term Model

Minimum Effective beam Thickness Required to Span the A-Zone, based on Back Analysis Results for the Geology Pi-Term Model (see Figure A42e)

Comparison of Back-Analysed (or measured (t') v. Predicted t' for the Geological PI-Term

$y = 1.2298x - 2.4954$
$R^2 = 0.8623$

Legend: Data (no outliers); Data (Outliers); Linear (Data (no outliers))

X-axis: Back Analysed (or Measured) t' (m)
Y-axis: Predicted t' (m)

Austar
Wyee TE Panel

Engineer:	S.Ditton	Client:	Review of Height of Fracturing Data		
Drawn:	S.Ditton				
Date:	01.05.14	Title:	Comparison of Back-Analysed (or measured (t') v. Predicted t' for the Geological PI-Term		
Ditton Geotechnical Services Pty Ltd					
		Scale:	NTS	Figure No:	A42g

DgS

Pi-term Equation:

$A/W' = 1.53(H/W')^{0.535}(T/W')^{0.464}(t'/W')^{-0.4}$ ($R^2 = 0.8$ & rmse = 0.09W' (15%))

and by re-arrangement:

$\underline{A = 1.52W'^{0.4}H^{0.535}T^{0.464}t'^{-0.4}}$

Legend:
- Best Fit Effective t'
- Predicted t'

Axis labels: Measured A/W' (y-axis), Predicted (A/W') (x-axis)

DgS	Engineer:	S.Ditton	Client:	Review of Height of Fracturing Data		
	Drawn:	S.Ditton				
	Date:	01.05.14	Title:	Results of Non-Linear Regession Analysis: Predicted v. Measured Value Analysis		
Ditton Geotechnical				for Height of A-Zone Fracturing for Geology Pi-Term Model		
Services Pty Ltd			Scale:	NTS	Figure No:	A42h

Results of Non-Linear Regession Error analysis for Height of A-Zone Prediction Model with Geology Included

	Engineer:	S.Ditton	Client:	Review of Height of Fracturing Data		
DgS	Drawn:	S.Ditton				
	Date:	01.05.14	Title:	Results of Non-Linear Regession Error analysis for Height of A-Zone Prediction		
Ditton Geotechnical				Model with Geology Included		
Services Pty Ltd	Scale:	NTS			Figure No:	A42i

Histograms

Cumulative distributions

Legend: ── Var1 ── Normal(0.008,0.080)

Legend: ── Var1 ── Normal(0.008,0.080)
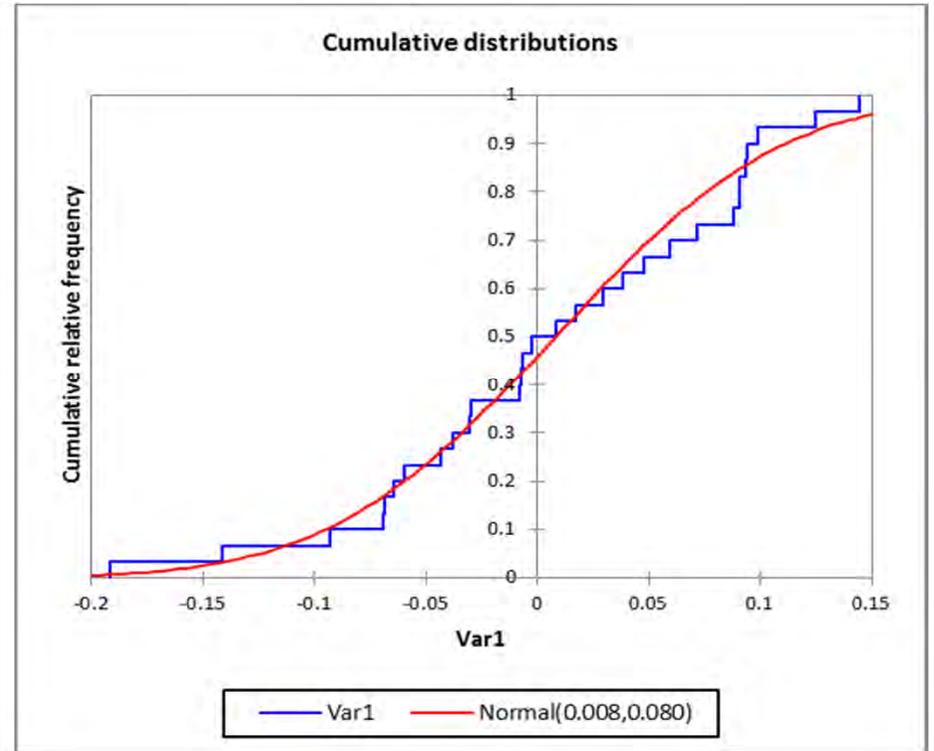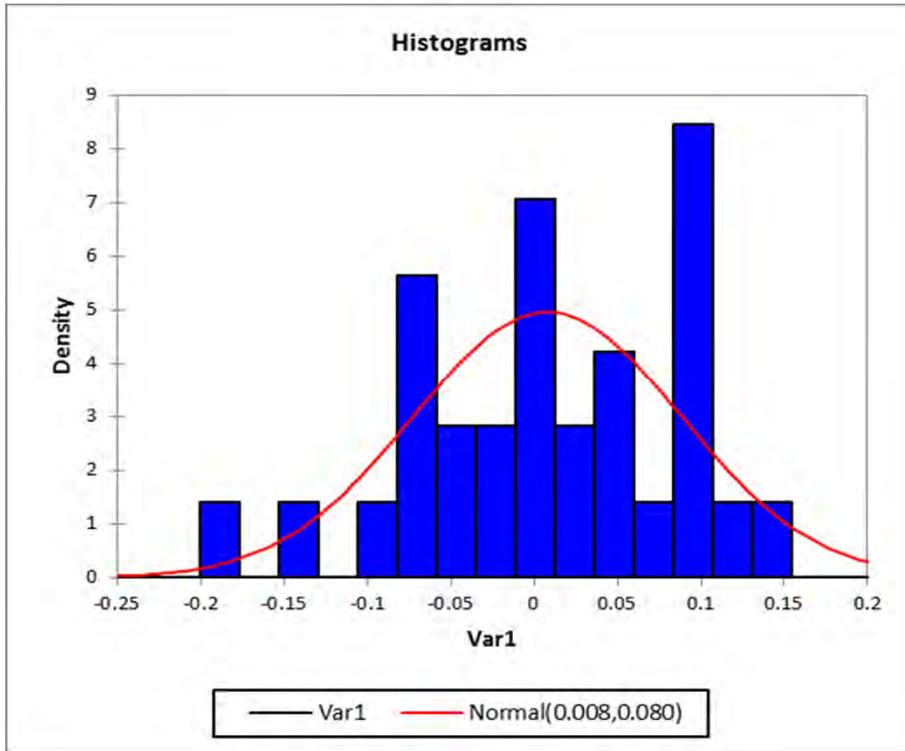
Kolmogorov-Smirnov test:

D	0.107
p-value	0.866
alpha	0.05

Test interpretation:
H0: The sample follows a Normal distribution
Ha: The sample does not follow a Normal distribution
As the computed p-value is greater than the significance level alpha=0.05, one cannot reject the null hypothesis H0.
The risk to reject the null hypothesis H0 while it is true is 86.6%.

DgS	Engineer:	S.Ditton	Client:	Review of Height of Fracturing Data
	Drawn:	S.Ditton		
	Date:	01.05.14	Title:	Results of Non-Linear Regession Error analysis for Geology Pi-Term Height of A-Zone
	Ditton Geotechnical			Prediction Model: Regression Error Normal Distribution Test
	Services Pty Ltd		Scale:	NTS Figure No: A42j

Geometry Model

PI-Term Equation for Height of Strata Dilation:

$B/W' = 1.621(H'/W)^{0.55}(T/W')^{0.175}$ ($R^2 = 0.86$ and rmse = 0.12W' (13%))

By re-arrangement:

$B=1.621W^{0.275}H^{0.55}T^{0.175}$

Measured B/W' (y-axis): 0.4, 0.6, 0.8, 1, 1.2, 1.4, 1.6, 1.8

Predicted B/W' (x-axis): 0.4, 0.6, 0.8, 1, 1.2, 1.4, 1.6, 1.8

Engineer:	S.Ditton	Client:	Review of Height of Fracturing Data
Drawn:	S.Ditton		
Date:	01.02.14	Title:	Results of Non-Linear Regession Error analysis for Height of B-Zone Predictions
DgS Ditton Geotechnical Services Pty Ltd			for Geometry Only Pi-Term Model
		Scale:	NTS
		Figure No:	A42k

Engineer:	S.Ditton	Client:	Review of Height of Fracturing Data		
Drawn:	S.Ditton				
Date:	01.02.14	Title:	Results of Non-Linear Regession Error analysis for Height of B-Zone Predictions		
Ditton Geotechnical Services Pty Ltd			for Geometry Only Pi-Term Model		
		Scale:	NTS	Figure No:	A42I

DgS

Kolmogorov-Smirnov test:

D	0.173
p-value	0.487
alpha	0.05

Test interpretation:

H0: The sample follows a Normal distribution
Ha: The sample does not follow a Normal distribution
As the computed p-value is greater than the significance level alpha=0.05, one cannot reject the null hypothesis H0.
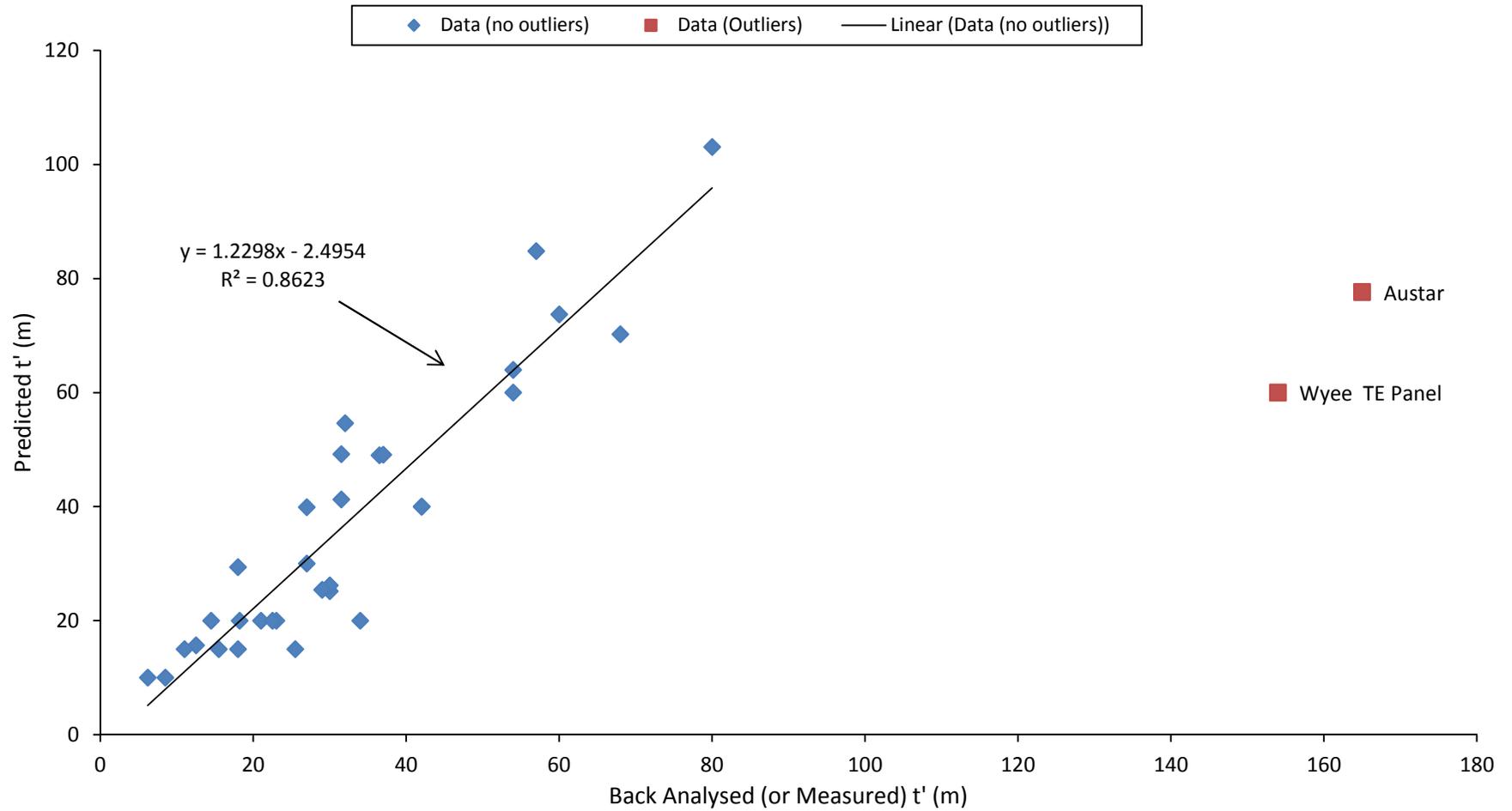The risk to reject the null hypothesis H0 while it is true is 48.70%.

DgS	Engineer:	S.Ditton	Client:	Review of Height of Fracturing Data
	Drawn:	S.Ditton		
	Date:	01.02.14	Title:	Results of Non-Linear Regession Error analysis for Height of B-Zone Predictions
Ditton Geotechnical				for Geometry Only Pi-Term Model
Services Pty Ltd	Scale:	NTS		Figure No: A42m

PI-Term Equation for Height of Strata Dilation:

$B/W' = 1.873(H/W')^{0.635}(T/W')^{0.257}(t'/W')^{-0.097}$ ($R^2 = 0.86$ and rmse = 0.12W' (14%))

By arrangement for B:

$B = 1.873W^{0.205}H^{0.635}T^{0.257}t'^{-0.097}$

Axis labels:
- Y-axis: Measured B/W'
- X-axis: Predicted B/W'

Engineer:	S.Ditton	Client: Review of Height of Fracturing Data
Drawn:	S.Ditton	
Date:	01.02.14	Title: Results of Non-Linear Regession Error analysis for Height of B-Zone Predictions for Geology Pi-Term Model
Dirton Geotechnical Services Pty Ltd		
Scale:	NTS	Figure No: A42n

DgS

Engineer:	S.Ditton	Client: Review of Height of Fracturing Data
Drawn:	S.Ditton	
Date:	01.02.14	Title: Results of Non-Linear Regession Error analysis for Height of B-Zone Predictions
Ditton Geotechnical		for Geology Pi-Term Model
Services Pty Ltd		Scale: NTS	Figure No: A42o

DgS
Ditton Geotechnical
Services Pty Ltd

Histograms — Density vs Var1, with legend: Var1, Normal(0.001,0.106)

Cumulative distributions — Cumulative relative frequency vs Var1, with legend: Var1, Normal(0.001,0.106)

Kolmogorov-Smirnov test:

D	0.126
p-value	0.849
alpha	0.05

Test interpretation:

H0: The sample follows a Normal distribution

Ha: The sample does not follow a Normal distribution

As the computed p-value is greater than the significance level alpha=0.05, one cannot reject the null hypothesis H0.

The risk to reject the null hypothesis H0 while it is true is 84.89%.

DgS	Engineer:	S.Ditton	Client:	Review of Height of Fracturing Data		
	Drawn:	S.Ditton				
	Date:	01.02.14	Title:	Results of Non-Linear Regession Error analysis for Height of B-Zone Predictions		
Ditton Geotechnical				for Geology Pi-Term Model		
Services Pty Ltd	Scale:	NTS			Figure No:	A42p

Legend: ◆ Panel Width ○ Effective Panel Width

W range: 110 m - 355 m (median = 179 m)

Y-axis: **W** (0 to 400)

X-axis: **W/H** (0.0 to 3.0)

Engineer:	S.Ditton
Drawn:	S.Ditton
Date:	03.12.12
Ditton Geotechnical Services Pty Ltd	

Client:	Modified from ACARP, 2003
Title:	Panel Width v. W/H Database for Sub-surface Fracturing Model
Scale:	NTS
Figure No:	A43a

DgS

H range: 75 m - 500 m (median = 213 m)

Engineer:	S.Ditton	Client: Modified from ACARP, 2003
Drawn:	S.Ditton	
Date:	03.12.12	Title: Cover Depth v. W/H Database for Sub-surface Fracturing Model
Ditton Geotechnical Services Pty Ltd		Scale: NTS	Figure No: A43b

DgS

T range: 1.9 m - 6.0 m (median = 2.8 m)

Engineer:	S.Ditton	Client:	Modified from ACARP, 2003		
Drawn:	S.Ditton				
Date:	03.12.12	Title:	Mining Height v. W/H Database for Sub-surface Fracturing Model		
Ditton Geotechnical Services Pty Ltd		Scale:	NTS	Figure No:	A43c

DgS

Figure A43d — Heights of Continuous Fracturing Predictions for the Geometry and Geology Pi-Term Models

Legend:
- ● Predicted A (mean +/- 95%CLs)
- ◇ Predicted Geometry Model (mean)
- △ Measured A
- ✕ Predicted Geometry Model (U95%CL)
- —— Surface
- ----- Power (Predicted A (mean +/- 95%CLs))

Y-axis: Height of Continuous Fracturing, A (m)
X-axis: W/H

Engineer:	S.Ditton	Client:	Review of Height of Fracturing Data
Drawn:	S.Ditton		
Date:	01.05.14	Title:	Heights of Continuous Fracturing Predictions for the Geometry and Geology Pi-Term Models
Ditton Geotechnical Services Pty Ltd			
		Scale:	NTS
		Figure No:	A43d

DgS

Chart axes:
- Y-axis: Changes to Continuous Height of Fracturing, ΔA (m), ranging 0 to 20
- X-axis: Input Parameter (m), ranging 50 to 500

Legend:
- dA/dW' — Ditton (Geometry only model)
- dA/dH — Ditton (Geometry only model)

Engineer:	S.Ditton	Client: Modified from ACARP, 2003
Drawn:	S.Ditton	
Date:	25.05.14	Title: Sensitivity Analysis of Geometry Only Pi-Term Model Input Parameters on Predicted Height of Continuous Fracturing: W' and H (as per Merrick, 2014)
Ditton Geotechnical Services Pty Ltd		Scale: NTS Figure No: A43e

DgS

Y-axis: Change to Height of Continuous Fracturing ΔA (m)

X-axis: Input Parameter (m)

Legend:
- dA/dT Ditton (Geology model)
- dA/dT Ditton (Geometry only model)

Engineer:	S.Ditton	Client:	Modified from ACARP, 2003		
Drawn:	S.Ditton				
Date:	25.05.14	Title:	Sensitivity Analysis of Geology & Geometry Pi-Term Model Input Parameters on Predicted Height of Continuous Fracturing: T (as per Merrick, 2014)		
Ditton Geotechnical Services Pty Ltd					
		Scale:	NTS	Figure No:	A43f

DgS

Ditton Geotechnical Services Pty Ltd

DgS	Engineer:	S.Ditton	Client: Modified from ACARP, 2003
	Drawn:	S.Ditton	
	Date:	25.05.14	Title: Sensitivity Analysis of Geology Pi-Term Model Input Parameters on Predicted Height of Continuous Fracturing: W' and H (as per Merrick, 2014)
	Ditton Geotechnical		
	Services Pty Ltd		Scale: NTS Figure No: A43g

Chart axes — Y-axis: Change in Continuous fracture height, ΔA (m); X-axis: Input Parameter (m)

Legend:
- dA/dW' Ditton (Geology model)
- dA/dH Ditton (Geology model)

Changes to Continuous Fracture Height ΔA (m)

Changes to Input Parameters (m)

DgS	Engineer:	S.Ditton	Client:	Modified from ACARP, 2003		
	Drawn:	S.Ditton				
	Date:	25.05.14	Title:	Sensitivity Analysis of Geology Pi-Term Model Input Parameters on Predicted Height of Continuous Fracturing: t' (as per Merrick, 2014)		
	Ditton Geotechnical Services Pty Ltd					
			Scale:	NTS	Figure No:	A43h

Legend:
- Cover Depth
- Surface Cracking Zone (Surface - 12m)
- Pi-Term Geology Model (mean)
- Pi-Term Geology Model (U95%CL)
- Pi-Term Geometry Model (mean)
- Pi-Term Geometry Model (U95%CL)
- Measured A Value
- Modified Theta Model (mean)
- Modified Theta Model (U95%CL)
- Tammetta, 2013 Model (mean)
- Tammetta, 2013 (U95%CL)
- SCT, 2008 (A=W)
- ACARP, 2007 (A=43T)
- Analytical Model
- Forster, 1995 (A=33T)

Case Study : Metropolitan LW10
Panel Type: Sub-Critical
W/H = 0.30
Cover Depth, H = 460 m
Panel Width, W = 140 m
Mining Height, T = 3.4 m
Effective Strata Unit thickness, t' = 31.5m
UCS = 70 MPa
E/UCS = 273

Y-axis: Height above Mine Workings, y (m)
X-axis: Panel Width, W (m)

Engineer:	S.Ditton	Client:	Modified from ACARP, 2003		
Drawn:	S.Ditton				
Date:	16.03.14	Title:	Predicted A-Zone Fracture Heights for Varying Panel Widths using Pi-Term Geometry and Geology Models and Current State of the Art Models		
Ditton Geotechnical Services Pty Ltd					
		Scale:	NTS	Figure No:	A43i

DgS
Ditton Geotechnical Services Pty Ltd

Legend:
- Cover Depth
- Surface Cracking Zone (Surface - 12 m)
- Pi-Term Geology Model (mean)
- Pi-Term Geology Model (U95%CL)
- Pi-Term Geometry Model (mean)
- Pi-Term Geometry Model (U95%CL)
- Measured A Value
- Modified Theta Model (mean)
- Modified Theta Model (U95%CL)
- Tammetta, 2013 Model (mean)
- Tammetta, 2013 (U95%CL)
- SCT, 2008 (A=W)
- Forster, 1995 (A=33T)
- Analytical Model
- Forster, 195 (A=21T)

Case Study : Mandalong LW5
Panel Type: Critical
Cover Depth, H = 179 m
Panel Width, W = 160 m
Mining Height, T = 3.7 m
Effective strata unit thickness, t' = 14.5 m
UCS = 67 MPa
E/UCS = 147

Height above Mine Workings, y (m) — vertical axis
Panel Width, W (m) — horizontal axis

Engineer:	S.Ditton	Client:	Modified from ACARP, 2003
Drawn:	S.Ditton		
Date:	16.03.14	Title:	Predicted A-Zone Fracture Heights for Varying Panel Widths using Pi-Term Geometry and Geology Models and Current State of the Art Models
Ditton Geotechnical Services Pty Ltd			
		Scale:	NTS	Figure No: A43j

DgS

Legend:
- Cover Depth
- Surface Cracking Zone (Surface - 12 m)
- Pi-Term Geology Model (mean)
- Pi-Term Geology Model (U95%CL)
- Pi-Term Geometry Model (mean)
- Measured A Value
- Pi-Term Geometry Model (U95%CL)
- Modified Theta Model (mean)
- Modified Theta Model (U95%CL)
- Tammetta, 2013 Model (mean)
- Tammetta,2013 (U95%CL)
- SCT,2008 (A=W)

Case Study: West Wallsend LW40
Panel Type: Supercritical
Cover Depth, H = 113 m
Panel Width, W = 178.6 m
W/H = 1.58
Mining Height, T = 3.8 m
Effective strata unit thickness, t' = 20 m
UCS = 25 MPa
E/UCS = 192

Y-axis: Height above Mine Workings, y (m)
X-axis: Panel Width, W (m)

Engineer:	S.Ditton	Client:	Modified from ACARP, 2003
Drawn:	S.Ditton		
Date:	16.03.14	Title:	Predicted A-Zone Fracture Heights for Varying Panel Widths using Pi-Term
Ditton Geotechnical			Geometry and Geology Models and Current State of the Art Models
Services Pty Ltd		Scale:	NTS	Figure No:	A43k

DgS

Legend:
- Cover Depth
- Surface Cracking Zone (Surface - 12 m)
- Pi-Term Geology Model (mean)
- Pi-Term Geology Model (U95%CL)
- Pi-Term Geometry Model (mean)
- Measured A Value
- Pi-Term Geometry Model (U95%CL)
- Modified Theta Model (mean)
- Modified Theta Model (U95%CL)
- Tammetta, 2013 Model (mean)
- Tammetta,2013 (U95%CL)
- SCT,2008 (A=W)

Case Study: West Wallsend LW41
Panel Type: Supercritical
Cover Depth, H = 97 m
Panel Width, W = 178.6 m
W/H = 1.84
Mining Height, T = 3.8 m
Effective strata unit thickness, t' = 22.5 m
UCS = 25 MPa
E/UCS = 150

Y-axis: Height above Mine Workings, y (m)
X-axis: Panel Width, W (m)

Engineer:	S.Ditton	Client:	Modified from ACARP, 2003
Drawn:	S.Ditton		
Date:	16.03.14	Title:	Predicted A-Zone Fracture Heights for Varying Panel Widths using Pi-Term Geometry and Geology Models and Current State of the Art Models
	Ditton Geotechnical Services Pty Ltd		
		Scale:	NTS	Figure No:	A43l

DgS
Ditton Geotechnical Services Pty Ltd

Note:
$\theta = 12°$ for W/H<0.45
$\theta = 9.63+4.42(W/H)+1.8(W/H)^2$ for 0.45<W/H<1.4
$\theta = 19.3°$ for W/H>1.4

$H' = W'/4\tan(\theta)$

South Bulga (LWE1) ?

Invincible (LW1)

Homestead (LW9)

Geology limits surface to seam connectivity for these cases

Legend: ◆ Measured A (All Coalfields) — Maximum Goaf Loading Height

X-axis: Panel Width/Cover Depth (W/H)
Y-axis: Distance Above Mine/Cover Depth (y/H)

Engineer:	S.Ditton	Client:	Review of Height of Fracturing Data		
Drawn:	S.Ditton				
Date:	01.05.14	Title:	Measured Heights of Continuous Fracturing in NSW and QLD Coalfields with Reported		
Ditton Geotechnical			Surface to Seam Connectivity Cases and Theoretical Goaf Loading Height		
Services Pty Ltd		Scale:	NTS	Figure No:	A43m

DgS
Ditton Geotechnical Services Pty Ltd

EXTENSION SIDE
OF BEAM

NEUTRAL AXIS

d_n

COMPRESSION SIDE
OF BEAM

Origin
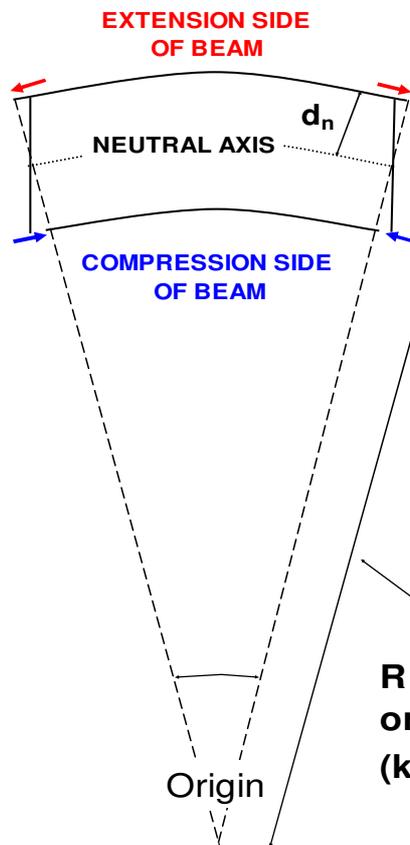
Strain E = (mm/m)
Curvature C = km^{-1}

$$E = C \times d_n$$

= Depth of Cracking

**R = Radius of curvature
or the curvature, C = 1/R
(km^{-1})**

Steep Slopes: 18° - 45°

Moderate Slopes: 8° - 18°

Mild Slopes: <8°

U95%CL E_{max} = 4 Mean C_{max}

K=30 (steep slopes)

K=20 (steep slopes)

K=15 (moderate slopes)

K=10 (mild slopes)

Mean E_{max} = 7.565C_{max}
R^2 = 0.6798

Note: Data includes all terrain types from gentle to steep slopes

Horizontal Strain (mm/m)

Curvature (km-1)

Legend: Tensile Data   Compressive Data   All Data   Series7   Linear (Compressive Data)   Linear (All Data)

Engineer:	S.Ditton	Client:	Extract from ACARP, 2003		
Drawn:	S.Ditton				
Date:	08.08.08	Title:	Empirical Model for Maximum Panel Strain Prediction Above Longwall Panels		
			for Smooth and Cracked Profiles in the Newcastle Coalfield		
		Scale:	NTS	Figure No:	A43o

DgS

Ditton Geotechnical
Services Pty Ltd

u = f (dsigma(z)/E, h/H, z/H) = far-field horizontal displacement

Horizontal stress, Sigma 1 , increases with depth.

u1 > u2 > u3; sum of $u_{1 \text{ to } n}$ = U

Notes:
1. Greater stress relief, dsigma(z), occurs at distance z in steep topography than if surface a constant depth, h.
2. E = Young's Modulus.
3. v = Poissons Ratio.
4. TSF = Tectonic or 'locked' in stress factor.
5. K = Sigma1/Sigma(v) ratio = v/(1-v) x Overconsolidation Ratio
6. Sigma(v) = vertical stress.
7. dSigma = f(Sigma1, T, H, z10mm and Smax)
8. T = Mining height.

Horizontal stress relieves by "dsigma(z)" at distance z from panel

H

S_{max}

u1

u2

U

u3

horizontal stress relieves by "dsigma" (MPa)

fractured and sheared rock

h

3~5T

disturbed/caved zone

Sigma1 = TSF.E + K.Sigma(v)

z

T Extracted Pillar or Longwall Panel of Width, W

z10mm is ~ 4 to 5 H with topographical effects and represents practical, measurable FFD limit.

Simple Analytical Model for Predicting Total FFD : U = 0.5(Sigma1 x 12.3/2)z10mm/[E(H+h)/2] + 'tail' of 10mm + Smax component (refer to text)

DgS	Engineer:	S.Ditton	Client:	DgS, 2007		
	Drawn:	S.Ditton				
	Date:	22.05.07	Title:	Conceptual Model of Far-Field Displacement Outside Angle of Draw Limits from Pillar Extraction or Longwall Panels		
Ditton Geotechnical Services Pty Ltd						
			Scale:	NTS	Figure No:	A44a

Left chart:

Sigma 1 (H) = 6.14 + 0.104H

Sigma 2 (h) = 0.104H

Sigma 3 (v) = 0.025H

Y-axis: Principal Stress (MPa)
X-axis: Depth, H (m)

Legend: Sigma 1 • Sigma 2 ◆ Sigma 3 (v) ▲

Key:
(v) = vertical
(H) = major horizontal
(h) = minor horizontal
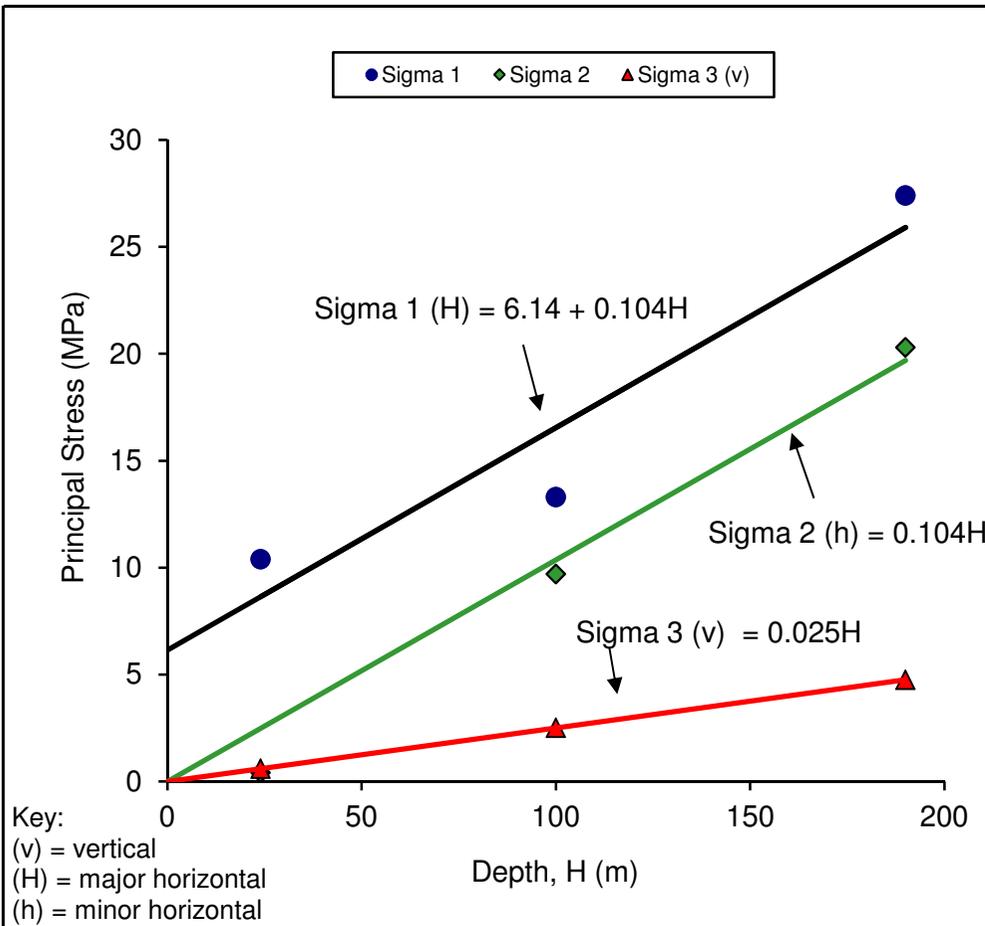
Measured Stress Field for F3 Freeway, West of Newcastle (Lohe & Dean Jones, 1995)

Right chart:

Sigma 1a = 6.5 + 0.025H

Sigma 2a = 4.5 + 0.025H

Sigma 1b = 0.05H

Sigma 2b = 0.0375H

Sigma 3a,b = 0.025H

Y-axis: Principal Stress (MPa)
X-axis: Depth, H (m)

Legend: Sigma 1a — Sigma 2a — Sigma 3a — Sigma 1b —— Sigma 2b ---- Sigma 3b —·—
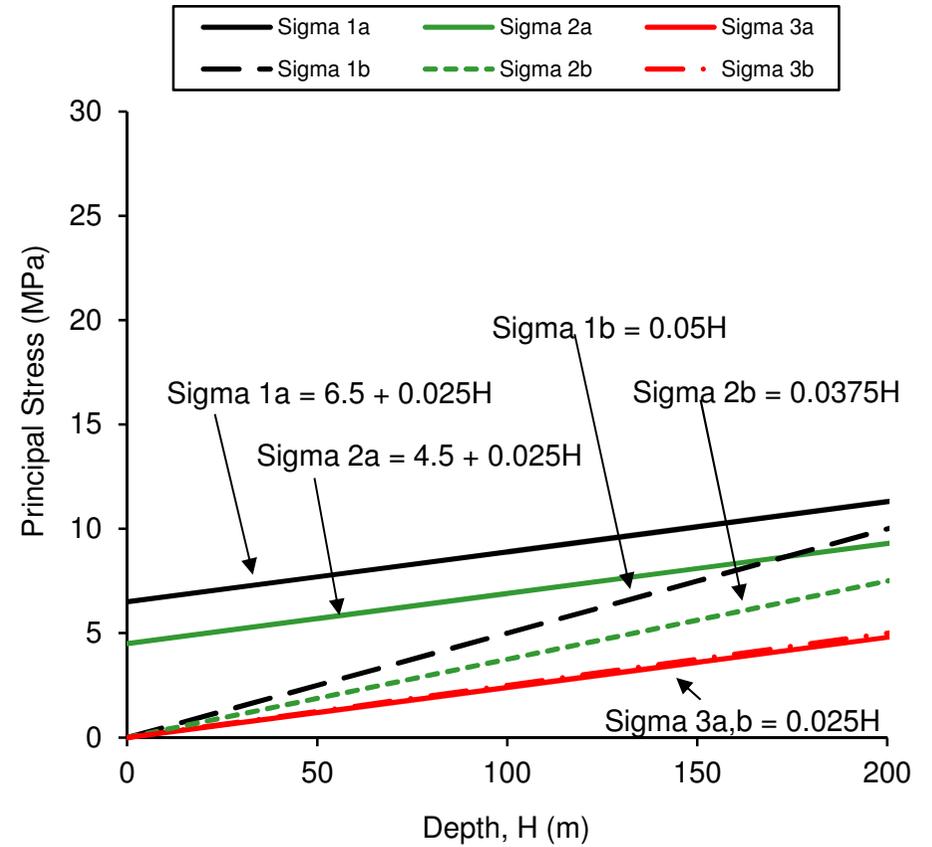
Typical Stress Field Models for Sydney Basin Overburden a) McQueen, 2004; b) Lohe & Dean Jones, 1995; c) Pells, 2002 not shown for clarity (refer to text).

DgS Ditton Geotechnical Services Pty Ltd	Engineer:	S.Ditton	Client:	DgS, 2007		
	Drawn:	S.Ditton				
	Date:	12.07.07	Title:	Published Principal Stress Field Models for Sydney Basin and		
				Western Area of Newcastle Coalfield		
	Scale:	NTS			Figure No:	A44b

Legend:
- ◆ F3 Freeway (Mine A, LW1: Finish End-Corner) Data
- ■ Transgrid Towers (Mine A, LWs 2 and 3: Start End-corner)
- △ RTA F3 Cut 7B (Mine A, LWs 2 and 3: Start End-corner)
- ● Mine B (LW2: Start end)
- ○ Mine B (LW1: Start end)
- – – – Expon. (F3 Freeway (Mine A, LW1: Finish End-Corner) Data)
- — Expon. (Transgrid Towers (Mine A, LWs 2 and 3: Start End-corner))
- — Power (Mine B (LW2: Start end))
- ····· Expon. (Mine B (LW1: Start end))

Y-axis: Measured Horizontal Displacement, u (mm)

X-axis: Distance from Longwall Extraction Limits/Cover Depth, z/H (m/m)

$y = 94.925e^{-1.3759x}$
$R^2 = 0.9598$

$y = 14.288e^{-1.5705x}$
$R^2 = 0.5108$

$y = 37.976e^{-1.3435x}$
$R^2 = 0.8459$

$y = 23.941x^{-0.5225}$
$R^2 = 0.8996$

DgS	Engineer:	S.Ditton	Client:	DgS, 2007		
	Drawn:	S.Ditton				
Ditton Geotechnical Services Pty Ltd	Date:	22.05.07	Title:	Empirical far-field displacement prediction model using total station electronic distance measurements from longwall panel ends		
	Scale:	NTS			Figure No:	A45

Legend:
- ◆ RTA F3 Freeway (Mine A, LW1: Finish end-corner) Data
- △ RTA F3 Cut 7B (Mine A, LWs 1 and 2: Start end - corner)
- ○ Mine B (LW1: Start end)
- ■ Transgrid Towers (Mine A, LWs 2 and 3: Start end-corner)
- ● Mine B (LW2: Start end)
- - - - Expon. (RTA F3 Freeway (Mine A, LW1: Finish end-corner) Data)
- — — Expon. (Transgrid Towers (Mine A, LWs 2 and 3: Start end-corner))
- — — Power (Mine B (LW2: Start end))
- - - - Expon. (Mine B (LW1: Start end))

$y = 0.0558e^{-1.3759x}$
$R^2 = 0.9598$

$y = 0.0089e^{-1.5705x}$
$R^2 = 0.5108$

$y = 0.0267e^{-1.3527x}$
$R^2 = 0.7923$

$y = 0.0109x^{-0.5225}$
$R^2 = 0.8996$

Y-axis: u/S_{max} (m/m)

X-axis: z/H

DgS	Engineer:	S.Ditton
	Drawn:	S.Ditton
	Date:	22.05.07
Ditton Geotechnical Services Pty Ltd		

Client:	DgS, 2007
Title:	Empirical far-field displacement prediction model using total station electronic distance measurements from longwall panel ends and normalised to maximum panel subsidence
Scale:	NTS
Figure No:	A46

Empirical far-field displacement prediction model using cummulative steel tape measurements from longwall sides and normalised to maximum panel subsidence

Legend: XL2(LWA), XL3(LWA), XL4(LWA), XL5(LWA), XL6(LWA), WN(LWB), LWC, LWD, LWE, LWF, LWG, LWH, Expon. (LWF)

$y = 0.1489e^{-1.6335x}$
$R^2 = 0.9902$

Horizontal Displacement/Smax (m/m)

Distance from Longwall Goaf Edge/Cover Depth (z/H)

DgS	Engineer:	S.Ditton	Client:	DgS, 2007		
	Drawn:	S.Ditton				
	Date:	22.05.07	Title:	Empirical far-field displacement prediction model using cummulative steel tape		
Ditton Geotechnical				measurements from longwall sides and normalised to maximum panel subsidence		
Services Pty Ltd	Scale:	NTS			Figure No:	A47

Legend:
- ◆ F3 (LW30 Finish End-Cnr) Data
- ■ Transgrid Towers (LWs 32,33:Start End-cnr)
- △ RTA F3 Cut 7B (LW31,32 Start-cnr)
- ● Newstan (LW16 start-end)
- ○ Newstan (LW15 start-end)
- ● LWF (XL Strain Data)

(Worst-case from panel sides)

$$y = 0.1489e^{-1.6335x}$$
$$R^2 = 0.9902$$

(Worst-case from panel ends for z/H <1)

$$y = 0.0558e^{-1.3759x}$$
$$R^2 = 0.9598$$

(Worst-case from panel corners)

$$y = 0.0267e^{-1.3527x}$$
$$R^2 = 0.7923$$

(Worst-case from panel ends for z/H > 1)

$$y = 0.0109x^{-0.5225}$$
$$R^2 = 0.8996$$

y-axis: u/S_{max} (m/m)

x-axis: z/H

DgS	Engineer:	S.Ditton
	Drawn:	S.Ditton
	Date:	22.05.07
Ditton Geotechnical Services Pty Ltd		

Client:	DgS, 2007
Title:	Combined empirical far-field displacement prediction models for longwall panel sides, ends and corners.
Scale:	NTS
Figure No:	A48

Ride (m)
MStep 2 minus 1

| 0.000000 | 0.010000 | 0.020000 | 0.030000 | 0.040000 | 0.050000 |

Major Principal Stress Direction

Calibration Locations

Engineer:	S.Ditton	Client:	DgS, 2007		
Drawn:	S.Ditton				
Date:	22.05.07	Title:	Example of Map-3D Elastic Boundary Element Model Far-Field Displacement Contours Around a Complex Pillar Extraction Mining Layout		
		Scale:	NTS	Figure No:	A49

DgS

Ditton Geotechnical Services Pty Ltd

Figure A50. Empirical far-field strain prediction model using cummulative steel tape measurements from longwall sides and normalised to maximum panel subsidence

Legend:
- XL2(LWB)
- XL3(LWB)
- XL4(LWB)
- XL5(LWB)
- XL6(LWB)
- WN(LWB)
- LWC
- LWD
- LWE
- LWF
- LWG
- LWH
- Expon. (Mean (All data))
- U95%CL
- U99%CL

Mean $E/S_{max} = 0.8000e^{-3.0291(z/H)}$

U95%CL $E/S_{max} = 1.4622e^{-1.9201(z/H)}$

U99%CL $E/S_{max} = 2.0200e^{-1.8018(z/H)}$

Y-axis: Measured Strain / Maximum Panel Subsidence (E/S_{max}) [mm/m^2]

X-axis: Distance From Goaf Edge/Cover Depth (z/H) [m/m]

Engineer:	S.Ditton	Client: DgS, 2007
Drawn:	S.Ditton	
Date:	22.05.07	Title: Empirical far-field strain prediction model using cummulative steel tape
Ditton Geotechnical		measurements from longwall sides and normalised to maximum panel subsidence
Services Pty Ltd		Scale: NTS	Figure No: A50

DgS

Ditton Geotechnical Services Pty Ltd